Chemical Engineering Department
PhD Program: Chemical Processes Engineering

TOWARDS THE RECOVERY OF RARE EARTH ELEMENTS FROM END-OF-LIFE PRODUCTS: HYDROMETALLURGICAL ROUTES AND MATHEMATICAL MODELLING OF EXTRACTION SYSTEMS

Author: Eleonora Obón Estrada

Director: Dr. Ana Maria Sastre Requena
Codiretor: Dr. Agustín Fortuny Sanromà

Escola Tècnica Superior d'Enginyeria Industrial de Barcelona (ETSEIB)
Universitat Politècnica de Catalunya,

Barcelona, July 2019

Thesis presented to obtain the qualification of Doctor awarded by the Universitat Politècnica de Catalunya

Abstract

The rare earth elements (REEs) are essential ingredients for the development of modern industry and the transition to a more sustainable economy model. The unique physicochemical features of these elements, such as their magnetism and optical properties, are greatly expanding their application. They have become key elements for the manufacture of many ordinary consumer goods like hybrid cars, fluorescent lamps or electronic devices like mobile phones or tablets. The growing popularity of the rare earth elements derivatives is leading to an increase in the global demand and the price of these elements. Unfortunately, the current availability of these resources is limited due to three main factors: their heterogeneous geological location, their low concentration in the ores, and the environmental issues related with their mining.

All these disadvantages concerning the supply of the rare earth elements have led to the study of new techniques to obtain them, such as the recycling of end-of-life products. Recycling of REEs arises as a new secondary source of supply of REEs, especially in Europe where large amounts of technological waste are generated every year. Currently, the recycling of rare earth elements represents less than 1% of the global supply. Nevertheless, some studies in the literature assume that by 2050 the recovery rate of REEs will be 90% for wind turbines, 70% for electrical vehicles and 40% for the rest of derivative products.

The research presented in this thesis relies on experimental investigation of new hydrometallurgical routes, the majority of them involving the use of ionic liquids, which could eventually be applied for the recovery of rare earth elements from end-of-life products. Matemathical modelling of the reported extraction systems has been carried out in order to provide a computational instrument that can be easily tailored for prediction of other collecting processes requiring minor adjustments.

Keywords

Rare Earth Elements; critical status; urban mining; hydrometallurgical routes; Solvent Extraction; Ionic Liquids; mathematical modelling; Supported Liquid Membranes; leaching process.

Resum

Les terres rares son ingredients essencials per al desenvolupament de la indústria moderna i la transició cap a un model economic més sostenible. Les seves característiques fisico-químiques úniques, com el seu magnetisme i propietats òptiques, han precipitat un increment accelerat en l'aplicació d'aquests elements. Les terres rares s'han convertit en elements clau per a la fabricació de molts articles d'ús diari com per exemple, cotxes elèctrics i dispositius electrònics com telèfons mòbils i tabletes. La creixent popularitat dels productes que contenen aquests metalls està provocant un escalat en la demanda global i el preu de les terres rares. Desafortunadament, en l'actualitat, la disponibilitat d'aquests recursos a la natura és limitada degut bàsicament a tres factors: heterogènia localització geològica, baixa concentració als minerals que els contenen i inconvenients mediambientals relacionats amb la mineria.

Els inconvenients relacionats amb el subministrament de les terres rares a nivell mundial han propiciat l'estudi de noves tècniques per a la obtenció d'aquests elements mitjançant el reciclatge de productes que els contenen. El reciclatge sorgeix com una font secundària alternativa a la mineria per tal d'assegurar el provisionament de terres rares especialment a Europa on generem grans quantitats de residus tecnològics cada any. Actualment, la taxa de reciclatge de terres rares se situa per sota l'1% del subministrament global. No obstant, alguns estudis publicats en la literatura assumeixen que l'any 2050, la taxa de recuperació haurà augmentat considerablement, de manera que es reciclarà fins a un 90% de les terres rares provinents d'aerogeneradors, 70% de vehicles elèctrics i 40% de la resta de productes que contenen aquests metalls.

La recerca presentada en aquesta tesi es basa, principalment, en la investigació de noves rutes hidrometalúrgiques, la majoria d'elles utilitzant líquids iònics, que puguin ser implementades en processos de recuperació de terres rares a partir de residus tecnològics. D'altra banda, s'han elaborat models matemàtics d'alguns dels sistemes d'extracció reportats que pretenen convertir-se en una eina computacional, fàcilment adaptable, per a la predicció del comportament d'extracció en d'altres processos de recuperació amb diferents condicions experimentals.

Preface

The increasing concerns about the environmental impact of fossil fuels and the uncertainty about their supply to be used as energy sources in the future are motivating a global switch towards new clean alternatives of emerging eco-efficient and globally competitive technologies.

The rare earth elements (REE) are vital to the modern technologies since their unique chemical features such as their magnetism and optical properties are needed to supply the required functionality in many high tech components, green technologies and material industries of NiHM batteries, hybrid cars, wind turbines, compact fluorescent lamps (CFLs), fluorescent lightning, liquid crystal displays (LCDs) and lasers, among other products (Kumar Jha et al., 2016).

The accelerating technological innovation cycles and the growth of emerging economies have led to increasing global demand of metals and minerals and securing access to a stable supply of many raw materials has become a major challenge (European Commission, 2017). Thus, the extraction costs are transferred to their prices since the sources of high quality ores have reduced and so lower quality mines must be now exploited.

About one hundred million tons of rare earth oxide reserves are presently accessible in the world, scattered in more than 30 countries. Nonetheless, the global mine production of rare earth metals is just 110.000 metric tons. The critical status of the rare earth elements is strongly tied to their heterogeneous geological location, low concentration in the ores and the environmental issues related with their mining due to the high volume of concentrate acids that are needed to separate them from their ores and the high amount of secondary waste generated after this process (Wübbeke, 2013).

Urban mining is a new concept based on reclaiming raw materials from end-of-life products. Higher recycling rates can reduce the pressure on demand for primary raw materials and minimise the energy consumption and other negative environmental impact from extraction and processing. The urban mining of REEs from end-of-life products and industrial waste streams started receiving more and more attention since it can provide another source of metals, alongside conventional mining in geological deposits (Tunsu et al., 2015a).

This thesis focuses on the development of hydrometallurgical routes for neodymium, terbium, and dysprosium recovery from aqueous solutions using ionic liquids. Mathematical modelling of the extraction systems developed has been carried out in order to predict the extraction extension of the metals providing a basis for further investigation on rare earth elements recycling from end-of-life products and contributing to the state of art on hydrometallurgical

REEs recovery. This work has been performed at the Chemical Engineering department of the Universitat Politècnica de Catalunya (UPC) in the framework of three research projects: *Técnicas avanzadas de separación utilizando liquidos iónicos como extractantes disolventes en tecnología de membranas con renovación de membrana liquida y en procesos (CTQ2011·22412); Separación/Recuperación de tierras raras mediante procesos de sorción en biopolímeros, composites y membranas (CTM2014-52770-R)* and *Estrategias de reciclado de residuos que contienen tierras raras: procesos de sorción mediante nanocomposites magnéticos y membranas líquidas para su separación y recuperación* (*CTM2017-83581-R*) funded by the Spanish Ministry of Science and Innovation (MICINN). A short stay in the Chalmers University of Technology also financed by the MICINN (Ref. EEBB-I-16-10674) completed the doctoral training.

Acknowledgements

This thesis has been conducted thanks to the Spanish Ministry of Science and Innovation (MICINN) since they have funded the three projects that have been the framework for the development of the whole investigation.

I consider myself very fortunate to have spent the last five years under the supervision of my thesis director Dr. Ana Sastre Requena whom has always kept an eye on me during all this time no matter how busy her schedule was. Thank you for your valuable advise, for taking me out of my confort zone when I was not convinced to go abroad and for encouraging me to keep going and never surrender. I can say now, that this experience has enabled me to grow personally and professionally.

I would like to thank my thesis codirector Agustí Fortuny and the professor Mª Teresa Coll for teaching me everything I know, and helping me define the goals of the investigation, which have been crucial for the development of this work.

During my studies, I had the pleasure of going abroad and staying at the Chalmers University of Technology in Gothenburg, Sweden. I want to thank my mentor Dr. Cristian Tunsu, who was absolutely willing to share his expertise, for his warm welcome, guidance and dedication throughout the time I was there. Also from Chalmers, I cannot forget to thank my beloved friends Gabrielle and Nicolas, for making the whole experience so much fun.

A special mention to all my friends, thank you for being so supportive and understanding, especially through the end of my studies when I may have been a little absent. I also want to thank my parents-in-law for their excitement and support, and for believing in me more than I do myself.

And finally, and most importantly, I want to thank my family. I am grateful to Carles for being an amazing laboratory assistant, for always spoiling me and taking good care of me during all these years. I wouldn't have made it to the end without your love and support. I am also deeply grateful to my mum, dad and sister because they started everything, they encouraged me to continue studying and I know for a fact that they are beyond proud. I am where I am as a direct result of you and your efforts.

"I was taught that the way of progress was neither swift nor easy"
- Marie Curie -

List of contents

Chapter 4: Results and discussion

List of Figures

List of Tables

List of Abbreviations and Acronyms

$\overline{HX}$ – Organic acid
[$C_n$mim] – Alkyl groups of Imidazolium
[P_n] – Phosphonium IL
% v/v – Volume volume percentage
% wt – Weight percentage
% w/v – Weight volume percentage
AliCy – [Aliquat336][Cyanex272]
AliD2EHPA - [Aliquat336][D2EHPA]
AliDec – [Aliquat336][Decanoic Acid]
AliOle – [Aliquat336][Oleic Acid]
Aliquat 336 - Methyl-tri(octyl/decyl)ammonium chloride
CFLs – Compact Fluorescent Lamps
CRT – Cathode Ray Tubes
Cyanex® 272 – Bis(2,4,4-trimethylpentyl)phosphinic acid
Cyanex® 923 – Mixture of trialkylphosphine oxides
Cyphos® 104 – Trihexyl(tetradecyl)phosphonium bis-2,4,4-(trimethylpentyl)phosphinate
D2EHPA – Di-(2-ethylhexyl)phosphoric acid
EDTA – Ethylene Diamine Tetraacetic Acid
FCC – Fluid Catalytic Cracking
H_2O_2 – Hydrogen Peroxide
H_2SO_4 – Sulphuric Acid
HCl – Hydrochloric Acid
HDD – Hard Disk Drives
HEHEPA – 2-ethylhexyl-2-ethylhexyl phosphoric acid
HEV – Hybrid Electric Vehicles
HNO3 – Nitric Acid
HREE – Heavy Rare Earth Elements
IE – Ion Exchange
IL – Ionic Liquids
Im – Ionic strength
K – equilibrium constant
LLE – Liquid – Liquid Extraction
LREE – Light Rare Rarth Elements
Me – metal
MP-AES – Microvawe Plasma Atomic Emission Spectroscopy
Na_2CO_3 – Sodium Carbonate
Na_2SO_4 – Sodium sulphate
NaOH – Sodium Hydroxide
O/A – Organic / Aqueous phase ratio

Primene 81-R – Mixture of highly-branched C12 to C14 tertiary alkyl primary amine isomers
PC88A – 2-ethylhexyl phosphonic acid mono 2-ethylhexyl ester
PM – Permanent Magnets
Primene JMT – Mixture of highly-branched C16 to C22 tertiary alkyl primary amine isomers
REE – Rare Earth Elements
REM – Rare Earth Metals
REO – Rare Earth Oxides
RTIL – Room Temperature Ionic Liquid
RTIL – Room Temperature Ionic Liquids
SE – Synergistic extractant
SLM – Supported Liquid Membranes
SX – Solvent Extraction
TBP – Tributylphosphate
USGS – U.S. Geological Survey
YSZ – Yttrium Stabilized Zirconia

Chapter 1: The Rare Earth Elements: state-of-the-art

The rare earth elements (REEs) are a group of 17 chemically similar metallic elements, 15 lanthanides plus yttrium and scandium. Lanthanides are a series of elements with atomic numbers within 57 and 71 and all of them occur in nature. They are held in a wide range of REE bearing minerals and are mined collectively. They are usually divided into two different categories: the light REE (LREE) and the heavy REE (HREE).

The rare earth elements are essential raw materials for a wide range of applications including metallurgy, catalysts, manufacture of glass and ceramics, phosphors, lasers, rechargeable batteries and others. Due to their unique chemical features like their magnetism and optical properties REEs are becoming increasingly important in the transition to a green economy because of their key role in the development of green technologies and many widespread domestic products (E. Obón et al., 2017b).

The first chapter of this manuscript covers the history and discovery of REEs as well as their physical and chemical properties and applications, and sets the background for understanding their current status as critical materials of use in technology and industry.

1. History of the Rare Earth Elements

The discovery of the rare earth elements started at Ytterby, a village near Stockholm in Sweden, by the end of the 18th century and went on for about 160 years.
In 1787, an army lieutenant and part-time chemist Carl Axel Arrhenius found a heavy black mineral, until then not mentioned by anyone, in an old quarry at Ytterby. The Finnish chemist and mineralogist Johan Gadolin was the first one to analyse and characterize the mineral composition. Gadolin found iron and silicate but also a new component, which accounted for 30% of the mineral. The mineral was called “gadolinite” and the new element “yttria” (Voncken, 2016a).

In 1804 the Swedish scientists Jöns Jakob Berzelius and Wilhelm Hisinger reported the discovery of another mineral, which contained the oxide of a new element. They named the element “cerium” and the mineral “cerite”. In 1839 Carl Gustaf Mosander, an associate of Berzelius, found and separated a new element from “cerite” and named it “lanthanum”. Nonetheless, he was convinced that the lanthanum he had separated was not a pure element but might contain yet another element. After further investigations, he finally detected that new element in 1842 and named it “didymium”, which in Greek word would be twins, to indicate that it occurred in conjunction with cerium and

lanthanum in the cerite mineral. Mosander also studied the gadolinite. In 1843 he published his results reporting that he had found not one but two more new elements in it, which were called “erbium” and “terbium”.

The emergence of the spectral analysis technique in the beginning of the 1850s marked a breaking point towards the identification of new elements. In 1864, Marc Delafontaine, a Swiss American chemist used the spectral analysis to definitely prove the existence of yttrium, terbium and erbium. In 1878 Delafontaine reported to have found didymium in “samarskite” a mineral discovered in 1838 by the German mineralogist Gustav Rose. Delafontaine reported in 1878 that the absorption spectrums of didymium separated from samarskite and from cerite were not fully identical. Therefore, he suspected that didymium was not a single element.

In 1879, the French chemist Paul Emile Lecoq found a new element in samarskite and named it “samarium”. At the same time, Lars Frederick Nilson separated a new element from the erbium fraction of gadolinite and named it “scandium”.

Also in 1878, the Swiss chemist Jean Charles Marignac while investigating gadolinite, separated a new element oxide named “ytterbium” since it stood between yttrium and terbium in its properties.

Shortly afterwards, in 1879 in Sweden, Per Theodor Cleve investigated the erbium fraction remaining after the separation of ytterbium in the gadolinite. Cleve suspected that it might contain more elements. With the aid of chemical separation techniques and spectral analysis, he identified two new elements and called them “thulium” and “holmium”.

In 1886, Lecoq de Boisbaudran following an intricate method for the chemical separation and spectroscopic fluorescence studies of the gadolinite elements, concluded that the holmium discovered by Cleve contained another new element, witch was called “dysprosium” (Adunka and Virginia Orna, 2018). Also in 1886, the Austrian chemist Carl Auer von Welsbach who had been investigating didymium for a year, succeeded separating two fractions of didymium ammonium nitrate, which were further investigated by absorption and spark spectrometry and so it was concluded that the fractions belonged to two different elements, which were called “praseodymium” and “neodymium”.

Almost fifteen years later, in 1901, the French chemist Eugene Demarcay announced he had separated a new element from samarium in the samarskite. He named the element “europium”. In 1904, europium was also separated from gadolinium by the French chemist Georges Urbain.

In 1905, Auer stated that after several studies he had found that the ytterbium described by Marignac probably contained new elements. Almost simultaneously, Urbain reported the same results and named the new elements “neoytterbium” and “lutetium”. Over the years, the name ytterbium replaced to neoytterbium and lutetium survived (Gupta and Krishnamurthy, 2005).

The discovery of lutetium closed the chapter of the disclosure of the natural occurring rare earth elements. The figure 1 summarizes the history of rare earth elements discovery throughout different pathways: a) gadolinite, b) cerite, c) samarskite.

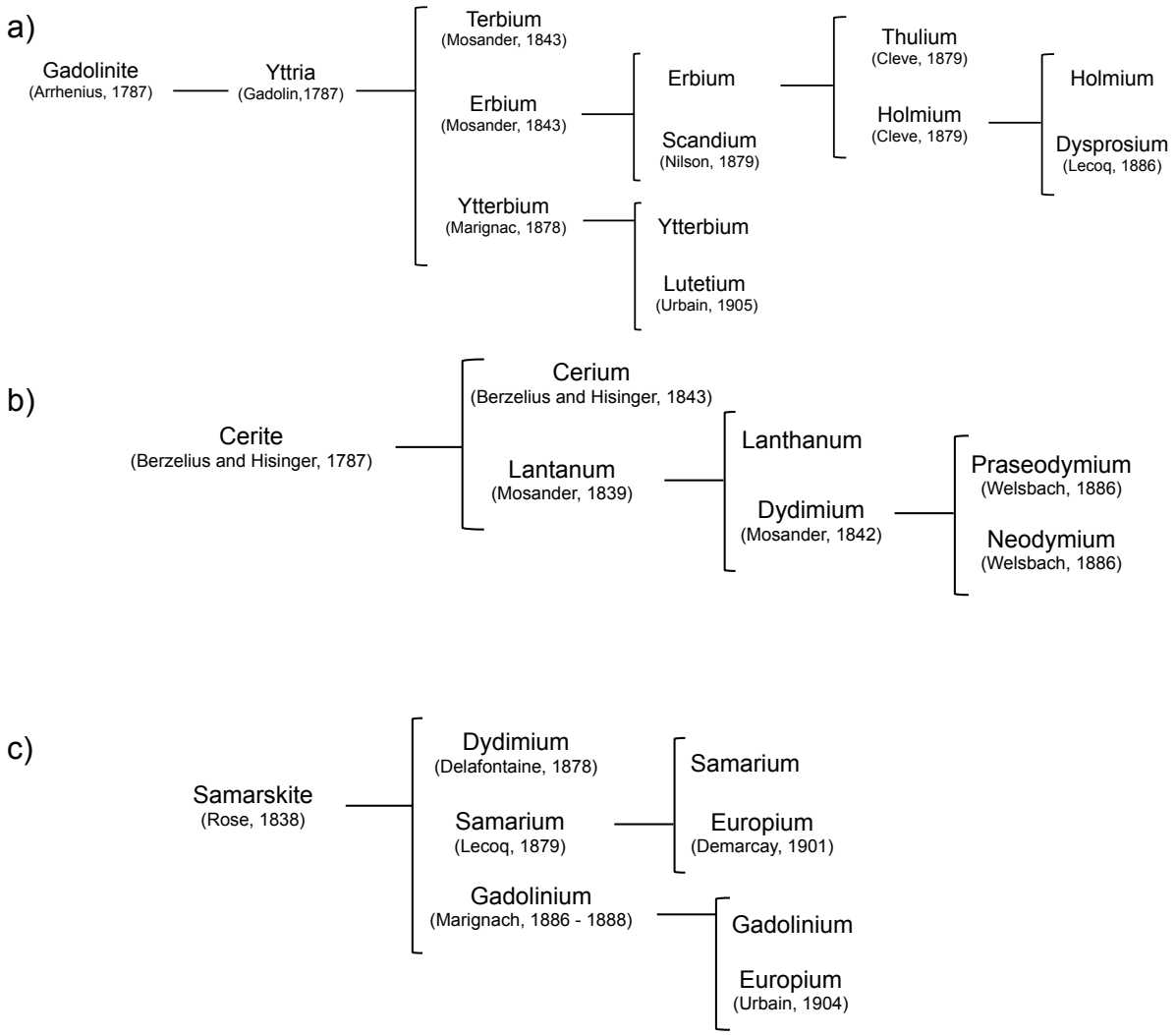

Figure 1. Discovery of the rare earth elements. Adapted from (Gupta and Krishnamurthy, 2005).

2. Physical and chemical properties

The US Department of Energy calls them “technology metals”. They make possible the high tech world we live in today. The Rare Earth Elements (REEs)

are a group of 17 metals in the bottom of the periodic table in the 6th period, specifically the fifteen lanthanides plus scandium and yttrium, which are considered REEs since they tend to occur in the same ore deposits as the lanthanides and exhibit similar chemical properties. The name of the series comes from lanthanum, the first element that sets the beginning of it. These elements are conventionally divided into two categories: the more common light rare earths from lanthanum to europium and the less abundant heavy rare earths, which include de rest of lanthanide elements along with yttrium. Scandium is not included in either of these groups due to its much smaller ionic radius (Kumar Jha et al., 2016).

All the lanthanides have close chemical properties due to their similar electron configurations; the majority of these elements have partially occupied 4f electron orbitals. As the atomic number increases, there is a decrease in the ionic radius that is larger than expected due to a phenomenon called lanthanide contraction. The lanthanide contraction may be explained by the fact that as one traverses the lanthanide series, the increasing charge on the nucleus (associated with the increase of protons according to the atomic number) causes electron shells of these elements to be pulled closer to the atom nucleus. The ionic radius is typically affected by shielding of the outer electron shells by the inner shells. The strength of this effect is higher in the s orbital and decreases through p, then d and finally f. Moving through the lanthanide series, electrons fill the 4f orbital which provides weaker shielding of the outer shells, resulting in a greater reduction of ionic radius (Richard and Fan, 2018). Figure 2 shows the ionic radius of the Ln^{3+} ions plus the trivalent ions of yttrium and scandium.

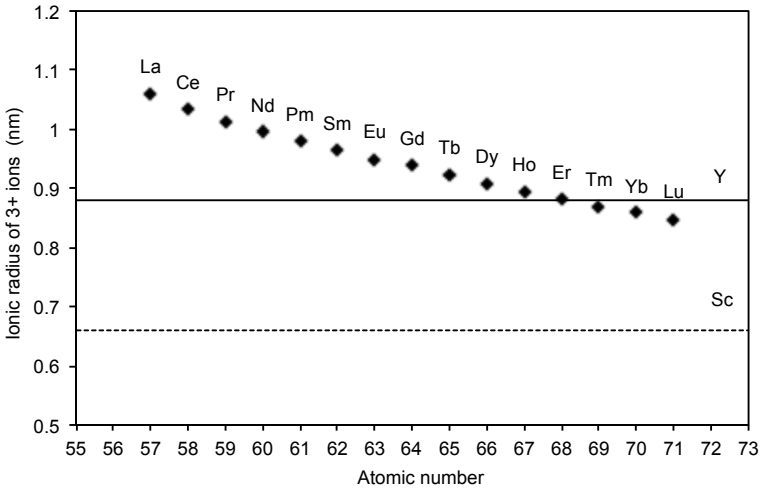

Figure 2. The lanthanide contraction. Adapted from (Jordens et al., 2013).

The figure above helps to understand why yttrium is considered to be a HREE and why scandium is often taken out of the REEs groupings since its ionic radius is much smaller.

The REEs have similar chemical properties, which translate into separation and purification difficulties. They are all soft, malleable, ductile and fairly dense (around 7 $g \cdot cm^{-3}$). Their melting points are nearby 1000ºC and their boiling points close to 3000ºC. The rare earth elements are poor electrical conductors. Within the lanthanides, room temperature resistivities are highest in the center of the series. Only lanthanum is superconducting at atmospheric pressure.

At room temperature, they are not affected by air the same way. Some of them corrode very rapidly (Eu) while some remain unspoilt for years (La). However, increasing the temperature and the humidity accelerates oxidation of rare earth metals. The rare earth oxides (REO) are among the most stable of the oxides of all elements in the periodic table (Voncken, 2016b).
Rare earth metals react with hydrogen to form hydrides at temperatures from 400 to 600ºC. The hydration of the metals increases their conductivities. They also have a strong affinity with nitrogen. However, nitridation of lanthanides is slow and high temperatures are required (Gupta and Krishnamurthy, 2005).

The REEs show similar reactivities, which is related to their electronic configuration since the 4f electrons do not take part in the formation of complexes (Rayner-Canham, 2000). The large size of the lanthanide ions makes it possible for only certain types of complexes to be formed; therefore the number of REEs complexes is limited. Only species that can attract the lanthanide cations because of their own small size, large charge and chelating abilities will form complexes, and bonding in all cases will be predominantly ionic. Besides, the properties that depend directly on the 4f electrons are not affected by complexation (Gupta and Krishnamurthy, 2005).

Despite the similarities, the lanthanide contraction facilitates their individual separation since it affects the strength of the complexes formed in aqueous solution. The slow decrease in ionic radius towards the lanthanides series increases the strength of cation-anion, ion-dipole and ion-induce dipole interactions, so that HREEs create stronger complexes with extractant molecules compared with LREEs (Tunsu et al., 2015a).

The trivalent ionic state ion is common for each lanthanide element. Cerium has also a second oxidation state (Ce^{+4}), which can be used for redox titrations because of its very oxidative nature. Most lanthanide ions are luminescent, and their emission lines cover the entire spectrum, from UV (Gd^{3+}) to visible (Pr^{3+}, Sm^{3+}, Eu^{3+}, Tb^{3+}, Dy^{3+}, Tm^{3+}) and near-infrared (Pr^{3+}, Nd^{3+}, Ho^{3+}, Er^{3+}, Yb^{3+}). The colours of the lanthanide ions in aqueous solution are listed in table 1.

Table 1. Colours of Ln^{3+} in aqueous solution. Adapted from (Cotton, 2006).

Ion	[Xe] $4f^n$	Colour
La^{3+}	[Xe] $4f^0$	Colourless
Ce^{3+}	[Xe] $4f^1$	Colourless
Pr^{3+}	[Xe] $4f^2$	Green
Nd^{3+}	[Xe] $4f^3$	Violet
Pm^{3+}	[Xe] $4f^4$	Pink
Sm^{3+}	[Xe] $4f^5$	Pale yellow
Eu^{3+}	[Xe] $4f^6$	Colourless
Gd^{3+}	[Xe] $4f^7$	Colourless
Tb^{3+}	[Xe] $4f^8$	Pale pink
Dy^{3+}	[Xe] $4f^9$	Pale yellow
Ho^{3+}	[Xe] $4f^{10}$	Yellow
Er^{3+}	[Xe] $4f^{11}$	Rose
Tm^{3+}	[Xe] $4f^{12}$	Pale green
Yb^{3+}	[Xe] $4f^{13}$	Colourless
Lu^{3+}	[Xe] $4f^{14}$	Colourless

The spectroscopic properties of the lanthanides arise from 4f-4f transitions. As the 4f shell has a low radial expansion, 4f electrons are shielded from the chemical environment because of the filled $5s^2$ and $5p^6$ orbitals. As a consequence, 4f-4f transitions are weakly affected by the environment and the ligand fields, resulting in narrow emission bands with discrete and characteristic energy levels. Figure 3 shows the emission spectra of terbium and europium complexes compared to an organic fluorophore (Alexa 488).

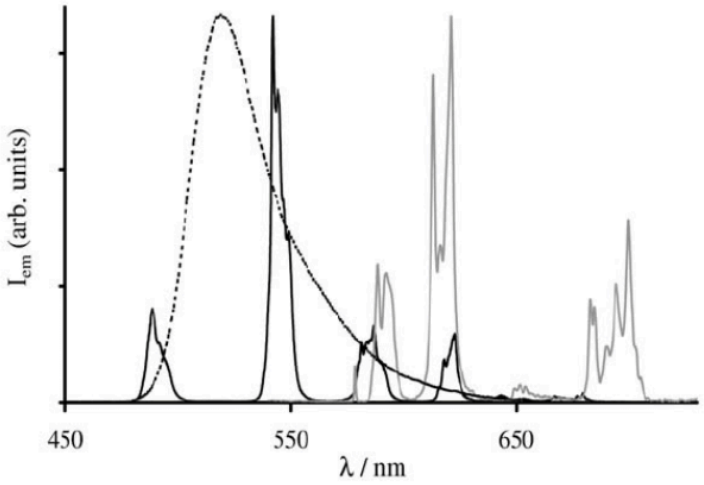

Figure 3. Emission spectra of Tb (black), Eu (grey) and Alexa 488 (doted black) (Charbonniere, 2011).

As can be observed in the figure, because of the f-f transitions, the terbium and europium emission bands are narrower than the Alexa 488 organic compound.

Similar layout would be found for the comparison of lanthanides and transition metals emission bands.

Across the lanthanide series, the electronic configuration of the elements affects their spectroscopic features. Europium and terbium, for example, have excited states that are slightly lower in energy than the excited states of typical ligands (Sturza et al., 2008). Thus, when they are excited by UV light the electrons fall to the excited state of their 3+ ion form and then to the metal ground state, producing luminescence spectra, which makes them key elements for lightning applications.

Figure 4 shows the electronic transitions between Eu^{3+} and an organic ligand. The absorption of a UV photon causes one of the electrons of the organic ligand to be promoted from the ground singlet state to the first excited singlet state. The organic ligand could return from the first excited state to the ground state by radiative emission generating fluorescence. Alternatively, the excited electron could also fall into an excited triplet state if one with a suitable energy is available. The transition of the excited electron from the singlet state to the triplet state does not involve electromagnetic radiation. The organic ligand may then fall from the triplet state to the ground singlet state generating phosphorescence. Nonetheless, when it is bound to the europium ion, radiationless energy transfer from the triplet state of the ligand to Eu^{3+} tends to occur promoting inner electronic transitions. As a result, the excited electron could fall into the Eu^{3+} ground state levels causing luminescence (Leif et al., 2006).

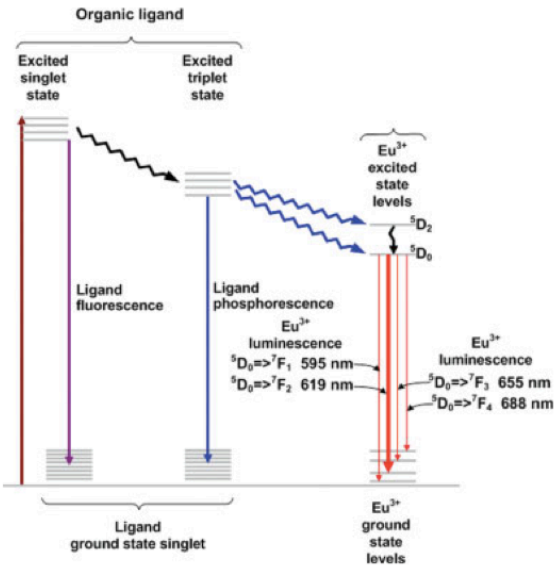

Figure 4. Luminescence of Eu^{3+} complexes of organic ligands (Leif et al., 2006)

With the exception of lanthanum, lutetium and yttrium, all the lanthanide ions contain unpaired electrons. In fact, the HREEs differ from LREEs in that they also have paired electrons in their atomic configurations. The 4f electrons determine the magnetic behaviour of the rare earth metals. The magnetic moments of the Ln^{3+} are assumed to be due to electron spin only as the orbitals occupied by unpaired electrons are located in the peripheries of the ions (Cotton, 2006).

The temperature also affects the magnetic structure of the lanthanides. For most of them, the Curie-temperatures are quite low, which results in the metals at room temperature generally displaying paramagnetism. The paramagnetism increases with increase in the number of unpaired electrons and it is only present in a magnetic field. The Curie-temperature is the point where the permanent magnetism of a material changes to paramagnetism (Voncken, 2016b).

Within all lanthanides, an exception is gadolinium, which has a Curie-temperature of 292 K (18.9ºC), thus it is ferromagnetic. In ferromagnetic materials, the parallel alignment of moments results in a large net magnetization even in the absence of a magnetic field.

The unique physical and chemical features of the rare earth metals are dominantly expanding their application in many high-tech components and green technologies. Although the REE have similar electron configurations, they also have distinctive physical and chemical properties that enable their use in a broad range of technologies that will be described further on in the 1.3 subsection of this chapter. These properties mean that the rare earths provide special magnetic, luminescence and strength characteristics to the products they are used in (Jowitt et al., 2018).

3. Applications

The rare earths have an ever-growing variety of applications in the modern technology. Many technological items that people are currently using on a daily basis depend critically on the rare earths (Kumar Jha et al., 2016).

The first application of the rare earth metals dates back to 1891, when Carl Auer von Welsbach used them for the production of bright light. In 1866 he discovered a gas mantle of zirconia doped with lanthanum that glowed when was brought into the hot zone of a gas flame. Nonetheless, it was too fragile so in 1891 Welsbach came up with a new gas mantle composed of 99% thoria and 1% ceria, which produced brighter light and was also cheaper than the first one. The use of the Welsbach mantle was extended until 1935 approximately, it is

estimated that about five billion gas mantles were produced and consumed in the world within those decades.

The following important application of the rare earths was an ignition system for the Welsbach gas mantle lamps, which was called flintstone. The flintstone was composed of 70% mischmetal (an alloy of cerium, lanthanum, neodymium, praseodymium) and 30% iron and it was used in the lighters for the gas mantle. The lighter flints are still very common and account for the consumption of a solid fraction of the mischmetal produced (Gupta and Krishnamurthy, 2005).

Historically, the third major application of the rare earth elements was the use of their fluorides as a fuse for the generation of intense light by electric arc to be used, for example, for cinema projectors.
From then up until now, many more industrial applications of rare earths have been developed in optics, chemical, electronics, magnets, ceramics, metallurgy and medical technologies (Jowitt et al., 2018). Table 2 displays a summary of the current most common uses of the lanthanide elements.

Table 2. Summary of the lanthanides and their common uses. Adapted from (Jowitt et al., 2018).

Element	Common uses
Lanthanum	Optics, batteries, catalysis
Cerium	Chemical applications, colouring, catalysis, optics
Praseodymium	Magnets, lighting, optics
Neodymium	Magnets, lighting, lasers, optics
Promethium	Limited use due to radioactivity, used in paint and atomic batteries
Samarium	Magnets, lasers, masers
Europium	Lasers, colour TV, lighting, medical applications
Gadolinium	Magnets, glassware, lasers, X-ray generation, computer applications, medical applications
Terbium	Magnets, Lasers, lighting
Dysprosium	Magnets, lasers
Holmium	Lasers
Erbium	Lasers, steelmaking, optics
Thulium	X-ray generation
Ytterbium	Lasers, chemical industry applications
Lutetium	Medical applications, chemical industry applications
Scandium	Alloys in aerospace engineering, lighting
Yttrium	Lasers, superconductors, ceramics, lighting

Currently, although there are no uniform classifications for rare earth applications, the REE markets are commonly divided into eight sectors: magnets, catalysts, phosphors and pigments, ceramics, metallurgy, batteries, glass and polishing and other minor uses. The estimated global REE consumption is shown in figure 5. Catalysts represent the largest consumption

segment, followed by magnets and glass polishing. Disclosure of the more prominent applications of the REEs for modern technologies is further developed in the following subsections.

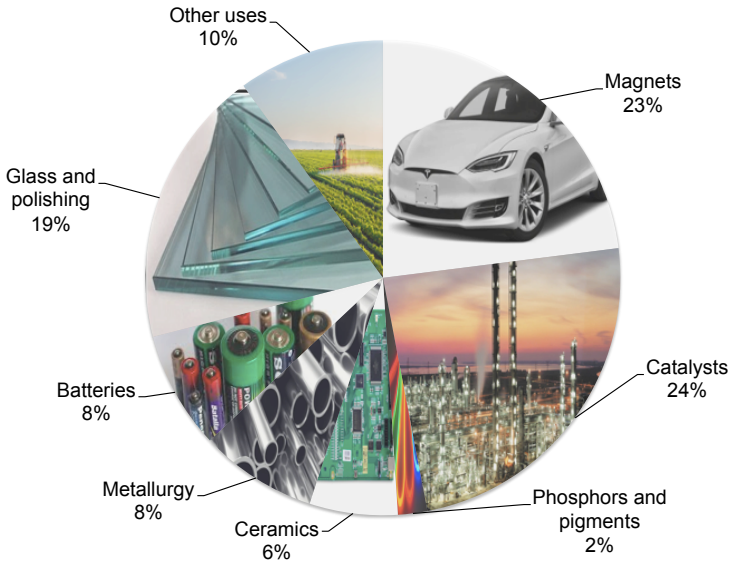

Figure 5. The distribution of global rare earth consumption in 2017, adapted from (EURare, 2017)

3.1. Optics

The 4f transitions of the lanthanides lead to narrow absorption-emission bands in the visible range with discrete and characteristic energy levels, which plays an essential role in the use of rare earths in the optics and phosphor industries.

One of the earlier applications of rare earths in optics was in the glass manufacture. Since iron oxide is a common impurity in glass and causes yellow green colouration decolorizing is often necessary. The addition of small amounts of CeO_2 decolorizes glass chemically, by oxidation of iron to the trivalent state. Physical decolouration can be achieved with erbium. The ferric impurities in the glass can be neutralized by erbium absorption, which results in the formation of a colourless shade (Molycorp, 1994). Erbium oxide gives a pink colour to the glass because of the stability of its trivalent ion. It is also used in ophthalmic materials like sunglasses and in decorative crystal glassware.
Some rare earth compositions containing 50 to 90% cerium oxide, the remainder being other LREEs, are used to polish glass surfaces without abrading. The rare earths are faster and cleaner polishing agents than silica and zirconia (Gupta and Krishnamurthy, 2005).

Many REEs are used for radiation shielding. Most cathode ray tube (CRT) faceplates use cerium-stabilized glass. Cerium prevents fogging of glass under nuclear radiation. Neodymium and vanadium oxides are used to manufacture

optical glass for photometers and nicol prisms. Neodymium is also used to absorb the yellow spectrum in typical incandescent applications.

The optical glass industry consumes rare earth oxides 99.9 – 99.995% in purity in the manufacture of different kinds of lenses. Optical glass for camera lenses is made from a lanthanum flint, which contains calcium, barium and lanthanum oxides. Gadolinium is added to optical glasses used in magnetooptical and electrooptical systems. Praseodymium is used for antireflection coating on lenses and as a constituent in tinted glass filters for selective absorption (Gupta and Krishnamurthy, 2005).

The rare earth elements act as activators in laser glasses. Neodymium is the most popular for this purpose. The Nd-YAG laser consists of neodymium atoms that are accommodated in a transparent host crystal (YAG = Yttrium Aluminium Garnet). The four level system of the Nd makes it ideal for induction of discrete emission by optical pumping (Dickman, 2008). Nd in the host (1 to 5 wt%) is exposed to intense broad-spectrum light and the Nd atoms absorb the light and are pumped to and excited energy state. Transition to a lower energy level generates radiation emission, which wavelength also depends on the host.

Optical telecommunications rely basically on signals transmitted down silica fibres. Rare earths are used for doping of the glass fibres to transmit data over long distances without booster stations. This is the current major high technology application of erbium.

3.2. Phosphors

The first application of rare earth elements in high-tech was the use of europium doped in an yttrium containing host Eu^{3+}-YVO_4 as a red phosphor in colour television picture tubes. Nowadays, colour for television, fluorescent lamps, LED lamps, CRTs and plasma screens is obtained through the use of three REE-based phosphors: an europium-yttrium compound for red, a terbium fluoride-zinc sulphide for green and a cerium-strontium sulphide for blue. When activated by photons, these phosphors emit luminescence, which makes the screen attractively colourful (Gupta and Krishnamurthy, 2005).

Rare earth phosphors are also used for conversion of X-radiation into visible light. They have allowed decreasing the X-ray dosage required for medical radiographies. The Tb^{3+}-Gd_2O_2S (terbium gadolinium oxysulfide) is the most common X-ray phosphor, which reduces the amount of radiation exposure to the patients up to 80%.

Phosphors for fluorescent lamps and compact fluorescent lamps (CFLs) are an important application of REEs. They convert the ultraviolet emission of rare-

gas/mercury discharge plasma into visible white light. Lamp phosphors consist of a mix of a red YOX (Y_2O_3:Eu^{3+}), green LAP or CAT ($LaPO_4$:Ce^{3+},Tb^{3+}; $CeMgAl_{11}O_{19}$:Tb^{3+}) and blue BAM ($BaMgAl_{10}O_{17}$:Eu^{2+}) phosphors (Loy et al., 2017). The blue phosphors represent only a minor weight fraction of the triphosphor blend. The emission spectrum of YOX is ideal for red colour generation. The commercial formulation contains high europium concentrations (3-5 mole percent). At lower europium concentrations emission in the green-yellow is enhanced at the expense of the red emission. The LAP phosphor is rapidly gaining popularity as an alternative to the CAT phosphor. The role of Ce^{3+} in this phosphor is that of the sensitizer. Considerable energy migration occurs over the cerium ions to the terbium ions reducing the amount of Tb^{3+} required for optimum performance (Srivastava and Sommerer, 1998).

3.3. Magnets

Currently, one of the most extensive applications of the lanthanides is their use in the permanent magnets (PM). Samarium alloyed with cobalt-sintered magnets were the first of the rare earth magnets to be available commercially. They possess specific magnetic properties much superior to ferrite and alnico magnets. The magnetic strength of Sm-Co compounds comes predominantly form the cobalt atoms. Samarium helps to maintain the crystalline structure locking the cobalt moments in place and impeding demagnetization. Both samarium and cobalt are expensive and limited in supply so praseodymium, which is more abundant than samarium is, in some cases, used to replace Sm in $SmCo_5$ materials. The superior properties of samarium magnets permitted extensive miniaturization in a wide variety of consumer and industrial products since they can be extremely short and still provide adequate magnetizing force (Gupta and Krishnamurthy, 2005).

Permanent magnets are critical components for electric motors and power generators nowadays. They are used for conversion between electricity and mechanical energy. The most powerful PM are based on intermetallic compounds containing REEs such as Nd, Sm, Dy, Tb and 3d metals, such as Fe and Co. The rare earths are necessary to provide strong spin-orbit coupling ensuring large magnetic hysteresis, while the 3d metals are responsible for high spontaneous magnetization and a significant Curie temperature (Skokov and Gutfleisch, 2018). Nd-Fe-B mangets have extensively penetrated commercial markets, they are widely used for the traction motor in electric vehicles, power generator in wind turbines, manufacture of particularly hard disc drives (HDD), magnetic resonance imaging (MRI) and some other minor applications such as acoustics (Cui et al., 2018). Partial substitution of neodymium by dysprosium or terbium or holmium (2 to 10% of Nd) improves the coercivity of Nd-Fe-B and leads to better thermal stability in high strength permanent magnets. Pr, Gd and

Ce can also be used in place of Nd in the manufacture of permanent magnets, although they produce weaker magnets.

3.4. Chemical

Rare earth oxides have been widely investigated in catalysis as structural and electronic promoters to improve the activity, selectivity and thermal stability of catalysts. Because of their chemical features, they showcase a unique catalytic performance when they are used as active components or as catalyst supports. Catalysis plays a major role in the consumption of rare earth elements, rare earth catalytic materials play and important role in such areas as the petroleum chemical industry, automotive emissions control and the purification of industrial waste air (Zhan et al., 2014).

In petroleum refining, catalysts are used to increase the yield of fuel obtained from the heavier oil fractions by cracking (FCC). Rare earth application in FCC emerged in the early 1960s when zeolites were introduced as cracking catalysts for oil refining. Zeolites are made catalytically more active and thermally more stable at the operating temperatures by replacing the sodium in them with rare earth ions. The use of rare earths can help preserve catalyst effectiveness and increase the yield of the gasoline fractions. Rare earths such as lanthanum and cerium are used in cracking catalysts to refine crude oil into gasoline, distillates, lighter oil products and other fuels (Akah, 2017). However, the use of rare earth in petroleum refining is decreasing since porous zeolite catalysts are used mainly in the production of leaded fuel, which is in the doldrums because of its negative environmental impact.

In recent years, the global automotive industry has developed rapidly and automotive emissions have increased the amount of atmospheric contaminants. Catalytic converters are devices used to convert toxic vehicle emissions to less harmful substances. They are used to convert hydrocarbons, carbon monoxide and nitrogen oxides in the engine exhaust to water, CO_2 and N_2. The catalyst components of a catalytic converter are usually γ-alumina and small amounts of precious metals and are activated by cerium, which is about 5% by weight. Cerium provides oxidation resistance to the mixture, stabilizes rhodium and palladium dispersions and minimizes the interaction of rhodium with alumina.

Besides automotive emissions, SO_x, NO_x and volatile organic compounds (VOCs) from industrial processes are the main atmospheric pollutants. The catalytic oxidation of VOCs has been considered to be the most effective technique for the purification of organic exhaust gas with high concentration. In catalysts for VOC purification, the rare earths can improve catalytic activity and thermal stability, and reduce the noble metal dosage. In the photocatalysts, incorporating rare earths into TiO_2 helps to extend efficiently light absorption

from UV to the visible, which promotes the application of TiO_2 in air purification for indoor conditions of dim and visible light (Zhan et al., 2014).

In the chemical process industry, rare earth elements are hesitantly used as catalysts for ammonia synthesis, alkylation, isomerization, hydrogenation, dehydrogenation, dehydration, polymerization, refining of hydrocarbons and oxidation (Gupta and Krishnamurthy, 2005).

3.5. Metallurgy

Rare earths have major applications as metallurgical alloys. They are used as additives to improve the properties of certain metals. The mischmetal aforementioned is the form in which the rare earths were introduced as constituents in many alloys for a variety of applications. The rare earths are primarily added to alloys to increase their strength at high temperature, improve their resistance to oxidation and/or corrosion and to improve ductility (EURare, 2017).

In the production of nodular iron, REEs are added to cleanse elements that prohibit spherical graphite growth, which avoids the formation of surface cracks and confers ductility to the metal.

The negative effect of sulphur on the mechanical properties of steel leads to a very brittle and fragile metal. Addition of rare earths, as mischmetal, silicides or alloys, captures the sulphur content in the form of very stable compounds such as RE_2S_3 or RE_2S_2O and enhances the ductility of the material (Gupta and Krishnamurthy, 2005).

Rare earth magnesium alloys have the potential to be used as light-weight structural alloys for lightweighting of vehicles, which is key to tackle the global issues of energy conservation and environmental protection. They possess a weakened crystallographic texture that leads to superior ductility over conventional magnesium alloys (Abedini et al., 2017).

In the aluminium manufacture, the addition of rare earths improves its tensile strength, heat resistance, vibration resistance, corrosion resistance and extrudability. Rare earths refine the grain, improve strength, ductility, toughness, weldability, machinability and corrosion resistance in the host alloy. However, the use of rare earths in metallurgy has shown a recent decline, since they are being gradually substituted for less expensive metals such as Mg and Ca (EURare, 2017).

3.6. Ceramics

Rare earth elements are mainly exploited for electronic devices, but far from negligible is their importance in materials for structural applications, which are also useful in modern technologies. Rare earth elements are used to produce three broad types of ceramic: refractory ceramics used in furnace linings, electronic ceramics used to manufacture capacitors and engineering ceramics used in high temperature applications. Yttrium and cerium are the most commonly used REEs in the production of ceramics, although neodymium, gadolinium, samarium and lanthanum are also utilised. The addition of rare earths in ceramics typically improves strength, wear resistance and high temperature performance (EURare, 2017).

Yttrium has a major use in the stabilization of zirconia. The stabilized zirconia (YSZ) is one of the best high temperature, high strength and thermal shock resistant refractory compositions that is stable under oxidation/reduction conditions at elevated temperatures (Gupta and Krishnamurthy, 2005). Due to its unique properties, yttria stabilized zirconia is a multifunctional material with a wide range of applications. These include: ion conductors, solid oxide fuel cells, oxygen and SO_2 sensors, catalysts and thermal barrier coatings (Cousland et al., 2018). An integral part of the emission control system in vehicles is the exhaust oxygen sensor, which is necessary to give information about the exhaust gas composition so that the catalytic converter system operates efficiently. YSZ are also used as oxygen sensors in industrial ovens.

Fuel cells are a promising clean energy technology for vehicle propulsion, auxiliary power and distributed power generation. Solid oxide fuel cells (SOFC's) generate electricity directly from the radiation of a fuel with an oxidant. Electricity is produced electrochemically by passing a hydrogen-rich fuel over the anode and air over the cathode and separating the two by an electrolyte. The only byproducts of the ceramic fuel cells are heat, water and CO_2, thus they are suitable for application in green technologies. Lanthanum, yttrium and cerium oxides along with Ni, Co, Cr or Zn are used as electrodes in fuel cells with zirconia-yttria solid electrolytes (U.S Department of Energy, 2011).

Sm, Eu, Gd and Dy oxides are used as radiation-shielding ceramic compositions in the nuclear industry.

3.7. Batteries

Electrochemical energy storage and conversion systems have received an increasing amount of attention because of the rapid development of portable electronic devices and the requirement for a greener and less energy-intensive transportation industry. Hydrogen is a new kindly energy, which can be stored through small rechargeable nickel-metal hydride (Ni-MH) batteries. Ni-MH

batteries are used in portable tools, consumer electronic and hybrid electric vehicles (HEV). This have essentially replaced nickel-cadmium batteries because of their technological and environmental advantages (Tunsu et al., 2015a). Eight to ten percent rare earth elements exist in the anode of Ni-MH batteries in the form of hydroxide, oxide and pure metal. The REEs include mainly lanthanum, cerium, praseodymium and neodymium. The crystal features of the REEs are related to their ability for hydrogen storage and release (Yang et al., 2014).

3.8. Other uses

Minor amounts of rare earths are used in many other applications, including: microwave devices, shielding in nuclear reactors, magnetic refrigeration, synthetic gemstones, textiles and paints. Microwave and gemstone applications tend to use heavy rare earth elements such as yttrium, gadolinium, erbium and ytterbium, whilst textile and paint industries are reliant on the light rare earth elements such as lanthanum, cerium and neodymium.

Rare earths have found a variety of applications in the nuclear power energy. Gadolinium oxide is used in boiling water reactors as a burnable portion. It is mixed with uranium oxide, because of their similar burn-up rate, to achieve a uniform neutron flux during the lifetime of the fuel element. Gadolinium and dysprosium are also used in neutron radiography, which is a handy tool for aerospace, nuclear and engineering industries. In the neutron radiography, radiation pass through an specimen and the negative is recorded to produce an image of the internal features of the material (Gupta and Krishnamurthy, 2005).

In the paint and pigments industry cerium compounds with aluminium or silicon are used to coat lead chrome paints. Cerium lanthanum and neodymium are added to paint to improve its fading resistance but also to reduce its drying time. In the textile industry, lanthanide caroxylates are used as paint dryers as well.

The REEs are used in some biological applications such as medicines, fertilizers and water treatment. Cerium and neodymium based medicines are used to treat conditions such as motion sickness and thrombosis. Cerium and lanthanum are used in fertilizers to increase crop yield and to remove phosphate during water treatment (EURare, 2017).

4. Sustainability of the Rare Earths Supply

As important strategic mineral resources, REEs have been a hot topic for research in recent years. The uneven distribution and difficulty to substitute rare earths led to studies on their supply and security trends.
The term rare, which gives name to REEs is, in fact, a misnomer, since these elements are widely present in the earths crust. The term refers to the historical

difficulty of identification and refining of REEs, since the challenge of their supply relates to their geological occurrence in high enough ore grades to be mined economically (Habib and Wenzel, 2014). Despite the abundance of more than 200 known REE-bearing minerals, only a few of them such as bastnatite, monazite and xenotime, have enough concentration of REEs to be considered the principal REE mineral ores feasible for the extraction of REMs.
As discussed before, because of their unusual physical and chemical properties, the REEs have become essential raw materials for the development of many high technologies for a wide variety of uses ranging in application from communications and entertainment to petroleum refining, lightning and renewable energies (Smith Stegen, 2015). Along with the growing market of green energy in the next decades, global demand for REEs will increase continuously, which will put great pressure on their current supply chain.

4.1. Rare earths availability

The rare earth elements are relatively abundant in the earth crust, however minable concentrations are less common than for most other ores. Their total crustal abundance is 169 ppm, where LREEs (La to Gd) are 137.8 ppm, far higher than HREEs, which are 31.3 ppm. The abundance of Ce is almost the same as environmentally much more studied elements, such as Cu and Zn. That said, the abundance of a particular element does not always mean ease of exploitation. The feasibility of exploitation typically depends on the geology, grade, tonnage, available processing technologies, costs and associative environmental issues (Baolu; et al., 2017).

The REEs are usually mixed in a variety of minerals such as phosphates, carbonates fluorides and silicates. They do not occur as native elemental metals in nature, only as part of a host mineral and rarely form continuous ore bodies. The rare earth elements are widely distributed all along the Earth. Figure 6 shows the estimated current distribution of the global reserves of REE according to the USGS survey.

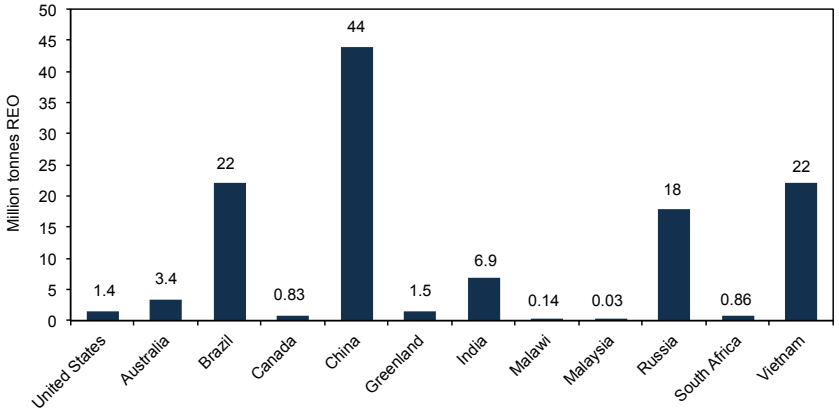

Figure 6. The estimated global distribution of rare earth reserves in 2017, adapted from (U.S. Geological Survey, 2018).

The term reserve is defined by the USGS as *"the part of the reserve base which could be economically extracted or produced at the time of determination"*. By contrast, the reserve base comprises the resources that are economically feasible (reserves) but also marginally economic reserves. As shown in figure 6, China has the largest reserve, which accounts for the 36.3% of the exploitable fraction of REEs, followed by Brazil and Vietnam (18.2% each), and Russia (14.9%). However, the global REE production is mainly carried out in a few countries. Figure 7 displays the estimated current production of REEs according to the USGS survey.

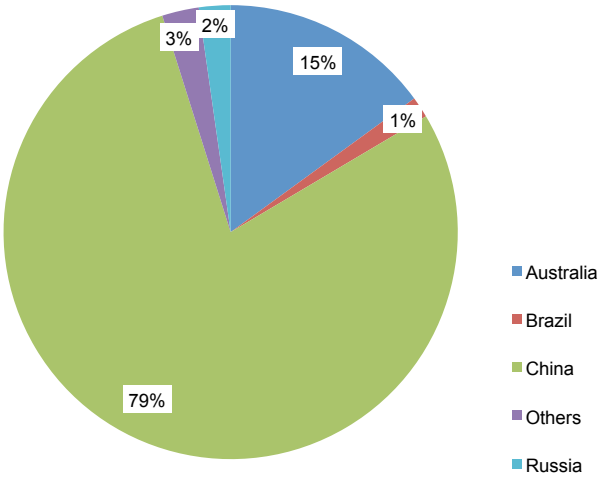

Figure 7. The estimated global production of rare earths in 2017, adapted from (U.S. Geological Survey, 2018). The others section represents the sum of the production estimated for Thailand, Malaysia, Vietnam and India.

The global production of REE in 2017 was 130,000 metric tonnes of REO, which was mainly comprised of China (78%) and Australia (15%), and the remainder distributed among Brazil, Russia, Thailand, Malaysia, Vietnam and India. The fact that China is the leading producer of REEs is not new, it has been the leading producer for decades, since the late 1990s. China's mine production takes place in the provinces of Fujian, Guangdong, Hunan, Jiangxi, Shandong, Sichuan and Yunnan, and in the autonomous regions of Guangxi and Nei Mongol. The largest mining operation is Baotou Rare Earth's Bayan Obo Mine, which produces iron ore as well as bastnasite and monazite. REE-bearing ion-adsorption clays are mined in various locations in the southeastern provinces. Heavy-mineral sands produced in Australia contain significant quantities of REEs, nonetheless, they are not economically exploited to avoid the concentration of naturally occurring radioactive materials. In 2011, Lynas Corporation Ltd. began production of rare-earth mineral concentrates at its Mount Weld carbonatite complex in Western Australia. Currently, Lynas capacity to produce mineral concentrates reaches 20,000 metric tonnes of REO. In Russia, loparite mineral concentrates are produced at the Lovozero

mining operation on the Kola Peninsula, Murmanskaya Oblast. Then, the concentrates are shipped to the Solikamsk magnesium plant. REE-bearing residues from the Solikamsk plant are treated for the recovery of rare earths. The Lovozero operation has the capacity to produce an estimated (Van Gosen et al., 2017). Brazil has the second largest reserve of rare earths in the world, however it only provides an estimated 1% of the global production. In Brazil, rare earths are extracted from the tailings of the niobium produced by the Companhia Brasileira de Metalurgia e Mineração (CBMM) (IPT, 2017). Thailand, Vietnam, India and Malaysia altogether account for the 3% global production of REEs. Monazite and xenotime are recovered from cassiterite mine tailings in the Malaysian states of Perak and Selangor. In India, REEs are produced from monazite contained in heavy-mineral sands by the Rare Earth Division of Indian Rare Earths Ltd. (IREL) and Kerala Minerals and Metals Ltd. (KMML) (Van Gosen et al., 2017).

Although a few countries domain the REEs global production, since the boom of rare earth market, investing in rare earth industry has been the hotspot. There are a lot of active projects on rare earth exploration, under preparation and exploitation, and some of them are promising to be the competitors of future supply of these elements (Chen, 2011). Figure 8 presents the distribution of the global locations of REE active mines and promising advanced exploration projects.

Figure 8. World map showing locations of active REE mines and advanced exploration projects in development in 2015 (Van Gosen et al., 2017).

The exploration projects are being evaluated to determine if they are economic to develop. For instance, in the United States, exploration and development assessment projects include Mountain Pass, California; Bokan Mountain, Alaska; La Paz, Arizona; Diamond Creek, Idaho; Lemhi Pass in Idaho and Montana; Pea Ridge, Missouri; Elk Creek, Nebraska; Thor Mine, Nevada; Round Top, Texas; and Bear Lodge, Wyoming (Van Gosen et al., 2017). Currently there are no REE producing mines in Europe, thus the European REE market begins at the stage of REE separation from mixed REE compounds (EURare, 2017).

Tables 3 and 4 are meant to give additional information about the deposits shown in Figure 8. In the tables, the hyphen express that the information is not reported.

Table 3. Active rare earth mines by deposit type (Van Gosen et al., 2017).

Deposit	Location	Reported resource (million tonnes)	REE grade (%wt)	Comment
Carbonatites				
Bayan Obo	Nei Mongol Autonomous Region, China	800.0	6.0	Estimated resource in the total deposit, not divided
Daluxiang	Sichuan, China	15.2	5.0	About 0.76 Mt (estimated) of REOs
Maoniuping	Sichuan, China	50.2	2.9	REO content of reserves is estimated to be more than 1.45 Mt
Weishan	Shandong, China	-	-	
Mountain Pass	California, United States	16.7	8.0	
Mount Weld	Western Australia, Australia	23.9	7.9	
Peralkaline igneous				
Karnasurt Mountain, Lovozero deposit	Northern region, Russia	-	-	Loparite concentrate contains 30 - 35 % REO
Heavy-mineral sand deposits				
Buena Norte mining district	East coast of Brazil	-	-	Historic and active producer of REEs from monazite in coastal sands
Ion-adsorption clay deposits				
Dong Pao Mine	Vietnam	-	-	Mine is reportedly in a late stage of development. Laterite clays overlie syenite intrusions
South China clay deposits	Jianxi, Hunan, Fujian, Guangdong and Guangxi Provinces, southern China	-	About 0.05 to 0.4	Numerous small mines. Little ore information is available. Best source of data may be Chi and Tian

Table 4. Advanced rare earth element exploration projects (Van Gosen et al., 2017).

Deposit	Location	Reported resources
Carbonatites		
Araxá	Minas Gerais, Brazil	Measured and indicated resources = 6.3 Mt at 5.0 % TREO; inferred resources = 21.9 Mt at 4.0 % TREO
Ashram project (formerly Eldor project)	Quebec, Canada	Measured resources = 1.6 Mt at 1.8 % TREO; indicated resources = 27.7 Mt at 1.9 % TREO; inferred resources = 219.8 Mt at 1.9 % TREO
Bear Lodge	Wyoming, United States	Measured and indicated resources = 16.3 Mt at 3.1 % TREO; inferred resources = 28.9 Mt at 2.6 % TREO
Cummins Range	Western Australia, Australia	inferred resources = 49.0 Mt at 1.7 % TREO
Elk Creek	Nebraska, United States	indicated resources = 80.5 Mt at 0.7 % Nb oxide; inferred resources = 99.6 Mt at 0.6 % Nb oxide; REE resources exist, but are not estimated
Glenover project	South Africa	indicated resources = 16.8 Mt at 1.5 % TREO; inferred resources = 12.1 Mt at 1.0 % TREO
Lavergne-Springer property	Ontario, Canada	indicated resources = 4.2 Mt at 1.1 % TREO; inferred resources = 12.7 Mt at 1.2 % TREO
Lofdal project	Namibia	indicated resources = 0.9 Mt at 0.6 % TREO; inferred resources = 0.8 Mt at 0.6 % TREO
Montviel project	Quebec, Canada	indicated resources = 82.4 Mt at 1.5 % TREO; inferred resources = 184.2 Mt at 1.4 % TREO
Mrima Hill	Kenya	Measured and indicated resources = 48.7 Mt at 4.4 % TREO; inferred resources = 110.7 Mt at 3.6 % TREO
Ngualla	Tanzania	Measured resources = 81.0 Mt at 2.7 % TREO; indicated resources = 94.0 Mt at 2.0 % TREO; inferred resources = 20.0 Mt at 1.8 % TREO
Nolans Bore	Northern Territory, Australia	Measured resources = 4.3 Mt at 3.3 % TREO; indicated resources = 21.0 Mt at 2.6 % TREO; inferred resources = 22.0 Mt at 2.4 % TREO
Sarfartoq	Greenland	indicated resources = 5.9 Mt at 1.8 % TREO; inferred resources = 2.5 Mt at 1.6 % TREO
Songwe Hill	Malawi	indicated resources = 6.2 Mt at 2.1 % TREO; inferred resources = 5.1 Mt at 1.8 % TREO
Wigu Hill	Tanzania	inferred resources = 3.3 Mt at 2.6 % TREO
Zandkopsdrift	South Africa	Measured resources = 23.0 Mt at 2.1 % TREO; indicated resources = 22.7 Mt at 1.8 % TREO; inferred resources = 1.1 Mt at 1.5 % TREO
Peralkaline igneous		

Bokan Mountain	Alaska, United States	Indicated resources for the Dotson Ridge deposit = 4.8 Mt at 0.6 % TREO; inferred resources = 1.1 Mt at 0.6 % TREO
Clay-Howells project	Ontario, Canada	inferred resources = 8.5 Mt at 0.7 % TREO
Dubbo Zirconia	New South Wales, Australia	Indicated resources = 35.7 Mt at 1.0 % TREO; inferred resources = 37.5 Mt at 0.8 % TREO
Foxtrot project	Newfoundland and Labrador, Canada	Indicated resources = 3.4 Mt at 1.1 % TREO; inferred resources = 5.9 Mt at 1.0 % TREO
Hastings project	Western Australia, Australia	Indicated resources = 27.0 Mt at 0.2 % TREO; additionally, 0.9 % Zr oxide and 0.4 % Nb oxide; inferred resources = 9.1 Mt at 0.2 % TREO
Hoidas Lake deposit	Saskatchewan, Canada	Measured resources = 1.0 Mt at 2.6 % TREO; indicated resources = 1.6 Mt at 2.4 % TREO; inferred resources = 0.3 Mt at 2.1 % TREO
Ilimaussaq complex, Kvenfjeld deposit	Greenland	Indicated resources = 437.0 Mt at 1.1 % TREO; inferred resources = 182.0 Mt at 1.0 % TREO
Ilimaussaq complex, Sørensen deposit	Greenland	Inferred resources = 242.0 Mt at 1.1 % TREO
Ilimaussaq complex, Zone 3 deposit	Greenland	Inferred resources = 95.0 Mt at 1.2 % TREO
Kipawa	Quebec, Canada	Indicated resources = 12.5 Mt at 0.5 % TREO; inferred resources = 3.8 Mt at 0.5 % TREO
Kutessay II project	Kyrgyzstan	Measured resources = 13.5 Mt at 0.3 % TREO; indicated resources = 2.7 Mt at 0.2 % TREO; inferred resources = 1.7 Mt at 0.2 % TREO
Nechalacho project (Thor Lake)	Northwest Territories, Canada	Measured resources = 12.6 Mt at 1.7 % TREO; indicated resources = 96.5 Mt at 1.6 % TREO; inferred resources = 160.3 Mt at 1.4 % TREO
Norra Kärr	Southern Sweden	Inferred resources = 60.5 Mt at 0.5 % TREO
Round Top	Texas, United States	Measured and indicated resources = 480.0 Mt at 0.1 % TREO; inferred resources = 342.0 Mt at 0.1 % TREO
Strange Lake	Quebec, and New foundland and Labrador, Canada	Indicated resources = 278.1 Mt at 1.0 % TREO; inferred resources = 214.4 Mt at 0.9 % TREO
TRE project	Northern Madagascar	Deposits include upper wethered bedrock of peralkaline intrusive complex and overlying argillaceous laterites (saprolite); inferred resources = 130 Mt at 0.1% TREO
Two Tom	Newfoundland and Labrador, Canada	Inferred resources = 41 Mt at 1.2 % TREO
Polymetallic deposits		
Eco Ridge Mine	Ontairo, Canada	Indicated resources = 22.7 Mt at 0.2 % TREO; inferred resources = 36.6 Mt at 0.2 % TREO
Milo project	Queensland, Australia	Inferred resources = 187.0 Mt at 0.1 % TREO; deposit contains REEs, Cu, Mo, Au, Ag and U
Plant in Stepnogorsk	Northern Kazakhstan	Resources and grade are not reported. Plant is being designed to extract Dy from uranium tailings

Steenkampskraal	South Africa	Measured resources = 85.0 Mt at 19.5 % TREO; indicated resources = 474.0 Mt at 14.1 % TREO; inferred resources = 60.0 Mt at 10.5 % TREO
Heavy-mineral sand deposists		
Charley Creek deposits	Northern Territory, Australia	Alluvial placers with I resources algon with monazite and xenotime; inferred total resources of 805.3 Mt at 0.03% TREO
Canakli deposit	Turkey	Inferred resource = 494.0 Mt at 0.1 % TREO
Kerala deposits	India	Total resources of 1.5 Mt of monazite reported in heavy-mineral sand deposits in the State of Kerala; resource grade is not reported

All things considered, the availability of REEs appears to be at risk based on a number of factors. First and foremost, as observed, one country monopolizes the current supply and production of these elements. Currently, China has almost the 80% of the market share although the country possesses less than a half of the global reserves. Until the mid-1980s, the Mountain Pass mine in California produced 60% of the world's rare earths. However, the Mountain Pass mine closed in 2002 partly because of the environmental problems and partly because it could not compete against China's lower-priced rare earths. Consequently, since then, China became the main global REE supplier. Nonetheless, in late 2000s China started decreasing its annual export quotas, which led to tremendous price increases and concerned importers around the world. As stated, due to the introduction of export quota, the world market experienced dramatic increase of prices. For instance, the Nd price increased from \$10 kg^{-1} in 2001 to \$350 kg^{-1} in 2011 (Habib and Wenzel, 2014). The Chinese government justified its restrictive decision by referencing an alleged concern about future supplies for its own industries, despite the country's substantial reserves. Chinese officials have also admitted that the quota restrictions are, in a certain sense, linked to the Chinese government's ambition to attract more end-use manufacturing industries: if manufacturers cannot be certain of Chinese exports of rare earths, then they might move their factories to China (Smith Stegen, 2015).

Another contributor to supply risk for REEs is the fact that they are found together in geological deposits, rendering mining of individual elements economically inefficient. Their similar chemical properties also translate into separation and purification difficulties.

Yet another factor to bear in mind is the REEs difficult and controversial mining conditions. The production of REEs is often associated with environmental issues. Mining, leaching, pre-concentration and the numerous separation stages needed to achieve the degrees of purity required in certain applications,

often lead to high amounts of secondary waste, which further increase their supply risk (Alonso et al., 2012; Tunsu et al., 2015a).
Finally, the REEs high demand, which is rapidly increasing due to the large variety of applications where they are used, some of which need very high specificity as previously outlined.

Regarding the aforementioned aspects, the rare earth elements are presently regarded as being among the most critical chemical elements. In 2010 the European Commission declared the REEs to have the highest supply risk among 41 different raw materials. The list was updated in 2014 and it was concluded that HREEs are the most critical followed by LREEs (European Comission, 2014a). The report reviewed the supply status of several raw materials fundamental for Europe's economy. The EU methodology, used to assess criticality, has a combination of two components: economic importance and supply risk. Similarly, in 2011 the U.S. Department of Energy (DOE) defined a medium-term criticality matrix, where neodymium, europium, terbium, dysprosium and yttrium were considered the five most critical REEs. Other elements such as cerium, indium, lanthanum and tellurium were found to be near critical. Figure 9 displays the DOE medium term critically matrix, which was intended to forecast the criticality of several elements from 2015 to 2025.

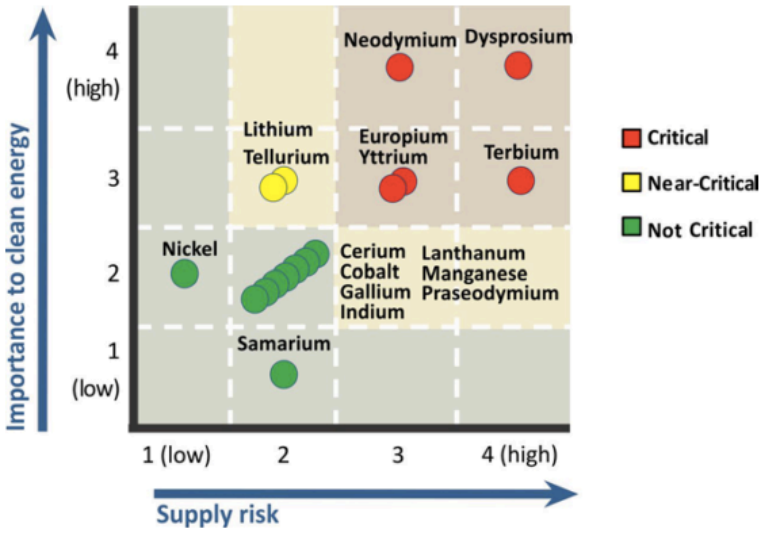

Figure 9. Medium-term (2015 – 2025) criticality matrix (U.S Department of Energy, 2011).

In order to tackle the increasing demand and current monopolistic market for REEs in the future, many authorities, companies and research groups have started focusing on recycling of REEs (Habib and Wenzel, 2014). Recycling of REEs from end-of-life products has gained a lot of attention in recent years due to the geopolitical nature of supply risk faced globally. Although recycling is not expected to meet the forecasted demand in the future, there are high hopes for

it to be able to balance the demand better on the longer term, when combined with virgin mining.

5. Rare earth sources

As mentioned before, contrary to received wisdom because of their historical name, the rare earth elements are relative abundant in Earth's crust. They occur naturally in many economically viable ore deposits throughout the world (Baolu; et al., 2017). Figure 10 shows the abundance of REEs compared to some well-known metals such as Cu, Zn, Ni, Sn and Pb. Due to their similar chemical properties such as their ionic radii, and valences REEs are often found altogether in the same minerals, where they are intimately mixed.

Among the rare earths, the relative abundance varies widely. Light rare earths are more concentrated in the continental crust than heavy rare earths because of their larger ionic radii, which makes them more incompatible. Thus, lanthanum, cerium, praseodymium and neodymium are the most abundant rare earths whilst thulium is the least abundant.

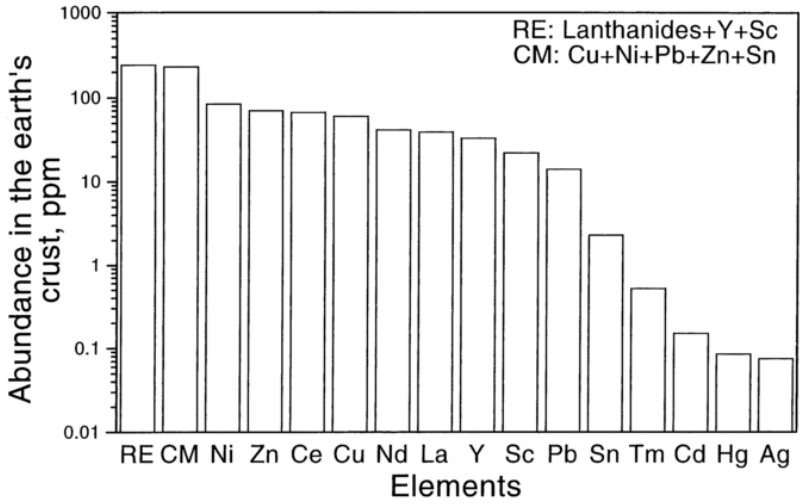

Figure 10. Natural abundance of rare earth elements and a few well-known metals (Gupta and Krishnamurthy, 2005).

The rapid progress in electronic manufacturing technologies has led to the generation of large number of end-of-life products and industrial waste containing rare earth elements. This has opened a new venue for the supply of REEs through recycling. Processing these streams for the recovery of REEs they contain can provide a secondary source of metals, alongside virgin mining although recycling cannot entirely replace mining and the production of metals from natural primary sources (Tunsu et al., 2015a). The following subsections of the manuscript discuss the most important primary and secondary sources of rare earth elements.

5.1. Primary sources: Natural occurrence, minerals and ores

Primary REE deposits are those formed by natural geological processes, including high-temperature processes, such as magmatism and hydrothermal activity; and low-temperature processes operating at the earth's surface, such as wathering, erosion and sedimentation (EURare, 2017). Minerals containing REEs are divided into groups depending upon their content of rare earths. They may be identified as cerium or yttrium type minerals based on whether the distribution of the lanthanides in the mineral is part of the light or heavy rare earth subgroups (Jordens et al., 2013). Bastnasite, monazite and xenotime are the three most frequently extracted rare earth minerals. Nonetheless, there are other sources such as ion-absorbed clays, which are also a significant source of HREEs mainly (Kumar Jha et al., 2016).

5.1.1. Bastnasite

Bastnasite is a fluorocarbonate mineral containing approximately 70% rare earth oxide that is primarily Ce, La, Pr and Nd (approximately 97.95% of total REOs). Its general formula is $Ce(CO_3)F$. It would be considered a selective, cerium type mineral although these classifications are not absolute due to the interchangeable nature of the lanthanide elements (Jordens et al., 2013). Of the HREEs, only Y is regularly found. Bastnasite originates in vein deposits, metamorphic zones and igneous carbonatites deposits. Major ore deposits are generally related to carbonatite intrusions. Carbonatites are often related to alkaline intrusives.

5.1.2. Monazite

Monazite is a phosphate mineral with the generalized chemical formula $CePO_4$. Its rare earth content is approximately 70% REO that is, similarly to bastnasite, primarily Ce, La, Pr and Nd (between 83.55% and 94.5% of total REO). It is considered to be a selective cerium type material, nonetheless unlike bastnasite, monazite also includes 4 to 12% thorium and small amounts of uranium(Jordens et al., 2013). It occurs generally as a minor mineral in granites and granodiorites and associated pegmatites, and also occurs in many metamorphic rocks and beach sands. It concentrates after weathering of the igneous or metamorphic host rock since it is a heavy mineral (5.15 average specific gravity) very resistant to weathering. The most important monazite resources for extraction are the beach sands.

5.1.3. Xenotime

Xenotime is an yttrium phosphate mineral with a REO content of 67% approximately, which is primarily HREEs. Unlike the bastnasite and monazite, xenotime has much smaller LREEs concentrations (around 8.4%). Xenotime is

typically found alongside monazite in 0.5 – 5.0% concentrations, it is commonly a by-product of monazite processing and so its processing follows a similar path to that of monazite (Jordens et al., 2013). Notwithstanding its oddity, xenotime is a major source of heavy rare earth elements along with ion absorbed bearing clays (Gupta and Krishnamurthy, 2005).

5.1.4. Ion-absorbed clays

Ion absorbed clays are an important source of HREEs since they have up to 60% yttrium group elements (HREEs) in their ionic state. The composition of ion-absorbed ores depends on location, but typically they are rich in Y, Eu, Sm and Gd. This ore is formed by the leaching of rare earth from seemingly rich primary rocks (granite or volcanic), followed by adsorption of soluble rare earth species on clays. Mild, humid and rainy climates facilitate these processes to occur (Gupta and Krishnamurthy, 2005).

5.1.5. Minor sources

There are many other minerals that contain REEs, however these are typically small-scale, unique operations. REE-bearing minerals are quite complex. Table 5 summarizes the REE-rich minerals currently known.

Table 5. Natural occurring minerals containing REEs, thorium and uranium. Adapted from (Jordens et al., 2013; Kumar Jha et al., 2016; Long et al., 2010).

[In the table, minerals in bold are the ones that have been exploited for the recovery of REEs. The hyphen in the content columns means the information is not available]

Metal name	Chemical formula	Content (weight percent)		
		REO	ThO2	UO2
Carbonates				
Acnylite (Ce)	$Sr(Ce,La)(CO_3)OH{\cdot}H_2O$	46-53	0-0.4	0.1
Acnylite (La)	$Sr(Ce,La)(CO_3)OH{\cdot}H_2O$	46-53	0-0.4	0.1
Bastnasite (Ce)	**$(Ce,La)(CO_3)F$**	**70-74**	**0-0.3**	**0.09**
Bastnasite (La)	**$(Ce,La)(CO_3)F$**	**70-74**	**0-0.3**	**0.09**
Bastnasite (Y)	**$Y(CO_3)F$**	**70-74**	**0-0.3**	**0.09**
Calcio-ancylite (Ce)	$(Ca,Sr)Ce_3(CO_3)_4(OH)_3{\cdot}H_2O$	60	-	-
Calcio-ancylite (Nd)	$Ca(Nd,Ce,Gd,Y)_3(CO_3)_4(OH)_3{\cdot}H_2O$	60	-	-
Doverite	$YCaF(CO_3)_2$	-	-	-
Parisite (Ce)	$Ca(Ce,La)_2(CO_3)_3F_2$	59	0-0.5	0-0.3
Parisite (Nd)	$Ca(Nd,Ce)_2(CO_3)_3F_2$	-	-	-
Synchysite (Ce)	$Ca(Ce,La)(CO_3)_2F$	49-52	1.6	-
Synchysite (Nd)	$Ca(Nd,La)(CO_3)_2F$	-	-	-
Synchysite (Y) (doverite)	$Ca(Y,Ce)(CO_3)_2F$	-	-	-
Halides				
Fluocerite (Ce)	$(Ce,La)F_3$	-	-	-
Fluocerite (La)	$(La,Ce)F_3$	-	-	-

Fluorite	$(Ca,REE)F_2$	-	-	-
Gagarinite (Y)	NaCaY(F,Cl)	-	-	-
Pyrochlore	$(Ca,Na,REE)_2Nb_2O_6(OH,F)$	-	-	-
Yttrofluorite	$(Ca,Y)F_2$	-	-	-
Oxides				
Anatase	$(Ti, REE)O_2$	-	-	-
Brannerite	$(U,Ca,Y,Ce)(Ti,Fe)_2O_6$	-	-	-
Cerianite (Ce)	$(Ce^{4+},Th)O_2$	-	-	-
Euxenite (Y)	$(Y,Ca,Ce,U,Th)(Nb,Ta,Ti)_2O_6$	-	-	-
Fergusonite (Ce)	$(Ce,La,Y)NbO_4$	-	-	-
Fergusonite (Nd)	$(Nd,Ce)(Nb,Ti)O_4$	-	-	-
Fergusonite (Y)	$YNbO_4$	-	-	-
Loparite (Ce)	$(Ce,Na,Ca)(Ti,Nb,)O_3$	-	-	-
Perovskite	$(Ca,REE)TiO_3$	<37	0-2	0-0.05
Samarskite	$(REE,Fe^{2+},Fe^{3+},U,Th,Ca)(Nb,Ta,Ti)O_4$	-	-	-
Uraninite	$(U,Th,Ce)O_2$	-	-	-
Phosphates				
Britholite (Ce)	$(Ce,Ca)_5(SiO_4,PO_4)_3(OH,F)$	56	1.5	-
Britholite (Y)	$(Y,Ca)_5(SiO_4,PO_4)_3(OH,F)$	56	1.5	-
Brockite	$(Ca,Th,Ce)(PO_4)\cdot H_2O$	-	-	-
Chevkinite (Ce)	$(Ca,Ce,Th)_4(Fe^{2+},Mg)_2(Ti,Fe_{3+})_3Si_4O_{22}$	-	-	-
Churchite (Y)	$YPO_4\cdot H_2O$	-	-	-
Crandallite	$CaAl_3(PO_4)_2(OH)_5\cdot H_2O$	-	-	-
Florencite (Ce)	$CaAl_3(PO_4)_2(OH)_6$	-	1.4	-
Florecnite (La)	$(La,Ce)Al_3(PO_4)_2(OH)_6$	-	1.4	-
Florencite (La)	$(Nd,Ce)Al_3(PO_4)_2(OH)_6$	-	1.4	-
Fluorapatite	$(Ca,Ce)_5(PO_4)_3F$	-	-	-
Gorceixite	$(Ba,REE)Al_3[(PO_4)_2(OH)_5]\cdot H_2O$	-	-	-
Goyazite	$SrAl_3(PO_4)_2(OH)_5\cdot H_2O$	-	-	-
Monazite (Ce)	**$(Ce,La,Nd,Th)PO_4$**	**35-71**	**0-20**	**0-16**
Monazite (La)	**$(La,Ce,Nd,Th)PO_4$**	**35-71**	**0-20**	**0-16**
Monazite (Nd)	**$(Nd,Ce,La,Th)PO_4$**	**35-71**	**0-20**	**0-16**
Rhabdophane (Ce)	$(Ce,La)PO_4\cdot H_2O$	-	-	-
Rhabdophane (La)	$(La,Ce)PO_4\cdot H_2O$	-	-	-
Rhabdophane (Nd)	$(Nd,Ce,La)PO_4\cdot H_2O$	-	-	-
Vitusite (Ce)	$Na_3(Ce,La,Nd)(PO_4)_2$	-	-	-
Xenotime (Y)	**YPO_4**	**52-67**	**-**	**0-5**
Silicates				
Allanite (Ce)	$(Ce,Ca,Y)_2(Al,Fe^{2+},Fe^{3+})_3(SiO_4)_3(OH)$	3-51	0-3	-
Allanite (Y)	$(Y,Ce,Ca)_2(Al,Fe^{3+})_3(SiO_4)_3(OH)$	3-51	0-3	-
Cerite (Ce)	$Ce_9Fe^{3+}(SiO_2)_6[(SiO_3(OH)](OH)_3$	-	-	-
Cheralite (Ce)	$(Ca,Ce,Th)(P,Si)O_4$	-	<30	-
Eudialyte	$Na_4(Ca,Ce)_2(Fe^{2+},Mn^{2+},Y)ZrSi_8O_{22}(OH,Cl)_2$	1-10	-	-
Gadolinite (Ce)	$(Ce,La,Nd,Y)_2Fe^{2+}Be_2Si_2O_{10}$	-	-	-
Gadolinite (Y)	$Y_2Fe^{2+}Be_2Si_2O_{10}$	-	-	-
Gerenite (Y)	$(Ca,Na)_2(Y,REE)_3Si_6O_{18}\cdot 2H_2O$	-	-	-

Hingganite (Ce)	$(Ce,Y)_2Be_2Si_2O_8(OH)_2$	-	-	-
Hingganite (Y)	$(Y,Yb,Er)_2Be_2Si_2O_8(OH)_2$	-	-	-
Hingganite (Yb)	$(Yb,Y)_2Be_2Si_2O_8(OH)_2$	-	-	-
Iimoriite (Y)	$Y_2(SiO_4)(CO_3)$	-	-	-
Kainosite (Y)	$Ca_2(Y,Ce)_2Si_4O_{12}(CO_3)\cdot H_2O$	-	-	-
Rinkite (rinkolite)	$(Ca,Ce)_4Na(Na,Ca)_2Ti(Si_2O_7)_2F_2(O,F)_2$	-	-	-
Sphene (titanite)	$(Ca,REE)TiSiO_5$	<3	-	-
Steenstrupine (Ce)	$Na_{14}Ce_6Mn_2Fe_2(Zr,Th)(Si_6O_{18})(PO_4)_7\cdot 3H_2O$	-	-	-
Thalenite (Y)	$Y_3Si_3O_{10}(F,OH)$	-	-	-
Thorite	$(Th,U)SiO_4$	<3	-	10-16
Zircon	$(Zr,REE)SiO_4$	-	0.1-0.8	-

All things considered, as aforementioned, the relative proportion of rare earth elements in the bearing minerals is variable. As shown in table 6, the deposits are normally rather enriched in the LREEs compared to the depleted HREEs proportion. Nonetheless, a few deposits mostly containing xenotime and ion-absorbed clays as principal REE ores are somewhat HREEs enriched.

Table 6. Rare earth elements distribution in selected deposits. Adapted from (Jordens et al., 2013; Long et al., 2010).

Element	**Bastnasite** Mountain Pass, USA	**Bastnasite** Bayan Obo, China	**Monazite** Green Cove Spring, USA	**Xenotime** Lehat, Malaysia	**High Y REE clay** Longnan, China	**Low Y REE clay** Xunwu, China
La (%)	33.8	23	17.5	1.2	1.8	43.3
Ce (%)	49.6	50.0	43.7	3.1	0.4	2.4
Pr (%)	4.1	6.2	5.0	0.5	0.7	7.1
Nd (%)	11.2	18.5	17.5	1.6	3.0	30.2
Sm (%)	0.9	0.8	4.9	1.1	2.8	3.9
Eu (%)	0.1	0.2	0.2	trace	0.1	0.5
Gd (%)	0.2	0.7	6.0	3.5	6.9	4.2
Tb (%)	-	0.1	0.3	0.9	1.3	trace
Dy (%)	-	0.1	0.9	8.3	7.5	trace
Ho (%)	-	trace	0.1	2.0	1.6	trace
Er (%)	-	trace	trace	6.4	4.9	trace
Tm (%)	-	trace	trace	1.1	0.7	trace
Yb (%)	-	trace	0.1	6.8	2.5	0.3
Lu (%)	trace	trace	trace	1.0	0.4	0.1
Y (%)	0.1	trace	2.5	61.0	65.0	8.0

5.2. Secondary sources: Urban mining

The transition from a linear to a circular approach when it comes to mining has characterised waste management strategies over recent decades. The increasing amount of end-of-life products, pre-consumer scrap and industrial

residues REE-enriched, linked to the expanding demand of the REEs has led to a growing interest in the recycling of these elements from secondary sources. The management of anthropogenic resources stocks and waste, in the view of long-term environmental protection, resource conservation, and economic benefits is commonly known as urban mining (Cossu and Bonifazi, 2013). Construction and demolition waste, combustion residues, sludges, exhausted oils, previously landfilled waste and industrial residues, among others, are considered urban mining targets (Tunsu et al., 2015a). Urban mining of REEs can reduce the environmental challenges associated with their virgin mining and processing, and it can also prevent some extent excessive mining by providing a new source in addition to natural deposits.

As previously mentioned, the streams viewed as potential targets for the recovery of rare earth metals are divided as follows: pre-consumer production scrap, end-of-life products, already landfilled streams and residues and by-products generated during REE processing. Because of the soaring application of REEs, the large amounts of REE-based products ensure the availability of secondary sources for many years. Research on the recycling of rare earths is typically directed towards three categories of end-of-life products: phosphors, permanent magnets and NiMH batteries.

5.2.1. Phosphor-based products

Products containing phosphors suitable enough for recovery of REEs are fluorescent lamps, LED lamps, CRTs and plasma screens. These products are mainly sources of yttrium and europium although they contain minor amounts of cerium, lanthanum, terbium or gadolinium. The rare earths content relies on application and can vary from one manufacturer to another. The generic chemical composition of pure tri-band phosphors in a fluorescent powder is given in table 7. As can be seen, yttrium is the major rare earth in lamp phosphors and the same applies to CRT phosphors.

Table 7. Chemical composition of some pure tri-band phosphors in a fluorescent lamp. Adapted from (Tunsu et al., 2015a).

Phosphor	Formula	Element content (%)							
		O	Y	Eu	Al	Mg	Ba	Ce	Tb
Red	$Y_2O_3:Eu^{3+}$	17.5	67.2	6.5					
Green	$CeMgAl_{10}O_{17}:Tb^{3+}$	42.6			31.3	5.7		9.5	5.3
Blue	$BaMgAl_{10}O_{17}:Eu^{2+}$	42.3		1.9	32.4	2.7	12.4		

A fluorescent lamp by weight consists of 88% glass, 5% metals, 4% plastic, 3% powder phosphors and 0.005% mercury. After crushing and sieving the lamps, the composition of the phosphor powder is generally 45% halophosphate

phosphor, 20 to 30% glass and silica, 12% alumina, 10 to 20% rare earth phosphors and 5% some other residual fractions. The resulting phosphor powder is either re-used directly in new lamps or processed for the recovery of REEs (Kumar Jha et al., 2016).

Compared to the recycling of phosphors from fluorescent lamps, relatively little research efforts have been devoted to the recycling of phosphors from cathode ray tubes (Binnemans et al., 2013). CRTs were one of the major components of monitors and televisions in the past. Nonetheless, because of the technological progress CRT have been replaced by LCDs and LEDs, which has led to the generation of a large amount of obsolete televisions and computer monitors year after year. CRT devices generally contain 1 to 7g of rare earth phosphors and so they constitute a source to thoroughly consider for REEs recovery (Yin et al., 2018).

5.2.2. Permanent magnets

The most common REE magnets are based upon neodymium-iron-boron (NdFeB). These magnets are primarily based on neodymium but they also contain minor amounts of dysprosium, praseodymium, gadolinium or terbium (Binnemans et al., 2013). Rare earths are generally recovered from three different magnet materials: metal scraps generated during magnet manufacturing, small magnets from end-of-life products and large magnets from hybrid vehicles and wind turbines (Kumar Jha et al., 2016). Hard disk drives (HDD) are regarded as an important source of REEs because of their intensive use. Taking into account the useful life of a hard disc, which is typically 5 years, the availability of end-of-life HDD for the recovery of rare earths seems to be guaranteed in the near future.

As in fluorescent lamps, the REEs content in the magnets varies depending on application needs and even among manufacturers. Table 8 lists REEs content in three different types of NdFeB magnets.

Table 8. Chemical composition of some Neodymium-iron-boron magnets. Adapted from (Tunsu et al., 2015a).

NdFeB magnet	Element composition (% wt.)						
	Co	Fe	Nd	Pr	Dy	B	Others
a		69	25		4	1	1
b		65 - 70	30		3	1	1
c	4.22	58.16	25.95	0.34	4.21	1	6.12

As already stated, dysprosium is sometimes added to magnets in order to increase their temperature stability against demagnetization, thus Dy content in

NdFeB magnets widely changes depending on the application (Binnemans et al., 2013).

5.2.3. NiMH batteries

Many electronic devices are powered by rechargeable batteries. One of the most effective rechargeable battery types is the nickel metal hydride battery (NiMH). NiMH batteries have replaced Ni-Cd batteries in many devices because of their better performance and lower environmental impact. They are mainly used in rechargeable AA and AAA batteries typically consumed in domestic applications and hybrid electric vehicles (HEVs). Generally, NiMH batteries have a lifespan of two years, resulting in the wastage of a large quantity of these batteries per year. With a finite lifetime for the batteries, recycling is key to recover their valuable inherent materials (Larsson et al., 2013a; Yang et al., 2014). Rare earth elements exist primarily in the anode of NiMH batteries in the form of hydroxide, oxide and pure metal (Assumpçao et al., 2009).

The chemistry of the batteries varies among manufacturers and types of batteries. Generic distribution of elements in different NiMH batteries is given in table 9.

Table 9. Chemical composition of different types of NiMH batteries. Adapted from (Tunsu et al., 2015a).

Application		Elemental composition (% wt.)													
		La	Ce	Nd	Pr	Y	Ni	Fe	Co	Al	K	Mn	C	Plastics	Others
Portable batteries	Button cells		6 - 8				29 - 39	31 - 47	2 - 3		1 - 2		2 - 3	1 - 2	2 - 3
	Prismatic cells		8 - 10				36 - 42	22 - 25	3 - 4		1 - 2		<1	3 - 4	2 - 3
	Cylidrical cells		7 - 8				38 - 40	6 - 9	2 - 3		3 - 4		<1	16 - 19	3 - 4
HEV batteries	Cathode					0.9	64.7		5.7	0.1	0.2	0.2			0.8
	Anode	20.2	7.4	2.4	1	0.7	52.3	0.1	3.6	1.5	0.4	5.6			

As shown, a typical portable NiMH battery contains 7% REEs, which accounts for 1g REEs per AAA battery. The fact that REEs in a HEV battery are present mostly in the negative electrode is a huge benefit since it considerably facilitates their separation and recovery. Up to 2 kg REEs can be obtained from a HEV battery.

6. Processing of primary resources

Beneficiation is the term used for the processing of the raw ore to remove gangue minerals, producing an REE concentrate that can be further processed. Many beneficiation methods are used depending on the deposit and the features of the bearing mineral such as grain size, mineralogy and texture. The form and location of the orebody determines whether REE ores should be

mined from the surface (open pit) or the underground. Chemical and physical processes are needed to convert the as-mined ore to a compound that is either an end product by itself or an intermediate for production of metals, alloys or other compounds (Gupta and Krishnamurthy, 2005). Chemical processing of the concentrated ore obtained after beneficiation usually involves hydrometallurgical and sometimes pyrometallurgical techniques.

This section incorporates a detailed account of the techniques for the processing of the rare earth primary sources, as well as an overview of the most commonly used individual rare earths separation procedures.

6.1. Processing of primary sources: beneficiation, extraction and concentration

The actual REEs mining process flowsheets are quite varied and tailored to the gangue and host ores. To extract rare earths, further processing/extraction and refining are required. The major factors to bear in mind regarding the selection of treatment processes are the type and nature of the deposit, its complexity and the presence of other valuable gangue minerals.
Initial step for ore processing generally involves beneficiation, which does not affect its chemical composition, but helps in liberation of the mineral from the host material. Many physical techniques such as gravity separation, flotation and electrostatic and magnetic separation are used in the beneficiation of rare earths. From there, different thermal and chemical reactions, mainly using hydrometallurgical techniques, transform the concentrated mineral into more valuable chemical forms (Kumar Jha et al., 2016).

6.1.1. Beneficiation operations: physical treatment

The following subsections of this chapter deal with theoretical aspects of the most widespread physical REM separation techniques, including gravity separation, magnetic separation, electrostatic separation and flotation.

6.1.1.1. Gravity separation

Gravity separations take profit of the differences in the specific gravity of minerals to achieve separation. It may be regarded as a form of particle classification. The settling speed of different materials in a fluid medium is determined by interaction of three different forces: gravity, buoyancy and fluid drag. Gravity separation involves the separation of minerals of different specific gravity by their relative movement in response to the three forces acting in a viscous medium such as heavy media, water or less commonly, air (Blankson Abaka-Wood et al., 2019). Depending on the particle size, the equilibrium among the forces follows Stokes' law (fine particles; < 50 μm) or Newton's law (thick particles; > 500 μm) (Jordens, 2016).

Rare earth metals are suitable for gravity separation since they have relatively larger specific gravity than the gangues they are typically associated with, which are often significantly less dense. Monazite separation from heavy mineral sands is the most frequent application of gravity separation involving rare earth bearing minerals. One of the simplest flowsheets for the concentration of monazite from placer deposits was actually not designed for rare earths exploitation, but to recover gold. Figure 11 shows the process used to recover gold and monazite from a placer deposit in Idaho.

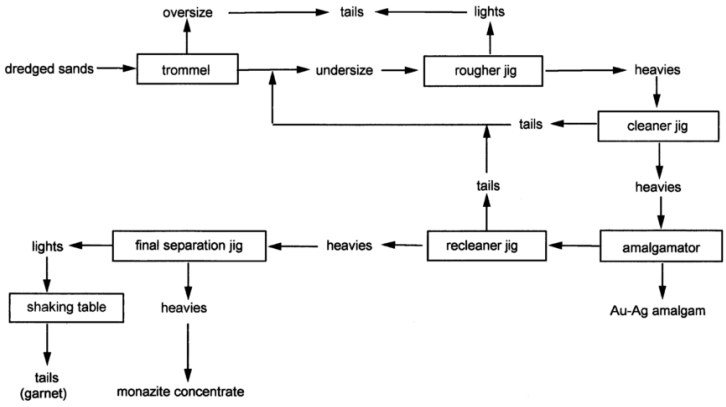

Figure 11. Concentration of gold and monazite from a placer deposit using gravity separation methods. Adapted from (Gupta and Krishnamurthy, 2005).

As can be seen, concentration of rare earth mineral is achieved by gravity separation only, whereas the gold is removed by amalgamation with Ag.

More sophisticated is the flowsheet specifically created for the concentration of monazite from Egyptian beach sands, which typically contain nearly 30 wt.% valuably heavy minerals (Moustafa and Abdelfattah, 2010). As shown in figure 12, wet separation is firstly used to discard low gravity gangue, followed by low intensity magnetic separation to discard any ferromagnetic minerals while avoiding the removal of paramagnetic monazite (Kumari et al., 2015). The resulting non-magnetic fraction is rich in monazite and zircon, and contains also xenotime, thorite, magnetic leucoxene, hematite and green silicates in a decreasing order of abundance (Moustafa and Abdelfattah, 2010).

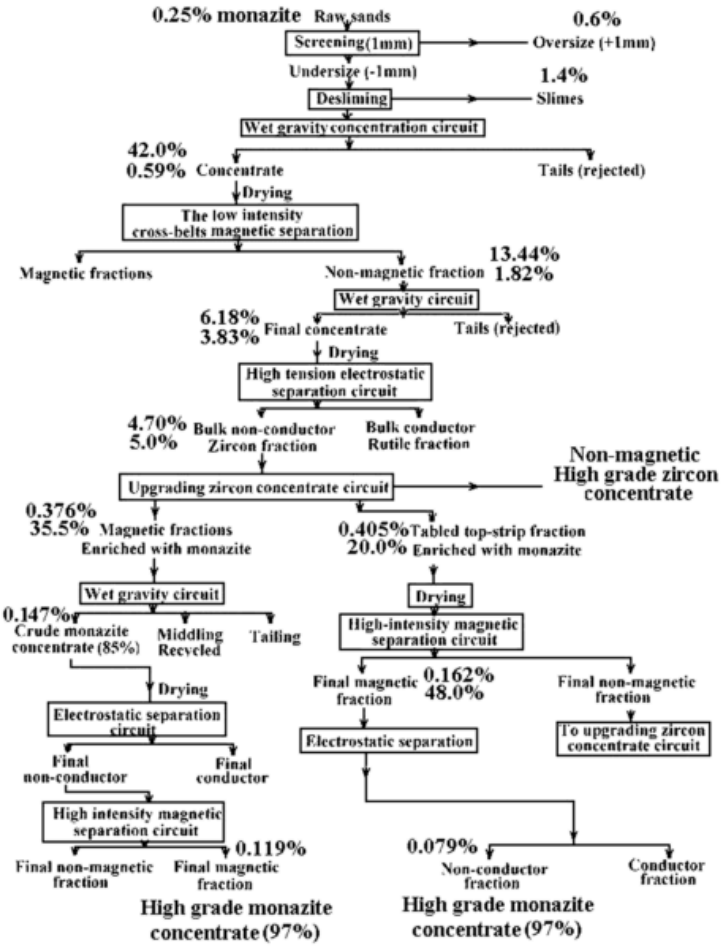

Figure 12. Concentration and separation of monazite from Egyptian beach sands using gravity and magnetic separation methods. Adapted from (Moustafa and Abdelfattah, 2010).

Gravity separation in combination with froth flotation is also applied for the recovery of monazite in many processing activities. At the Bayan Obo deposit in China, gravity separation has been used between rougher and cleaner flotation circuits to separate monazite and bastnatsite from the iron-bearing and silicate gangue material (Jordens et al., 2013). In this particular case, the challenge associated with gravity separation is that gangue materials have similar specific gravities to the desired rare earth minerals. Moreover, they are presented in the form of very fine particles, which translates in large losses of rare earths since simple gravity separation techniques are rather ineffective in such cases. Thus, separation of very fine particles is only achieved by employing centrifugal gravity separators such as the Knelson, Falcon and Mozley gravity concentrators (Blankson Abaka-Wood et al., 2019). Figure 13 provides a schematic illustration of the separation mechanism taking place within the Knelson concentrator. The mixed heavy and light particles are introduced in the bottom of the bowl using the central pipe. Heavy particles are concentrated inside the ribs and light particles leave the bowl from its upper part.

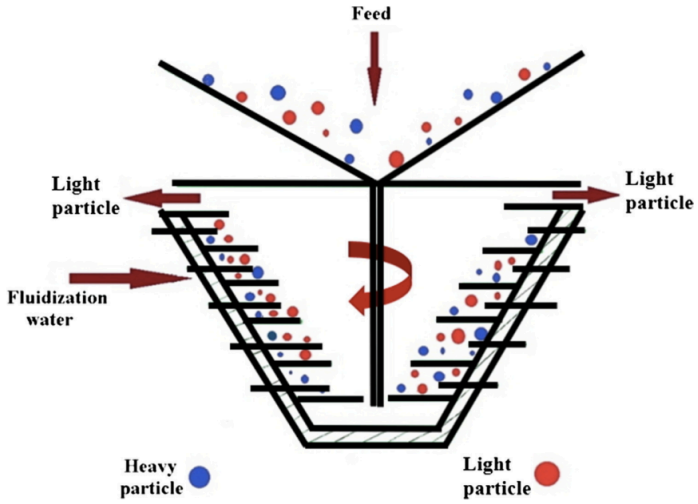

Figure 13. Schematic illustration of a Knelson concentrator (Fatahi and Farzanegan, 2018).

Besides the applications aforementioned, gravity separation has been successfully implemented at lab-scale on Turkish and Australian deposits with fine-grained mineralizations (Jordens et al., 2013). Many REE resources are contained in tailings generated from the extraction of primary commodities such as copper, gold, silver, cobalt, uranium and lead, into the very fine particle size range (< 5 μm). In order to recover ultrafine particles, the initial grinding procedure was modified to homogenize particle sizes (300 μm). From there, the recovery of rare earth light particles was achieved using a gravity separator that was specifically designed for that purpose.

6.1.1.2. Magnetic separation

Magnetic separation of minerals is based on the different behaviours of mineral particles being exposed to an external magnetic field. The presence of unpaired electrons in the material determines its magnetic response. Application of a magnetic field to a mineral containing unpaired electrons induces magnetic dipoles, which align with the external magnetic field generating a magnetic force. The magnetism of mineral particles is classified into three categories: ferromagnetic, paramagnetic and diamagnetic, depending on the material behaviour in the presence of an applied magnetic field. Ferromagnetic and paramagnetic minerals are both attracted among the lines of an external magnetic field, although ferromagnetic materials align its magnetic moments much more rapidly. Conversely, diamagnetic minerals are repelled along the magnetic field lines (Jordens, 2016).

Magnetic separation is a method commonly used in the rare earth mineral beneficiation to eliminate highly magnetic gangue or to concentrate the desired paramagnetic rare earth bearing minerals such as monazite and xenotime (Kumari et al., 2015). As explained previously in the first chapter of this thesis,

almost all lanthanides have a series of electrons occupying a 4f sub-shell and these electrons typically have magnetic moments which do not cancel out, resulting in a material with some degree of magnetism (Jordens et al., 2013).

Magnetic separators are used in combination with gravity separators for the recovery of REE-bearing minerals from beach sands. They are used, prior to more selective separation steps, to remove strongly magnetic minerals such as magnetite and are also used to separate monazite from diamagnetic heavy mineral gangue such as zircon and rutile (Jordens et al., 2013). Figure 14 presents a schematic illustration of the separation mechanism taking place within a particular type of magnetic separator. This particular device consists essentially of a feed silo, a conveyor belt and a roller with rare earth permanent magnets, which produce a magnetic field. Classification of mineral fractions is achieved with the use of high-intensity dry magnetic separation (Miceli et al., 2017).

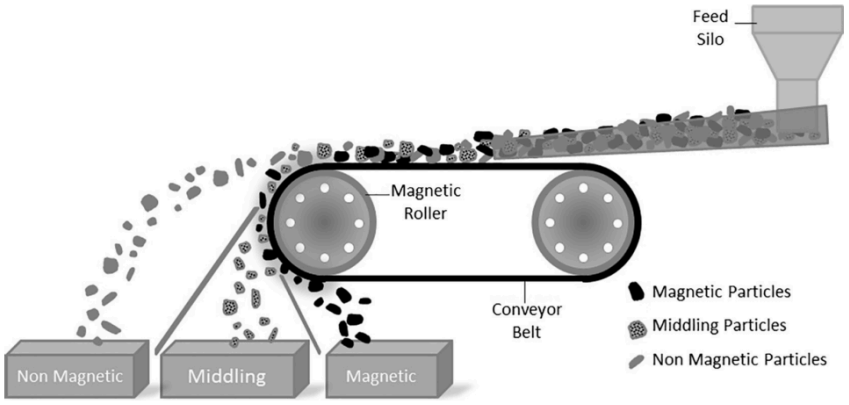

Figure 14. Schematic illustration of a RE-ROLL dry rare-earth magnetic separator (Miceli et al., 2017).

Magnetic separators are also successfully used, in combination with gravity separation, in the beneficiation of Chinese bastnasite rare earth ores to eliminate iron-bearing gangue minerals as a cleaning step before further REE specific separation steps.

6.1.1.3. Electrostatic separation

Electrostatic separation is based on the differences in mineral conductivities. It is regarded as an alternative processing technique and is limited in mineral processing applications because of its feed requirements (low feed moisture, inability to treat very fine particle sizes). Nonetheless, it is often used in the concentration of monazite and xenotime from beach sand deposits.

The most common electrostatic separator used for beneficiation of rare earth minerals is the high-tension roll (HTR) separator. Figure 15 provides a schematic illustration of the separation mechanism achieved using a HTR. The

high-tension separators are ionic field separators employing a grounded roll. As the particles move within the roll they pass through a discharge ionizing electrode which imparts surface charge to the minerals. The strongly conductive minerals lose this charge whereas the weaker conducting minerals maintain it and remain attached to the roll. Strongly conductive mineral particles follow a trajectory depending on the centrifugal force developed by the speed of the rotor while the weakly conducting minerals are removed from the roll mechanically by a brush (Jordens, 2016; Sunil Kumar Tripathy et al., 2010).

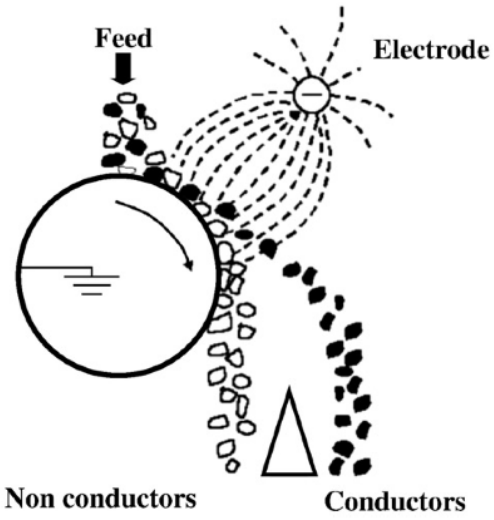

Figure 15. Schematic illustration of high-tension roll separator (Sunil Kumar Tripathy et al., 2010).

In the rare earth mineral processing, electrostatic techniques are mainly used for separation of monazite and xenotime from gangue materials with similar specific gravity and magnetic properties. For instance, electrostatic separators are used for xenotime beneficiation when it is concentrated with ilmenite after magnetic separation of heavy mineral sands. Xenotime can be recovered from the mixture since ilmenite is conductive but xenotime is not (Kumari et al., 2015).

6.1.1.4. Flotation

The flotation technique is based on the ability of a mineral to float, which depends upon its surface properties. Chemical modification of these properties enables the mineral particles to attach to an air bubble in a flotation cell. The bubbles and the mineral particles rise to the surface of the froth that is presented on the flotation cell and even though the bubbles may break, the mineral remains on the surface of the froth. Thus, the mineral is physically separated from the remaining gangue material and can be removed for further processing (Jordens, 2016). Figure 16 shows the separation of the froth enriched with REE minerals in a flotation cell.

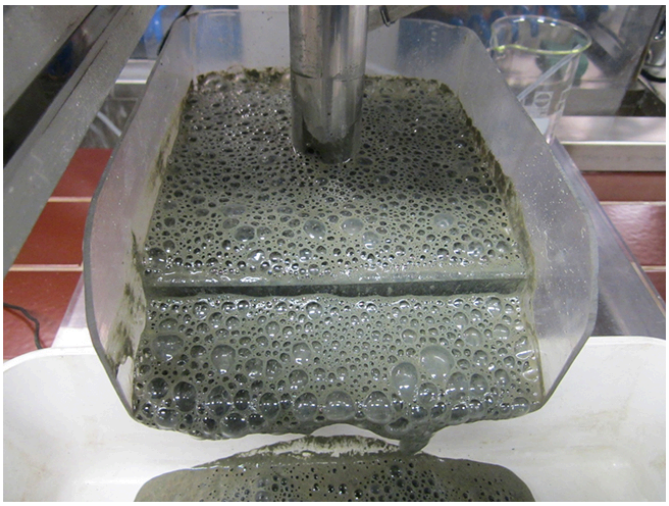

Figure 16. Froth flotation of REE concentrate (EURare, 2013).

Crushing and grinding the ore to a fine size is required to carry on froth flotation separation. It separates individual mineral particles from the waste rock and other mineral particles and it is typically done in water with the resultant slurry called pulp. The pulp is processed in the flotation cells, which agitate the mixture and introduce air as small bubbles.

Froth flotation is often applied to the beneficiation of rare earth ores because it allows to process a wide range of fine particle sizes and the process can be tailored to the unique mineralogy of a given deposit (Jordens et al., 2013). This process relies on the ability of certain chemicals, called collectors, to modify the surface properties of the minerals. Other chemicals are used to generate the froth, to adjust the pH and even to depress the flotation of the minerals in order to enhance the concentration of REEs through reverse flotation.

Bastnasite often has similar physical and chemical properties to the gangue materials and so it requires selective flotation reagents. Flotation of bastnasite is achieved using a variety of collectors such as hydroxamates, fatty acids, dicarboxylic acids and organic phosphoric acids. These collectors are all considered oxhydryl collectors as they contain a double-bonded oxygen to which a metal cation will bind (Jordens, 2016). Beneficiation of bastnasite through flotation is carried out in many mineral deposits including Mountain Pass in the EEUU and Bayan Obo in China. The flotation process of monazite is similar to that of bastnasite regarding the collectors used. However, two of the typical monazite gangue minerals, zircon and rutile, require the addition of a depressant in order to fulfil selective flotation of monazite. The most commonly depressants used for this purpose are sodium silicate, sodium sulphide and sodium oxalate (Jordens, 2016).

6.1.2. Hydrometallurgical operations: chemical treatment

Once the ore minerals have been concentrated through beneficiation, they are chemically treated to recover the rare earth elements. The recovery is generally carried out by pyro/hydrometallurgical processes consisting of heat treatment followed by leaching, precipitation, solvent extraction and ion exchange. The following subsections deal with the most widely known REEs recovery techniques including leaching, precipitation, ion exchange and solvent extraction.

6.1.2.1. Leaching of REEs

Leaching of the physically beneficiated concentrate with suitable acidic or alkaline solutions directly or after heat treatment is required to dissolve the metallic fraction of the minerals. The lixiviant solutions used determine the rare earth complexes formed under different pH conditions. Several leaching techniques to obtain REE concentrated liquors from bastnasite, monazite and xenotime have been described in the literature.

Bastnasite is susceptible to weathering, which causes REO to dissolve and combine with available phosphates. One of the main concerns related with bastnasite processing in the past was the extraction of REE fluorides. Nonetheless, alkaline treatment consisting in initial treatment with an HCl mild solution to extract the REE carbonates followed by reaction with NaOH at 96ºC to convert the REE fluorides to hydroxides, which are easily dissolved by leaching with HCl, has proven to successfully overcome this issue (Peelman et al., 2016).

Another technique widely employed is the acidic roasting. The main process used in Bayan Obo for the recovery of rare earths is the sulphuric acid roasting of bastnasite, in which the concentrated ore is heated with 98% H_2SO_4 solution to approximately 500ºC for several hours. This process decomposes the fluorocarbonate matrix converting rare earths to their sulphates and releases CO_2 and HF gas, which is highly dangerous and so, has to be carefully treated. The rare earth sulphates are selectively precipitated as sodium double sulphates by leaching the residue with a NaCl solution (Kumar Jha et al., 2016). Figure 17 presents a schematic flowsheet for the leaching process used for Baotou rare earth concentrates in China following the steps described above.

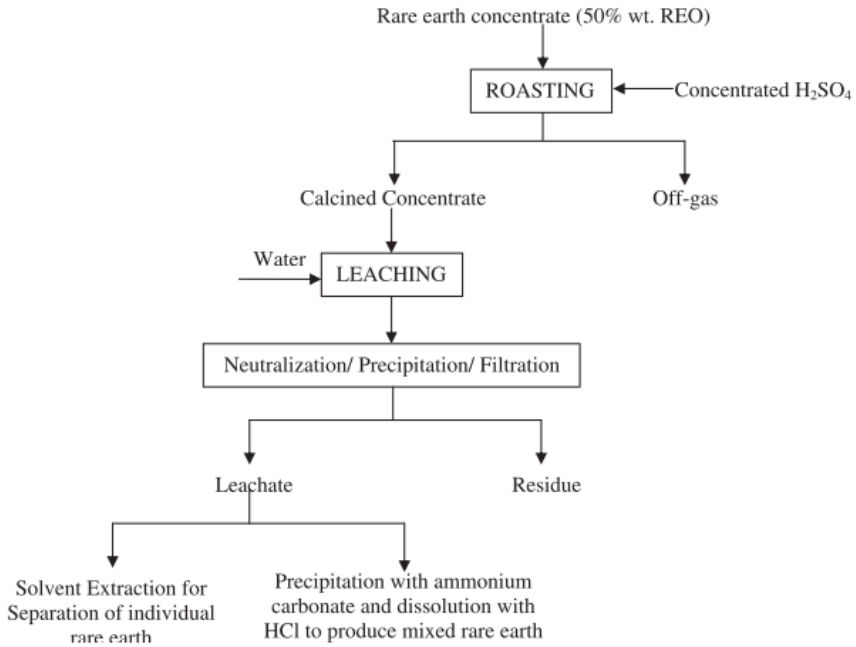

Figure 17. Leaching process used for Baotou bastnasite in China (Kumar Jha et al., 2016).

Similarly to bastnasite, monazite requires suitable conditions to leach out the metals present in it. The high content of thorium is the main drawback during monazite processing. In some cases, grinding of the concentrated fraction is required before leaching. In order to decompose the monazite, sulphuric acid or sodium hydroxide leaching at high temperatures are preferred above other techniques. NaOH is commonly employed for monazite leaching at 140 – 150ºC. The resultant product is a thick paste, which is slurried in water, filtered, washed and dried. Then, the cake concentrate, containing rare earth metals and thorium hydroxide, is leached with a hot acidic solution resulting in a REE concentrated stream suitable for further separation. The trisodium phosphate, which is a by-product of the alkali treatment, is recovered and commercialised. However, thorium is leached simultaneously, which brings radioactive concern to this process.

Another method currently used consists in heating the monazite ore with $CaCl_2$ and $CaCO_3$ under a reducing and sulphidizing atmosphere. This leads to the conversion of REE phosphates to REE oxysulphides (RE_2O_2S) and oxychlorides (REOCl) and creates a stable Th oxide and chloropatite ($Ca_5Cl(PO_4)_3$). Then, REEs can be selectively leached from the mixture with HCl 3%. This process eliminates the environmental threat caused by Th however, the REE recovery rate is lower than the alkaline method and the valuable Na_3PO_4 by-product is not generated (Peelman et al., 2016).

Table 10 gathers the leaching technologies currently used with bastnasite and monazite to produce rare earth elements.

Table 10. Summary of leaching technologies currently used in primary REE production. Adapted from (Peelman et al., 2016).

Mineral	Process	REE yield	Remarks
Bastnasite	I) Alkaline conversion of REF3 into $RE(OH)_3$ II) Leaching wiht HCl	-	The process can be preceded with HCl leach to extract REE carbonates before alkaline conversion
	I) Sulphuric acid roast II) Leaching with NaCl solution III) Precipitaton as Na dobule sulphates	-	Precipitates are converted to chlorides for further purification
Monazite	I) Digestion in hot NaOH 60-70% II) Washing residue with hot water III) Leaching with acidic solution	98%	Thorium is leached together with rare earths. Generates markeatable Na_3PO_4 by-product
	I) Heat under reducing and sulphidizing atmosphere with $CaCl_2$ and $CaCO_3$ II) Leaching with HCl 3%	89%	Thorium does not leach, remains in the residue as thorium oxide

Like bastnasite and monazite, experimental studies of leaching for the recovery or rare earths from xenotime have also been approached. As previously mentioned, xenotime is usually a by-product of monazite processing and so its own processing follows a similar path to that of monazite. Either sulphuric acid leaching or alkali leaching are used for the extraction of rare earth metals from xenotime (Habashi, 2013).

Regardless of the original rare earth mineral or the leaching technique employed, the leaching solution will always contain impurities such as iron, aluminium, calcium, which make further processing of REE concentrates for selective extraction of lanthanides necessary.

6.1.2.2. Precipitation

The small differences in basicity resulting from the decrease in ionic radius from lanthanum to lutetium influence the solubility of REE salts, the hydrolysis of ions and the formation of complex species. These properties form the basis of separation procedures such as precipitation, ion exchange and solvent extraction, which are the most common separation techniques currently used.

Precipitation of rare earths denotes the removal of part of these elements from the solution by the addition of a chemical reagent to form a less soluble compound. Several compounds have been tested for the separation of rare earths by precipitation. Hydroxides and double sulphates have been widely employed. The rare earth double sulphates $RE_2(SO_4)_3 \cdot Na_2SO_4 \cdot nH_2O$ are usually precipitated by the addition of sodium sulphate to the concentrated

streams. LREEs such as lanthanum, cerium, praseodymium, neodymium and samarium from sparingly soluble double sulphates, whereas all HREEs complexes are generally soluble. Precipitation of rare earths as double sulphates is typically followed by their conversion into rare earth hydroxides ($RE(OH)_3$) and then to rare earth oxides through metathesis reaction (Gupta and Krishnamurthy, 2005; Kumari et al., 2015).

Selective precipitation of rare earths is also achieved with oxalates. For instance, separation of thorium and the lanthanides from the sulphuric leachate of monazite and xenotime concentrates is often based on oxalate precipitation. Thorium and REE oxalates ($Th(C_2O_4)_2$; $RE(C_2O_4)_3$) are converted into hydroxides through reaction with NaOH and then calcined to obtain oxides. The oxides are dissolved in strong acidic solutions for later separation of thorium via solvent extraction (Habashi, 2013).

6.1.2.3. Ion exchange

Ion exchange (IE) takes place when the leachate solution containing the lanthanides is allowed to flow through a cationic exchange resin bed. The ion exchange technique involves the adsorption stage in which the ions from the solution get loaded or absorbed on the exchanger and an elution stage is required for desorption. When more than one anion or cation is present in the solution, and if certain selectivity is exhibited, the ion exchange process becomes an ion exchange separation (Gupta and Krishnamurthy, 2005).

Before 1960, ion exchange was the only method used to separate rare earth metals but nowadays it is only used to recover small REE quantities from highly purified ores. During ion exchange process, different cationic or anionic resins are used depending on the leachate features. The affinity of the exchanged ions depends majorly on their charge, size and degree of hydration. Because the stability constants of the lanthanide complexes differ from one to another, the most stable complexes move faster down the resins, which is a critical factor to bear in mind for the design of REE separation flowsheets (Kumar Jha et al., 2016).
Different complexing agents have been used as eluents for the recovery of REEs through ion exchange: 5% citric acid adjusted at pH 3 with ammonium hydroxide, 0.1% citric acid adjusted at pH 5-8 with ammonium hydroxide, $1 mol \cdot L^{-1}$ lactate at pH 3 and $0.26 mol \cdot L^{-1}$ EDTA at pH 3.6 (Habashi, 2013). The effect of ion exchange resins on the separation yield has also been extensively studied. Table 11 displays a detailed summary of IE separation studies carried out employing different resins.

Table 11. Summary of REE separation studies performed employing different ionic exchange resins (Kumar Jha et al., 2016).

Resin used	Study details
Tulsion CH-96 and T-PAR	Solid-phase extraction of heavy rare earths like Tb, Dy, Ho, Y, Er, Yb and Lu from phosphoric acid using Tulsion CH-96 and T-PAR resin has been reported.
IR-120P (cation-exchange polymeric resin)	Recovery of Y and rare earths using electroelution of a cation-exchange polymeric resin IR-120P Rohm & Haas-USA from chloride medium is reported.
N-methylimidazolium functionalized anion exchange resin	N-methylimidazolium functionalized anion exchange resin was used for adsorption of Ce(IV) from nitric acid medium by reducing it to Ce(III).
Tulsion CH-93	Solid–liquid extraction of Gd from phosphoric acid medium using amino phosphonic acid resin, Tulsion CH-93 is reported. The log D vs. equilibrium pH plot gave straight line with a slope of 1.8. The loading capacity of Tulsion CH-93 for Gd was 10.6 mg/g.
Dowex I-X8 anion-exchange resin	The distribution coefficients on Dowex I-X8 was determined for all rare earths at different proportions of nitric acid and acetone which is found to be sufficient for the separation of rare earths by ion-exchange chromatography.
D113-III resin	The adsorption and desorption behaviors of Er(III) ion using resin D113-III were investigated. The loading of Er(III) ion onto D113-III increased on increasing the initial concentration.
D72 (acid ion exchange resin)	The loading of Pr (III) ions was dependent on pH and adsorption kinetics of Pr (III) ions onto D72 resin followed pseudo-second-order model. The maximum adsorption capacity of D72 for Pr (III) was evaluated to be 294 mg/g for the Langmuir model at 298 K.
D151 resin	The adsorption and desorption behaviors of Ce(III) on D151 resin was achieved at pH 6.50 in HAc–NaAc medium. The maximum loading capacity of Ce(III) was 392 mg/g resin at 298 K.
Bio-Rad AG 50W-X2 cation-exchange resin	A new method for determining the stability constants for the mono- and difluoro-complexes of Y and rare earths, using a cation-exchange resin Bio-Rad AG 50W-X2 has been reported.
TODGA resin	A two-stage method to separate Lu and Hf from silicate rock and mineral samples digested by flux melting or HF–HNO3 dissolution using TODGA resin from Eichrom Industries is presented.
Amberlite XAD-4	The pre-concentration and separation of La(III), Nd(III) and Sm(III) in synthetic solution was achieved using Amberlite XAD-4 with monoaza dibenzo 18-crown-6 ether. The adsorbed rare earth elements were eluted by 2M HCl.
D152 resin	The sorption of rare earth ions from HAC–NaAC buffer solution using D152 resin containing –COOH function groups at 298 K are presented.
XAD-4 (crosslinked polystyrene resin)	A new chelating agent bis-2[(O-carbomethoxy)phenoxy]ethylamine has been synthesized using a facile microwave induced process. The ligand was appended on to XAD-4 resin and adsorption properties of La(III), Nd(III) and Sm(III) towards this resin were studied. The selectivity sequences of the resin for these metals were in agreement with their stability constants.
Tertiary pyridine resin	The novel separation method of rare earths using tertiary pyridine type resin with methanol and nitric acid mixed solution was developed. The adsorption and separation behaviors of rare earths were investigated and found that it can be well separated mutually.

6.1.2.4. Solvent extraction

The separation of rare earths by solvent extraction (SX) depends upon the preferential distribution of individual rare earths between two immiscible liquid phases that are in contact with each other (Gupta and Krishnamurthy, 2005). Separation processes based on solvent extraction techniques have been developed to produce high purity single rare earth solutions or compounds (Xie et al., 2014). Solvent extraction is generally accepted as the most appropriate

commercial technology for separating rare earths. Typically, multiple contacts are needed to transfer the metal ions from the aqueous to the organic phase. This is also the case of the stripping stage, in which the loaded organic phase is treated with an aqueous solution to recover the valuable species and close the mass balance.

There are many advantages of using solvent extraction for rare earth separation. One of them is that extractants can hold large amounts of REE, and so highly concentrated streams can be treated. Another advantage is that the extraction can be tailored in order to separate the valuable compounds from impurities such as Ca^{2+}, Fe^{3+}, Al^{3+} and Pb^{2+}.

Several extractant solutions have been described in the literature. However, only a few are currently used in the industry. Conventional extractants can be classified mainly into three categories: cation exchangers (or acidic extractants), solvation extractants (or neutral extractants), and anion exchangers (or basic extractants). Solvent extraction of rare earths is also extensively carried out using ionic liquids, which will be discussed in depth further on in this manuscript. The extractants are generally too viscous to be used in a practical system and so they are typically dissolved to ensure a good contact with the aqueous phase. The solvents most commonly used are kerosene and certain aromatics. Modifier substances such as decanol are often added to the organic phase to improve the hydrodynamics of the system (Gupta and Krishnamurthy, 2005). Table 12 summarizes some of the commercial extractants reported in the literature for rare earth SX.

Cationic extractants are employed for the extraction and separation of REM as they form cationic species in the aqueous solution. The overall extraction from aqueous media by cationic extractants can generally be simplified as (Kumar Jha et al., 2016; Xie et al., 2014):

$$\mathrm{Ln^{3+}} + 3\,\overline{\mathrm{HA}} \leftrightarrow \overline{\mathrm{LnA_3}} + 3\,\mathrm{H^+} \qquad \text{(R.1)}$$

Where Ln represents any lanthanide, A is the organic anion and over scoring denotes that the species are present in the organic phase.

Acidic extractants used for extractive separation of lanthanides are grouped as two categories: carboxylic acids and organophosphorus extractants. Carboxylic acids such as versatic and napthenic acids are commercially available and relatively inexpensive.

Table 12. Summary of some commercial extractants for rare earth solvent extraction (Xie et al., 2014).

Reagents class	Structure	Extractants
1. Cation exchangers		
Carboxylic acids		Versatic acids: $R_1 + R_2 = C_7$, Versatic 10; $R_1 + R_2 = C_6 - C_8$, Versatic 911
	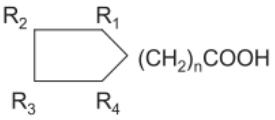	Naphtenic acids: $R_1 - R_4$: varied alkyl groups
Phosphorous acids	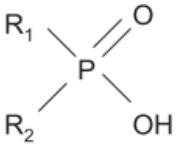	Phosphoric acids: $R_1 = R_2 = C_4H_9CH(C_2H_5)CH_2O–$, di-2-ethylhexylphosphoric acid (D2EHPA) Phosphonic acids: $R_1 = C_4H_9CH(C_2H_5)CH_2O–$, $R_2 = C_4H_9CH(C_2H_5)CH_2–$, 2-ethylhexylphosphonic acid mono-2-ethylhexyl ester (EHEHPA, HEHEHP, P507, PC88A) Phosphinic acids: $R_1 = R_2 = C_4H_9CH(C_2H_5)CH_2–$, di-2-ethylhexylphosphinic acid (P229) $R_1 = R_2 = CH_3(CH_2)_3CH_2CH(CH_3)CH_2–$, di-2,4,4-trimethylpentylphosphinic acid (Cyanex 272)
	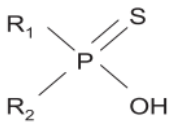	Monothiophosphorous acids: $R_1 = R_2 = CH_3(CH_2)_3CH_2CH(CH_3)CH_2–$, di-2,4,4-trimethylpentyl-monothiophosphinic acid (Cyanex 302)
	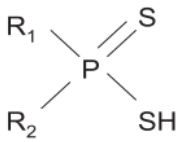	Dithiophosphorous acids: $R_1 = R_2 = CH_3(CH_2)_3CH_2CH(CH_3)CH_2–$, di-2,4,4-trimethylpentyl-dithiophosphinic acid (Cyanex 301)
2. Chelating exchangers	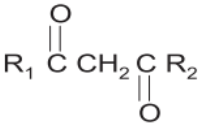	β-diketones: R_1 = R-C_6H_5,$R_2 = CH_3(CH_2)_5–$, R: unknown side alkyl, (LIX 54)
3. Solvating extractants	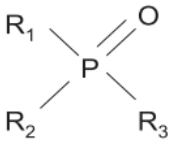	Phosphorous ester: $R_1 = R_2 = R_3 = CH_2(CH_2)_2CH2O–$, tri-n-butyl-phosphate (TBP) $R_1 = R_2 = CH_2(CH_2)_2CH_2O–$, $R_3 = CH_2(CH_2)_2CH_2–$, dibutylbutylphosphonate (DBBP) Phosphine oxides: $R_1 = R_2 = R_3 = CH_2(CH_2)_6CH_2–$, tri-n-octylphosphine oxide (TOPO, Cyanex 921)
4. Anion exchangers	RNH_2	Primary amines $R = (CH_3)_3C(CH)_2C(CH_3)_2)_4$ (Primene JMT, N1923)
	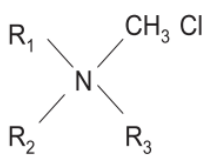	Quaternary amines: $R_1 = R_2 = R_3 = C_8–C_{10}$ mixture (Aliquat 336, Adogen 464)

The use of different carboxylic acids for extracting rare earth metal ions has been reported in the literature. Much attention has been paid towards Y extraction. The extraction behaviour of yttrium differs for these reagents. It is extracted along with the middle earths by Versatic 10, whereas it is extracted with the light rare earths by naphtenic acid. The yttrium extraction pattern is related with the acidity of the extractant. Napthenic acid has been widely used for separating yttrium from lanthanides in China. However, the extractant composition changes through use and its solubility in water lead to significant reagent losses (Xie et al., 2014).

Several organophosphorous extractants have been tested in rare earth separation processes. Organophosphorous extractants are typically classified into five categories: phosphoric, phosphonic, phosphinic, monothiophosphorous and dithiophosphororous acids. D2EHPA (or HDEHP, di(2-ethylhexyl) phosphoric acid) and HEHEHP (or EHEHPA, 2ethylhexyl phosphonic acid mono-2-ethylhexyl) are the most widely used organophosphorous extractants in the industrial REE production and also the most studied ones.
D2EHPA-impregnated resins were investigated by (Lee et al., 2009) for the separation of Ce, Pr, Nd and Sm from La. The D2EHPA impregnated resins showed higher adsorption ability and large separation factors than those impregnated with Cyanex 923 and PC88A (HEHEHP). However, although D2EHPA shows better sorption rates, PC88A is often preferred as an extractant for total separation of the rare earth elements because it is easier to strip. Extraction of REEs with D2EHPA requires low pH values of the aqueous phase, which implies that the equilibrium of Eq. (1) is strongly shifted towards the right side. Therefore, high concentrated acidic solutions are needed for stripping of the metals loaded in D2EHPA.
D2EHPA has been used for the separation of light rare earths from chloride solution of monazite on bench scale and validated on pilot extent. A batch process was developed to separate Sm, Eu, and Gd from the lanthanide hydrous oxide cake produced from monazite mineral (Rabie, 2006). The process was based on extraction by D2EHPA diluted in kerosene from nitric-hydrochloric acid mixture. Five stripping contacts were required to close the extraction balance. Separation of LREEs and HREEs was achieved through the stripping stages. LREEs were stripped almost completely in the first contact whereas HREEs needed further contacts to be recovered. A concentrate containing 98% of Sm, Eu, and Gd as a group was obtained with 78% recovery from their concentration in mother monazite mineral.

Combination of both D2EHPA and EHEHPA has also been described. The equilibrium separation of the trivalent rare earth elements Nd, Dy and Y from HCl by D2EHPA and EHEHPA separately and in mixtures was studied by (Mohammadi et al., 2015). The extraction order in both cases was found to be Y > Dy > Nd. The combination of both phosphorous acids increased the extraction

yield only when the total concentration of extractants was above 0.15 mol·L^{-1}. For lower total extractant concentrations, the highest extraction efficiencies were obtained using pure D2EHPA.

EHEHPA is a suitable extractant for selective separation of HREEs from LREEs extensively used for the industrial solvent extraction separation of rare earths (Gupta and Krishnamurthy, 2005). It is amenable for rare earths separation at lower acidity and can be stripped off using lower concentration of acid compared to D2EHPA (Hidayah and Abidin, 2018). As aforementioned, the organophosphorous acids are cationic exchangers and liberate hydrogen ion during the loading with REEs. This liberated hydrogen ion, increases the solution acidity, which adversely affects the metal extraction. This issue is often solved saponifying the EHEHPA with NaOH. The saponification is restricted, however, to avoid solubility of saponified solvent in the aqueous phase.
High separation factors were obtained for Ce/La (60.85), Nd/La (72.17) and Pr/La (98.33) at equilibrium pH 2 from the chloride leach liquor of monazite using PC88A mixed with modifier isodecanol and diluted in kerosene (Archana Kumari et al., 2018).
SX studies carried out using D2EHPA and EHEHPA showed increase in the extraction efficiency for REMs based on their atomic number: La < Ce < Pr < Nd < Sm < Eu < Gd < Tb < Dy < Ho < Er < Tb < Yb < Lu.

Some di-alkyl phosphinic acids have also been investigated for rare earths separation, although only Cyanex 272 (bis(2,4,4-trimethylpentyl) phosphinic acid) has been used commercially. In the separation of rare earth elements by SX with organophosphorous extractants, Cyanex 272 leads to lower extraction percentages but higher separation factors. Solvent extraction experiments have been performed to separate La from chloride solution containing Pr and Nd. The synthetic chloride solution was similar to the leach liquor of monazite sand after NaOH digestion. Cyanex 272 and saponified Cyanex 272 were able to selectively separate La from Pr and Nd after three contacts at an aqueous – organic phase ratio 1.5 (Banda et al., 2012a). The competitive simultaneous extraction and separation of 14 lanthanide elementsfrom perchloric acid aqueous solution by solvent extraction with Cyanex 272 was reported by (Swain and Otu, 2011). Cyanex 272 did not extract REM from very acidic solutions. However, it exhibited excellent physical phase separation properties at low acid concentrations. The lanthanides were separated into two broad groups: LREEs and HREEs. The extraction order was La < Ce < Pr < Nd < Sm < Eu < Gd < Tb < Dy < Ho < Er < Tm < Yb < Lu.

Chelating extractants act as ion donors and so they extract metals by cationic ion exchange, similarly to cation exchangers. The essential feature of chelating extractants is the presence of a ring structure within the extractant molecule that acts as a ligand to the metal ions (Hidayah and Abidin, 2018). Chelating

extractants have been tested for europium extraction from nitrate solutions and cerium and lanthanum from chloride solutions, but they have been neglected by the REEs extraction industry because of their unfavourably performance compared with acidic extractants (Xie et al., 2014).

Several types of solvation extractants have been used for rare earth separations. In extraction by solvation, the extractant replaces the coordinated water molecules from the aquated metal ion to form a species that is soluble in the organic phase. The most important solvating extractant for rare earth recovery is tri-n-butyl-phosphate (TBP) and the extraction of a trivalent rare earth by TBP can be represented by the general reaction (Gupta and Krishnamurthy, 2005):

$$3\,\mathrm{RE(NO)_3} + \cdot\,\mathrm{xH_2O} + 3\,\overline{\mathrm{TBP}} \;\leftrightarrow\; \mathrm{RE(NO_3)_3(TBP)_3} + \mathrm{xH_2O} \qquad \text{(R.2)}$$

According to the reported studies dealing with the extractability of lanthanides with TBP the distribution coefficients seem to be much lower in chloride solutions than in nitric media. Concentrated nitric systems appear to be promising for separating rare earths lighter than samarium. However, rare earths heavier than samarium could not be separated effectively in nitric systems (Xie et al., 2014). TBP has proved to be useful in the bulk recovery of the rare earth product from nitrate liquors. However, it is less useful in separations among the trivalent lanthanides because the observed separation factors for adjacent REE pairs are generally small (Gupta and Krishnamurthy, 2005).

Anion exchangers require the presence of strong anionic ligands to extract metal ions as anionic complexes. Liquid anion exchangers have been effectively used for rare earths separation. They are based on long-chain alkali amines classified as primary (RNH_2), secondary (R_2NH), tertiary (R_3N) and quaternary ammonium halides. Primene JMT is a liquid anion-exchanger that requires the formation of ion-pairs or ion association to act as extractant. The liquid-liquid extraction of yttrium (III) from sulphate medium using Primene JMT dissolved in kerosene was investigated by (Desouky et al., 2008). Bench scale experiments were carried out for the recovery of yttrium (III) from an yttrium rich fraction of monazite concentrate, which resulted in a crude yttrium oxide recovery of 76.3%. Recovery of yttrium and rare earth elements from copper pregnant leach solutions sing Primene JMT dissolved in kerosene was also successfully demonstrated by (Hiskey and Copp, 2018). Yttrium extraction was found to be 88.4%, LREEs averaged approximately 95% extraction and the HREEs a little lower at 92% for Primene JMT concentration of 0.147 mol·L^{-1} (5 %v/v).
Extraction of rare earth elements from aqueous solutions using quaternary ammonium salts such as Aliquat 336 as well as many other liquid salts has

been largely discussed in the literature. However, as previously mentioned, since the focus of this thesis is the recovery of rare earths using mainly ionic liquids, these SX processing techniques will be addressed in detail further on in the document.

7. Processing of secondary sources: REE recycling

When it comes to the recycling of REEs from secondary sources, common mining and metallurgical hydro-, pyro- or electro-chemical processes are typically carried out. The nature and the chemical features of the feed to be processed determine the recovery techniques applied. As previously mentioned, the current implementation of industrial REE recycling methods is still scare, mainly because of the inhomogeneity of the REE-bearing streams along with the drawbacks related to collection, dismantling and separation requirements, which difficult rare earths recovery from end-of-life products. Nonetheless, in spite of the disadvantages, the high content of REEs in certain products compared to natural deposits and the large amount of REE-based products sold and disposed annually, favour urban mining, which is increasingly attracting attention.

Three different areas collect the advantages of urban mining of REEs compared to virgin ore mining. Firstly, the environmental sector, as the recovery of REEs from secondary sources prevents the spreading of radioactive isotopes present in natural ores such as monazite. A reduction of landfill areas is achieved, since mining tailings and disposal of discarded products or fractions from discarded products is avoided. Recycling of REEs also helps to maintain cleaner landscapes, reduces exploitation and helps conserving natural deposits. The REEs supply chain is also affected positively by urban mining. The materials can be recycled back into production cycles for the same or different applications. The availability of certain compounds increases because the concentrations of important metals are higher in discarded products compared to ores. Finally, it has an important economic impact, reducing the costs of raw materials by creating additional supply (Tunsu et al., 2015a).

REEs recovery from end-of-life products typically implies the following stages: collection and sorting of the products; characterization, assay and pre-treatment of the material; leaching and separation of metal ions; and refining of the product to a desired form (pure metal or pure metal compounds) (Tunsu et al., 2015a). Efficient separation and pre-concentration methods for the fractions of interest are needed in order to assure the economic feasibility of potential industrial processes for reclaiming the rare earths in such products and also to minimize chemical consumption. Dismantling or concentrating the fraction of interest can be difficult in some cases. For instance, separating the permanent magnets from hard disk drives (HDD) is particularly challenging due to the

compact product design, where the magnets are generally glued to other components. As in ordinary mining processes, after pre-concentration, the leaching of REEs is carried out using concentrated acid and basic solutions at elevated temperatures. Tailings may be left behind after this step. Separation of rare earths from other elements present in the leachates requires a multi-stage solvent extraction, scrubbing and stripping separation process, which also leads to the generation of secondary waste streams that can be hazardous for the environment and so have to be properly treated before disposal.

The streams regarded as potential targets for REE recovery are typically divided into three categories: pre-consumer production scrap, end-of-life products and landfilled streams. Moreover the residues generated during the production of REE-based products are also valuable resources for metal recycling (Tunsu and Retegan, 2016). However, recycling of REEs is often directed towards end-of-life products, specifically phosphors, permanent magnets and NiMH batteries (Binnemans et al., 2013).

7.1. Products containing phosphors

Phosphors-based products comprise fluorescent lamps, LED lamps and CRT plasma screens. However, the research efforts have been directed to the recycling of REEs from large fluorescent lamps and compact fluorescent lamps. These products are mainly viewed as sources of yttrium and europium but they also contain minor amounts of other REEs such as cerium, lanthanum, terbium or gadolinium. There are three possible routes available for recycling the phosphor fraction of used fluorescent lamps: direct re-use of the recycled lamp phosphors in new lamps, recycling of individual components obtained by physicochemical separation methods to re-use them in new lamps, and chemical attack of the phosphors to recover their rare earths content (Binnemans et al., 2013). The direct re-use of the lamp phosphors is a very simple method in which, no chemical processing is required and so reagent consumption and generation of waste streams is null. Nonetheless, it is only applicable to one type of fluorescent lamps at a time, since different lamps make use of different phosphor mixtures. Moreover, phosphors deteriorate over lifetime of the lamp, which leads to poorer quality secondary products. Separation of phosphors in individual components is also a relatively simple process and it requires limited amounts of chemicals or reagents, but despite these advantages, it is very difficult to obtain very pure phosphor fractions, and again, due to the fact that phosphors deteriorate over time, the quality of recycled lamps is lower. Finally, recovery of the rare earth content by chemical attack of the phosphors is generally applicable to all types of phosphor mixtures. The hydrometallurgical processing routes used are similar to those followed for extraction of rare earths from primary ores, and high grade REO are obtained. These REO can be then used for other applications. However, as

in virgin mining, many processing steps are involved, large amounts of chemicals are required and great volumes of environmentally hazardous streams are typically generated.

After collection, the end-of-life fluorescent lamps are processed by specialized companies to separate glass, metal, plastics, phosphor powders and mercury. Linear tubes are relatively easy to recycle by cutting the ends of the tube and blowing the phosphor powder out. Separation of different components in compact fluorescent lamps (CFLs) is much more difficult, since they have to be crushed and shredded into fine particles to recover glass, metals, phosphor powder and mercury. After this procedure, the lamp phosphor can contain up to 50 wt.% of glass. The largest glass pieces can be removed by a sieving operation, either via dry or wet process; however, it is not possible to remove the very fine glass particles from the phosphor powder. The remaining glass fraction hampers the recycling of the lamp phosphors since treatment of the phosphor fraction with Na_2CO_3 at high temperatures transforms the fine glass particles into soluble silicates, contaminating REE feed solutions (Binnemans et al., 2013).

7.1.1. Separation of phosphor powder mixtures by physicochemical procedures

In the literature, the froth flotation separation technique has been approached for the separation of phosphor mixtures from the lamp particles. Nonetheless, it is not as easy as separation of mineral ore particles in the mining industry, because all phosphor components are phosphates, oxides, aluminates or borates with similar hydrophobicity and particle sizes. Pneumatic separation from a mixture of lamp phosphor particles in an air stream has also been described. However, these methods are only recommended for pre-treatment of the phosphor mixture before recycling of its REE content. Some disadvantages of the reuse of separated pure phosphor compounds in new lamps are: (1) low purity end products; (2) degradation of phosphors over time; (3) mercury build-up in the phosphor layer over time; (4) heterogeneous qualities of the phosphors in the mixture, since the purity of the REOs differ from one manufacturer to another; (5) changes in the particle size distribution of the phosphors. All in all, as previously stated, the quality of the recycled phosphor powders is lower to that of the starting product (Binnemans et al., 2013).
Despite the disadvantages, direct recycling of lamp phosphors is often indicated for the special case when the lamp producers can recycle the phosphors from their own end-of-life fluorescent lamps.

Mercury removal is an issue closely related to the recycling of REEs from lamp phosphors. Not only it is considered an environmental hazard because of its high toxicity but it is also an unwanted impurity in the solvent extraction

batteries of a rare earth separation plant. Different processes have been developed for removal of mercury from the lamp phosphor fraction, such as: thermal treatment at 400 - 600ºC in a vacuum, which allows to remove the largest part of mercury; heating the phosphor powders to at least 800ºC, to completely decompose the inorganic mercury compounds; or to heat the phosphor powders with organic reducing agents (Wu et al., 2014).

Many companies have dealt with the development of different techniques and pathways to separate and recover glass, mercury, and fluorescent powders from discarded fluorescent lamps. For instance, Nomura Kohsan, a Japanese company working towards mercury recycling, designed a flow sheet including some of the recycling routes followed in fluorescent lamps waste management (figure 18).

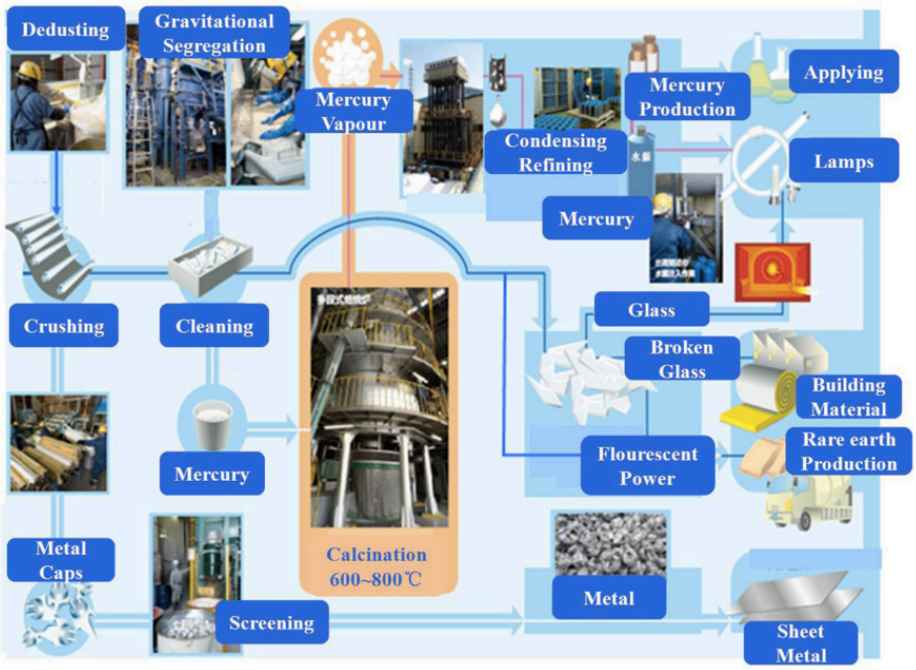

Figure 18. Flow sheet showing the crushing recycling technologies of waste fluorescent lamps developed by the Nomura Kohsan Company (Wu et al., 2014).

7.1.2. Recovery of REEs from powder phosphor mixtures

7.1.2.1. Leaching

The reclaimed lamp phosphor mixtures are a rich source of REEs, particularly HREEs. Chemical attack of the phosphor mixture is required in order to dissolve REEs and bring them into solution for further separation by precipitation or SX. Based on the literature, the recovery of REEs from fluorescent lamp waste is focused primarily through the hydrometallurgy route, which is mainly based on yttrium and europium recovery and involve acidic leaching.

Due to the chemical differences between the red, green and blue phosphors in fluorescent lamps, different types of leaching are needed to recover the REEs. Yttrium and europium from the red phosphor can be easily dissolved at room temperature using mineral or organic acids of mild concentrations, whereas dissolution of cerium, lanthanum, gadolinium and terbium is tougher and requires high temperatures and concentrated acids. Most studies focus on the recovery of yttrium and europium from the red phosphor (YOX), because they are the easiest elements to recover and they represent the highest value in the phosphor waste. Recycling of the green phosphors is also very interesting due to the high concentration of the critical and expensive terbium (Loy et al., 2017). The differences in solubility of the phosphor fractions allow for selective separation of REEs during leaching. The following reactions (R.3 – R.5) present the chemical transformations involved during leaching of REEs from phosphor powders using acidic solutions (Tunsu and Retegan, 2016):

Red phosphor:

$$Y_2O_3{:}\,Eu^{3+} + 6H^+ \rightarrow 2Y^{3+} + Eu^{3+} + 3H_2O \quad \text{(R.3)}$$

Blue phosphor:

$$CeMgAl_{10}O_{17}{:}\,Tb^{3+} + 34H^+ \rightarrow Ce^{2+} + Mg^{2+} + 10Al^{3+} + Tb^{3+} + 17H_2O \quad \text{(R.4)}$$

Green phosphor:

$$BaMgAl_{10}O_{17}{:}\,Eu^{2+} + 34H^+ \rightarrow Ba^{2+} + Mg^{2+} + 10Al^{3+} + Eu^{2+} + 17H_2O \quad \text{(R.5)}$$

Several lab-scale leaching experiments have been carried out using a variety of agents. Table 13 summarizes the most common reviewed leaching operations for REE recovery from end-of-life fluorescent lamps.

Table 13. Literature review for the leaching of REEs from phosphors. Adapted from (Tanvar and Dhawan, 2019).

Phosphor sample		Leaching solutions	Leaching conditions	Authors
Y_2O_3	6.0 - 27.0 %	HNO_3	3.0 - 5.0 M acid	(Tunsu et al., 2014c)
Eu_2O_3	0.1 - 1.4 %	H_2SO_4	1 - 24 h	(Tunsu et al., 2016)
Tb_2O_3	0.6 - 0.7 %	HCl	50 - 80ºC	(Innocenzi et al., 2017a)
Ce_2O_3	1.0 - 2.0 %			(Miskufova et al., 2018)
CaO	26.0 %			(Ella Y. Lin et al., 2018)

As shown in table 13, nitric, sulphuric and hydrochloric acid behave similarly, ensuring yttrium and europium dissolutions over 90%. Decrease in the leaching time can be achieved by adding 4 – 10% v/v of H_2O_2. Selective leaching of REEs from phosphor powders will be further discussed and tested in Chapter 4.

Alternatively to acidic leaching, an alkali digestion step, similar to the one used for monazite, can be employed to dissolve blue and green phosphors in the solution. The combination of selective leaching and alkali fusion seems to be one of the most efficient ways to dissolve all the REEs in lamp phosphors (Tunsu et al., 2015a). The chemical structures of $BaMgAl_{10}O_{17}:Eu^{2+}$ and $CeMgAl_{10}O_{17}:Tb^{3+}$ are so stable that they are really difficult to be decomposed by inorganic acids (Wu et al., 2014).
This method makes further separation by SX easier, since it will leave a concentrated solution of one HREE (Tb) along with two LREEs (La and Ce).

7.1.2.2. Precipitation

Chemical precipitation is one of the easiest methods for obtaining REEs in a solid form from an acidic solution. The purpose is to transfer the rare earth ions in a solution into insoluble precipitation adding chemical reagents such as oxalic acid or oxalate. The rare earth oxalates obtained can be further converted to oxides upon heating (Tunsu et al., 2015a):

$$2RE^{3+}{}_{(aq)} + 3C_2O_4^{2-}{}_{(aq)} \leftrightarrow RE_2(C_2O_4)_{3(s)} \quad \text{(R.6)}$$

$$RE_2(C_2O_4)_{3(s)} + 3O_{2(g)} \leftrightarrow 2RE_2O_{3(s)} + 12CO_{2(g)} \quad \text{(R.7)}$$

Recovery of REEs using this method is closely related to the inorganic acid used during the leaching stage. It is also strongly dependent on the nature of the phosphors-containing leachate and on the precipitation pH. The presence in solution of impurity elements such as calcium and zinc can lead to lower purity product due to co-precipitation.

7.1.2.3. Solvent extraction

Solvent extraction of REEs ions from phosphors leachates has been effectively carried out with several conventional extractants such as: HEHEPA, Cyanex 923, Cyanex 272, Cyanex 572 and TBP, but also ionic liquid systems. Table 14 recaps some of the latest SX investigations dealing with the separation of rare earths from phosphor leachates.

As can be seen in the table, the use of bifunctional ionic liquid extractants seems to be promising for the recovery or REEs. Separation of REEs from a simulated phosphor leachate using the custom made ionic liquids P81R·D2EHPA and P81R·Cy572 was achieved by (Pavón et al., 2018a). The separation process proposed is able to obtain ≥99.9% cerium, yttrium and europium individually. The separation factors reached were compared to those achieved with D2EHPA and Cyanex 572 and it was found that Y/Eu and Y/Ce selectivities are higher when using the ionic liquids prepared. Similarly, the

extraction of individual REEs contained in real fluorescent leach liquors was investigated by (Innocenzi et al., 2018).

Table 14. Summary of some of the solvent extraction studies dealing with separation of REEs from lamp phosphors leachates.

Material	Extraction system	Extraction conditions	Considerations	Authors
Simulated mixture solutions	P81R·D2EHPA and P81R·Cy572 ionic liquids	4 M HCl	≥99.9% efficiency	(Pavón et al., 2018a)
Lamp phosphor leachates	Cyanex 272, Cyanex 572 and D2EHPA	1 M H2SO4	D2EHPA best performance: 47.9% Y, 7% Tb, 4% Ce	(Innocenzi et al., 2018)
Real fluorescent lamp waste leachates	Cyanex 923	HNO3 media, batch tests at various temperatures (23 -60ºC)	Co-extraction of Fe and Hg. Optimum extraction conditions: <1M HNO3; <1M Cyanex 923; room temperature	(Tunsu et al., 2014a)
Real fluorescent lamp waste leachates	TBP and Cyanex 923 in various diluents (TetraPropylene Hydrogenated, kerosene, terbutyl benzene, 1-octanol)	Batch tests at room temperature	Higher distribution ratios for Cyanex 923	(Tunsu et al., 2014b)

Cyanex 272, Cyanex 572 and D2EHPA acidic extractants diluted in kerosene were tested out. The preliminary assays showed the difficulty to selectively separate the REEs using the Cyanex 272 and Cyanex 572, however D2EHPA allowed separating terbium and yttrium from other rare earths following the proposed recovery process, which includes six stages of extraction with 15% v/v D2EHPA in kerosene, room temperature and pH 0.5. Studies dealing with extraction of REEs from lamp phosphors using the solvating extractants TBP and Cyanex 923 were carried out by (Tunsu et al., 2014a, 2014b). It was found that the diluent used plays an important role in the solvent extraction of rare earth ions from nitrate media when using both Cyanex 923 and TBP. Better results were obtained using aliphatic diluents over aromatic ones or alcohols. Higher distribution ratios were obtained by using Cyanex 923 over TBP, since TBP requires a much high concentration of weakly coordinating counter-ions in solution to achieve satisfactory extraction. However, the extraction of HNO_3 by Cyanex 923 was shown to compete with the REM ions at high acidities in the aqueous phase.

In order to achieve higher performances, solvent extraction and precipitation processes can be used together. Precipitation of rare earths from the stripping solution can be carried out after SX to obtain the elements in solid form. Alternatively, the rare earths ions can be precipitated prior to solvent extraction. Then the precipitate, which contains fewer impurities than the initial leachate, is re-dissolved leading to a cleaner and easer to separate solution (Tunsu et al., 2015a).

7.2. Products containing permanent magnets

Neodymium-iron-boron (NdFeB) magnets are the most common REE-based magnets. They are primarily based on neodymium but they also contain minor amounts of dysprosium, praseodymium, gadolinium or terbium. Hard disk drives are regarded as an important source or REEs due to the large mass flows. Similar to fluorescent lamps, there are variations in the REEs content in various types of magnets. The composition varies among manufacturers and typically depends on application needs. For instance, as previously stated, higher amounts of dysprosium are used for high-performance applications.

Three different material flows are considered for the recovery of REEs from permanent magnets: (1) swarf originating from magnet manufacturing; (2) small magnets in end-of-life consumer products; (3) large magnets in hybrid and electric vehicles, as well as in wind turbines (Binnemans et al., 2013). The manufacturing process of REE magnets produces large amounts of scrap because of grinding and polishing operations. Up to 30% of the starting REE alloy can be lost during the manufacturing process.

Different routes have been described for recycling rare earth elements from end-of-life magnets: direct re-use of the discarded permanent magnets; reprocessing of alloys through hydrogen decrepitation; hydrometallurgical methods; pyrometallurgical methods; and gas-phase extraction (Binnemans et al., 2013). Direct recycling and re-use is the most economical way of recycling because of its low energy input and also because it does not imply chemical consumption, thus no waste is generated. However, it is only relevant for the large magnets, such as those used in wind turbines, large electric motors and generators in hybrid an electric vehicles, in other cases it is recommended to separate the rare earths from the transition metals and other elements present in the magnet alloys. Reprocessing of magnets from HDDs through hydrogen decrepitation is carried out in a reactor, where hydrogen is introduced and selectively reacts with the Nd-Fe-B at room temperature, forming a demagnetized hydrogenated powder that is easily separated from the auxiliary materials. The resultant powder can be further processed into new sintered magnets (Önal Recai et al., 2017). This recycling route requires less energy input than hydrometallurgical and pyrometallurgical routes; moreover no waste streams are generated. Nevertheless, since it is especially suited for hard disk drives, it cannot be applied to mixed scrap feed, which contains magnets with large compositional variations, neither to oxidized magnets. Hydrometallurgical methods overcome that issue, since they are generally applicable to all types of magnet compositions as well as to non-oxidized and oxidized alloys. The hydrometallurgical processing routes used are similar to those followed for extraction of rare earths from primary ores and so, many steps are required before obtaining new magnets. The main drawbacks of hydrometallurgical

methods are the consumption of large amounts of chemicals and the generation of great volumes of wastewater. Like hydrometallurgical processing, pyrometallurgical methods are generally applicable to all types of magnet compositions. Some of the advantages of this technique are that it does not generate wastewater, that only a few processing steps are required and that it is possible to obtain REEs in metallic state by liquid metal extraction. However, large energy inputs are required and large amounts of solid waste are generated with electroslag refining. Direct smelting and liquid metal extraction cannot be applied to oxidized magnets. Finally, the gas phase extraction is also generally applicable to all types of magnet compositions, either oxidized or non-oxidized alloys. Application of gas-phase extraction methods does not generate wastewater, but large amounts of chlorine gas are required and aluminium chloride, which is very corrosive, is involved.

7.2.1. Pre-processing of end-of-life REE magnets

Before shredding and smelting, the magnets have to be removed from end-of-life products and so they have to be identified and extracted from the waste prior to application of further recycling techniques. However, sintered magnets are difficult to separate because of the strong magnetic fields they generate and also because they are typically glued into position. It would be possible to demagnetise the magnets by heating them to above 300ºC but this would result in melting of organic binders and glues, generating hazardous vapors. For this reason, non-thermal demagnetization is recommended (Binnemans et al., 2013). Figure 19 displays the typical steps followed for separation and demagnetization of permanent magnets before further processing.

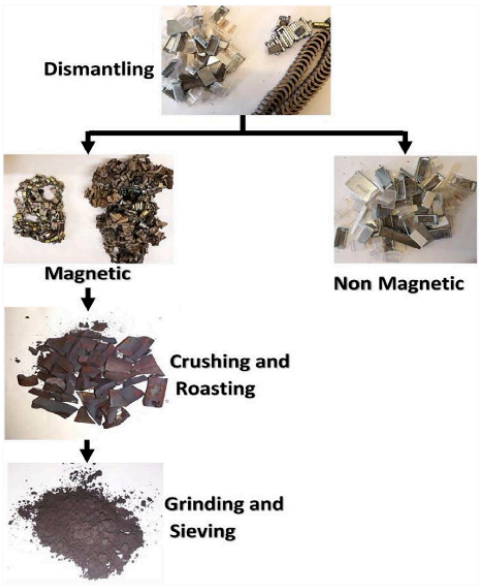

Figure 19. Process flowsheet of dismantling and demagnetization of NdFeB magnets (Ni'am et al., 2019).

The Hitachi Company was selected by Japan's Ministry of Economy, Trade and Industry in 2009, to participate in a project to promote recycling rare earth metals from "urban mines". Separate machinery was developed to separate and collect rare earth magnets from HDDs. The separation machine consist on a drum-type unit, which spins to shake and prang the HDDs continuously, so that the screws holding the magnets loosens and the HDDs break up into their structural components (casing, disk, rare earth magnet, etc.). Because the components containing rare earth magnets emerge from the machinery separately, the workers are able to pick out the desired components easily, just by screening out visually (Hitachi, 2010).

Decrepitation of magnets from HDDs has also been suggested. As explained earlier, the process consists in the expansion of NdFeB magnets by absorbing hydrogen. Upon expansion, the magnet breaks into coarse granules or powder, which makes it easier to collect. However, in order to allow a rout out for the hydrogen decrepitation process, HDDs have to be sectioned first in order to remove the non-profitable fraction (Önal Recai et al., 2017).

The fine powder extracted from HDDs can be directly reprocessed into new sintered magnets with magnetic properties similar to those of the original magnets, or further treated by chemical attack during the subsequent hydro- and pyrometallurgical processing routes. Even though, these routes would require significant energy input compared to direct re-processing of the alloys, it would be possible to process mixed scrap feeds containing magnets with a large compositional range, which would not be suitable for direct use (Binnemans et al., 2013).

7.2.2. Hydrometallurgical routes for separation of REEs from permanent magnets

7.2.2.1. Leaching

In order to achieve separation through hydrometallurgical routes, selective leaching of the magnet alloys is required, since more than 70% of the magnets content is iron, which is cannot be recycled as a marketable product and should be disposed of as a waste product. Ideally, the magnets would be dissolved in strong mineral acids and the REEs would be selectively precipitated as double sulfates, oxalates and fluorides. However, even selective leaching cannot avoid unwanted elements going into solution, for instance nickel and copper from the protective coating of the magnets, and boron.

Studies dealing with recovery of rare earths from permanent magnets through selective leaching are mainly focused on relatively clean magnets and preconsumer production swarf, not the end-of-life magnet scrap mixed with

other waste materials (Binnemans et al., 2013). Common mineral acids are used after thermal demagnetization of the material. Selective leaching of REEs from waste permanent magnets is accomplished under the optimized parameters of 5 mol·L^{-1} HCl, 368 K temperature, 24 h reaction time, 2% solid-liquid ratio, 800 ppm stirring speed and 0.250 mm particle size of magnets powder. The results on the statistical analysis carried out through the Taguchi method, show that the acid type is the most influential parameter for separation of REEs (Ni'am et al., 2019). Recovery of approximately 98% Nd and 81% Dy from magnetic sludge keeping iron dissolution below 15% by using 1 mol·L^{-1} HNO_3^+ and 0.3 mol·L^{-1} H_2O_2 at 353 K has been achieved by (Pana Rabatho et al., 2013). The oxidation of rare-earth metals by roasting produces oxides/mixed-oxides, which are readily soluble in acids. Selective dissolution of rare earth metals from roasted magnet powder with HCl and HNO_3 has been reported by (Hoogerstraete et al., 2014). Under the optimized conditions of 0.5 mol·L^{-1} HCl, 368 K temperature, 100g·L^{-1} pulp density and 500 rpm stirring speed, 98 wt% REE have been selectively leached from spent NdFeB magnets from a wind turbine, leaving iron oxide in the residue (Aarti Kumari et al., 2018). REE oxalates 99.9 wt% purity have been achieved using a combined ionic liquid leaching/extraction system (Dupont and Binnemans, 2015). The process is based on the leaching on (microwave) roasted NdFeB magnets in the carboxyl-functionalized ionic liquid [Hbet][Tf_2N]. The special thermomorphic properties of the IL – water system causes the mixture to be homogeneous during leaching at 80ºC, and biphasic when cooling back down to room temperature. The formation of a biphasic system induces metal separation where Fe(III) goes to the organic phase and the REE(III) and Co(II) ions to the water phase. Then, oxalic acid is used to precipitate the REEs and the cobalt, which is finally removed from the oxalate product using aqueous ammonia. The final REE oxalate can be calcined to obtain pure oxides, which could be used as precursors for the production of new NdFeB magnets. Figure 20 presents an overview of the proposed leaching process for REEs recovery from NdFeB magnets.

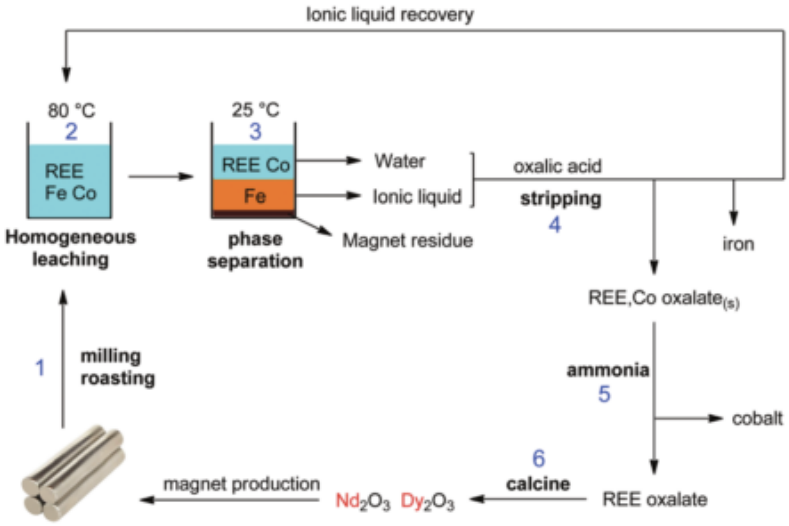

Figure 20. Process flowsheet of the proposed recycling process for microwaved roasted NdFeB magnets, based on the acidity and thermomorphism of the functionalized ionic liquid [Hbet][Tf2N] (Dupont and Binnemans, 2015).

7.2.2.2. Precipitation

Due to the presence of impurities such as iron and boron ions in NdFeB magnets leachates, selective precipitation is a commonly used method to remove REMs from solutions. The precipitation process usually adjusts pH and adds chemicals that stimulate precipitation; therefore, the metal ions convert into metal hydroxides or insoluble metal salts (Lee et al., 2013).

An aqueous process for reclaiming REEs, iron and boron from NdFeB magnets by means of precipitation has been developed (Lyman and Palmer, 1992). Magnetic scrap is leached with 2 $mol \cdot L^{-1}$ sulphuric acid solution. The pH of the leachate is subsequently raised to 1.5 by adding sodium, potassium and ammonium hydroxide after which, a double sulphate salt containing neodymium is formed. By using hydrofluoric acid in the leaching process it is possible to obtain REE trifluoride salts, which can be reduced to produce pure metallic REEs. Oxalic acid solution can be used to treat the solution containing the double salt from which the rare earth oxalates can be selectively precipitated and then thermally converted to oxides. This process seems to be feasible and efficient, but the use of large amounts of chemicals limits its applicability (Tunsu et al., 2015a).

Selective precipitation of Nd from NdFeB leachates has been achieved by double salt precipitation of $Nd(SO_4)_3 \cdot Na_2SO_4 \cdot 6H_2O$ (Lee et al., 2013). Precipitation through this method offers an economically affordable separation of neodymium from iron and boron without filtration problems. The chemical process is presented in the following equation (Tunsu et al., 2015a):

$$Nd^{3+}{}_{(aq)} + 3Na^{+}{}_{(aq)} + 4SO_4{}^{-2}{}_{(aq)} \leftrightarrow Nd(SO_4)_3 \cdot Na_2SO_{4(s)} + Na^{+}{}_{(aq)} \quad \text{(R.8)}$$

Rare earth elements have been recovered from NdFeB wastes by a selective leaching and precipitation process using 1.5:1 optimized oxalic acid dosage and pH 1.5 during 2 hours at 313 K, with a stirring rate of 300 r/min (Tian et al., 2019). Efficient precipitation of REM ions with oxalic acid, after dissolution of roasted magnets into a mixture of hydrochloric acid and ammonium chloride solution has also been reported (Hoogerstraete et al., 2014). Iron chloride, formed during leaching is not stable above pH 2 and undergoes hydrolysis in water, precipitating as $Fe(OH)_3$. High purity products are obtained after precipitation with oxalic acid with low reagents consumption.

Selective precipitation of neodymium from iron ions as phosphate has been achieved (Onoda and Nakamura, 2014). A prepared solution from iron nitrate and neodymium chloride was mixed with 0.2 $mol \cdot L^{-1}$ phosphoric acid to precipitate the iron and neodymium ions. A highly concentrated sodium hydroxide solution was used to adjust the pH in the range 2.3 – 4.3. To reduce the oxidation state of iron, ascorbic acid was added. Then, the precipitates were filtered and dried, leaving iron in an ionic form in the filtrate. The phosphate precipitation process appears to be promising for NdFeB recycling, since recovery of neodymium is close to 100%.

7.2.2.3. Solvent extraction

Although most extraction experiments have been performed at a small laboratory scale, several studies assess the recovery and separation of REM from permanent magnets through solvent extraction.

Recycling strategies for recovery of Nd and Dy from permanent magnets using numerous extractants including Aliquat 336 and P-based extractant systems such as TBP, D2EHPA, PC 88A and saponified PC 88A have been reviewed (Yoon et al., 2016). The recoveries of dysprosium and neodymium from permanent magnet scrap leach liquors using D2EHPA and PC 88A are compared and it is concluded that both are feasible for RE recovery from permanent magnets scrap leach liquors with meaningful recovery efficiencies. However, compared to each other, PC 88A outperforms D2EHPA with kerosene as a diluent system.

Separation of neodymium and dysprosium from NdFeB permanent magnet swarf by hydrometallurgical route including solvent extraction with NaCyanex 302 has been achieved (Padhan et al., 2017). Maximum separation factor (D_{Dy}/D_{Nd}) of 53.65 is obtained at equilibrium pH 1.2. Dy is separated from Nd at this pH with 0.125M NaCyanex 302. This leads to 98% extraction of Dy and

7.22% co-extraction of Nd in two stages of counter current extraction with 0.125M NaCyanex 302 at A:O=1:1. After Dy separation, 99.79% Nd is extracted, with 0.2M NaCyanex 302 in two counter current extraction stages at 1:1 phase ratio.

Apart from the conventional commercial extractants, ionic liquids seem to be promising for the recovery and separation of REEs in solvent extraction processes. Separation of neodymium and praseodymium from a simulated NdFeB magnet leach liquor using bi-functional ionic liquids such as trioctylmethylammonium bis(2,4,4-trimethylpentyl)phosphate (R_4NCy) and trioctylmethylammonium di(2-ethylhexyl)phosphate (R_4ND) has been reviewed (Padhan and Sarangi, 2017). Compared to the conventional extractants Aliquat 336, Cyanex 272 and D2EHPA, the bi-functional ionic liquids performance is more efficient under same experimental condition. The extraction efficiency is in the order: R_4NCy > R_4ND > Cyanex 272 > D2EHPA > Aliquat 336. Using R_4NCy, two stages counter-current contact at 1:1 phase ratio are required to achieve 98.97% Nd and 99.02% Pr extraction. The following equation describes the proposed extraction mechanism:

$$\mathrm{Nd^{3+}} + 3\mathrm{Cl^-} + \overline{3\mathrm{R_4NCy}} \leftrightarrow \overline{\mathrm{MCl_3 \cdot 3R_4NCy}} \qquad \text{(R.9)}$$

The P81R·Cy572 IL has been suggested as extractant to recover neodymium from synthetic magnet waste leaching through an industrial counter-current process (Pavón et al., 2018b). High selective separation of neodymium from the mixture at pH 1.2 is achieved by means of two counter-current stages with an organic phase composition of 0.3 mol·L^{-1} P81R·Cy572 (1:1 molar ratio) in kerosene.

7.2.3. Pyrometallurgical routes

Pyrometallurgical routes have been developed as an alternative for hydrometallurgical processes. Whereas the hydrometallurgical routes are very comparable to those used for the extraction of REEs from minerals, their main disadvantages are the large amount of chemicals used and the number of stages required. Generally, for the recycling of REE magnets, the alloys first have to be converted to oxides and then reduced back to the metal. Some of the pyrometallurgical routes allow remelting of the REE alloys or extraction of the REEs from transition metals in the metallic state. Other routes are more suitable for recycling of REEs from partly oxidized REE magnet alloys (Binnemans et al., 2013).

When the material to be recycled is available as relatively clean pieces, for instance magnets broken during the manufacturing process, electroslag refining is a viable process for upgrading scrap. In this process, scrap material is melted

either as a consumable electrode of by addition to a molten bath. A reactive flux is used to remove carbon, hydrogen, nitrogen and oxygen and metallic impurities, such as Li, Na, Al, Zn, Mg, Ca and Si. The flux used is typically a molten mixture of CaCl2 and CaF2, to which optionally a rare-earth fluoride is added. After sufficient time of reaction and separation, the metal is transferred from the crucible into a water-cooled chill mold, which leads to purification of metallic alloys. Figure 21 outlines the operation of the electroslag refining process. The process does not lend itself to the separation of rare earths from the transition metals, however, it shows to be promising for a closed loop recycling of large volumes of high quality material (Binnemans et al., 2013).

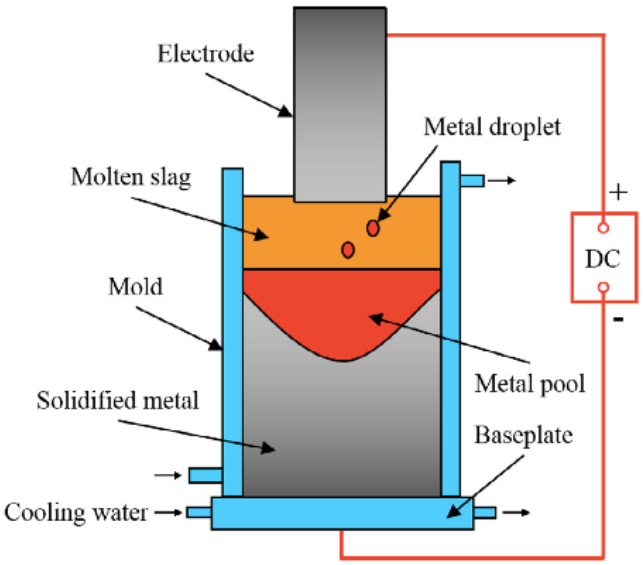

Figure 21. Schematic of electroslag remelting process (Wang et al., 2017).

The liquid metal extraction process has been developed to overcome the disadvantages of the electroslag remelting technologies. Allegedly, this process allows the handling of a wide variety of scrap feed to produce very clean materials. It consists of selective dissolution of the rare-earth alloy by a liquid alloy system. The rare earths and transition metals are distributed between two immiscible liquid metal phases.

The glass slag method arises as a more selective approach compared to those described above. Selective extraction of neodymium from NdFeB alloys has been successfully achieved. Through this process, the REE alloy is brought into contact with a molten flux that is able to selectively dissolve the rare earths from the alloys. After extraction, the loaded flux is cooled into a glass form. The rare earths can be recovered from the glass after dissolution followed by precipitation or after roasting of the glass slag. However, this method generates large amounts of inorganic wastes.

Direct melting of new and clean magnet scrap to produce new magnet alloys has also been addressed. Nonetheless, the oxygen and carbon content of the scrap hampers this process because of the significant loss of rare earths due to their strong affinity for the oxide slags formed. Moreover, smelting cannot remove carbon impurities and the carbon-containing alloys have inferior magnetic properties, which results in poorer quality products.

All things considered, the pyrometallurgical routes described have many important drawbacks, which are difficult to bridge, mainly because of their high energy consumption, their limited applicability and the need of additional processing to obtain pure REEs (Swain and Mishra, 2019).

7.2.4. Gas-phase extraction

In the gas-phase extraction method, rare earth metals are recovered from scrap by chlorination with Cl_2 in a N_2 stream, and carbochlorination with Cl_2 and CO in a N_2 stream. Through this process, the metals are transformed into volatile chlorides and separated based on differences in volatility. However, separation of rare earths from transition metals is difficult since the rare earth chlorides are less volatile and can hardly be separated from other less volatile chlorides, especially from alkaline-earth chlorides. Moreover, because the rare-earth chlorides have a very similar volatility, mutual separation cannot be achieved in the sublimation processes (Binnemans et al., 2013; Swain and Mishra, 2019).

7.3. NiMH batteries

In recent years NiMH batteries for use in various technological purposes are replacing Ni-Cd accumulators. The only difference between NiMH batteries and Ni-Cd accumulators is the composition of the anode. In the NiMH battery, nickel oxyhydroxide (NiOOH) is used as a cathode whilst the anode is a highly porous structure comprising a hydrogen absorbing material consisting of nickel, manganese, cobalt, aluminium and lanthanoids (La, Ce, Nd and Pr) in an AB_x type of structure (B = Ni, Co, Mn, Al; A = lanthanoids) with Y_2O_3 or Yb_2O_3 added for corrosion resistance (Larsson et al., 2013a). The AB_x designation refers to the ratio of the A type elements (lanthanoids) to that of the B type elements (Ni, Co, Mg, Al) (Tunsu et al., 2015a). To reduce the price, mischmetal is used instead of single lanthanum or neodymium (Kumar Jha et al., 2016). The composition of the mischmetal used varies depending on the origin and processing of the rare earth minerals and it affects the characteristics of the hydrogen storage alloys. Hybrid electric cars represent more than a half of the usage of NiMH batteries. Every Toyota Prius contains about 2.5 kg of REEs (mischmetal) in its battery pack (Binnemans et al., 2013).

With the increase in the generation of spent NiMH batteries, recycling of their metal contents is being increasingly investigated to avoid the disposal of tons of

dangerous waste in the environment. In addition, because of the economic value of metals such as nickel, cobalt and rare earths, different recycling routes have been developed to achieve the goals of urban mining (Assumpçao et al., 2009). Hydrometallurgical processes have shown to be able to recycle different waste fractions from the NiMH batteries (cathode and anode materials, metals from casting) that can be separately marketed with low investment costs. However, in order to achieve separation, many manual operations are required for dismantling of batteries and separating the different components and large consumption of chemicals is involved. Pyrometallurgical routes have also been proposed. Similar processing steps to those used for extracting REEs from primary ores can be used to extract them from the slags and the energy invested can be recovered, to a certain extent, from the organic components of the batteries. Nonetheless, pyrometallurgical techniques generally lead to REEs mixtures and so further separation is required. Furthermore, the REEs have to be extracted from slags, which necessarily involves hydrometallurgical processes and consumption of chemicals (Binnemans et al., 2013).

7.3.1. Pre-processing of NiMH batteries

Hydrometallurgical treatment of spent portable batteries requires a mechanical pre-treatment step, the separation of the active material containing the rare earth elements. For large batteries such as the ones used in electric vehicles, manual dismantling and separation of the anode from the cathode is preferred, since it minimizes chemical consumption in the leaching and separation steps (Larsson et al., 2013a).

Mechanical pre-treatment of mixed spent small portable batteries is generally carried out via crushing and grinding. The mechanical processing of 50 NiMH batteries has been performed through the following series of operations (also displayed as a flowsheet in figure 22): hammer milling; a first magnetic separation to release the metallic fraction from the polymeric fraction; knife milling of the accumulators to separate the metallic cases and screen from paste and separators; a second magnetic separation of the Ni-containing parts of the accumulators; finally, a last magnetic separation to release the strong magnetic material (metallic cases and screen) from weak magnetic material (powder, containing the material from positive and negative electrodes) (Assumpçao et al., 2006).

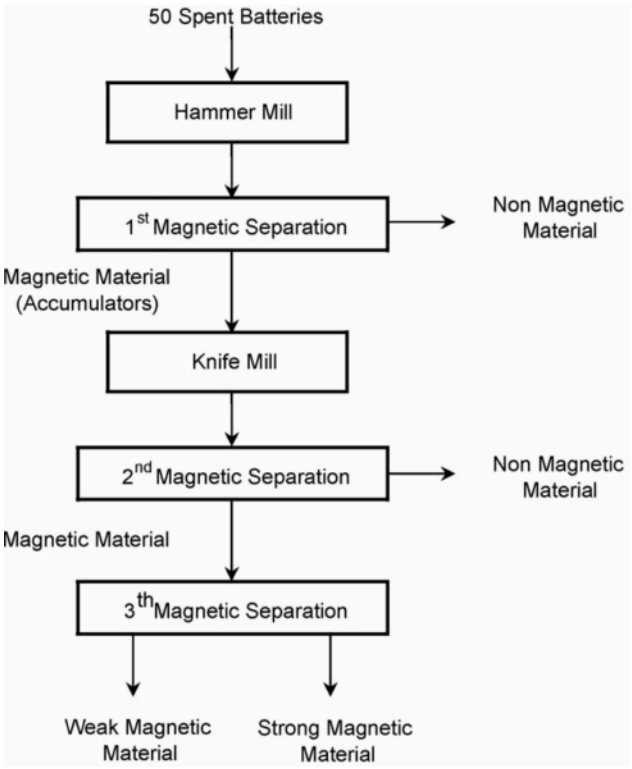

Figure 22. Mechanical separation flowsheet proposed for the separation of materials from NiMH small portable batteries (Assumpçao et al., 2006).

Similarly, another separation route has been described using simple and inexpensive mechanical processes such as grinding, sieving and elutriation, which is a process for separating particles based on their size, shape and density, using a liquid flowing in the opposite direction of sedimentation. Through this method, the materials present in spent NiMH batteries can be separated into three different fractions: 24.21% of metals mixture, 28.20% of polymers and 42.00% of powder (positive and negative electrodes) (Tanabe et al., 2016). First of all, the batteries are ground in a hammer mill with a 10 mm sieve in the output (first separation). From this sample, part of the remaining powder is removed using a 65 mm sieve (second separation). Elutriation of the leftovers, is performed in a spouted bed and concludes the separation system.

7.3.2. Hydrometallurgical routes for separation of REEs from NiMH batteries

7.3.2.1. Leaching

Most hydrometallurgical techniques proposed are based on metals recovery by selective precipitation or solvent extraction after leaching of the marketable fraction of NiMH batteries. In general, sulphuric and hydrochloric acids are preferred for leaching electrode materials. Because of its chemical structure and

composition, mildly acidic solutions are enough to almost completely dissolve the REEs, even at lower temperatures (Tunsu et al., 2015a).

Complete dissolution of the anode active material can be achieved with hydrochloric, nitric or sulphuric acid. Leaching of REEs using sulphuric acid solutions 2 mol·L^{-1} at 20ºC during two hours has proven to be successful to recover about 80% of the rare earths contained in spent NiMH batteries (Pietrelli et al., 2002). After mechanical pre-treatment, the powder removed from the accumulators can be dried and leached using sulphuric acid 2 mol·L^{-1} at 90ºC during 4 hours under constant stirring to recover more than 98 wt% of the rare earths in the solution (Assumpçao et al., 2009). Two consecutive leaching processes with sulphuric acid solutions at different conditions (2 mol·L^{-1} during 3 hours at 80ºC, and 1 mol·L^{-1} during 1 hour at 25ºC) have shown to be efficient to dissolve 100% of Ni, Co, Zn, Mn, La and Ce from NiMH batteries (Innocenzi and Vegliò, 2012). Hydrochloric acid 8 mol·L^{-1} in an inert atmosphere has proven to successfully dissolve rare earth metals from the anode of the NiMH batteries (Larsson et al., 2013b). Because of the high metal concentration, the anode material cannot be fully dissolved in a single step, but the problem is solved by using a two-step method whereby the HCl 8 mol·L^{-1} is contacted with the residue material after the initial leaching to leach the last metals, and then the acid is added to the first step to reuse it. This method has been also used for the leaching of valuable critical metals from spent NiMH batteries from hybrid electric vehicles (Petranikova et al., 2017). In this case, to simplify the leaching process, leaching experiments were done in the presence of oxygen. After dissolution, the leachates are typically filtered in order to separate them from the solid residue and facilitate the following steps such as precipitation or solvent extraction of the metals.

7.3.2.2. Precipitation

Selective precipitation after leaching is a common practice to recover pure REMs from NiMH batteries. Many studies in the literature deal with precipitation of rare earths from leachates containing other valuable metals such as Ni, Co, Zn and Mn.

A mixture of 6.5 wt.% NaOH and 3.5 wt.% Na_2CO_3 has been successfully used to precipitate over 94% of lanthanum and cerium and also praseodymium and neodymium from sulphuric acid media by adjusting the pH to 1.6 (Nan et al., 2006). After leaching with 2 mol·L^{-1} sulphuric solution and a pH of approximately zero, rare earths have been selectively precipitated by adding 5 mol·L^{-1} NaOH (Assumpçao et al., 2009). The pH range has to be maintained below 2.5 – 3.0 because precipitation of iron hydroxide usually begins at that range of pH. Compared to several acid solutions such as nitric, hydrochloric and aqua regia, leaching with sulphuric acid seems to be more appropriate, since it

boosts the subsequent selective precipitation of REEs. Recovery rates of 99% for cerium and lanthanum when using this method have been reported, with the major impurities being manganese (2.16%) and aluminium (2.93%). Similarly, separation of rare earth sulphates from leach solution by precipitation with NaOH has been described. This time, as a new feature, a cooling step is added before the filtration of unleached residue because the solubility of RE sulphates decreases with the increase of the temperature (Innocenzi and Vegliò, 2012). Recovery rates of 64 wt.% lanthanum sulphate and 28 wt.% cerium sulphate have been obtained, with impurities of manganese and aluminium (about 2 – 3.5 wt.% each) and some other metals like nickel and zinc.

Precipitation of rare earths from a concentrated hydrochloric acid solution with ammonium oxalate at pH 0.5 leads to 98.5% rare earths recovery (Fernandes et al., 2013). However, despite the simplicity of the method, selective precipitation of lanthanides as oxalate requires a rigid control of the experimental parameters.

A newer study dealing with precipitation of rare earths as double sulphates from concentrated sulphuric leach solutions has revealed the fact that precipitation efficiencies not only rely upon pH but, they also heavily depend on both H_2SO_4 and Na_2SO_4 concentrations (Porvali et al., 2018). Different additions of Na_2SO_4 to initial samples of the leachate solution, result in changes of Na/REE and SO_4/REE stoichiometric ratio and change of the H_2SO_4 molarity in the leaching solution. The best precipitation efficiency achieved, which is La > 98%, Ce > 99% and Pr > 99%, can be obtained by adjusting the ratios to 21.2 Na^+/REE and 58.3 SO_4^{2-}/REE.

7.3.2.3. Solvent extraction

Solvent extraction is a more complex operation compared to selective precipitation. Several extraction routes have been described using conventional commercial extractants as well as ionic liquids. D2EHPA, Cyanex 272, Aliquat 336, TBP and Cyanex 923 have been investigated for metals separation after dissolution (Innocenzi et al., 2017b). For instance, REEs, aluminium, iron and zinc have been separated from cobalt and nickel from hydrochloric acid leachates at pH 2 using 25% D2EHPA in kerosene (Zhang et al., 1998). The loaded organic phase is scrubbed first with 0.3 $mol \cdot L^{-1}$ HCl to remove the co-extracted cobalt, then stripping of the rare earths is carried out with 2 $mol \cdot L^{-1}$ HCl. A mixed REE oxide containing 53.3% La_2O_3, 3.4% CeO_2, 10.5% Pr_6O_{11}, 32.1% Nd_2O_3 and 0.8% Sm_2O_3 is obtained after precipitation of the rare earth fraction from the stripping solution with oxalic acid followed by calcination.

PC-88A 20% has been also successfully used for separation of rare earth metals from cobalt, nickel, manganese and zinc in sulphuric media. Through

this method, the rare earth elements can be recovered after 8 extraction stages, maintaining the pH at 3.5 (Wu et al., 2009). Co-extraction of cobalt and nickel can be solved by scrubbing with 0.2 mol·L^{-1} sulphuric acid. Zinc and manganese are separated by stripping of the loaded organic phase with 2 mol·L^{-1} hydrochloric acid. However, 17 stripping stages are needed to remove these impurities and so a high amount of chemical reagents is required. Finally, the rare earth metals can be stripped using 4 mol·L^{-1} hydrochloric acid in 6 stages. The total recovery rate of REEs achieved using this technique is 98.9%.

Mixtures of Cyanex 923 and TBP have been effectively used to separate metals from HEV. The REEs are separated from nickel, potassium and magnesium in 4 extraction stages with 70% Cyanex 923, 10% TBP, 10% kerosene, 10% 1-decanol (Larsson et al., 2013b, 2012). The loaded organic phase is stripped with ammonium nitrate and nitric acid to remove the majority of the manganese and cobalt ions. Cerium, lanthanum, neodymium, praseodymium and yttrium are recovered from the organic phase by using 1 mol·L^{-1} hydrochloric acid after initial stripping with 1 mol·L^{-1} ammonium nitrate.

The organic system consisting of 10% N1923 primary amine and 4% isooctanol in sulphonated kerosene has been used to highly separate rare earths over Fe, Ni, Cu, Mn and Zn from sulphuric acid solutions (Yun et al., 2015). The proposed extraction reaction can be expressed as follows:

$$5\overline{(\mathrm{RNH_3})_2\mathrm{SO_4}} + 2\mathrm{RE^{3+}} + 3\mathrm{SO_4^{2-}} \leftrightarrow 2\overline{(\mathrm{RNH_3})_5\mathrm{RE(SO_4)_4}} \qquad \text{(R.10)}$$

Using optimized stripping conditions (2.5 mol·L^{-1} HCl) the recovery of rare earths can reach 99.5% (99.94% purity) in a single stage.

A flow sheet has been developed for recovery of metals from nickel metal hydride batteries using the neutral extractant Cyanex 923 dissolved in the ionic liquid tricaprylylmethylammonium nitrate [A336][NO_3], and a synthetic chloride-based aqueous leach solution (Larsson and Binnemans, 2015). Figure 23 shows the process scheme, which consists on three selective strip operations using sodium nitrate first, to strip cobalt and manganese; then adding hydrochloric acid to remove the REEs from the mixture, and finally stripping of iron and zinc with nitric acid.

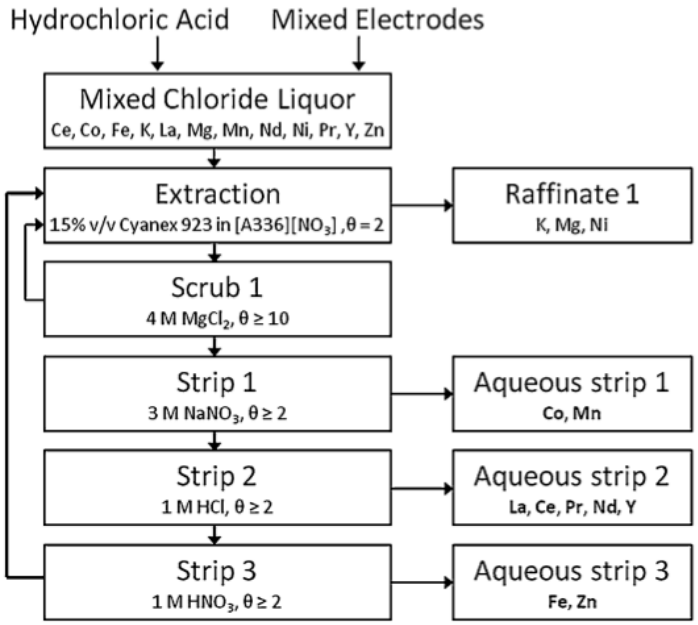

Figure 23. Flowsheet describing the extraction and stripping steps of the separation method proposed (Larsson and Binnemans, 2015).

7.3.3. Pyrometallurgical routes

The use of pyrometallurgical processes for the recovery of REM from nickel metal hydride batteries has not been as widely investigated as hydrometallurgical processes.

The recycling of different metals including cerium and lanthanum from a mixture of different types of household batteries has been investigated using thermal methods during preliminary treatment (Provazi et al., 2011). The material is grounded, briquetted and submitted to reduction tests in which it is calcined at 1000ºC for 4 hours under inert atmosphere to eliminate volatile metals present in the charge, such as cadmium, zinc and mercury. The residue is then submitted to magnetic separation and the remainder is leached with sulphuric acid for further precipitation or solvent extraction of the marketable metals.

Umicore and Rhodia have developed a process for the treatment of spent NiMH batteries with the aim of recovering base metals and rare earths. The general process, which has not been publicly disclosed yet, consists on treatment of the batteries in a vertical furnace with coke, air and a slag former (Innocenzi et al., 2017b). Then, part of the metals such as nickel, cobalt, copper and iron are converted into an alloy. Moreover, a slag of a mixture of oxides (calcium, aluminium, silicon, iron and rare earths) is recovered and treated to produce a concentrate of REEs that may be sent to the solvent extraction plant of Rhodia in la Rochelle (France).

8. Conclusions

This chapter details the discovery of the lanthanides as well as their unique physical and chemical features, which are invariably related to the development of an extensive range of technological fields. An overview of the main applications of rare earths was given including the most widespread and other minor uses. Transitioning to a green, low-carbon economy is becoming more and more important and so it is causing an increase in the demand and price of REEs. This fact, linked to the issues arising from their mining and recycling procedures confers the REEs the status of critical materials, which is defined by the value each material adds to the economy and the material's potential for an international supply shortage (U.S Department of Energy, 2011).

There are several challenges associated with the virgin mining of REEs. First of all, their heterogeneous geological location, since REE-containing minerals are rarely concentrated, which makes their exploitation difficult. Secondly, rare earth-containing minerals rarely form continuous ore bodies, which means that mining of large amounts of ores are required to obtain REEs. Moreover, they occur together with either uranium or thorium, thus mining of rare earths often generates radioactive waste that is hard to address.

To tackle the REEs supply challenge investing in sustainable primary mining is a feasible option. Many companies are actively seeking for new exploitable rare-earth deposits and old mines are being reopened. Nonetheless, as REEs range in different ratios in their ores, mining of one metal in particular produces large amounts of by-products that need to be capitalized. For instance, neodymium is less common than lanthanum or cerium, so that mining of REE ores for neodymium extraction generates great volume of Ce and La that need to be sold.

Recycling of rare earth elements may mitigate the large-scale mining needed to meet the global demand of these metals. Despite commercial recycling is still low (less than 1% in 2011), many research efforts are devoted on the REE recovery from secondary sources. Major drawbacks of urban mining relate to collection and dismantling requirements, difficult separation, matrix heterogeneity and low REEs content.

Regarding the beneficiation of rare earth element-bearing ores, monazite, bastnasite and xenotime are the main rare earth minerals of commercial importance. Several processing techniques have been developed to recover rare earths from these ores starting from physical beneficiation methods such as gravity, magnetic, electrostatic and flotation separation. The concentrated streams from beneficiation stages are then typically treated using hydrometallurgical procedures to yield individual rare earths or mixed rare earth

solutions or compounds. Solvent extraction of rare earth elements has been extensively studied. The selection of extractants and aqueous solution conditions is generally influenced by cost considerations, environmental concerns and by technical requirements, such as selectivity. The use of cation exchangers, solvation extractants and anion exchangers has been widely assessed. Commercially, D2EHPA, HEHEPA, Versatic 10, TBP and Aliquat 336 are largely used to separate rare earth elements. However, as the extraction technology continues to expand, the use of ionic liquids to support a more efficient design of the REEs extraction process is increasingly attracting the attention of the scientific community.

Nonetheless, because of the recent economic and political changes surrounding the REEs beneficiation and the need for a more sustainable society, the scientific community is nowadays focusing the attention towards the potential recovery of REEs from various end-of-life products, also called urban mining. Recycling of REEs has an important economic impact, reducing the costs of raw materials by creating additional supply. A drastic improvement in end-of-life recycling rates for REEs is needed to ensure the supply of these critical raw materials in the future. The main targets today are products containing phosphors, permanent magnets and NiMH batteries. This is due to their wide use, which ensures their availability as urban mining sources for the near future. In addition, the five most critical REEs (neodymium, dysprosium, europium, yttrium and terbium) are used in such devices. The relatively high content of critical rare earth elements when compared to natural ores makes these streams attractive targets.

Hydrometallurgical processes are generally the first methods of choice for the recovery of high purity fractions of REEs from complex streams. Some of their associated disadvantages are the use of large amounts of chemicals and the generation of great volumes of hazardous secondary wastes. The hydrometallurgical approaches for the recovery of REEs from batteries, phosphors and magnets are pretty similar. They typically consist on a leaching step followed by selective precipitation or solvent extraction of the REMs. Amongst the hydrometallurgical methods described, the use of ionic liquids for REEs separation is receiving increasing attention in the hopes of developing more environmentally friendly separation techniques by eliminating phosphorous or sulphur containing compounds. The properties and advantages of ionic liquids used for rare earths extraction will be further discussed in the chapter 3 of this thesis.

Chapter 2: Aim of the Thesis

1. Aim and objectives

The goal of this thesis is to investigate hydrometallurgical routes to recover these essential metals for the sake of eventual implementation in urban mining operations. Among all the hydrometallurgical processes described in this manuscript, greater efforts have been conducted towards evaluation of the feasibility of ionic liquid separation through different sorts of extraction techniques. Mathematical modelling of the reported extraction systems has been undertaken with the aim of providing a computational tool that could be easily tailored to predict the performance of other collecting processes. The effectiveness, efficiency and the technical viability of the proposed procedures have been discussed in depth.

In order to accomplish the general aim of this thesis, some specific objectives were defined early on in the research program to facilitate the gradual development of the study by targeting of small goals:

- Establish base line information to bring into focus the importance of the rare earth elements for the development of modern industry and green technologies, illustrate the current rare earths critical status regarding their economic importance and supply risk, and review the most common recovery and recycling approaches found in the literature.
- Assess the performance of different conventional extractants and diluted ionic liquids for the liquid-liquid extraction of rare earth elements from aqueous solutions.
- Evaluate the effectiveness of ionic liquid solutions in supported liquid membranes (SLM) for selective separation of REEs.
- Develop mathematical models to predict the extraction behaviour of the proposed extraction systems.
- Perform leaching tests to recover rare earth elements from end-of-life fluorescent lamps.

Chapter 3: Experimental Methods

This chapter gathers the materials, separation methods, characterization techniques and data analysis tools used throughout the experimental program on which this thesis is based. A detailed description of ionic liquids is provided in order to highlight the benefits of these materials for application in rare earths separation technologies.

1. Materials

1.1. Commercial Reagents

Neodymium oxide (Nd_2O_3), terbium oxide (Tb_2O_3), dysprosium oxide (Dy_2O_3), hydrochloric acid, citric acid, tartaric acid, kerosene, 1-decanol, sodium chloride, sodium hydroxide and sodium carbonate were purchased from Sigma-Aldrich. Oleic acid was provided by Fluka Analytical. Aliquat 336 (methyl-tri(octyl/decyl)ammonium chloride) and D2EHPA (bis(2-ethylhexyl)phosphate, 95%$_w$) were obtained from Alfa Aesar. Cyphos® IL 104 (trihexyl(tetradecyl)phosphonium bis-2,4,4-(trimethylpentyl)phosphinate), Cyanex® 923 (mixture of trialkylphosphine oxides) and Cyanex® 272 (Bis(2,4,4-trimethylpentyl)phosphinic acid) were gently provided by Cytec Canada INC. TBP (tributylphosphate) was purchased from Merck.

A sample of end-of-life fluorescent lamp waste containing phosphors obtained after crushing the lamps and separation of glass, aluminium end-caps, electronic modules, etc., was used for the recovery of rare earths via selective leaching. The sample was kindly supplied by the Chalmers University of Technology (Gothenburg, Sweden). Their samples were provided in turn by Nordic Recycling AB (a member of the Hans Andersson Group AB).

1.2. Ionic liquids: tailored reagents

Ionic liquids are typically used as diluents, but they can also act as selective extractants. They are increasingly gaining attention as alternative solvents in hydrometallurgical separation of metals, mostly because they are regarded to be more environmentally friendly than the conventional organophosphorus solvents and also because of their suitable properties. Their low volatility, adjustable miscibility and polarity, and electrical conductivity make them better substitutes for common solvents (Tunsu and Retegan, 2016). Ionic liquids are considered “designer solvents” because their anions and cations can be tailored to meet the needs of the extraction system. Their valuable physicochemical properties include a low melting point (below 100ºC), very low vapour pressure, high thermal stability, high electrical conductivity, a wide electrochemical window, a low surface tension and an adjustable solvent viscosity and/or

polarity and/or hydrophobicity associated with low or high water miscibility (Berthod et al., 2018).

Ionic liquids (ILs) are organic molten salts with melting points lower than 100ºC. Those with melting points below room temperature are called room temperature ionic liquids (RTIL). They are viscous and non-volatile because of their negligible vapour pressure. ILs have an elevated molecular polarity range. However, unlike most molecular solvents of similar polarity range, they are typically poorly soluble in water and their solubility is highly dependent on the anion. This is the most important property from the point of view of solvent extraction, because it will determine environmental and economic management related issues.

ILs are made by associating large organic cations with a wide variety of anions. They are formed by big asymmetrical ions with diffused charge density. Figure 24 shows some of the most common used cations and anions in ILs. Large organic cations are preferred for solvent extraction applications since their hydrophobicity prevents the loss of the ionic liquids into aqueous solutions by dilution (Hidayah and Abidin, 2018). For instance, imidazolium and pyridinium bonded with hexafluorophosphate offer low extraction performances because they tend to be miscible with aqueous phase. Primary ammonium salts like Primene JMT, which is a mixture of primary amines with 18 to 22 carbon atoms, face the same problem, and so the use of phase modifiers such as 1-decanol and isooctanol is required to avoid the extractant losses due to the miscibility drawback and to facilitate the phase separation.

Imidazolium has good reputation as being highly selective for metal ions. It is versatile, has flexibility in design and can be used in different kinds of metal separation techniques. The alkyl groups of imidazolium ([$C_n$mim]) are extendable and it has been found that the longer the chains the better the hydrophobicity and the viscosity (Hidayah and Abidin, 2018). Separation of REEs with imidazolium ILs has been broadly investigated in the literature. However, it has become more common in synergistic extractant systems. N,N-dioctyldiglycol amic acid (DODGAA) in the ionic liquid [C4mim][Tf2N] (1-butyl-3-methylimidazolium bis(trifluoromethylsulfonyl)imide) shows good extraction of rare earth metals from acidic leachates of phosphors collected from fluorescent lamps (Yang et al., 2013). When comparing it with PC88A, DODGAA-IL shows better separation and extraction efficiency between rare earths and transition metals at 30ºC in sulphate media. In another study, a mixture of Cyanex 923 and ionic liquids phases containing the bis(trifluoromethylsulfonyl)imide anion have been tested for the extraction of neodymium and some other REEs from nitrate media (Alok Rout and Binnemans, 2014a). The extraction efficiency has shown to be strongly dependent on the hydrophilicity of the ionic liquid cation as well as its solubility in the aqueous phase. Ionic liquids with a small hydrophilic

cation, like [C4mim][Tf2N] extract Nd(III) efficiently via an ion-exchange mechanism, however ionic liquids with a hydrophobic cation, like [P66614][Tf2N] extract Nd(III) much less efficiently because the ion-exchange is suppressed by the low solubility of the ionic liquid cation.

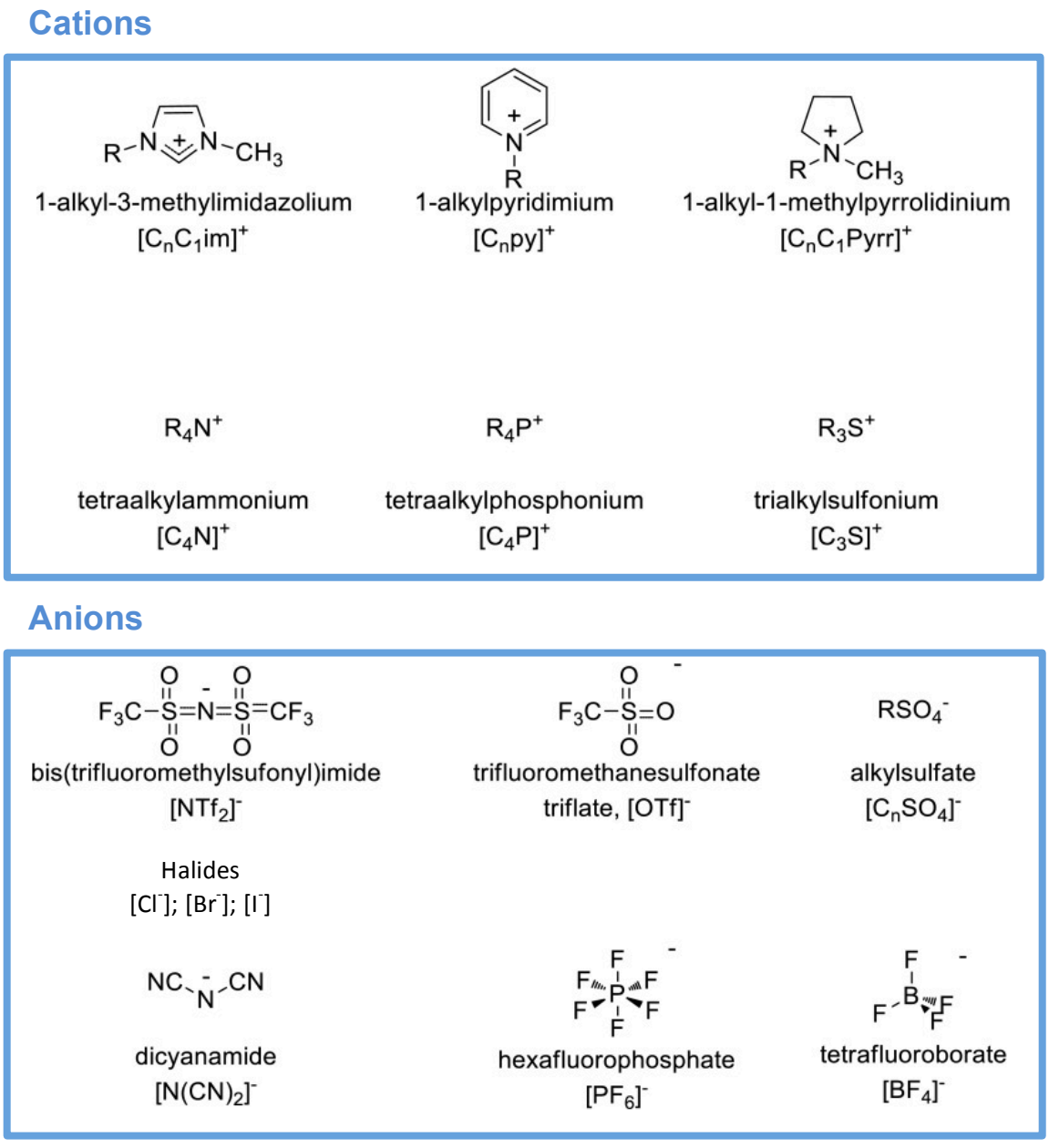

Figure 24. Examples of some commonly used cations and anions for ionic liquids. Adapted from (Welton, 2018).

Phosphonium ILs have lower density than the imidazolium ones but have higher electronic polarisabilities. Many phosphonium ILs used for separation are based on the widely known and applied Cytec Industries trialkylphosphine oxides (Cyphos IL 101, Cyphos IL 104, Cyphos IL 109 and Cyphos IL 111) (Regel-Rosocka and Materna, 2014). The extraction of several rare earths from nitric solutions by solvent extraction has been achieved using the non-fluorinated

functionalised ionic liquid $[P_{66614}][MA]$ diluted in the ionic liquid $[P_{66614}][NO_3]$ (Alok Rout and Binnemans, 2014b). A $[P_{66614}][MA]$ concentration of 0.05 $mol \cdot L^{-1}$ is sufficient to recover almost 100% of REEs despite the relatively high viscosity of the ionic liquid diluent $[P_{66614}][NO3]$. The proposed ionic liquid system is able to separate efficiently the rare-earth ions from transition metal ions, which are normally present along with rare earth ions in end-of-life products. Similarly, synergistic extraction of trivalent rare earth elements from hydrochloric acid solution using mixtures of methyltrioctylammonium sec-octylphenoxy acetate ($[N_{1888}][SOPAA]$) and trihexyl(tetradecyl)phosphonium bis(2,4,4-trimethylpentyl)phosphinate ($[P_{66614}][BTMPP]$, Cyphos IL 104) has been investigated (Ma et al., 2017). The extractabilities of mixed $[N_{1888}][SOPAA]$ and $[P_{66614}][BTMPP]$ seem to be much better than those of mixed HSOPAA and HBTMPP.

Pyridinium has higher viscosity compared to other types of ILs. Pyrrolidinium is a new alternative to pyridinium and imidazolium ILs with higher thermal stability. It is hygroscopic but insoluble in water. Pyridinium and pyrrolidinium ionic liquids have been tested on metal ions such as silver palladium and gold but there is not much information available yet about their application in rare earths separation in the literature.

Quaternary ammonium compounds such as Aliquat 336 have lower melting points and higher viscosity than their phosphonium analogues. Extraction systems involving the use of Aliquat 336 can operate very efficiently without a ligand complexing metal ions (Regel-Rosocka and Materna, 2014). They can also be easily altered by selection of the conjoined anion. With the right settings, Aliquat 336 can be successfully used in the separation and extraction of rare earths due to its hydrophobic characteristics (Hidayah and Abidin, 2018). Aliquat 336 has high potential as an affordable and versatile IL to be used for solvent extraction of REEs by simple substitution reaction. An ionic liquid extraction system has been designed for the separation of neodymium (III) from aqueous solutions using the functionalized ionic liquid [A336][DGA] (Trioctylmethylammonium Dioctyl Diglycolamate) diluted in the ionic liquid $[A336][NO_3]$ (trioctylmethylammonium nitrate) (Alok Rout and Binnemans, 2014c). The distribution ratios obtained in [A336][DGA] were compared with those observed with the molecular extractant N,N-dioctyl diglycol amic acid (HDGA), from which the anion of the ionic liquid extractant is prepared. The distribution ratio for extraction of neodymium(III) by [A336][DGA] in $[A336][NO_3]$ was higher than that for extraction by HDGA in $[A336][NO_3]$, at pH values >2. Under the experimental conditions investigated, nearly 100% extraction of neodymium(III) is possible, despite the relatively high viscosity of the ionic liquid diluent $[A336][NO_3]$. Moreover, The ionic liquid system [A336][DGA]/ $[A336][NO_3]$ is environmentally friendlier than solvent extraction systems with fluorinated ionic liquids or with volatile organic solvents. In a similar context,

Aliquat 336 has been applied for recycling of REE-containing end-of-life products. Selective extraction of REEs from NiMH batteries leachates has been achieved using Aliquat 336 first to extract cobalt, iron manganese and zinc, and then Cyanex 923 (10%) diluted in [A336][NO_3] (methyl-tri(octyl/decyl)ammonium nitrate; 90%) to selectively extract the rare earth metals from the obtained raffinate (Larsson and Binnemans, 2014). During the investigation it was found that Aliquat 336 yields to higher distribution ratios for rare earths extraction compared with Cyphos IL 101 (trihexyl(tetradecyl)phosphonium chloride) and so lower concentration of Cyanex 923 is required.

As can be noted, most REE extraction attempts with ionic liquids in the literature are made by combining different solvents to design new synergistic extractants (SE). Figure 25 displays the evolution of the extractant trends used for solvent extraction of rare earth elements.

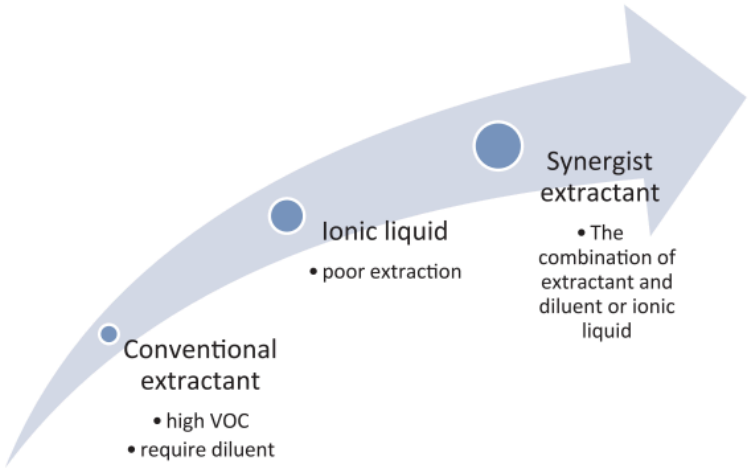

Figure 25. The evolution of the extractants used in extraction of REE in solvent extraction procedures (Hidayah and Abidin, 2018).

The use of synergistic extractants has become very common in SX of REEs to increase separation, selectivity and avoid solubilisation of the organic phase. SE is a combination of two or more solvents to form a new dynamic solvent.

In this regard, several synergistic ionic liquids have been prepared and tested during this investigation. AliOle, AliCy, AliDec and AliD2EHPA ionic liquids were prepared by reacting Aliquat 336 with equimolar amounts of Oleic Acid, Cyanex 272, Decanoic Acid and D2EHPA, respectively, diluted in kerosene. The commercial ionic liquid Aliquat 336 and the acidic extractants were mixed in a separatory funnel. Reactions (11) and (12) summarize the synthesis of the extractants. Aliquat 336 ($\overline{R_4N^+Cl^-}$) provided the cationic part of the ionic liquid and the organic acids ($\overline{HX}$) the anionic part. The bar over the species denotes that they are in the organic phase.

$$\overline{R_4N^+Cl^-} + \overline{HX} \leftrightarrow \overline{R_4N^+Cl^- \cdot HX} \quad \text{(R.11)}$$

During the reactions HCl was formed. In order to eliminate it, the organic solution was washed with a 0.5 mol·L^{-1} $NaHCO_3$ solution until no further Cl- was present in the aqueous phase.

$$\overline{R_4N^+Cl^- \cdot HX} + NaHCO_3 \leftrightarrow \overline{R_4N^+X^-} + CO_2 \uparrow + NaCl + H_2O \quad \text{(R.12)}$$

The transfer of HCl from the organic to the aqueous phase was measured by Cl^- titration with $AgNO_3$. Two washing steps were required to eliminate the HCl completely.

2. Separation techniques

A summary of the separation techniques approached in this thesis is presented below.

2.1. Liquid – liquid extraction

Liquid – liquid extraction (LLE) is a separation process consisting of the transfer of a solute from one solvent to another, the two solvents being ideally immiscible with each other. Typically, one of the solvents is an aqueous mixture and the other is a non-polar organic liquid. The liquid – liquid extraction can comprise the following steps (SX Kinetics, 2002):

- Extraction: The operation of transferring the metal of interest from the feed to the organic phase by mixing, followed by phase separation. The extraction stage produces a loaded organic phase containing the solute and an aqueous phase depleted of the metal known as raffinate.
- Scrubbing: The selective removal of impurity metals from the loaded organic phase by treatment with an aqueous scrub solution. The scrubbing step leaves the organic phase loaded with the metal of interest.
- Stripping: The removal of the valuable solute from the scrubbed organic phase by reversing the extraction chemical reaction. The strip liquor is the product of the extraction process.
- Regeneration: The treatment of the stripped organic phase for removal of metals that were not scrubbed or stripped. This stage produces a regenerated organic phase to be used once again as organic feed.

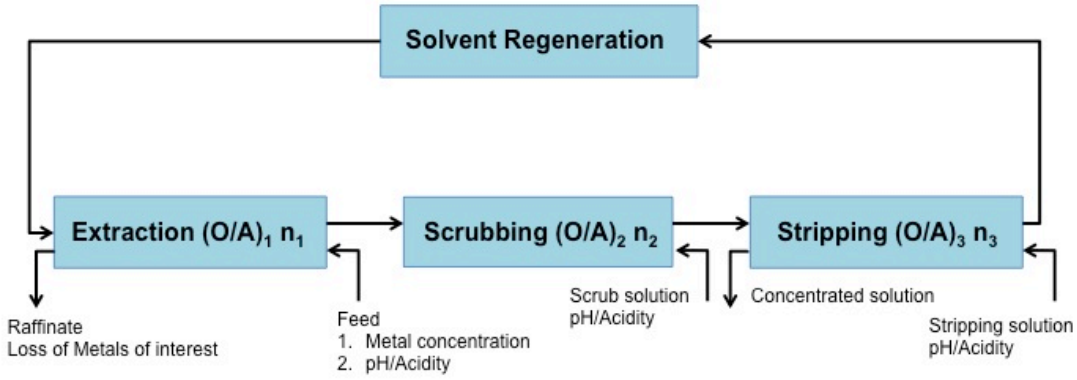

Figure 26. Typical solvent extraction block diagram for separation and purification of metals.

The metal recovery in liquid – liquid extraction is mainly dependent on the composition and pH of the aqueous phase (feed, scrub and strip solutions), the composition of the organic phase (solvent, diluent and phase modifier), the number of stages in extraction, scrubbing and stripping units (n_i) and the O/A ratios in the three units. In this particular investigation, only extraction and stripping were carried out because of the features of the separation experiments, since they were performed in individual steps, not in a counter-current system, which would require regeneration of the organic phase for it to be reused.

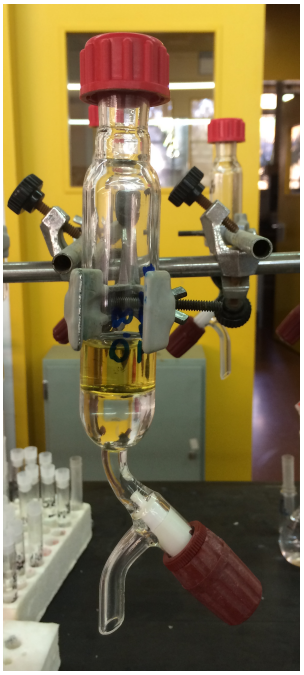

Figure 27. Separatory funnel used for LLE.

The extraction experiments were carried out by shaking equal volumes of aqueous and organic phases (10 mL) in separatory funnels using an MVH-40 SBS horizontal mechanical shaker (150 rpm) at room temperature (21±2ºC). Figure 27 shows the detail of the separatory funnels used for liquid-liquid extraction. After phase separation, the aqueous phase was collected and its pH was measured with a calibrated Crison micropH 2002 pH meter. After analysis, the following equation was used to calculate the extraction percentages of the metals:

$$\%E = \frac{[\overline{Me}]}{[Me]_{ini}} \cdot 100 = \frac{[Me]_{ini} - [Me]_{aq}}{[Me]_{ini}} \cdot 100 \qquad \text{(Eq.1)}$$

Where $[\overline{Me}]$, $[Me]_{ini}$ and $[Me]_{aq}$ are the metal concentrations in the organic phase, in the feed solution and in the aqueous phase after extraction,

respectively.

Acidic stripping solutions were used to close the mass balance and recover the metals loaded in the organic phase after extraction. The stripping experiments were performed following the same steps as in the extraction experiments. After analysis of the concentrated stripping solution, equation 2 was used to determine the stripping percentages:

$$\%S = \frac{[\mathrm{Me}]_{\mathrm{strip}}}{[\overline{\mathrm{Me}}]} \cdot 100 \qquad \text{(Eq.2)}$$

where $[\mathrm{Me}]_{\mathrm{strip}}$ is the metal concentration in the stripping solution.

The extraction and stripping percentages can be calculated from the metals concentrations in the aqueous solutions because the A:O ratio is 1:1 in all the experiments performed. The number of stages or contacts required for complete stripping of the metals will be further addressed in the following chapter, as it can vary from one experiment to another.

2.2. Supported liquid membranes

Supported liquid membranes (SLM) consist of a tri-phase separation technique to extract solutes from a continuously flowing aqueous stream through a thin layer of a hydrophobic organic phase immobilized onto a polymeric support with subsequent stripping into another aqueous phase. The microporous support offers mechanical resistance and the organic solution conforms the selective barrier.

Transportation in liquid membranes is a dynamic and non-equilibrium process. It is influenced by both physical and chemical parameters. Physical parameters that could influence the transportation are the stirring speed of the aqueous phases and the membrane surface. The chemical parameters are mainly the pH of the solutions, their ionic strength, the analyte concentration, the organic phase formulation and the stripping solution used. The solute that is to be transported is extracted first by the organic phase and then diffused to the aqueous stripping phase. The driving force of the separation process is the concentration gradient between the fluids. The organic extractant facilitates the selective distribution of the metals between the feed and the stripping solution. Figure 28 displays schematically the operation of a supported liquid membrane. The following steps are involved in the transport of metallic species from the feed to the stripping solution (Padwal et al., 2018):

- Diffusion of the metal ions from the bulk of the feed phase to the inner surface of the membrane.
- Selective extraction of species from the feed to the membrane interface.
- Convective transport of the complex across the liquid membrane.

- Diffusion of the complex across the outer surface of the membrane in the strip side.
- Stripping of the metal ions from the outer surface of the membrane.

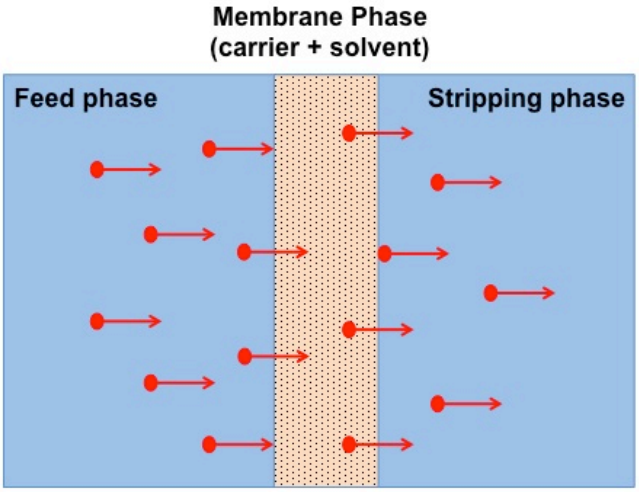

Figure 28. Schematic operation solute transport in a supported liquid membrane.

In this investigation, the supported liquid membrane assays were carried out based on the optimum extraction conditions found with the liquid-liquid extraction experiments. The membrane tests were performed in a device consisting of two acrylic semicircular extraction cells in contact through a flat membrane. The cells had circular windows of 40 mm in diameter to place the supported liquid membrane and a volume of 230 mL each. The system provided agitation by two electric stirrers of variable speed, which were set to 1000 rpm. A vigorous agitation is required to minimize the interface thickness formed on either side of the liquid membrane that could hamper the diffusion. As a support for the organic phase, a hydrophobic Durapore HVHP04700 membrane with an effective area of 11.4 cm^2, pore size of 0.4 µm, 75% porosity, 45 mm diameter and 125 µm thickness was used. Figure 29 gives detailed pictures of the different parts of the SLM assembly performed.

For preparation of the SLM, the porous film was soaked in the carrier (ionic liquid + dissolvent + phase modifier) during at least five minutes at room temperature. The impregnation of the microporous solid support was achieved by capillarity.

After attaching the membrane in between the cells, the stripping and feed solutions were added (210 mL), one in each cell. The addition of the feed solution ushers the experiment. The pH of the feed phase was continuously monitored using a calibrated pH meter in order to ensure that the optimum pH transport conditions set were maintained.

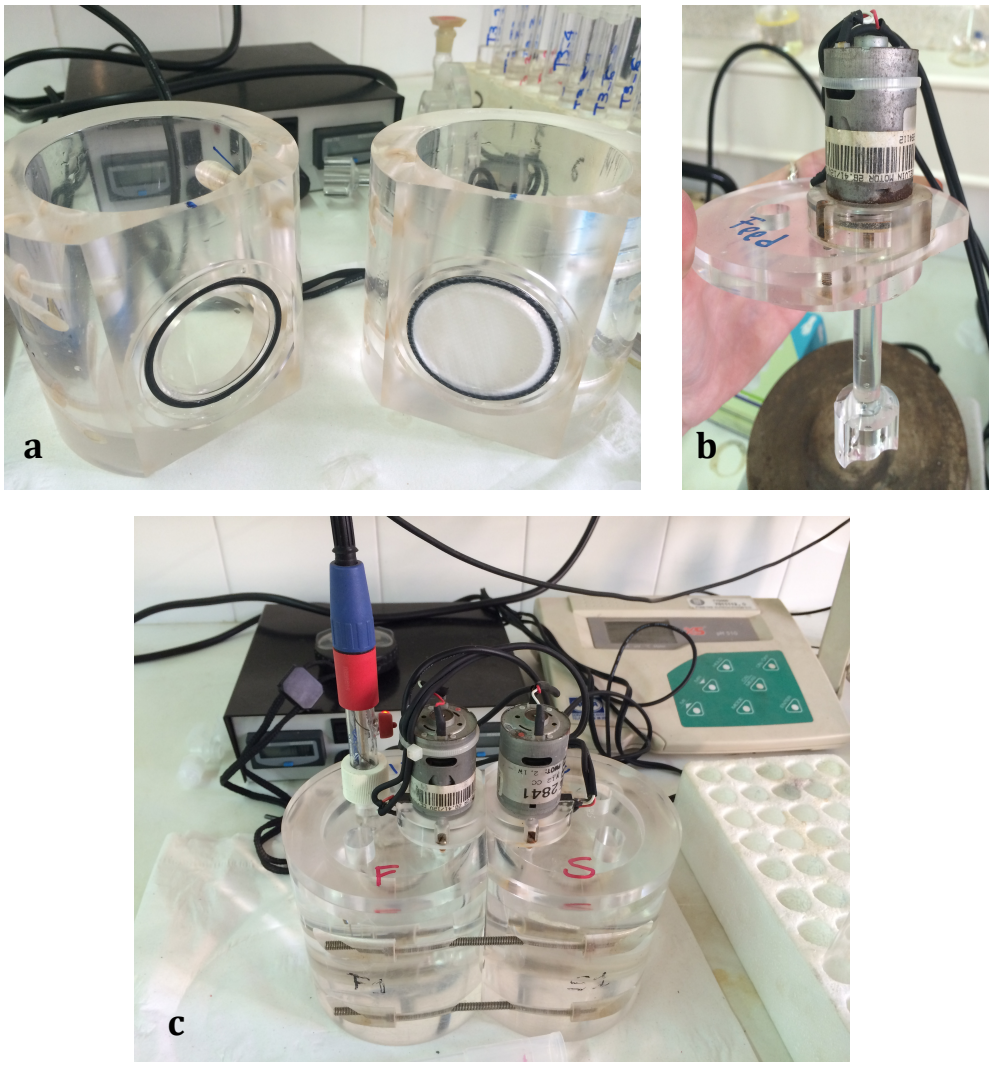

Figure 29. Pictures of the supported liquid membrane assembly: a) extraction cells with SLM attached; b) detail of electric stirrer; c) complete assembly of the SLM device.

The assay took around 7 to 8 hours to perform. For the first two hours, 10 mL stripping samples were taken every 30 minutes, to check on the initial transport kinetics. After that time, the samples were taken every hour. The volume of the solutions taken was replaced with fresh stripping solution and so the concentrations of metals in the samples were diluted and the analysis results had to be corrected following equation 3:

$$C_T = \frac{V_{cell} \times C_{t'} + \sum_{i=2}^{T} C_{ti} \times V_m}{V_{cell}} \qquad \text{(Eq.3)}$$

Where, C_T is the real metal concentration in the stripping cell in a specific time frame; V_{cell} is the total volume of the stripping cell; C_t is the metal concentration analysed in a specific time frame; $C_{t'}$ is concentration in the present time and V_m is the volume of the sample taken.

The mass balance of each cell was studied to quantify the metal transport and to calculate the permeability of the SLM, which is a key factor to numerically compare different operation conditions and to generate mathematical models for prediction of metal transport. The calculation of the permeability coefficient will be further addressed in the following chapter, as it depends on the experimental conditions and so different expressions were inferred.

3. Characterisation techniques

3.1. Microwave plasma atomic emission spectroscopy (MP-AES)

The REEs content of the selected samples was determined by Microwave Plasma Atomic Emission Spectroscopy using an MP-AES 4100 spectrophotometer from Agilent Technologies. Figure 30 displays a simplified diagram of a microwave plasma atomic emission spectrometer.

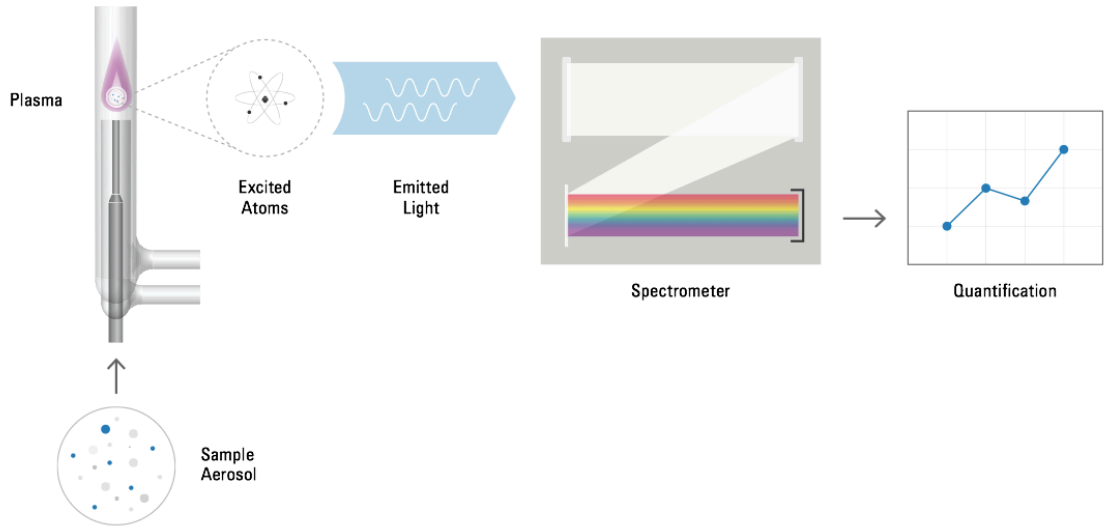

Figure 30. Schematic diagram of the different parts of a microwave plasma atomic emission spectrometer (Agilent Technologies, 2016).

An aerosol is created from the liquid samples using a nebulizer and a spray chamber. The aerosol is then introduced into the centre of a nitrogen-fuelled microwave plasma, which reaches temperatures nearing 5000 K. At these temperatures, atomic excitation is strong and leads to excellent detection limits. The excited atoms emit light at characteristic wavelengths for each element as they return to lower energy states, Table 15 gathers the characteristic emission wavelengths of Nd(III), Tb(III) and Dy(III). The emission is directed towards a fast scanning monochromator where the selected wavelength range is imaged onto a high efficiency detector that measures both spectra and background

simultaneously. Quantification of the metallic elements is achieved by comparing their emission to that of known concentration of the same elements plotted on a calibration curve (Agilent Technologies, 2016).

The determination of the metallic content was carried out analysing the aqueous samples (feed and stripping) diluted in a matrix of 0.5 $mol \cdot L^{-1}$ nitric acid, whereas the concentration of the analytes in the organic phase was calculated by means of mass balance.

Table 15. Characteristic emission wavelengths of Nd(III), Tb(III) and Dy(III).

Element	Wavelength (nm)
Nd (III)	430.4
Tb (III)	350.9
Dy (III)	353.2

4. Data analysis: Mathematical modelling

Mathematical modelling of solvent extraction systems was undertaken using the Matlab software R2016a and R2017b versions (Mathworks, 1984). The mathematical models proposed were based on the equilibria equations and mass balances involved in the separation systems, which were treated as optimization parameters to find the values of the unknown formation and equilibrium extraction constants that match experimental and calculated data with the minimum error. The resolution method applied is shown in Figure 31.

According to the flowchart, the resolution of the solvent extraction system started setting a matrix of experimental data. The experimental matrices typically contain, separated by columns, the initial conditions of the aqueous and organic solutions and the experimental values of the extraction percentages obtained.

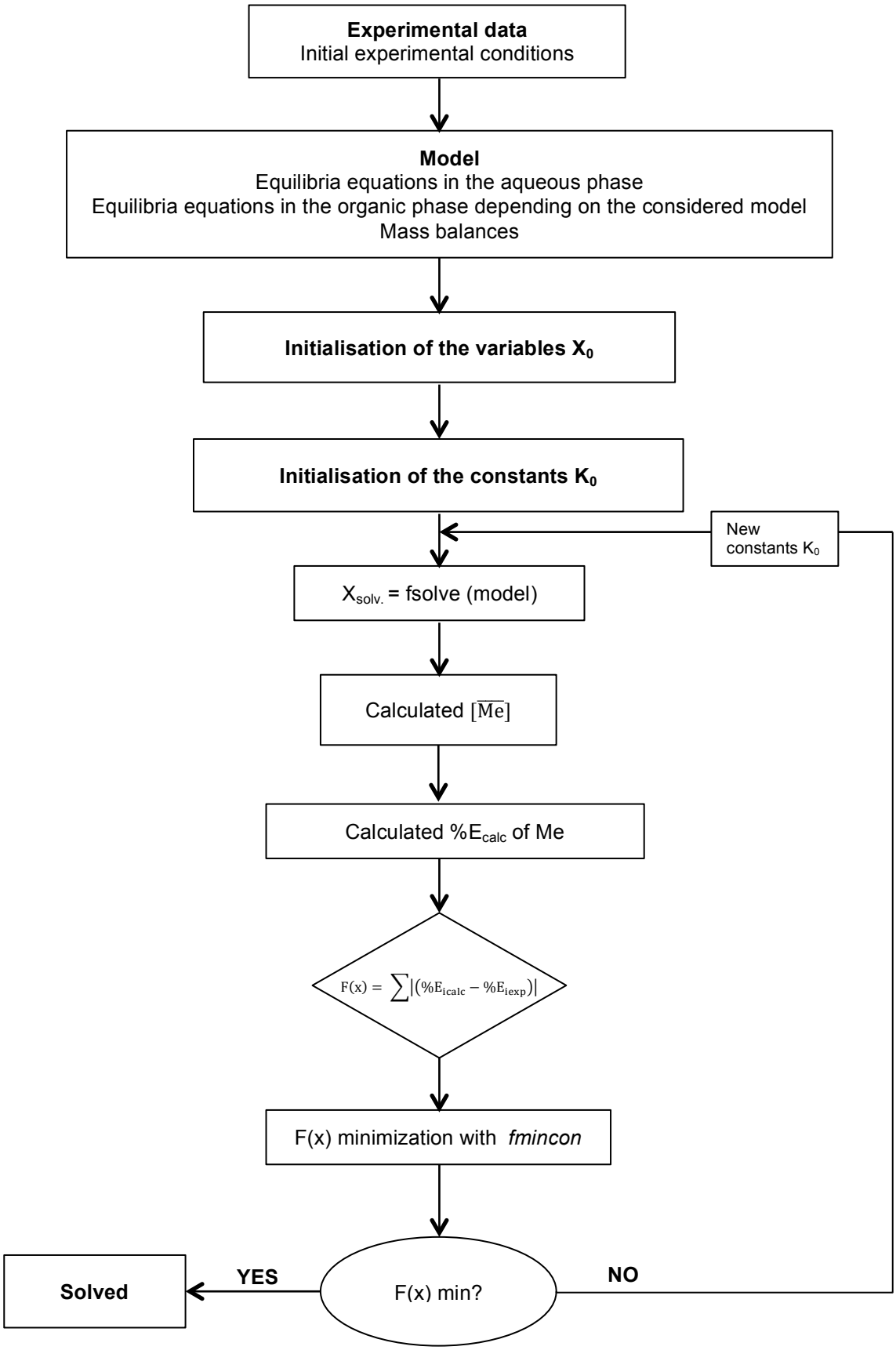

Figure 31. Flow chart of the generic resolution of REEs separation applicable to different solvent extraction systems. Adapted from (E. Obón et al., 2017a).

Next, the equilibria equations in the aqueous and the organic phase as well as the mass balances involved in the extraction system were introduced and grouped in a balance block, and the initial guesses for all the species concentrations and the equilibrium/formation constants (X_0 and K_0, respectively) were entered. The nonlinear equations system was solved with the Matlab function *fsolve*. Eq. 1 was then applied to obtain the calculated metal extraction percentages from the calculated metal concentrations in the organic phase after extraction.

The calculated extraction percentage is a key parameter in the model resolution since the optimization of the stability and equilibria constants depends on the sum of the square of the differences between the calculated and the experimental percentages of extraction. The function F(x) was defined as:

$$\mathrm{F(x)} = \sum \left| \left(\%\mathrm{E_{icalc}} - \%\mathrm{E_{iexp}} \right)^2 \right| \qquad \text{(Eq.4)}$$

The F(x) function was minimized using the Matlab function *fmincon,* which finds the minimum constrained of a nonlinear multivariable function. The optimization led to the determination of the stability and equilibria constants, whose values allowed the experimental extraction extension of the metals to be reproduced with the minimum error.

Chapter 4: Results and discussion

This chapter recaps the experimental results and mathematical modelling obtained over the course of this thesis, divided into different subsections. The experimental results have been thoroughly discussed in order to justify the assessments made in terms of the viability of the separation procedures proposed. The findings of this research provide the guidelines for further investigation in terms of recovery of rare earth elements from end-of-life products based on hydrometallurgical routes and mathematical modelling of solvent extraction systems.

1. Experimental studies of neodymium, terbium and dysprosium extraction from acidic solutions

The effect of different types of extractants, the concentration of salting-out reagents in the aqueous phase, the pH of the feed solution and the organic phase composition, was studied in order to set a suitable work frame and to evaluate and compare the performance of different REEs extraction systems for further mathematical modelling investigation. Stripping studies using acidic agents were carried out in order to recover the metals loaded in the organic phase and close the mass balance.

1.1. Screening of extractants

Chemical characteristics of the extractants play a determining role in their extraction efficiency. For purposes of ease and clarity, the solvent extractants used in this investigation were originally classified as shown in Figure 32.

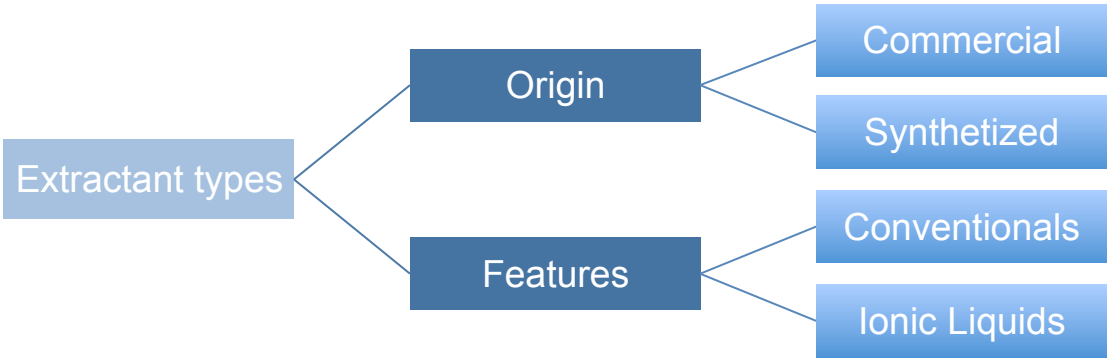

Figure 32. Classification diagram of different extractant types regarding their origin and characteristic features.

As can be seen in figure 32, in the early stages of the research, the extractants were sorted based upon their origin and their characteristic features. Regarding

their origin, they were divided into commercial and synthetized. The commercial extractants supplied by the manufacturers were used without additional purification or saponification. The commercial extractants chosen were Cyanex 272, Oleic Acid, Cyanex 923, TBP, Cyphos 104 and Aliquat 336. The synthetized solvents were prepared in the laboratory following the procedure described in the section 1.2 of chapter 3. The synthetized ionic liquids were called: AliOle, AliCy, AliDec and AliD2EHPA, and were used dissolved in kerosene.

Apart from their origin, the extractants were also classified based on their chemical features. Acidic and solvating extractants as well as ionic liquids solutions were tested to compare their REEs extraction performances under different experimental conditions. Table 16 summarizes the organic extractants used regarding their chemical characteristics, which determine the metal ion extraction mechanisms.

Table 16. Organic extractants used classified according their chemical features.

Extractant type	Name	Simplified chemical formula
Acidic	Cyanex 272	$\overline{\mathrm{HCy}}$
	Oleic acid	$\overline{\mathrm{HA}}$
Solvating	TBP	$\overline{\mathrm{RO_3PO}}$
	Cyanex 923	$\overline{\mathrm{R_3PO}}$
Ionic liquids	Aliquat 336	$\overline{\mathrm{R_4N^+Cl^-}}$
	Cyphos 104	$\overline{\mathrm{R_4P^+Cy^-}}$
	AliCy	$\overline{\mathrm{R_4N^+A^-}}$
	AliDec	
	AliOle	
	AliD2EHPA	

The simplest and most generic metal ion extraction mechanisms expected with the extractants selected are listed below, metal speciation in the aqueous solution will be addressed further on in this chapter.:

Acidic extractants (Cyanex 272 and Oleic Acid):

$$3\,\overline{\mathrm{HA}} + \mathrm{Me^{3+}} \leftrightarrow\ \overline{\mathrm{MeA_3}} + 3\,\mathrm{H^+} \qquad \text{(R.13)}$$

Solvating extractants (Cyanex 923 and TBP):

$$\mathrm{n}\,\bar{\mathrm{L}} + \mathrm{MeCl_3} \leftrightarrow\ \overline{\mathrm{L_n \cdot MeCl_3}} \qquad \text{(R.14)}$$

Ionic liquids (Aliquat 336, Cyphos 104, AliCy, AliDec, AliOle, AliD2EHPA):

$$3\,\overline{\mathrm{R_4N^+A^-}} + \mathrm{Me^{3+}} + 3\,\mathrm{Cl^-} \leftrightarrow 3\,\overline{\mathrm{R_4N^+Cl^-}} + \overline{\mathrm{MeA_3}} \quad \text{(R.15)}$$

$$3\,\overline{\mathrm{R_4N^+A^-}} + \mathrm{MeCl_3} \leftrightarrow 3\,\overline{\mathrm{R_4N^+A^- \cdot MeCl_3}} \quad \text{(R.16)}$$

In the reactions above, $\mathrm{Me^{3+}}$ represents the neodymium, terbium or dysprosium metallic ions.

As depicted in reactions R.15 and R.16, ionic liquids are able to extract metal ions either by ionic exchange or by solvation. In order to compare the extractants behaviour, several experiments were carried out using neodymium, terbium and dysprosium solutions 7 mmol·L^{-1} each, in chloride media 0.05 and 4 mol·L^{-1}. Different molar concentrations of the commercial solvents were used because it was a first approach to finding which ones are able to extract the chlorinated species and the dilutions with kerosene were done in volume/volume terms. Figure 33 shows the Nd(III), Tb(III) and Dy(III) extraction percentages achieved by each extractant tested. This assay permitted to guess their interaction with REEs species formed.

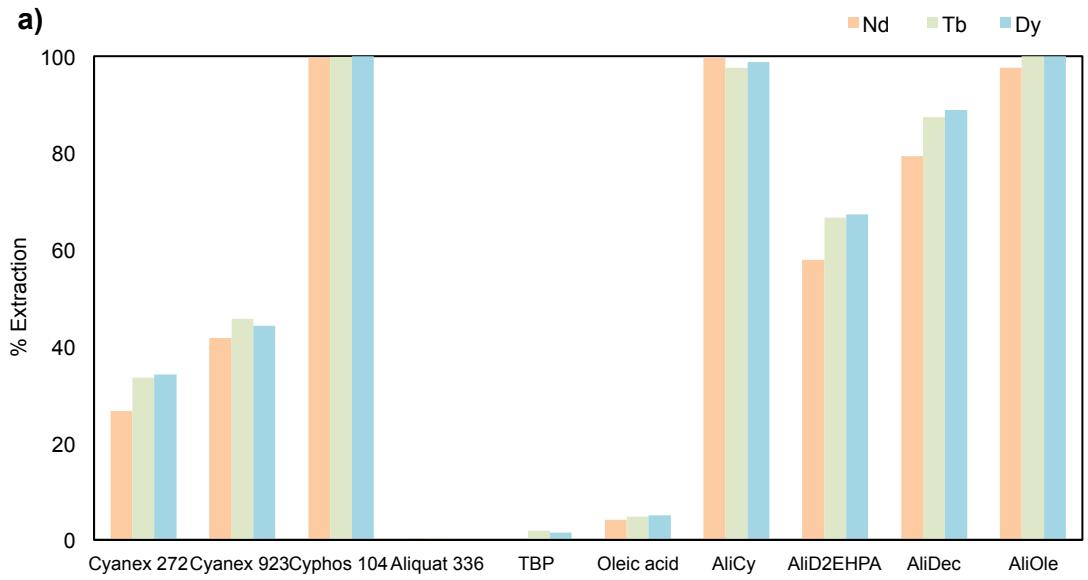

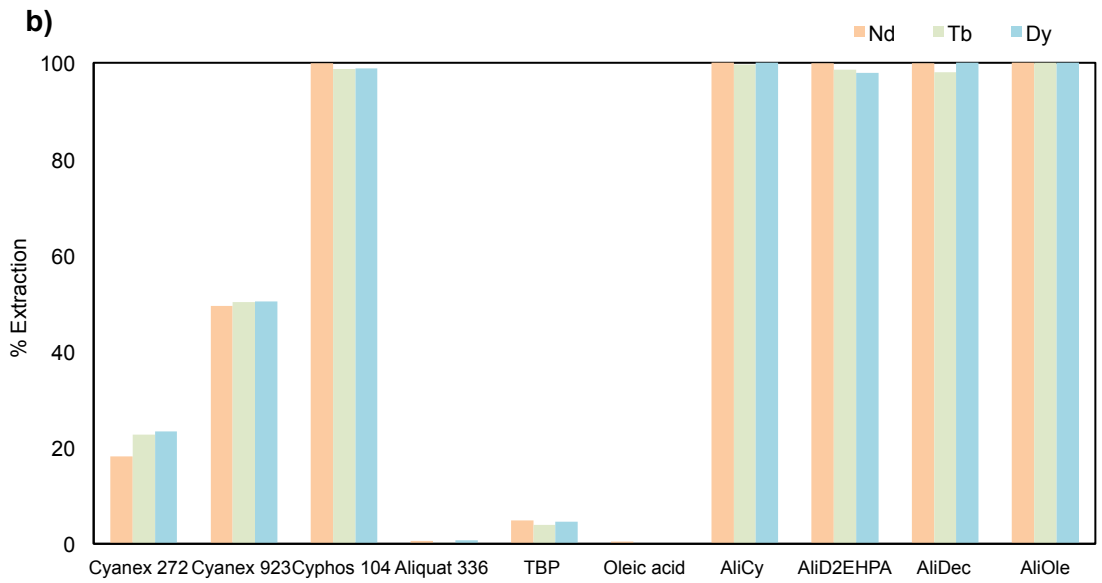

Figure 33. Effect of different extractants on the extraction extension of neodymium(III) terbium(III) and dysprosium(III) solutions, 7 mmol·L^{-1} each, in 0.05 mol·L^{-1} a) and 4 mol·L^{-1} b) chloride solutions, using the extractants listed in Table 16. pHfeed = 3.5. Shaking time = 15 min, at room temperature. [Cyanex 272] = 0.27 mol·L^{-1}, [Cyanex 923] = 0.25 mol·L^{-1}, [Cyphos 104] = 0.27 mol·L^{-1}, [Aliquat 336] = 0.1 mol·L^{-1}, [TBP] = 0.37 mol·L^{-1}, [Oleic Acid] = 0.31 mol·L^{-1} and [synthetized ILs] = 0.1 mol·L^{-1}.

It can be observed that, the extraction yields achieved with the homemade ionic liquids and Cyphos 104 are generally greater than the rest of extractants in both low (a) and high (b) chloride concentration solutions, despite the concentrations of the synthetized ILs are lower (0.1 mol·L^{-1}). As expected, the extraction performance of REEs slightly increases with increasing atomic number, due to the lanthanide contraction. However, the differences are not significant enough to raise a selective extraction system under these experimental conditions.

Aliquat 336 shows very low extraction, throughout the chloride concentration range, compared with the rest of extractants. This behaviour is related to the metal species extracted. Regarding their chemical features, AliD2EHPA, AliCy, AliDec, AliOle and Cyphos 104 can extract both cationic and anionic species by ion exchange and neutral species by solvation, whereas Aliquat 336 needs anionic species to extract by exchanging the Cl^-. Since anionic species are not formed in chloride media under the experimental conditions established, the Aliquat 336 extraction efficiency is found to be null.

Solvating extractants such as Cyanex 923 and TBP typically show better extraction performances in high chloride media. Increasing chloride concentration in the aqueous phase promotes the formation of neutral species that can be extracted by solvation. The REEs speciation in chloride aqueous solutions will be fully disclosed later in the following subsection of this chapter. Nonetheless, as shown in the figure, very low extraction values were obtained

with TBP even for 4 mol·L^{-1} chloride media. According to the literature, the TBP concentration might be low (Michaud et al., 2012). In this regard, extraction experiments with TBP 30% v/v (about 1 mol·L^{-1}) were carried out to evaluate the extraction of 4 mmol·L^{-1} neodymium, terbium and dysprosium from 4 mol·L^{-1} solutions. Extraction percentages around 60% were achieved for each single metal here.

REEs extraction with Cyanex 272 is favoured by low chloride concentrations in the aqueous phase. As a cationic extractant, it will extract preferentially Me^{3+} species from the media and release H^+ acidifying the aqueous phase (R.13). Conversely, the extraction percentages achieved with Oleic Acid are very low compared to the extraction yield of the IL AliOle, which proves the synergistic effect of combining both Aliquat 336 and Oleic Acid for the extraction of rare earths from chloride media.

The synthetized ionic liquids proved to be a good option for rare earth extraction from chloride media. Since all of them were suitable at 0.1 mol·L^{-1}, a comparative study of the extraction efficiency achieved with AliCy, AliDec, AliD2EHPA and AliOle at lower concentration (0.01 mol·L^{-1}) was taken to determine the most suitable one for REEs recovery. Figure 34 shows the extraction percentages of neodymium, terbium and dysprosium achieved with the homemade ILs.

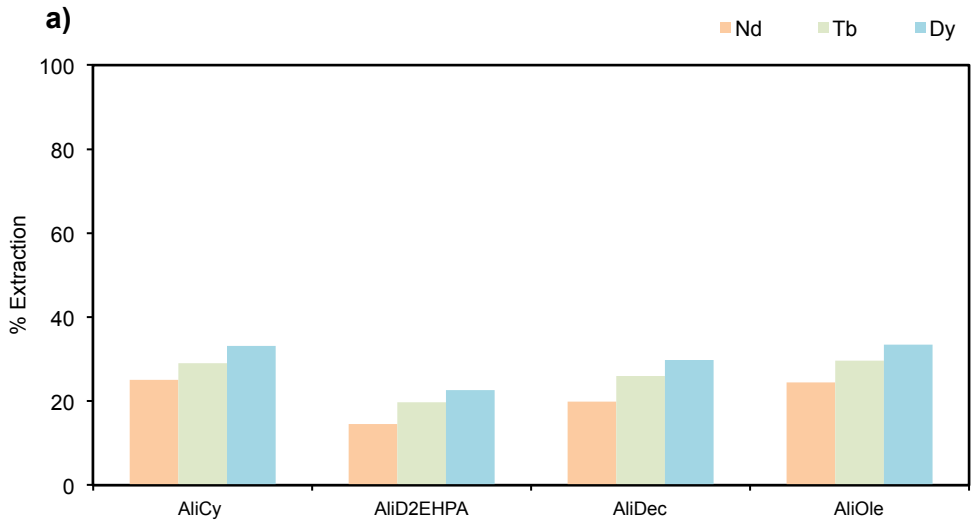

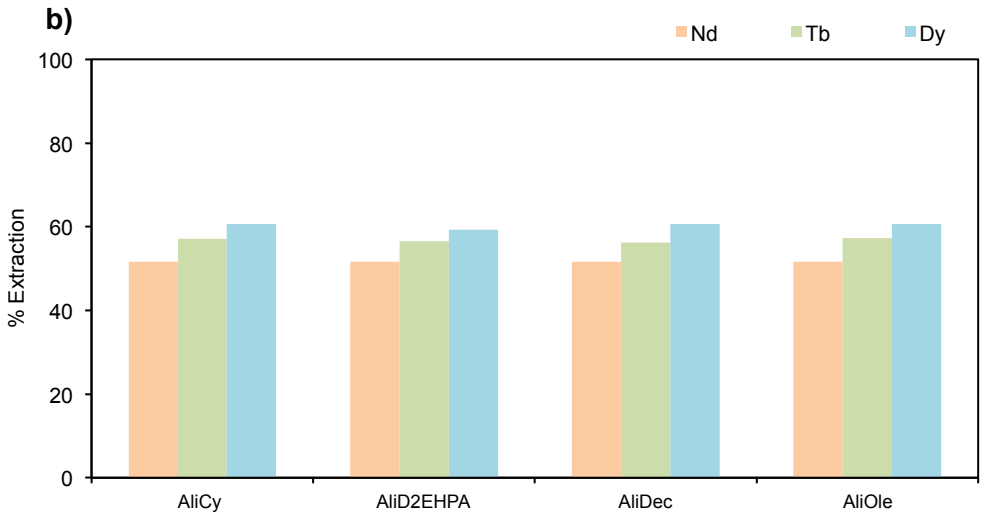

Figure 34. Effect of 0.01 mol·L^{-1} synthetized ionic liquids: AliCy, AliD2EHPA, AliDec and AliOle on the extraction extension of neodymium(III), terbium(III) and dysprosium(III) 7 mmol·L^{-1} each, in 0.05 mol·L^{-1} a) and 4 mol·L^{-1} b) chloride solutions. pHfeed = 3.5. Shaking time = 15 min, at room temperature.

As can be seen, the extraction percentages achieved with the synthetized ionic liquids were all very close. However, because of its faster phase separation, AliOle was chosen among the ILs to further carry on solvent extraction studies of neodymium, terbium and dysprosium.

1.2. Effect of the salting-out reagent in the feed: Metal Speciation

The effect of the salting out agent in the aqueous phase was studied. The extraction performance is typically related to the interaction of the ionic liquid with the metallic species; hence speciation of neodymium, terbium and dysprosium in aqueous phase was assessed. Extraction experiments of Nd(III), Tb(III) and Dy(III) were carried out with AliOle 0.01 mol·L^{-1} from chloride and nitrate aqueous solutions. Figure 35 shows the effect of the chloride and nitrate ions on the extraction efficiency of the REEs.

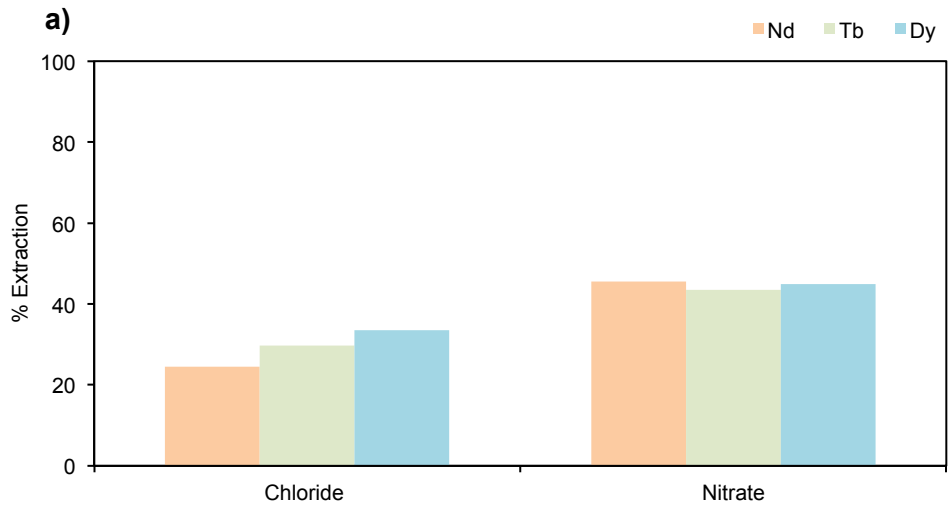

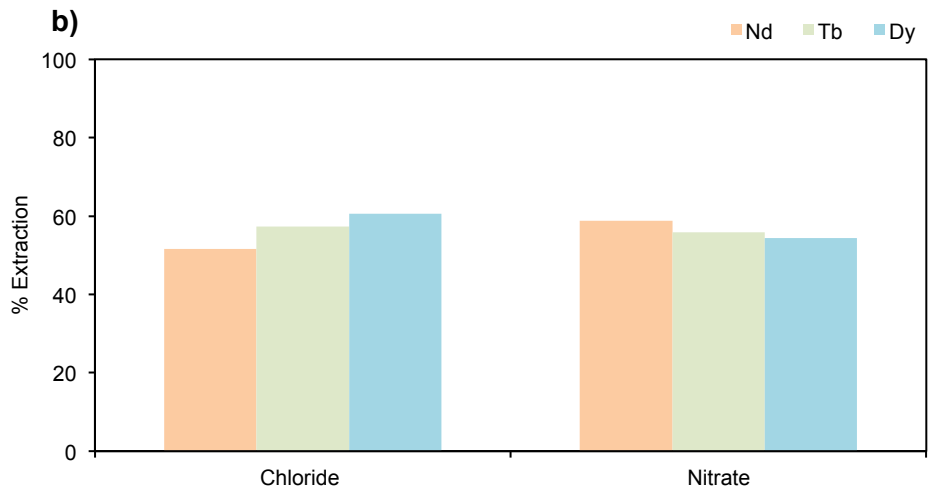

Figure 35. Effect of chloride and nitrate ions in the aqueous phase on the extraction extension of neodymium(III), terbium(III) and dysprosium(III). [AliOle] = 0.01 mol·L^{-1}; [Metals] = 7 mmol·L^{-1} each; pHfeed = 3.5. Shaking time = 15 min at room temperature; a) 0.05 mol·L^{-1} chloride / nitrate ions b) 4 mol·L^{-1} chloride / nitrate ions.

As can be observed, extraction of REEs with AliOle is possible from chloride and nitrate media with similar distribution ratios. In this regard, chemical equilibrium diagrams come in handy to understand the formation of metallic species in the aqueous media and to relate it with the potential extraction mechanisms. Figures 36 and 37 represent the chemical equilibrium diagrams of neodymium, terbium and dysprosium in chloride and nitrate media, respectively. The diagrams were obtained using the Medusa software (KHT Royal Institute of Technology) (Puigdomenech, 2013).

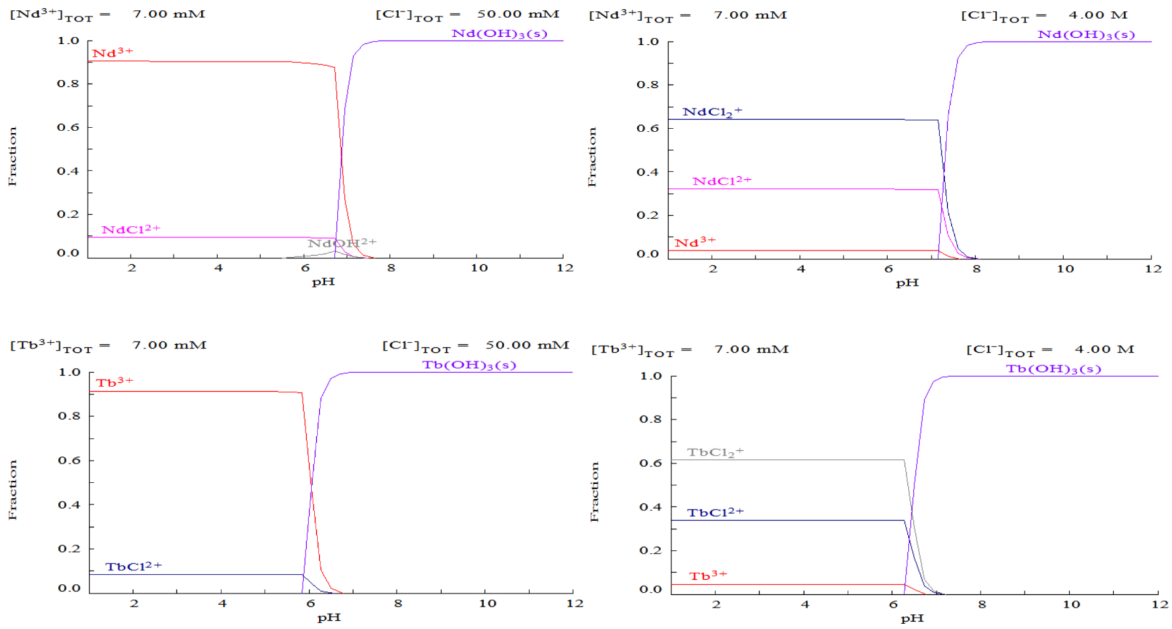

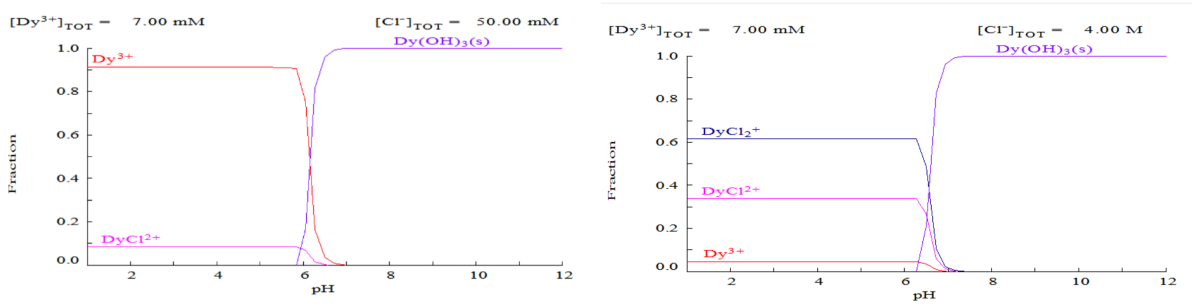

Figure 36. Chemical equilibrium diagrams of 7 mmol·L^{-1} neodymium, terbium and dysprosium in chloride media. The diagrams on the left side correspond to the metal speciation in 0.05 mol·L^{-1} chloride media and on the right side, the metal speciation in 4 mol·L^{-1} chloride media.

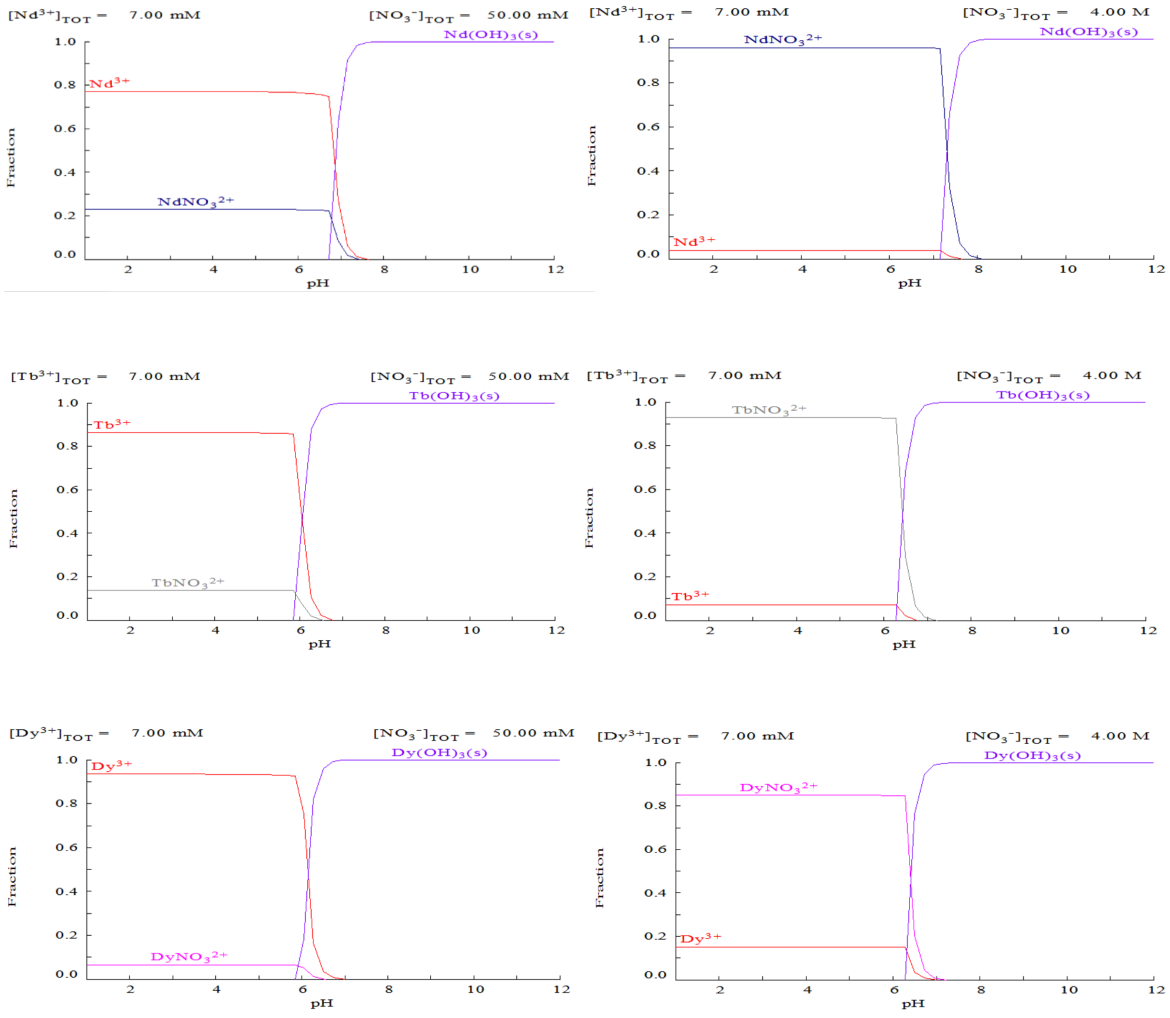

Figure 37. Chemical equilibrium diagrams of 7 mmol·L^{-1} neodymium, terbium and dysprosium in nitrate media. The diagrams on the left side correspond to the metal speciation in 0.05 mol·L^{-1} nitrate media and on the right side, the metal speciation in 4 mol·L^{-1} nitrate media.

The extraction yield showed by ILs in general and AliOle in particular, could be explained by how they interact with the rare earths species formed in the aqueous phase. According to the Medusa diagrams, the speciation of neodymium, terbium and dysprosium is practically identical under the defined experimental conditions (pH = 3.5). Nonetheless, the fractions of the species slightly differ from one metal to another. At low chloride media (0.05 mol·L^{-1} Cl^{-1}) the generic metallic species allegedly formed are Me^{3+} and $MeCl^{2+}$, being Me^{3+} the higher fraction (about 90% of the total concentration). Increasing the chloride concentration to 4 mol·L^{-1} stimulates the formation of $MeCl_2^{+}$ as well. The species distribution proposed is 5% Me^{3+}, 35% $MeCl^{2+}$ and 60% $MeCl_2^{+}$, approximately. However, in the preliminary extraction experiments using neutral extractants such as Cyanex 923 and TBP, extraction of neutral species by solvation was achieved, which means that neutral species have to be formed as well.

Regarding the nitrate media, low nitrate concentrations (0.05 mol·L^{-1} NO_3^{-}) lead to the formation of Me^{3+} and $MeNO_3^{2+}$ species in the aqueous phase, being Me^{3+} the majority (from 77% in the case of Nd to 93% in the case of Dy). According to figure 36, increasing the nitrate concentration up to 4 mol·L^{-1}, does not promote the formation of new metallic species under the experimental conditions, but changes the distribution of the species already formed. The distribution of $MeNO_3^{2+}$ increases beyond 85% and the Me^{3+} species decrease until 15% and below. However, it does not take into account the formation of $Me(NO_3)_2^{+}$, neither the formation of neutral species ($MeNO_3$), which is in disagreement with a large number of studies in the literature that propose extraction mechanisms of REEs neutral species (Panda et al., 2012a; Rout et al., 2013; Alok Rout and Binnemans, 2014a).

The configuration features of the ionic liquids allow them to be able to extract all the species available despite their distribution in the aqueous phase. The extraction performance is primarily dependent upon the distribution coefficient (K). Regardless the chemical equilibrium diagrams provided, it is common knowledge, that positively charged metallic complexes are extracted by the anionic part of the ILs and neutral species are extracted by solvation. Their versatility is one of the main reasons why ionic liquids are considered strategic extractants for the recovery of REEs from aqueous solutions. Despite their limitations, the Medusa diagrams were helpful to choose the pH range to work with, since they show the pH in which nonsoluble species ($Me(OH)_3$) will appear under the working conditions. According to the diagrams, it is advisable to monitor the pH in both nitrate and chloride media and keep it low enough to avoid the precipitation of metals in the aqueous phase, which may distort the extraction values obtained.

The chloride media was chosen to continue the extraction study of neodymium, terbium and dysprosium with AliOle, since a slightly higher potential for separation of the metals was spotted and also because of its easier phase separation. Nonetheless, a parallel study focusing on REEs extraction from nitrate media with AliOle would be ideal to complement and enrich this investigation.

1.3. The effect of the pH in the feed

During the screening of extractants, it was noticed that after metal extraction with the ionic liquids (Cyphos 104, AliCy, AliD2EHPA, AliDec and AliOle) the pH in the aqueous phase increased from 3.5 to 6.0, approximately. According to the chemical equilibrium diagrams in figure 36, approaching pH 6.0 in the feed may generate precipitation of the metals, especially in low chloride media, since nonsoluble metallic species begin to form thereafter. Nonetheless, no precipitation issues were spotted in chloride media in the working pH range. Regarding this observation, a pH study was carried out to investigate the effect of equilibrium pH on the neodymium, terbium and dysprosium extraction with AliOle. Figure 38 shows the extraction percentages of Nd(III), Tb(III) and Dy(III) achieved using 0.015 mol·L^{-1} AliOle IL by varying the pH of the feed adding sodium hydroxide.

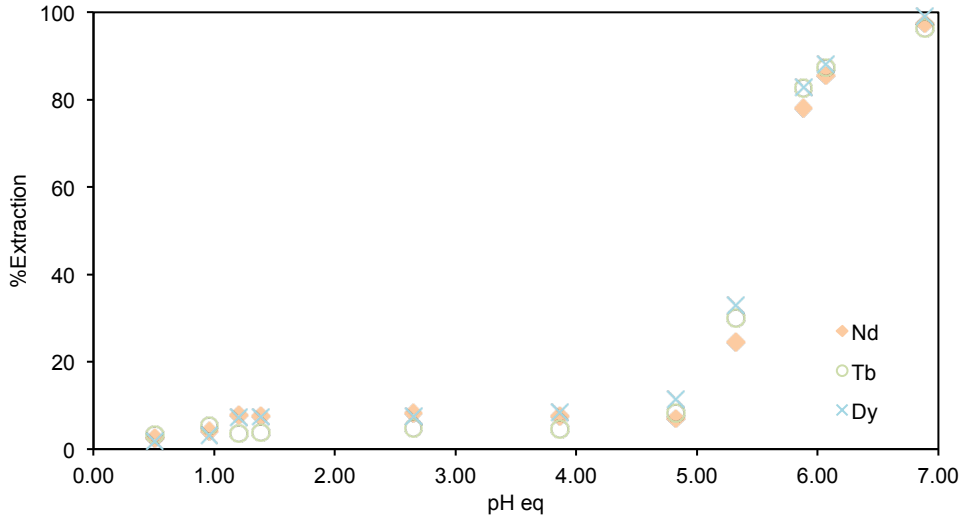

Figure 38. Effect of equilibrium pH on the single extraction of neodymium, terbium and dysprosium 7 mmol·L^{-1}, each in 4 mol·L^{-1} chloride media. [AliOle] = 0.015 mol·L^{-1}. Shaking time = 15 min at room temperature.

As shown, the extraction of the REEs with AliOle is strongly influenced by the pH of the aqueous phase. The pH dependence can be explained by the competition between the extraction of protons (or acid molecules) and the extraction of metal ions. The extraction curves obtained for each metal were

very similar, which is in agreement with the work of Parmentier et al. regarding the extraction of REEs by the Tetraoctylphosphonium Oleate IL (Parmentier et al., 2015b). From pH 0.5 to 5, the extraction percentages were very low (below 10%), but an inflection point appeared between pH 5 and 6 (matching up with the Oleic Acid pKa = 4.99) where extraction percentages increase from less than 10% all the way up to almost 90%. From pH 6 onwards the extraction of the metals kept increasing until reaching 100% approximately. When the H+ concentration in the aqueous phase is higher than the extractant concentration, only hydrochloric acid is extracted and no further ionic liquid remains available to extract the metal ions. Decreasing HCl concentration in the aqueous phase releases part of the ionic liquid and so the REEs extraction performance is boosted.

An HCl extraction test was carried out to evaluate HCl extraction with AliOle. Figure 39 displays the extraction performance of 0.39, 0.22, 0.07 and 0.04 mol·L-1 HCl solutions using different concentrations of AliOle from 0 to 0.1mol·L^{-1}. A calibrated pH meter was used to determine the HCl concentration in the aqueous phase.

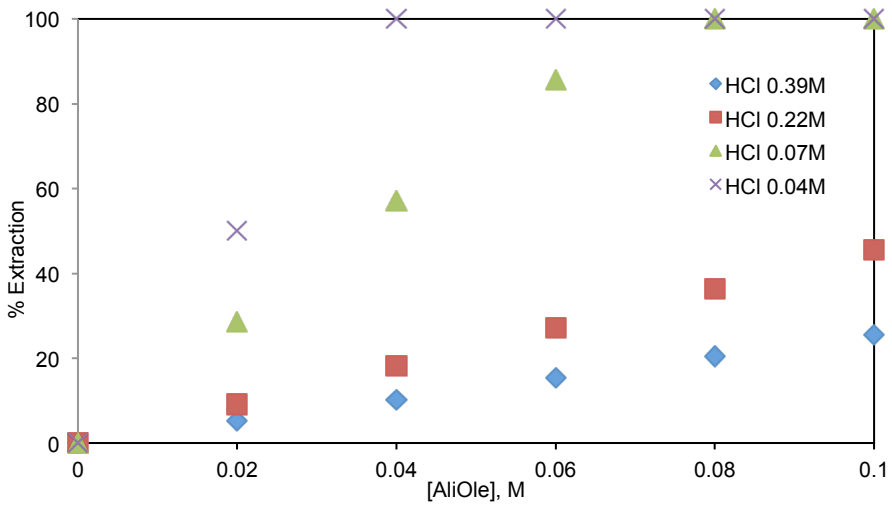

Figure 39. Effect of the AliOle IL concentration on the hydrochloric acid extraction. [HCl] = 0.39; 0.22; 0.07; 0.04. Shaking time = 15 min at room temperature.

As can be observed, when the HCl concentration is lower than the AliOle concentration, all the acid is extracted, neutralizing the solution and showing an acid-extractant ratio of 1:1. Therefore, increasing the pH in the feed solution promotes higher extraction percentages, since more free extractant remains available to react with metal species.

All in all, despite the extraction yield increases with the pH in the aqueous phase, it is advisable to keep the equilibrium pH as low as possible, in order to

avoid precipitation issues and not to let it increase further than 6.5 – 7, especially while working with low chloride concentrations in the feed. In this regard, the pH of the feed was fixed at 3.5 since it has been proven to maintain the equilibrium pH in the range 5 – 6.5.

1.4. The effect of AliOle concentration in the organic phase

Experimental studies were performed to determine the effect of the AliOle concentration on the individual extraction of neodymium terbium and dysprosium from different aqueous solutions containing 0.05, 2 and 4 mol·L^{-1} chloride concentrations. The AliOle IL was dissolved in kerosene to obtain a concentration range between 0.005 and 0.1 mol·L^{-1}. The pH of the feed was set at 3.5. Figure 40 shows the extraction values achieved for each metal in the experimental series.

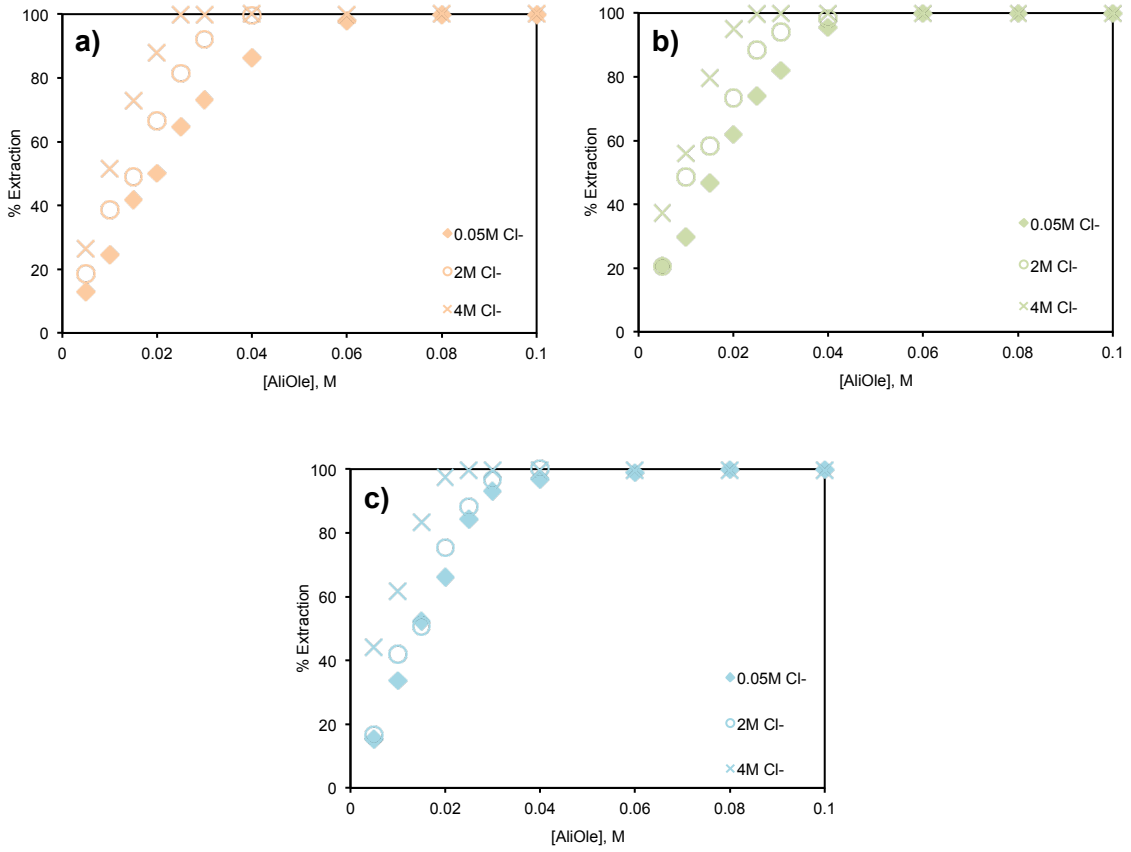

Figure 40. Effect of the AliOle IL concentration on the neodymium, terbium and dysprosium individual extraction: a) 7 mmol·L^{-1} neodymium (III), b) 7 mmol·L^{-1} terbium (III), b) 7 mmol·L^{-1} dysprosium (III); pH_{feed} = 3.5. Shaking time = 15 minutes at room temperature.

As expected, an increase in the AliOle IL concentration enhances the extraction of the neodymium, terbium and dysprosium metal ions with similar performance. However, the competitive extraction of HCl is also promoted. The equilibrium pH of the aqueous phases measured after extraction increased with the increase of the ionic liquid concentration, which may generate precipitation

issues, as explained above. Nevertheless, precipitation of metals was not observed in any of the experimental trials.

At this point, it can be seen that chloride concentration in the aqueous phase has a visible effect on the metal ions extraction yield. Higher chloride concentrations tend to increase neodymium, terbium and dysprosium extractability due to the promotion of the formation of metal chlorinated species in the aqueous phase, at least when using small concentrations of ionic liquid. In order to give more detailed information on this matter, the extraction of the metals as a function of the chloride concentration in the feed will be further addressed in the following subsection of this chapter.

1.5. The effect of chloride concentration in the feed

The extraction experiments of neodymium, terbium and dysprosium in 0.05, 2 and 4 $mol \cdot L^{-1}$ chloride solutions with AliOle IL showed that the extraction of the metal ions is related someway with the anion concentration in the aqueous phase. In this regard, experimental trials focused on the effect of the salting out agent concentration in the feed were carried out to evaluate in depth how chloride concentration could influence the extraction process. The chloride concentration was increased by adding NaCl to the aqueous solutions. Figure 41 shows the extraction of the metal ions as a function of the chloride concentration in the feed. The ionic liquid concentration was maintained here.

It is observed that increasing the chloride concentration in the aqueous phase enhances the extraction of the metal ions as expected regarding the first approach in figure 40. The extraction percentages of the metals in 4 $mol \cdot L^{-1}$ chloride media are around 1.5 times higher than the extraction percentages reached for 0.05 $mol \cdot L^{-1}$ Cl^-. This trend is maintained for each of the metals, the differences in their extraction yields seem to rely only on the lanthanide contraction. This notable increment of the extraction values with an increase of the chloride concentration in the feed suggests that the neodymium, terbium and dysprosium metal ions extracted by AliOle IL may be chlorinated species.

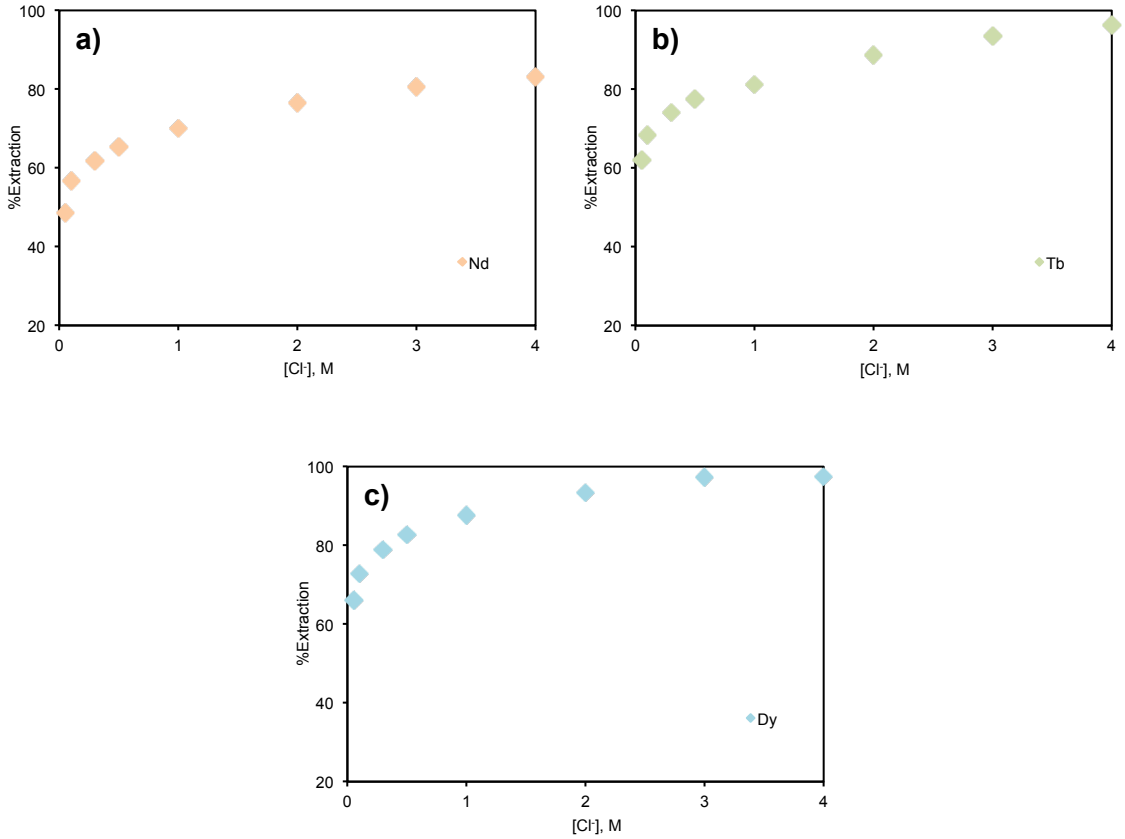

Figure 41. Effect of the chloride concentration on the neodymium, terbium and dysprosium individual extraction: a) 7 mmol·L^{-1} neodymium (III), b) 7 mmol·L^{-1} terbium (III), b) 7 mmol·L^{-1} dysprosium (III); pH_{feed} = 3.5; [AliOle] = 0.02 mol·L^{-1}; Shaking time = 15 minutes at room temperature.

The equilibrium diagrams of neodymium, terbium and dysprosium as a function of the chloride concentration in the feed were made to get a better picture of the metal speciation in the aqueous phase under the experimental conditions. Figure 42 shows the distribution diagrams of the neodymium, terbium and dysprosium species in the feed as a function of the chloride concentration using the Medusa software (Puigdomenech, 2013).

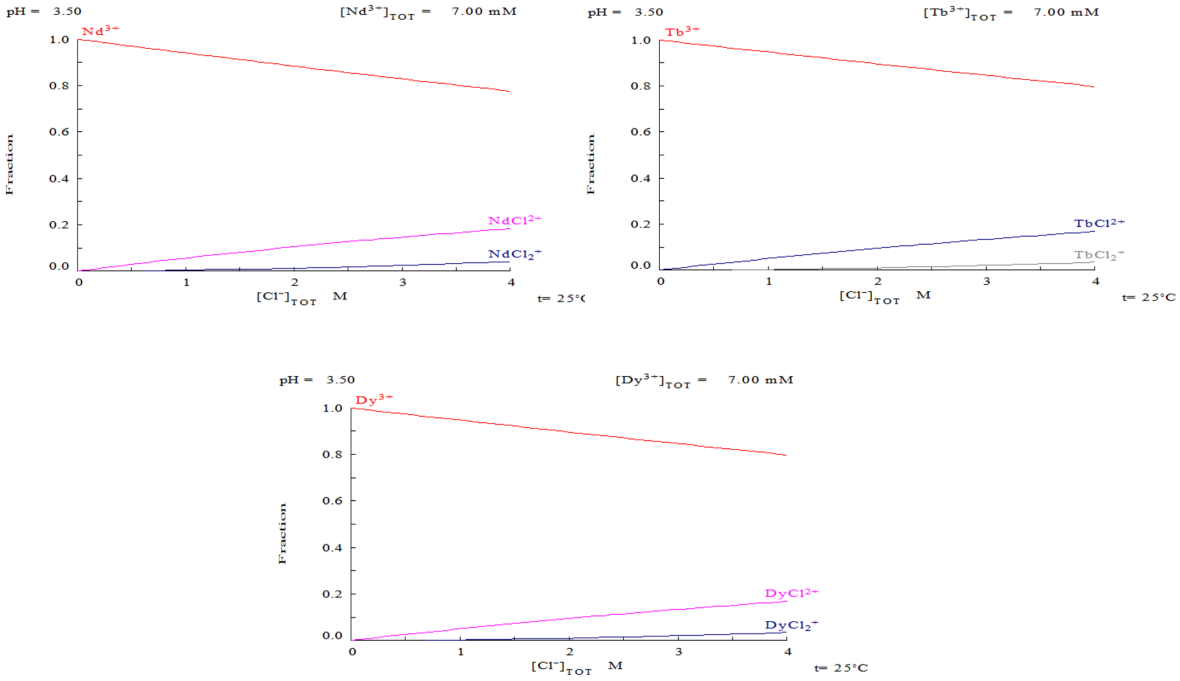

Figure 42. Effect of the chloride concentration on the neodymium, terbium and dysprosium speciation in the aqueous phase under the experimental conditions. [Metals] = 7 mmol·L^{-1}; pH = 3.5.

As can be seen, increasing the chloride concentration promotes the formation of different metal species in the aqueous phase available to be extracted by the ionic liquid. The diagrams obtained with Medusa for neodymium, terbium and dysprosium speciation are almost identical, which suggests that the formation constants of the chlorinated species of these metals may be of a similar magnitude order. Taking into account the equilibrium diagrams and comparing them to the experimental results in figure 41 it can be assumed that the metal ions must be extracted as chloride complexes. Furthermore, high chloride concentrations in the aqueous phase increase the ionic strength of the media and displace the precipitation of metals in the form of $Me(OH)_3$ to higher pHs as can be observed in figure 36.

1.6. Stripping studies

Acidic solutions were tested for the stripping of Nd(III), Tb(III) and Dy(III) from the loaded AliOle IL phase since they have proven to strip metal ions efficiently from tetraoctylammonium oleate IL, which is very similar to AliOle IL (Parmentier et al., 2015a). The metal ions can be easily stripped from the IL with acidic solutions because of the protonation of the oleate anion. Consequently, oleic acid is formed as well as a new IL, which could be methyl-tri-(octyl/decyl)ammonium chloride, nitrate, sulphate or citrate, depending on the stripping solution used. Therefore, direct reuse of AliOle was impossible after stripping, but it was easily regenerated after washing it with sodium bicarbonate

as described in R.12. The use of oxalic acid as stripping agent was dismissed although it has been proven to be able to strip 100% of the metals loaded in the organic phase without protonation of the of the oleate anion of the tetraoctylphosphonium oleate IL (Parmentier et al., 2015b). The oxalic acid forms oxalate salts with the metals, which are insoluble in the aqueous phase and, since one of the goals of this thesis is to provide suitable hydrometallurgical routes to be used for the recovery or rare earth elements in urban mining operations, the precipitation stripping is not the most appropriate option.

According to the assumptions made in the previous subsection of this chapter about the extraction of chlorinated species, the acidic stripping of the metals from the organic phase may occur as shown the following general reaction:

$$\overline{(\mathrm{R_4N^+Cl^-})_{(3-n)} \cdot \mathrm{MeCl_n}^{(3-n)+}\mathrm{A}_{(3-n)}} + \mathrm{HX} \leftrightarrow (3-\mathrm{n})\overline{\mathrm{R_4N^+X^-}} + (3-\mathrm{n})\overline{\mathrm{HA}} + 3\ \mathrm{Cl^-} + \mathrm{MeCl_n}^{(3-n)+} \qquad \text{(R.17)}$$

Where $\overline{(\mathrm{R_4N^+Cl^-})_{(3-n)} \cdot \mathrm{MeCl_n}^{(3-n)}}$ represents the IL-Me complex in the organic phase, HX an acid stripping solution, $MeCl_n^{(3-n)+}$ embraces all the metal chlorinated species and n could be any value in the range 0-3.

Stripping of the metal ions was investigated using HCl, HNO_3, H_2SO_4 and citric acid solutions. Table 17 shows the stripping yields achieved after individual extraction experiments with AliOle 0.02 mol·L^{-1}.

Table 17. Stripping extension of the neodymium, terbium and dysprosium loaded in the organic phase after a single contact of HCl, HNO_3, H_2SO_4 and citric acid 0.5 mol·L^{-1}. Shaking time = 15 min at room temperature. Organic phase: [AliOle] = 0.02 mol·L^{-1}; Metals concentration loaded in the organic phase after individual extraction: [Nd(III)] = 650 mg·L^{-1}; [Tb(III)] = 730 mg·L^{-1}; [Dy(III)] = 754 mg·L^{-1}.

	% Stripping		
Stripping Agent	**Nd**	**Tb**	**Dy**
HCl	33.2	40.1	36.8
HNO_3	36.0	43.1	40.0
H_2SO_4	33.4	40.0	37.1
Citric acid	32.6	39.1	36.2

As shown in table 17, the stripping percentages obtained for Tb and Dy were slightly higher than the Nd ones, which may be caused by the lanthanide contraction. Moreover, the stripping values obtained after the first contact using different acidic agents were practically identical for each of the metals, which suggests that the strength of the acids has not a particular effect on the back extraction. On another note, the complexing power of the citric acid has proven to be appropriate for the stripping purpose. Nonetheless, three stripping contacts were required to remove >90% of the metals from the loaded organic phase with all the stripping agents.

The effect of the acidity of the stripping solution was also tested. HCl solutions at concentrations in the range 0.05 – 6 mol·L^{-1} were used. HCl was chosen among the rest of acidic solutions to avoid the mixture of anions in the system. Figure 43 shows the stripping extension of the metals as a function of the HCl concentration after the first contact.

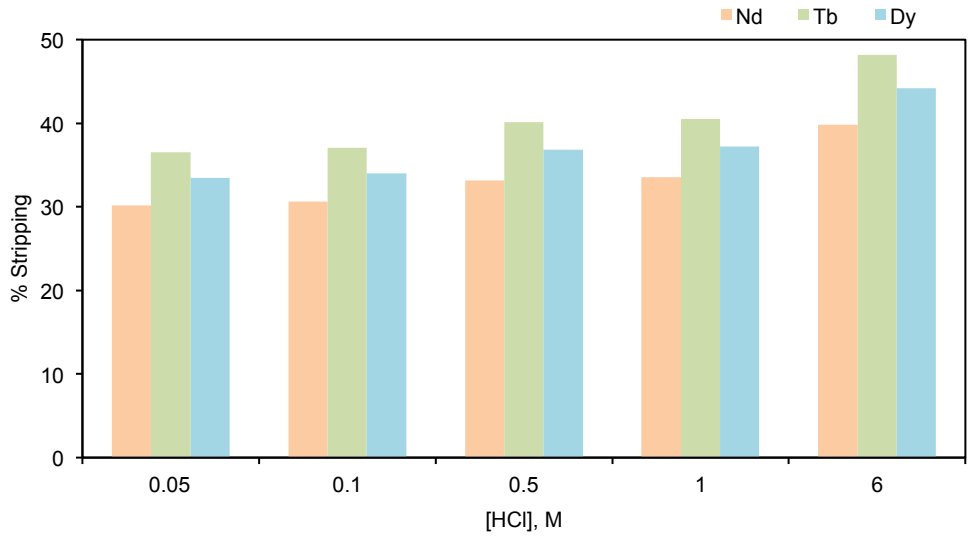

Figure 43. Effect of the chloride concentration on the neodymium, terbium and dysprosium stripping extension. Shaking time = 15 min at room temperature. Metals concentration loaded in the organic phase after individual extraction: [Nd(III)] = 650 mg·L^{-1}; [Tb(III)] = 730 mg·L^{-1}; [Dy(III)] = 754 mg·L^{-1}.

As can be observed, an increase of the hydrochloric acid concentration does not have a strong impact on the stripping extension. Thus, in order to avoid the use of highly concentrated acidic solutions, which is not interesting from an economical and environmental point of view, and because the performance is similar, low hydrochloric acid solutions are proposed to strip the metal ions from the organic phase.

1.7. Competitive extraction between neodymium, terbium and dysprosium with AliOle IL

Extraction experiments were carried out to evaluate the competitive extraction of Nd(III), Tb(III) and Dy(III) from chloride media with AliOle IL. The extraction performance was studied as a function of the chloride anion and the ionic liquid concentrations. The AliOle IL was dissolved in kerosene to obtain a concentration range between 0 and 0.08 mol·L^{-1}.The pH of the feed was set at 3.5 for each experimental trial. Figure 44 shows the extraction values achieved in the experimental series.

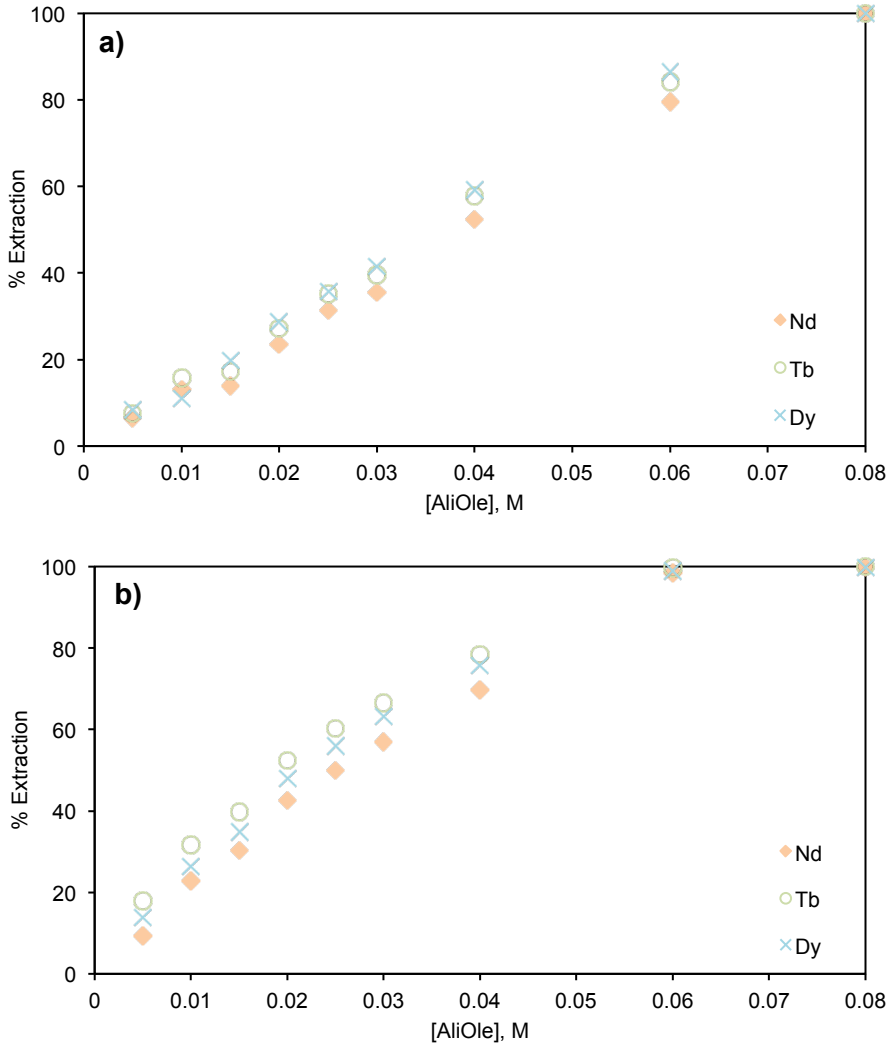

Figure 44. Effect of the AliOle IL concentration on the simultaneous extraction of neodymium, terbium and dysprosium: 7 mmol·L^{-1} neodymium, terbium and dysprosium (21 mmol·L^{-1} in total); pH_{feed} = 3.5; shaking time = 15 minutes at room temperature; a) [Cl$^-$] = 2 mol·L^{-1}; b) [Cl$^-$] = 4 mol·L^{-1}.

As can be seen, the extraction yield of neodymium, terbium and dysprosium in both cases is very similar. No selective extraction of the metals was observed under the experimental conditions, not even at low ionic liquid concentrations where it would act as a limiting factor of the extraction equilibrium. Therefore, it can be assumed that AliOle IL may not be suitable for selective separation of lanthanides from concentrated streams. Nonetheless, because of the high extraction values obtained when increasing its concentration over 0.04 mol·L^{-1} it may be useful for the recovery of rare earths from leachates containing other metals.

As in previous experimental trials dealing with the individual extraction of neodymium, terbium and dysprosium, high concentrations of chloride anions have a beneficial effect on the extraction efficiency since the formation of chlorinated species in the aqueous phase is promoted.

1.8. Conclusions

This first section of chapter 4 reports on the liquid-liquid solvent extraction of neodymium, terbium and dysprosium from aqueous media. Different types of extractants were tested, however the ionic liquids Cyphos 104, AliCy, AliDec, AliD2EHPA and AliOle showed the best extraction potential. Although they all share a similar behaviour, AliOle IL was chosen to carry out a detailed extraction study due to its high extraction ability and its effortless phase separation. The effect of the salting out reagent in the aqueous phase was studied and it was found that the extraction of REEs with AliOle is possible from chloride and nitrate medias with similar distribution ratios, nevertheless the chloride media was chosen to continue the extraction study also because of its easier phase separation. The effect of the chloride concentration in the aqueous phase was studied and it was found that higher chloride concentrations boost the extraction of the metals by promoting the formation of chlorinated species. The initial pH of the feed was fixed at 3.5 to maintain the equilibrium pH in the range 5-6.5. The extraction efficiency of the metals was studied as a function of the AliOle concentration and it was found that it is favoured by an increase of the ionic liquid concentration in the range 0.05 – 0.1 $mol \cdot L^{-1}$. The recovery of the metals from the loaded organic phase was achieved completely after three stripping contacts with HCl. The simultaneous extraction of neodymium, terbium and dysprosium from chloride media was studied and it was found that AliOle IL was not selective enough for separation of the lanthanides under the experimental conditions set but that it could be useful for the recovery of rare earths from leachates containing other metals.

The experimental data gathered was then arranged in different matrices and used for the resolution of different mathematical models derived from the mass balances and chemical equilibria involved in the extraction systems proposed. The mathematical modelling computed with Matlab software will be addressed in depth in the 3.1 subsection of this chapter.

2. Experimental studies of neodymium, terbium and dysprosium from alkaline solutions

Previously in this chapter, the extraction of cationic metal chlorinated species was discussed. On the contrary, this section describes, a solvent extraction study of neodymium, terbium and dysprosium anionic species from chloride alkaline solutions using the ionic liquid Aliquat 336, which needs anionic species to extract by exchanging the Cl^-. Anionic extractants such as primary or tertiary amines have proven to be useful to separate anionic species of REEs from impurities in mixed alkaline solutions. Nonetheless, the use of anionic extractants to recover lanthanides from aqueous solutions has been sparsely

studied. Aliquat 336 and Primene JMT have been tested since they are strong-base anion exchangers (Kumar Jha et al., 2016). However, solvent extraction of REEs from acidic solutions is still predominant in the metal recovery field.

The proposed hydrometallurgical processing route consists in the removal of lanthanides from aqueous solutions using complexation plus solvent extraction. The complexing agents are often organic substances, usually with oxygenated groups. In this investigation citric acid was used to form anionic metallic species in the aqueous phase suitable to be extracted with Aliquat 336 IL. In this investigation, the metal extraction efficiency was studied as a function of the citric acid concentration, the pH of the feed, the chloride concentration and the Aliquat 336 concentration.

2.1. Liquid-liquid extraction: the effect of the complexing agent

A series of batch trials was carried out to evaluate the feasibility of removing simultaneously neodymium, terbium and dysprosium from the feed solution. The citric acid capability to form anionic species with the rare earth elements in alkaline solutions was put to the test. The effectiveness of the extraction system proposed was determined by comparing the extraction of Nd(III), Tb(III) and Dy(III) achieved with and without the addition of citric acid to the aqueous phase. Figure 45 depicts the effect of the addition of citric acid on the extraction efficiency.

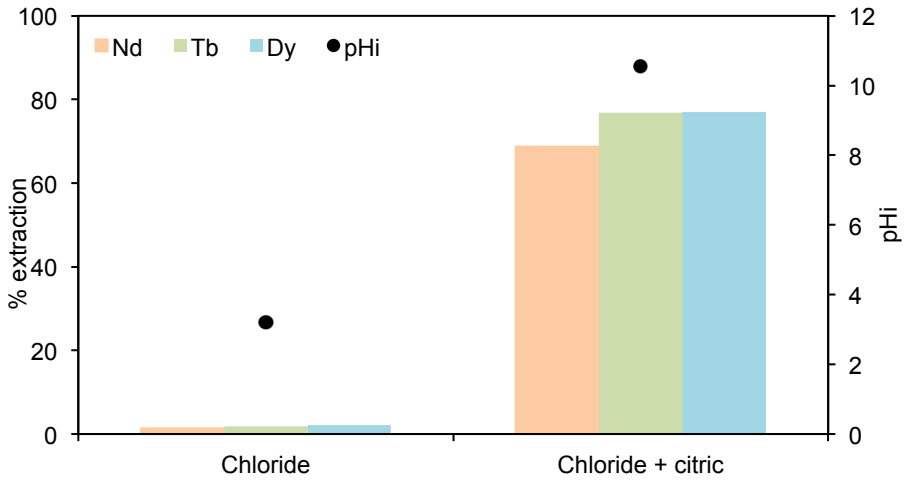

Figure 45. Effect of the citric acid addition in the feed on the Nd(III), Tb(III) and Dy(III) extraction. [Metal ions]$_i$ = 7 mmol·L^{-1} each; [Cl$^-$] = 0.1 mol·L^{-1}, [Aliquat336] = 10%, [Citric acid] = 42 mmol·L^{-1}

As expected, the addition of citric acid into the feed along with an increase in the pH using sodium hydroxide, leads to the formation of metal anionic complexes in the aqueous phase that can be extracted by the ionic liquid Aliquat 336.

The effect of the citric acid concentration in the aqueous phase was also addressed. The total concentration of the metals (21 mmol·L^{-1} in total, 7 mmol·L^{-1} each) was taken as a benchmark and the citric acid concentration was increased from there. A series of experiments were done at 21, 42 and 60 mmol·L^{-1} citric acid to achieve 1:1, 1:2 and 1:3 metal-citrate stoichiometries, respectively. Figure 46 displays the effect of the metal-citrate stoichiometry on the extraction performance.

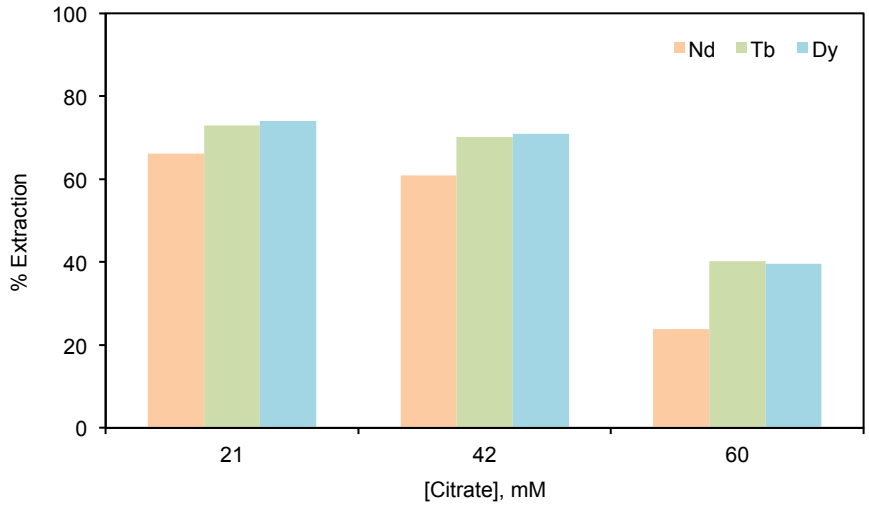

Figure 46. Effect of the citrate concentration in the feed on the Nd(III), Tb(III) and Dy(III) extraction. [Metal ions]$_i$ = 7 mmol·L^{-1} each; [Cl$^-$] = 0.1 mol·L^{-1}, [Aliquat336] = 10% (0.23 mol·L^{-1}).

As can be seen, increasing the citrate concentration in the aqueous phase from 21 to 60 mmol·L^{-1} causes a decrease in the extraction yield of the metals, around 50% in the case of terbium and dysprosium and approximately 40% in the case of neodymium, indicating that there might be competitive extraction of citrate by anionic exchange with Aliquat 336:

$$\mathrm{Cit^{3-}} + 3\,\overline{\mathrm{R_4N^+Cl^-}} \overset{\mathrm{Kie}}{\leftrightarrow} \overline{\mathrm{(R_4N^+)_3Cit^{3-}}} + 3\,\mathrm{Cl^-} \qquad \text{(R.18)}$$

Moreover, metal precipitation was observed in the aqueous phase for the 21 mmol·L^{-1} citrate concentration experiment, which seems to confirm this assumption. Having a metal-citric acid molar ratio of 1:1, the extraction of citrate might leave free metal ions in the solution that would precipitate in the Me(OH)$_3$ form when increasing the pH in the feed. In this regard, the extraction percentages obtained after analysis of the 1:1 raffinate would be distorted because of the precipitation issues.

Thus, to avoid precipitation and minimize the competitive extraction of citrate at the same time, the citric acid concentration in the feed was set to 42 mmol·L^{-1}, which is twice the total concentration of metals in the aqueous phase.

2.2. The effect of the pH in the feed

To determine the effect of the pH on the neodymium, terbium and dysprosium extraction efficiency, the distribution of citrate ions in the aqueous phase as a function of the pH was investigated. The Medusa software was used to figure out the citrate speciation in the feed. Figure 47 shows the effect of the pH on the citrate speciation in the media.

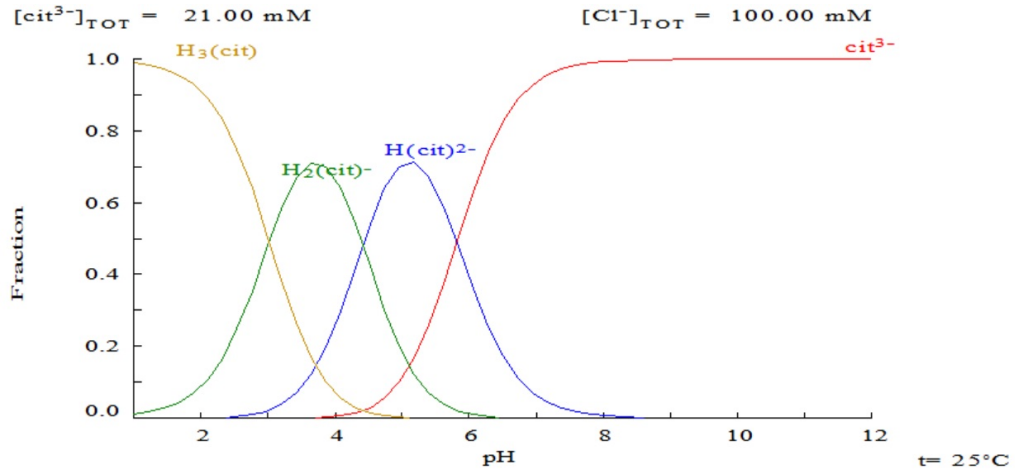

Figure 47. Effect of the pH in the aqueous media on the citrate ion distribution (Puigdomenech, 2013). [Citric acid] = 21 mmol·L^{-1}; [Cl$^-$] = 0.1 mol·L^{-1}; pH within 1–12.

As can be seen, the pH determines the formation of citrate species in the aqueous phase. As the pH increases, the proton concentration decreases, which promotes the formation of cit^{3-} ions. Since the effect of the pH was tested in the pH range 8 – 11, it can be assumed that the citrate species available to form anionic complexes with the metals is the cit^{3-}.

The effect of the pH in the feed on the extraction performance was studied as well. As previously mentioned, a series of experiments were carried out in the pH range 8 – 11 to investigate the effect of equilibrium pH on the neodymium, terbium and dysprosium extraction with Aliquat 336 IL. Figure 48 shows the extraction of the metals as a function of the pH in the feed.

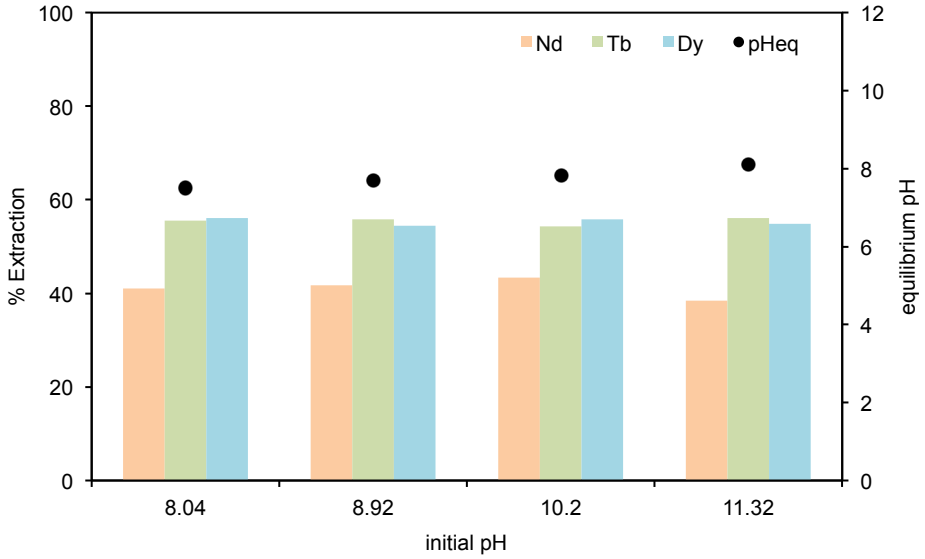

Figure 48. Effect of the pH in the feed on the metals extraction yield. $[Metal]_i$ = 7 mmol·L^{-1} each; [Citric acid] = 42 mmol·L^{-1}; [Cl^-] = 0.1 mol·L^{-1}; [Aliquat 336] = 0.17 mol·L^{-1}.

Based on the experimental results obtained, it can be assumed that the pH in the aqueous phase does not have a significant effect on the metal extraction efficiency in the working pH range. As can be observed, the extraction extension remained constant throughout all the experimental series. The pH of the solution does not affect the extraction because hydroxide ions are not involved in the formation of chloro-metal-citrate species. Since the main citrate species in the feed, in the working pH range, is cit^{3-} (figure 47) the formation of chloro-metal-citrate anionic species relies only on the stability constants:

$$MeCl^{2+} + Cit^{3-} \overset{Kcit1}{\longleftrightarrow} MeClCit^{-} \quad \text{(R.19)}$$

$$MeCl_2^{+} + Cit^{3-} \overset{Kcit2}{\longleftrightarrow} MeCl_2Cit^{2-} \quad \text{(R.20)}$$

$$Me^{3+} + Cit^{3-} \overset{Kcit3}{\longleftrightarrow} MeCit \quad \text{(R.21)}$$

And the list could go on because of the excess of citric acid in the media, which may lead to formation of more metal chlorinated anionic species. In the reactions, Me represents Nd(III), Tb(III) or Dy(III) and $Kcit_1$, $Kcit_2$ and $Kcit_3$ represent the stepwise stability constants of the potential anionic complexes formed.

Nonetheless, since the equilibrium pH did not change regardless of the initial pH in the feed, the competitive extraction of hydroxide ions from the aqueous phase must be taken into account:

$$\overline{R_4N^+Cl^-} + OH^- \overset{Kex\ OH}{\longleftrightarrow} \overline{R_4N^+OH^-} + Cl^- \quad \text{(R.22)}$$

As can be seen, the competitive extraction of hydroxide ions does not affect the metal extraction efficiency in the experimental conditions established, because of the excess of Aliquat 336 (0.23 mol·L^{-1}) compared to the OH^- concentration in the aqueous phase. This is in agreement with the results obtained by (Sun et al., 2017). In their investigation about separation of V from alkaline solutions using the primary amine N1923 with the addition of Na_3Cit, a decrease of the V(V) extraction percentages is experimented when equilibrium pH values are higher than 12, whereas the extraction performance is maintained throughout the pH range 7.5 – 11.5. This may be due to the nonlinear increasing OH^- concentration with increasing aqueous pH.

2.3. The effect of chloride concentration in the aqueous phase

The metal extraction performance was studied as a function of the chloride concentration in the feed to determine the effect of the salting out reagent on the extraction extension of the metals. Figure 49 depicts the influence of the Cl^- concentration in the feed on the metal extraction percentages.

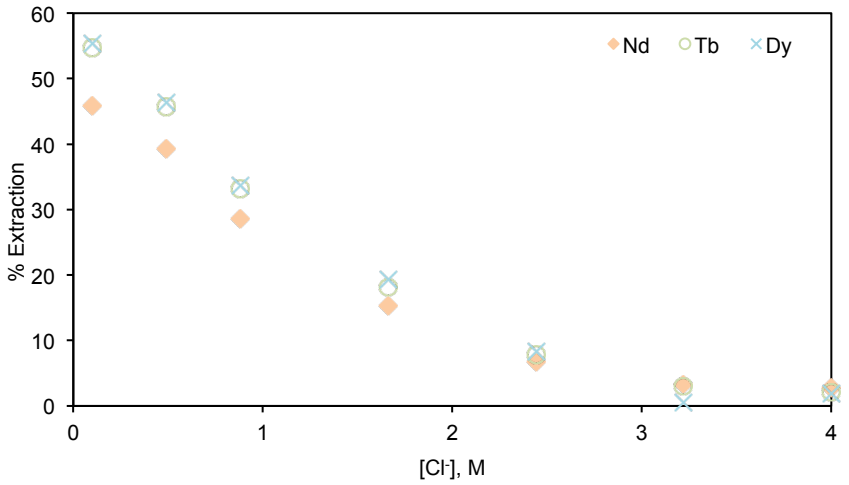

Figure 49. Effect of chloride concentration in the aqueous phase on the extraction extension. $[Metal]_i$ = 7 mmol·L^{-1} each; [Citric acid] = 42 mmol·L^{-1}; [Aliquat336] = 0.17 mol·L^{-1}; pH = 10.3.

As can be observed, low concentrations of chloride ions in the aqueous phase lead to higher extraction values. High chloride concentrations in the feed have a detrimental effect on the extraction performance. Increasing the chloride concentration in the aqueous phase may harm the extraction performance of the metals by shifting the extraction equilibrium towards the release of the REE anionic species to the aqueous phase:

$$\overline{R_4N^+Cl^-} + X^- \overset{Kex}{\longleftrightarrow} \overline{R_4N^+X^-} + Cl^- \qquad \text{(R.23)}$$

Where X^- represents whatever metallic anionic species extracted

In fact, NaCl has been tested as a stripping agent in the literature when working with Aliquat 336 to recover the metals from the organic phase and close the mass balance (Peng and Tsai, 2014; Usapein et al., 2009).

2.4. The effect of the Aliquat 336 concentration in the organic phase

The effect of the Aliquat 336 concentration on the extraction performance was studied as well. Several trials were carried out using Aliquat 336 dissolved in kerosene / decanol (90/10 %v/v) to cover a concentration range of 0.023 – 0.34 $mol \cdot L^{-1}$. Figure 50 shows the neodymium, terbium and dysprosium extraction percentages achieved as a function of the ionic liquid concentration in the organic solution.

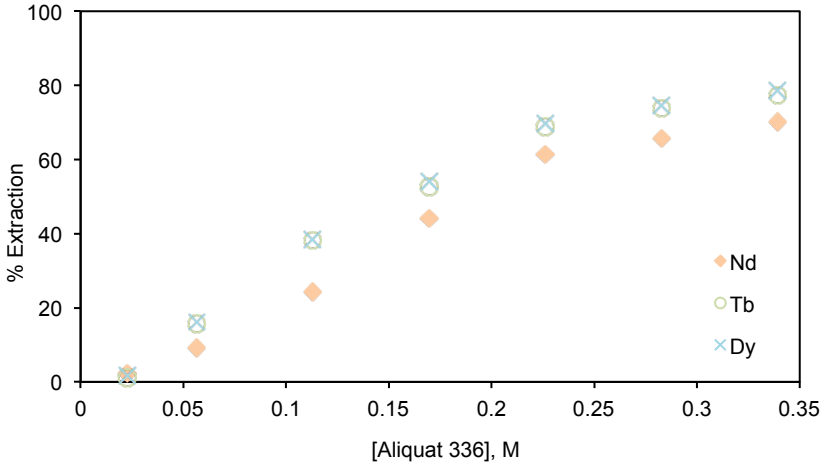

Figure 50. Effect of the Aliquat 336 molar concentration on the extraction of Nd(III), Tb(III) and Dy(III). $[Metal]_i$ = 7 $mmol \cdot L^{-1}$ each; [Citric acid] = 42 $mmol \cdot L^{-1}$; pH = 10.3.

As expected, an increase of the Aliquat 336 IL concentration leads to an increase in the extraction yield because of the higher extraction capacity of the organic phase. The extraction yield of neodymium, terbium and dysprosium is very similar for each of the experimental points. The slight differences observed are caused by the lanthanide contraction. Therefore, it can be assumed that the separation of neodymium, terbium and dysprosium anionic complexes with Aliquat 336 IL may not be suitable under the experimental conditions established. Nonetheless, the proposed extraction system may be useful for the recovery of rare earths from leachates containing other metals such as aluminium or chromium.

At this point, in order to get closer to the mechanism involved in the extraction system, the logarithm of the distribution coefficient (D) of the metals, which is typically described as: $[Metal\ ion]_{aq}$ / $[Metal\ ion]_{org}$ was plotted vs. the logarithm of Aliquat 336 concentration. Figure 51 shows the effect of the Aliquat 336

concentration on the neodymium, terbium and dysprosium distribution coefficients:

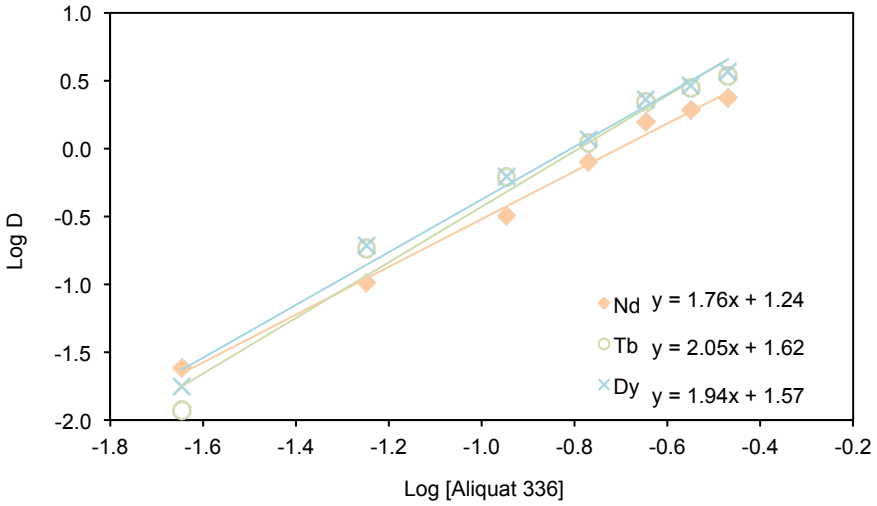

Figure 51. Effect of the Aliquat 336 IL concentration on the distribution ratios of neodymium, terbium and dysprosium. $[Metal]_i$ = 7 mmol·L^{-1} each; [Citric acid] = 42 mmol·L^{-1}; pH = 10.3.

The linear regression analysis of Log D versus Log [Aliquat 336] of the experimental extraction data gave straight lines with slope values of 1.76 for neodymium, 2.05 for terbium and 1.96 for dysprosium. This suggests that 2 molecules of Aliquat 336 may be involved during the extraction of the metals. Therefore, taking into account the speciation of citrate in the aqueous media, the extraction of Nd(III), Tb(III) and Dy(III) is most likely to occur via a $MeCl_2Cit^{2-}$ complex in combination with two IL molecules:

$$MeCl_2Cit^{2-} + 2\,\overline{R_4N^+Cl^-} \overset{Kex}{\leftrightarrow} \overline{(R_4N^+)_2MeCl_2Cit^{2-}} + 2\,Cl^- \qquad \text{(R.24)}$$

This was used as a starting point to develop a mathematical model of the solvent extraction of Nd(III), Tb(III) and Dy(III) which can be found further on in the 3.3 subsection of this chapter.

2.5. Stripping studies

The stripping studies were performed using acidic solutions for the stripping of the metals from the loaded organic phase. Since Nd(III), Tb(III) and Dy(III) chloro-citrate complexes are anionic species, they may be easily stripped by ion exchange.

Hydrochloric acid and sulphuric acid were used as stripping agents. The stripping of neodymium, terbium and dysprosium occurs according to the general reactions written below:

$$\overline{(R_4N^+)_2MeCl_2Cit^{2-}} + 3\,HCl \leftrightarrow 2\,\overline{R_4N^+Cl^-} + Me^{3+} + H_3Cit + 3\,Cl^- \qquad \text{(R.25)}$$

$$2\ \overline{(R_4N^+)_2MeCl_2Cit^{2-}} + 3\ H_2SO_4 \ \leftrightarrow\ 2\ \overline{(R_4N^+)_2SO_4} + 2\ Me^{3+} + 2\ H_3Cit + 4\ Cl^- + SO_4^{2-} \qquad \text{(R.26)}$$

The stripping performance was assessed as a function of the hydrochloric and sulphuric acid concentrations in the stripping solutions. Figure 52 shows the effect of HCl and H_2SO_4 concentrations on the stripping of the metals after the first contact.

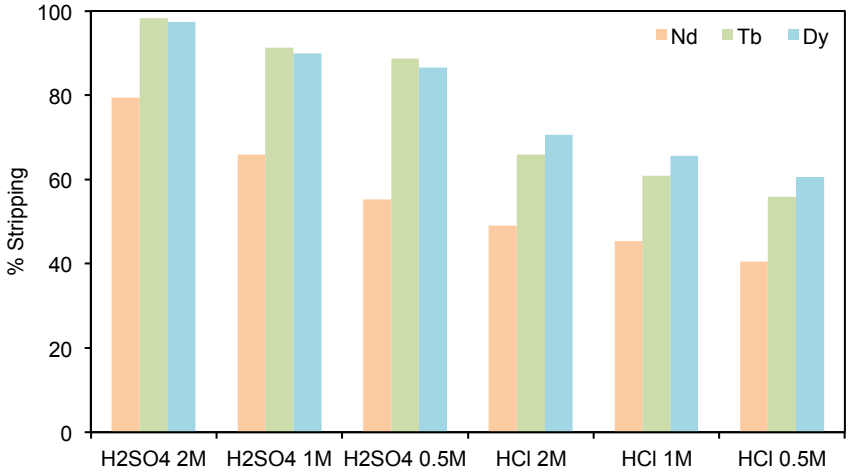

Figure 52. Effect of the Stripping agent on the stripping performance of Nd(III), Tb(III) and Dy(III). $[Metal]_i$ = 7 mmol·L^{-1} each; [Aliquat336] = 0.17 mol·L^{-1}, [Citric acid] = 42 mmol·L^{-1}, $[Cl^-]$ = 0.1 mol·L^{-1}.

As can be observed, the stripping of the metals relies significantly on the acidic solution used. Higher stripping performances were achieved with the sulphuric acid solutions. The ionic strength of the stripping solutions may explain this trend:

$$I_m = 0.5 \sum z_i^2 c_i \qquad \text{(Eq.5)}$$

Where c_i represents the molar concentration of the ions in the solution and z_i is the charge of each ion.

According to Eq.6, the ionic strength of H_2SO_4 1 mol·L^{-1} is 3, whereas the ionic strength of HCl 2 mol·L^{-1} is 2. The higher amount of ions available for the ionic exchange of the metals in the sulphuric solutions may be the reason why sulphuric acid 1 mol·L^{-1} leads to higher stripping values than HCl 2 mol·L^{-1}. Two stripping contacts were required to remove the metals completely from the loaded organic phase with H_2SO_4 2 mol·L^{-1}.

Regarding the effect of the concentration of the acidic solutions, it was noted that increasing the HCl and H_2SO_4 concentrations improves the stripping performance. Moreover, it can be observed that the stripping of the neodymium

is lower than the stripping of terbium and dysprosium. This could provide a basis for investigation of REEs separation in the future.

2.6. Conclusions

Section 2 of this chapter reports on the extraction of Nd(III), Tb(III) and Dy(III) anionic species from chloride media using Aliquat 336 IL with the addition of citric acid. First of all, the effectiveness of the addition of the complexing agent to create extractable anionic species of the metals in the aqueous phase was proven. The pH was found to be non-critical when working in the range 8–11, since the main citrate species in the feed is cit^{3-} and therefore, the formation of chloro-metal-citrate species only relies on the stability constants. The effect of chloride in the aqueous phase was studied and it was seen that high concentrations are detrimental since chloride ions seem to shift the equilibrium decreasing the extraction of the metallic species. The effect of Aliquat 336 concentration on the extraction efficiency was investigated and based on the results, it was found that 2 molecules of Aliquat 336 might be involved in the extraction of the metals. The stripping performance was found to rely significantly on the ionic strength of the acidic solution; the stripping yield achieved with sulphuric acid was higher than with hydrochloric acid. The stripping of neodymium species was lower than the stripping of terbium and dysprosium species, which could provide a basis for investigation of REEs separation in the future.

The experimental results obtained were used as a base to create a mathematical model of the solvent extraction system proposed by solving the mass balances and equilibria equations involved. The mathematical modelling computed with Matlab software will be outlined in detail in the following section of this chapter.

3. Mathematical modelling of neodymium, terbium and dysprosium solvent extraction systems

This chapter gathers the mathematical models of neodymium, terbium and dysprosium solvent extraction from acidic and alkaline solutions based on the experimental results obtained with the extraction systems previously proposed using AliOle and Aliquat 336 ILs. The Matlab software was used to solve the equilibria equations and mass balances involved in the extraction systems to determine the equilibria constants. The validity of the models was confirmed by comparing the plotted experimental and calculated data. The extraction models suggested can be tailored to predict the extraction extension in separation systems entailing other REEs and different organic extractants.

3.1. Modelling studies of neodymium solvent extraction with methyl-tri(octyl/decyl)ammonium oleate ionic liquid from chloride media

A preliminary modelling approach was developed, based on the experimental results of the neodymium single extraction from chloride media with AliOle, to determine the potential metal ion extraction mechanism involved. Regarding the chemical equilibrium diagrams displayed in figure 36, which show the speciation of Nd (III), Tb(III) and Dy(III) in chloride media, and taking into account the experimental results presented in figure 33, where the neutral extractants are also able to extract the metals, the theoretical equilibrium IL-Nd(III) reactions that could take place in the chloride media are the ones listed below. All these equilibriums consider that the neodymium species extracted is the only one in the aqueous phase.

a. $$3\,\overline{R_4N^+A^-} + Nd^{3+} + 3\,Cl^- \overset{K_a}{\leftrightarrow} 3\,\overline{R_4N^+Cl^-} + \overline{NdA_3} \quad \text{(R.27)}$$

$$K_a = \frac{\left[\overline{R_4N^+Cl^-}\right]^3 \cdot \left[\overline{NdA_3}\right]}{\left[\overline{R_4N^+A^-}\right]^3 \cdot [Nd^{3+}] \cdot [Cl^-]^3} = \frac{\left(3 \cdot \left[\overline{Nd}\right] + \Delta[H^+]\right)^3 \cdot \left[\overline{Nd}\right]}{\left[\overline{E_{free}}\right]^3 \cdot [Nd]_{aq} \cdot [Cl^-]_{aq}^3} \quad \text{(Eq.6)}$$

b. $$3\,\overline{R_4N^+A^-} + Nd^{3+} + 3\,Cl^- \overset{K_b}{\leftrightarrow} \overline{(R_4N^+Cl^-)_3 \cdot NdA_3} \quad \text{(R.28)}$$

$$K_b = \frac{\left[\overline{(R_4N^+Cl^-)_3 \cdot NdA_3}\right]}{\left[\overline{R_4N^+A^-}\right]^3 \cdot [Nd^{3+}] \cdot [Cl^-]^3} = \frac{\left[\overline{Nd}\right]}{\left[\overline{E_{free}}\right]^3 \cdot [Nd]_{aq} \cdot [Cl^-]_{aq}^3} \quad \text{(Eq.7)}$$

c. $$3\,\overline{R_4N^+A^-} + Nd^{3+} + 3\,Cl^- \overset{K_c}{\leftrightarrow} \overline{(R_4N^+Cl^-)_2 \cdot NdA_3} + \overline{R_4N^+Cl^-} \quad \text{(R.29)}$$

$$K_c = \frac{\left[\overline{(R_4N^+Cl^-)_2 \cdot NdA_3}\right] \cdot \left[\overline{R_4N^+Cl^-}\right]}{\left[\overline{R_4N^+A^-}\right]^3 \cdot [Nd^{3+}] \cdot [Cl^-]^3} = \frac{\left[\overline{Nd}\right] \cdot \left(\left[\overline{Nd}\right] + \Delta[H^+]\right)}{\left[\overline{E_{free}}\right]^3 \cdot [Nd]_{aq} \cdot [Cl^-]_{aq}^3} \quad \text{(Eq.8)}$$

d. $$3\,\overline{R_4N^+A^-} + Nd^{3+} + 3\,Cl^- \overset{K_d}{\leftrightarrow} \overline{R_4N^+Cl^- \cdot NdA_3} + 2\,\overline{R_4N^+Cl^-} \quad \text{(R.30)}$$

$$K_c = \frac{\left[\overline{(R_4N^+Cl^-)_2 \cdot NdA_3}\right] \cdot \left[\overline{R_4N^+Cl^-}\right]}{\left[\overline{R_4N^+A^-}\right]^3 \cdot [Nd^{3+}] \cdot [Cl^-]^3} = \frac{\left[\overline{Nd}\right] \cdot \left(\left[\overline{Nd}\right] + \Delta[H^+]\right)}{\left[\overline{E_{free}}\right]^3 \cdot [Nd]_{aq} \cdot [Cl^-]_{aq}^3} \quad \text{(Eq.9)}$$

e. $$2\,\overline{R_4N^+A^-} + NdCl^{2+} + 2\,Cl^- \overset{K_e}{\leftrightarrow} 2\,\overline{R_4N^+Cl^-} + \overline{NdClA_2} \quad \text{(R.31)}$$

$$K_e = \frac{\left[\overline{R_4N^+Cl^-}\right]^2 \cdot \left[\overline{NdClA_2}\right]}{\left[\overline{R_4N^+A^-}\right]^2 \cdot [NdCl^{2+}] \cdot [Cl^-]^2} = \frac{\left(2 \cdot \left[\overline{Nd}\right] + \Delta[H^+]\right)^2 \cdot \left[\overline{Nd}\right]}{\left[\overline{E_{free}}\right]^2 \cdot [Nd]_{aq} \cdot [Cl^-]_{aq}^2} \quad \text{(Eq.10)}$$

f. $$2\,\overline{R_4N^+A^-} + NdCl^{2+} + 2\,Cl^- \overset{K_f}{\leftrightarrow} \overline{(R_4N^+Cl^-)_2 \cdot NdClA_2} \quad \text{(R.32)}$$

$$K_f = \frac{\left[\overline{(R_4N^+Cl^-)_2 \cdot NdClA_2}\right]}{\left[\overline{R_4N^+A^-}\right]^2 \cdot [NdCl^{2+}] \cdot [Cl^-]^2} = \frac{\left[\overline{Nd}\right]}{\left[\overline{E_{free}}\right]^2 \cdot [Nd]_{aq} \cdot [Cl^-]_{aq}^2} \quad \text{(Eq.11)}$$

g. $$2\,\overline{R_4N^+A^-} + NdCl^{2+} + 2\,Cl^- \overset{K_g}{\leftrightarrow} \overline{R_4N^+Cl^- \cdot NdClA_2} + \overline{R_4N^+Cl^-} \quad \text{(R.33)}$$

$$K_g = \frac{\left[\overline{R_4N^+Cl^- \cdot NdClA_2}\right] \cdot \left[\overline{R_4N^+Cl^-}\right]}{\left[\overline{R_4N^+A^-}\right]^2 \cdot [NdCl^{2+}] \cdot [Cl^-]^2} = \frac{\left[\overline{Nd}\right] \cdot \left(\left[\overline{Nd}\right] + \Delta[H^+]\right)}{\left[\overline{E_{free}}\right]^2 \cdot [Nd]_{aq} \cdot [Cl^-]_{aq}^2} \quad \text{(Eq.12)}$$

h. $$\overline{R_4N^+A^-} + NdCl_2{}^+ + Cl^- \overset{K_h}{\leftrightarrow} \overline{R_4N^+Cl^-} + \overline{NdCl_2A} \quad \text{(R.34)}$$

$$K_h = \frac{[\overline{R_4N^+Cl^-}]\cdot[\overline{NdCl_2A}]}{[\overline{R_4N^+A^-}]\cdot[NdCl_2{}^+]\cdot[Cl^-]} = \frac{([\overline{Nd}]+\Delta[H^+])\cdot[\overline{Nd}]}{[\overline{E_{free}}]\cdot[Nd]_{aq}\cdot[Cl^-]_{aq}} \quad \text{(Eq.13)}$$

i. $$\overline{R_4N^+A^-} + NdCl_2{}^+ + Cl^- \overset{K_i}{\leftrightarrow} \overline{R_4N^+Cl^-\cdot NdCl_2A} \quad \text{(R.35)}$$

$$K_i = \frac{[\overline{R_4N^+Cl^-\cdot NdCl_2A}]}{[\overline{R_4N^+A^-}]\cdot[NdCl_2{}^+]\cdot[Cl^-]} = \frac{[\overline{Nd}]}{[\overline{E_{free}}]\cdot[Nd]_{aq}\cdot[Cl^-]_{aq}} \quad \text{(Eq.14)}$$

j. $$\overline{R_4N^+A^-} + NdCl_3 \overset{K_j}{\leftrightarrow} \overline{R_4N^+A^-\cdot NdCl_3} \quad \text{(R.36)}$$

$$K_j = \frac{[\overline{R_4N^+A^-\cdot NdCl_3}]}{[\overline{R_4N^+A^-}]\cdot[NdCl_3]} = \frac{[\overline{Nd}]}{[\overline{E_{free}}]\cdot[Nd]_{aq}} \quad \text{(Eq.15)}$$

The HCl extraction reaction has to be also taken into account due to the high impact of the pH on the extraction process (figure 38):

$$\overline{R_4N^+A^-} + HCl \overset{Ke_{HCl}}{\longleftrightarrow} \overline{R_4N^+Cl^-} + \overline{HA} \quad \text{(R.37)}$$

Therefore, the concentration of protons in the aqueous phase before and after the extraction ($\Delta[H^+] = [H^+]_{ini} - [H^+]_{aq}$) is employed for the determination of $[E_{free}]$, $[Cl^-]_{aq}$ and $[\overline{R_4N^+Cl^-}]$ bearing in mind that the reaction is complete.

In the equations above, $[E_{free}]$ is the concentration of extractant that remains free and available after extraction, and it is taken as:

$$[E]_{free} = [E]_{ini} - (n\cdot[\overline{Nd}] - \Delta[H^+]) \quad \text{(Eq.16)}$$

Where n can be 1, 2 or 3 depending on the reaction's stoichiometry.

$[\overline{R_4N^+Cl^-}]$ represents the chloride concentration in the organic phase and it is expressed as the sum of the fraction extracted in the metal chloride form plus the fraction extracted in the hydrochloric acid form:

$$[\overline{R_4N^+Cl^-}] = p\cdot[\overline{Nd}] + \Delta[H^+] \quad \text{(Eq.17)}$$

Where p is the stoichiometric coefficient of $[\overline{R_4N^+Cl^-}]$.

$[Cl^-]_{aq}$ is the chloride concentration remaining in the aqueous phase after extraction:

$$[Cl^-]_{aq} = [Cl^-]_{ini} - m\cdot[Nd]_{aq} - 3\cdot[\overline{Nd}] - \Delta[H^+] \quad \text{(Eq.18)}$$

Where m can be 0, 1, 2 or 3 depending on the number of chlorides associated with the Nd(III) species in the aqueous phase. In the equation, Cl^-_{ini} refers to the

chloride concentration in the feed calculated as the sum of chloride concentration from HCl and NaCl.

Subscripts are used to categorize the species of the process: *ini* indicates initial concentration, *aq* means the concentration of species in the aqueous phase and *free* is used to designate the extractant available after the HCl and metal ions extraction. As previously mentioned, the bar over the species denotes that they belong to the organic phase.

The equilibrium equations of the reactions presented above are linearized in terms of [E_{free}]. Table 18 shows, sorted by axis, the obtained linearizations, the theoretically expected slopes (T. Slope) and the slopes experimentally obtained (Exp. Slope). The experimental slopes were split in two groups regarding the concentration of chloride in the feed due to the effect of the anion on the extraction behaviour. This procedure is a handy guide to determine the reaction that better fits the extraction values obtained in the experimental trials.

Table 18. Linearized equilibria of the extraction reactions listed in R.27 – R.36.

Model	Axes	Logarithmic function represented	T. Slope	Exp. Slope	
				Low [Cl⁻]	High [Cl⁻]
a	Ordinate	$\log\left(\frac{\left(3\cdot[\overline{Nd}]+\Delta[H^+]\right)^3\cdot[\overline{Nd}]}{[Nd]_{aq}\cdot[Cl^-]_{aq}^3}\right)$	3	4.61	3.64
	Abscissa	$\log([\overline{E_{free}}])$			
b	Ordinate	$\log\left(\frac{[\overline{Nd}]}{[Nd]_{aq}\cdot[Cl^-]_{aq}^3}\right)$	3	2.90	2.05
	Abscissa	$\log([\overline{E_{free}}])$			
c	Ordinate	$\log\left(\frac{[\overline{Nd}]\cdot\left([\overline{Nd}]+\Delta[H^+]\right)}{[Nd]_{aq}\cdot[Cl^-]_{aq}^3}\right)$	3	3.74	2.54
	Abscissa	$\log([\overline{E_{free}}])$			
d	Ordinate	$\log\left(\frac{[\overline{Nd}]\cdot\left(2\cdot[\overline{Nd}]+\Delta[H^+]\right)^2}{[Nd]_{aq}\cdot[Cl^-]_{aq}^3}\right)$	3	4.25	3.49
	Abscissa	$\log([\overline{E_{free}}])$			
e	Ordinate	$\log\left(\frac{\left(2\cdot[\overline{Nd}]+\Delta[H^+]\right)^2\cdot[\overline{Nd}]}{[Nd]_{aq}\cdot[Cl^-]_{aq}^2}\right)$	2	4.36	3.22
	Abscissa	$\log([\overline{E_{free}}])$			
f	Ordinate	$\log\left(\frac{[\overline{Nd}]}{[Nd]_{aq}\cdot[Cl^-]_{aq}^2}\right)$	2	2.92	2.01
	Abscissa	$\log([\overline{E_{free}}])$			
g	Ordinate	$\log\left(\frac{[\overline{Nd}]\cdot\left([\overline{Nd}]+\Delta[H^+]\right)}{[Nd]_{aq}\cdot[Cl^-]_{aq}^2}\right)$	2	3.76	2.50

	Abscissa	$\log([\overline{E_{free}}])$			
h	Ordinate	$\log\left(\frac{([\overline{Nd}]+\Delta[H^+])\cdot[\overline{Nd}]}{[Nd]_{aq}\cdot[Cl^-]_{aq}}\right)$	1	3.29	1.40
	Abscissa	$\log([\overline{E_{free}}])$			
i	Ordinate	$\log\left(\frac{[\overline{Nd}]}{[Nd]_{aq}\cdot[Cl^-]_{aq}}\right)$	1	2.37	2.59
	Abscissa	$\log([\overline{E_{free}}])$			
j	Ordinate	$\log\left(\frac{[\overline{Nd}]}{[Nd]_{aq}}\right)$	1	3.08	2.21
	Abscissa	$\log([\overline{E_{free}}])$			

Regarding the experimental slopes obtained and comparing them with the theoretical ones, it could be assumed that the fitting of the Nd(III) extraction models depends on the chloride concentration in the aqueous phase. It has been observed that model b, whose stoichiometry metal:extractant is 1:3, is the most suitable model for Nd(III) extraction from low chloride solutions (0.05 mol·L^{-1}) and model f, whose stoichiometry metal:extractant is 1:2, is the most appropriate model for Nd(III) extraction from high chloride solutions (2 and 4 mol·L^{-1}). To determine the fitting of the models, the equilibrium equations K_b from Eq. 8 and K_f from Eq. 12 are taken as the starting point. Then, the equilibrium equations are linearized taking logarithms.

Taking the linearization in terms of the expression y = mX + a:

- *Model b*

$$Y = \log\left(\frac{([Nd]_{ini}-[Nd]_{aq})}{[Nd]_{aq}\cdot\left([Cl^-]_0-3\cdot([Nd]_{ini}-[Nd]_{aq})-([H^+]_{ini}-[H^+]_{eq})\right)^3}\right)$$

$$X = \log([\overline{E_{free}}]) = \log\left([\overline{E}]_{ini}-3\cdot([Nd]_{ini}-[Nd]_{aq})-([H^+]_{ini}-[H^+]_{eq})\right)$$

- *Model f*

$$Y = \log\left(\frac{([Nd]_{ini}-[Nd]_{aq})}{[Nd]_{aq}\cdot\left([Cl^-]_0-3\cdot([Nd]_{ini}-2\cdot[Nd]_{aq})-([H^+]_{ini}-[H^+]_{eq})\right)^2}\right)$$

$$X = \log([\overline{E_{free}}]) = \log\left([E]_{ini}-2\cdot([Nd]_{ini}-[Nd]_{aq})-([H^+]_{ini}-[H^+]_{eq})\right)$$

Figure 53 depicts the representations of the experimental values obtained by applying the expression Y = mX + a, for the models b and f.

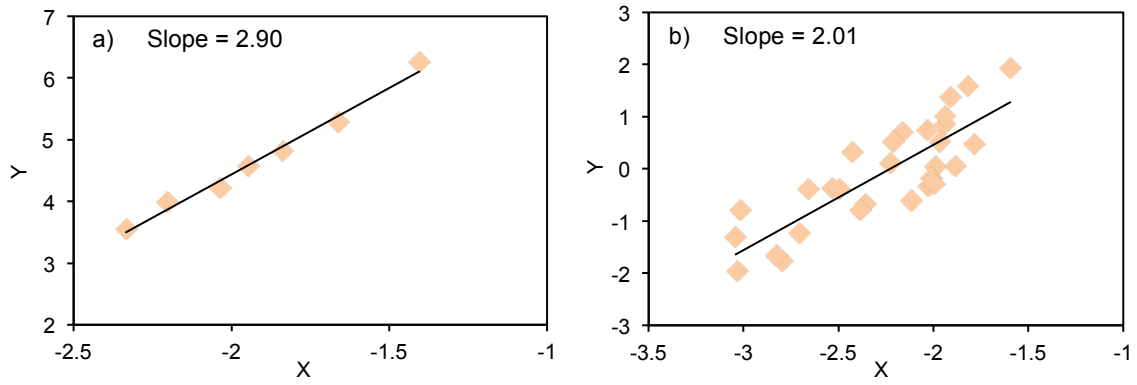

Figure 53. Variation of Y as a function of free AliOle concentration logarithm (X) in the equilibrium. a) Model b: Nd(III) extraction from low chloride media (0.05 mol·L^{-1}); b) Model f: Nd(III) extraction from high chloride media (2 and 4 mol·L^{-1}).

The linear regression analysis of the plot 53.a) shows a straight line with a slope = 2.90 and a $K_b = 1.00 \cdot 10^{10}$ and the linear regression analysis of the plot 53.b) shows a straight line with a slope = 2.01 and a $K_f = 5.54 \cdot 10^{3}$.

Figure 54 shows the fitness of the calculated extraction percentages obtained using models b and f with the experimental ones.

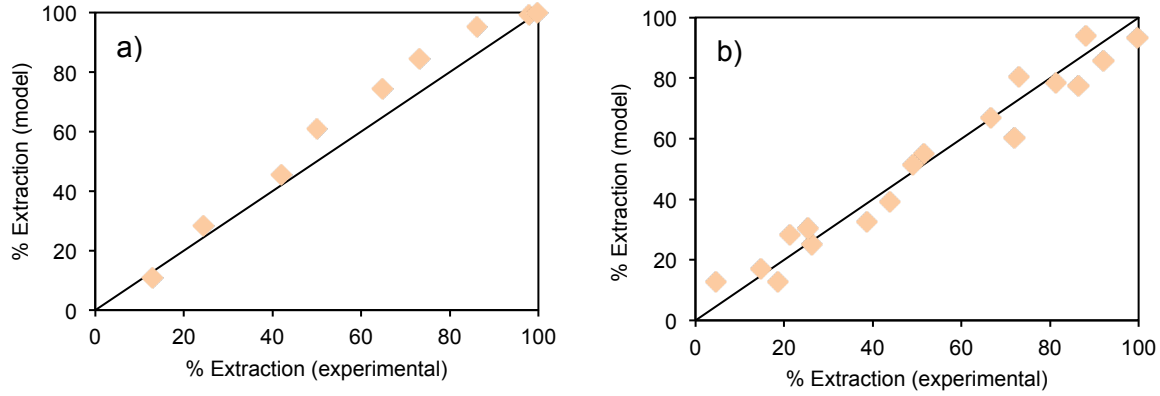

Figure 54. Comparison between experimental and calculate data: a) Calculated data using model b for 0.05 mol·L^{-1} chloride concentration ($K_{ex} = 1.00 \cdot 10^{10}$); b) Calculated data using model f for 2 and 4 mol·L^{-1} chloride concentrations ($K_{ex} = 5.54 \cdot 10^{3}$).

As can be seen, models b and f are able to accurately recreate the experimental extraction points achieved in low and high chloride media respectively. Even though the models do not take into account metal speciation in the aqueous phase, the results obtained show that they are reliable instruments to predict experimental data for this extraction system.

All in all, the preliminary extraction models proposed for the Nd(III) extraction with AliOle, assume extraction of Nd^{3+} species ($K_{ex} = 1.00 \cdot 10^{10}$) at low chloride concentrations (model b) and $NdCl^{2+}$ species ($K_{eq} = 5.54 \cdot 10^{3}$) for chloride concentrations higher than 2 $mol \cdot L^{-1}$ (model f). As shown in figure 54 the models are able to accurately reproduce the experimental Nd(III) extraction extension and predict the extraction behaviour under different experimental conditions and so they have been used as the starting point to further develop more sophisticated and detailed models with Matlab software.

3.2. Mathematical modelling of neodymium, terbium and dysprosium solvent extraction from chloride media using methyl-tri(octyl/decyl)ammonium oleate ionic liquid as extractant

This subsection develops a mathematical model of single Nd(III), Tb(III) and Dy(III) solvent extraction. Matlab R2016a software was used to solve the equilibria equations and mass balances involved in the extraction system to determine the equilibria constants. Several equilibria equations were tried to find out the most suitable model. The proposed extraction model has proven to fit perfectly the individual metal extraction data and to faithfully predict the simultaneous extraction of neodymium, terbium and dysprosium mixed in the aqueous phase. The validity of the approached equilibria constants was confirmed by comparing the plotted experimental and calculated data.
Similar extraction models can be applied in the future to predict the extraction of other REEs with AliOle under different experimental conditions and establish this information as a background for the metals transport in an SLM system.

The mathematical model proposed was developed taking into account the equilibria equations involved in the REEs extraction process with AliOle. Model equations of individual solvent extraction of Nd(III), Tb(III) and Dy(III) incorporate the equilibria and mass balance equations. Different equilibria (speciation and extraction) were considered regarding the speciation of the metals in chloride media in order to figure out the most suitable extraction model.

3.2.1. Equilibria equations

In the previous subsection, the extraction mechanism of Nd(III) was superficially investigated (E. Obón et al., 2017b). As mentioned, the neodymium extraction with AliOle was found to be in the form $NdCl^{2+}$ when the chloride concentration in the feed was above 2 $mol \cdot L^{-1}$, which resembles the chloride concentration usually found in the leachates from end-of-life products (Tunsu et al., 2014c). The first modelling approach was drawn from the premise that there was just one metal species in the aqueous phase. However, in the current work, the metal speciation is taken into account as several chloride complexes can be formed according to the formula $MeCl_n^{3-n}$, where Me can be Nd(III), Tb(III) or

Dy(III) and n = 1, 2 or 3 depending on the number of chlorides bonded with the metal ion. Therefore, the REEs distribution in the aqueous phase can be described as follows:

$$Me^{3+} + Cl^- \overset{K_1}{\leftrightarrow} MeCl^{2+} \quad \text{(R.38)}$$

$$MeCl^{2+} + Cl^- \overset{K_2}{\leftrightarrow} {MeCl_2}^+ \quad \text{(R.39)}$$

$${MeCl_2}^+ + Cl^- \overset{K_3}{\leftrightarrow} MeCl_3 \quad \text{(R.40)}$$

Where Me can be Nd(III), Tb(III) or Dy(III) and K_1, K_2 and K_3 represent the stepwise stability constants.

The equilibria expressions of the complex formation constants expressed as a function of the activities of the species (a_i) are listed below:

$$K_1 = \frac{a_{MeCl^{2+}}}{a_{Me^{3+}} \cdot a_{Cl^-}} = \frac{[MeCl^{2+}]}{[Me^{3+}]\cdot[Cl^-]} \cdot \frac{\gamma_{MeCl^{2+}}}{\gamma_{Me^{3+}} \cdot \gamma_{Cl^-}} \quad \text{(Eq.19)}$$

$$K_2 = \frac{a_{{MeCl_2}^+}}{a_{MeCl^{2+}} \cdot a_{Cl^-}} = \frac{[{MeCl_2}^+]}{[MeCl^{2+}]\cdot[Cl^-]} \cdot \frac{\gamma_{{MeCl_2}^+}}{\gamma_{MeCl^{2+}} \cdot \gamma_{Cl^-}} \quad \text{(Eq.20)}$$

$$K_3 = \frac{a_{MeCl_3}}{a_{{MeCl_2}^+} \cdot a_{Cl^-}} = \frac{[MeCl_3]}{[{MeCl_2}^+]\cdot[Cl^-]} \cdot \frac{\gamma_{MeCl_3}}{\gamma_{{MeCl_2}^+} \cdot \gamma_{Cl^-}} \quad \text{(Eq.21)}$$

Where γ_i represents the activity coefficient of the species i and the stepwise formation constants can be converted easily into their cumulative form taking into account that they are described as the product of the simple ones: $\beta_1 = K_1$; $\beta_2 = K_1 \cdot K_2$; $\beta_3 = K_1 \cdot K_2 \cdot K_3$.

The ionic strength of the metals was calculated from Eq. 6. The Davies equation was used to calculate the activity coefficients of the species in the aqueous phase when $I_m \neq 0$:

$$\log_{10} \gamma_i = -0.5102 \cdot z_i \cdot \left(\frac{\sqrt{I_m}}{(1+\sqrt{I_m})} - 0.3 \cdot I_m\right) \quad \text{(Eq.22)}$$

According to the speciation described, several extraction mechanisms of REEs from chloride medium were considered. A distinction was made between extraction of REEs by ionic exchange (Alok Rout and Binnemans, 2014a) and by solvation (Aba et al., 2011; Kubota et al., 2011), since both mechanisms have been depicted in the literature.

The proposed equilibria equations assume that there can be just one Me-organic species in the organic phase, meaning that the extraction of several

metal species simultaneously does not occur. The model takes also into account the competitive extraction of HCl. On this basis, the extraction reactions that could take place in this extraction system are the same as the ones presented in the previous preliminary work on the neodymium individual extraction R.27 – R.37, but taking them as generic reactions where Me can be Nd(III), Tb(III) or Dy(III).

$$3\,\overline{R_4N^+A^-} + Me^{3+} + 3\,Cl^- \overset{K_a}{\leftrightarrow} 3\,\overline{R_4N^+Cl^-} + \overline{MeA_3} \quad \text{(R.27a)}$$

$$3\,\overline{R_4N^+A^-} + Me^{3+} + 3\,Cl^- \overset{K_b}{\leftrightarrow} \overline{(R_4N^+Cl^-)_3 \cdot MeA_3} \quad \text{(R.28a)}$$

$$3\,\overline{R_4N^+A^-} + Me^{3+} + 3\,Cl^- \overset{K_c}{\leftrightarrow} \overline{(R_4N^+Cl^-)_2 \cdot MeA_3} + \overline{R_4N^+Cl^-} \quad \text{(R.29a)}$$

$$3\,\overline{R_4N^+A^-} + Me^{3+} + 3\,Cl^- \overset{K_d}{\leftrightarrow} \overline{R_4N^+Cl^- \cdot MeA_3} + 2\,\overline{R_4N^+Cl^-} \quad \text{(R.30a)}$$

$$2\,\overline{R_4N^+A^-} + MeCl^{2+} + 2\,Cl^- \overset{K_e}{\leftrightarrow} 2\,\overline{R_4N^+Cl^-} + \overline{MeClA_2} \quad \text{(R.31a)}$$

$$2\,\overline{R_4N^+A^-} + MeCl^{2+} + 2\,Cl^- \overset{K_f}{\leftrightarrow} \overline{(R_4N^+Cl^-)_2 \cdot MeClA_2} \quad \text{(R.32a)}$$

$$2\,\overline{R_4N^+A^-} + MeCl^{2+} + 2\,Cl^- \overset{K_g}{\leftrightarrow} \overline{R_4N^+Cl^- \cdot MeClA_2} + \overline{R_4N^+Cl^-} \quad \text{(R.33a)}$$

$$\overline{R_4N^+A^-} + {MeCl_2}^+ + Cl^- \overset{K_h}{\leftrightarrow} \overline{R_4N^+Cl^-} + \overline{MeCl_2A} \quad \text{(R.34a)}$$

$$\overline{R_4N^+A^-} + {MeCl_2}^+ + Cl^- \overset{K_i}{\leftrightarrow} \overline{R_4N^+Cl^- \cdot MeCl_2A} \quad \text{(R.35a)}$$

$$\overline{R_4N^+A^-} + MeCl_3 \overset{K_j}{\leftrightarrow} \overline{R_4N^+A^- \cdot MeCl_3} \quad \text{(R.36a)}$$

$$\overline{R_4N^+A^-} + HCl \xrightarrow{K_{eHCl}} \overline{R_4N^+Cl^-} + \overline{HA} \quad \text{(R.37a)}$$

In this case, the equilibrium equations of the extraction constants are expressed as a function of the activities of the species (a_i):

$$K_a = \frac{a^3_{\overline{R_4N^+Cl^-}} \cdot a_{\overline{MeA_3}}}{a^3_{\overline{R_4N^+A^-}} \cdot a_{Me^{3+}} \cdot a^3_{Cl^-}} = \frac{[\overline{R_4N^+Cl^-}]^3 \cdot [\overline{MeA_3}]}{[\overline{R_4N^+A^-}]^3 \cdot [Me^{3+}] \cdot [Cl^-]^3} \cdot \frac{\gamma^3_{\overline{R_4N^+Cl^-}} \cdot \gamma_{\overline{MeA_3}}}{\gamma^3_{\overline{R_4N^+A^-}} \cdot \gamma_{Me^{3+}} \cdot \gamma^3_{Cl^-}} \quad \text{(Eq.23)}$$

$$K_b = \frac{a_{\overline{(R_4N^+Cl^-)_3 \cdot MeA_3}}}{a^3_{\overline{R_4N^+A^-}} \cdot a_{Me^{3+}} \cdot a^3_{Cl^-}} = \frac{[\overline{(R_4N^+Cl^-)_3 \cdot MeA_3}]}{[\overline{R_4N^+A^-}]^3 \cdot [Me^{3+}] \cdot [Cl^-]^3} \cdot \frac{\gamma_{\overline{(R_4N^+Cl^-)_3 \cdot MeA_3}}}{\gamma^3_{\overline{R_4N^+A^-}} \cdot \gamma_{Me^{3+}} \cdot \gamma^3_{Cl^-}} \quad \text{(Eq.24)}$$

$$K_c = \frac{a_{\overline{(R_4N^+Cl^-)_2 \cdot MeA_3}} \cdot a_{\overline{R_4N^+Cl^-}}}{a^3_{\overline{R_4N^+A^-}} \cdot a_{Me^{3+}} \cdot a^3_{Cl^-}} = \frac{[\overline{(R_4N^+Cl^-)_2 \cdot MeA_3}] \cdot [\overline{R_4N^+Cl^-}]}{[\overline{R_4N^+A^-}]^3 \cdot [Me^{3+}] \cdot [Cl^-]^3} \cdot \frac{\gamma_{\overline{(R_4N^+Cl^-)_2 \cdot MeA_3}} \cdot \gamma_{\overline{R_4N^+Cl^-}}}{\gamma^3_{\overline{R_4N^+A^-}} \cdot \gamma_{Me^{3+}} \cdot \gamma^3_{Cl^-}} \quad \text{(Eq.25)}$$

$$K_d = \frac{a_{\overline{R_4N^+Cl^- \cdot MeA_3}} \cdot a^2_{\overline{R_4N^+Cl^-}}}{a^3_{\overline{R_4N^+A^-}} \cdot a_{Me^{3+}} \cdot a^3_{Cl^-}} = \frac{[\overline{R_4N^+Cl^- \cdot MeA_3}] \cdot [\overline{R_4N^+Cl^-}]^2}{[\overline{R_4N^+A^-}]^3 \cdot [Me^{3+}] \cdot [Cl^-]^3} \cdot \frac{\gamma_{\overline{(R_4N^+Cl^-)_2 \cdot MeA_3}} \cdot \gamma^2_{\overline{R_4N^+Cl^-}}}{\gamma^3_{\overline{R_4N^+A^-}} \cdot \gamma_{Me^{3+}} \cdot \gamma^3_{Cl^-}} \quad \text{(Eq.26)}$$

$$K_e = \frac{a^2_{\overline{R_4N^+Cl^-}} \cdot a_{\overline{MeClA_2}}}{a^2_{\overline{R_4N^+A^-}} \cdot a_{MeCl^{2+}} \cdot a^2_{Cl^-}} = \frac{[\overline{R_4N^+Cl^-}]^2 \cdot [\overline{MeClA_2}]}{[\overline{R_4N^+A^-}]^2 \cdot [MeCl^{2+}] \cdot [Cl^-]^2} \cdot \frac{\gamma^2_{\overline{R_4N^+Cl^-}} \cdot \gamma_{\overline{MeClA_2}}}{\gamma^2_{\overline{R_4N^+A^-}} \cdot \gamma_{MeCl^{2+}} \cdot \gamma^2_{Cl^-}} \quad \text{(Eq.27)}$$

$$K_f = \frac{a_{\overline{(R_4N^+Cl^-)_2 \cdot MeClA_2}}}{a^2_{\overline{R_4N^+A^-}} \cdot a_{MeCl^{2+}} \cdot a^2_{Cl^-}} = \frac{[\overline{(R_4N^+Cl^-)_2 \cdot MeClA_2}]}{[\overline{R_4N^+A^-}]^2 \cdot [MeCl^{2+}] \cdot [Cl^-]^2} \cdot \frac{\gamma_{\overline{(R_4N^+Cl^-)_2 \cdot MeClA_2}}}{\gamma^2_{\overline{R_4N^+A^-}} \cdot \gamma_{MeCl^{2+}} \cdot \gamma^2_{Cl^-}} \quad \text{(Eq.28)}$$

$$K_g = \frac{a_{\overline{R_4N^+Cl^-\cdot MeClA_2}} \cdot a_{\overline{R_4N^+Cl^-}}}{a^2_{\overline{R_4N^+A^-}} \cdot a_{MeCl^{2+}} \cdot a^2_{Cl^-}} = \frac{\left[\overline{R_4N^+Cl^-\cdot MeClA_2}\right]\cdot\left[\overline{R_4N^+Cl^-}\right]}{\left[\overline{R_4N^+A^-}\right]^2\cdot\left[MeCl^{2+}\right]\cdot\left[Cl^-\right]^2} \cdot \frac{\gamma_{\overline{R_4N^+Cl^-\cdot MeClA_2}} \cdot \gamma_{\overline{R_4N^+Cl^-}}}{\gamma^2_{\overline{R_4N^+A^-}} \cdot \gamma_{MeCl^{2+}} \cdot \gamma^2_{Cl^-}} \quad \text{(Eq.29)}$$

$$K_h = \frac{a_{\overline{R_4N^+Cl^-}} \cdot a_{\overline{MeCl_2A}}}{a_{\overline{R_4N^+A^-}} \cdot a_{MeCl_2^+} \cdot a_{Cl^-}} = \frac{\left[\overline{R_4N^+Cl^-}\right]\cdot\left[\overline{MeCl_2A}\right]}{\left[\overline{R_4N^+A^-}\right]\cdot\left[MeCl_2^+\right]\cdot\left[Cl^-\right]} \cdot \frac{\gamma_{\overline{R_4N^+Cl^-}} \cdot \gamma_{\overline{MeCl_2A}}}{\gamma_{\overline{R_4N^+A^-}} \cdot \gamma_{MeCl_2^+} \cdot \gamma_{Cl^-}} \quad \text{(Eq.30)}$$

$$K_i = \frac{a_{\overline{R_4N^+Cl^-\cdot MeCl_2A}}}{a_{\overline{R_4N^+A^-}} \cdot a_{MeCl_2^+} \cdot a_{Cl^-}} = \frac{\left[\overline{R_4N^+Cl^-\cdot MeCl_2A}\right]}{\left[\overline{R_4N^+A^-}\right]\cdot\left[MeCl_2^+\right]\cdot\left[Cl^-\right]} \cdot \frac{\gamma_{\overline{R_4N^+Cl^-\cdot MeCl_2A}}}{\gamma_{\overline{R_4N^+A^-}} \cdot \gamma_{MeCl_2^+} \cdot \gamma_{Cl^-}} \quad \text{(Eq.31)}$$

$$K_j = \frac{a_{\overline{R_4N^+A^-\cdot MeCl_3}}}{a_{\overline{R_4N^+A^-}} \cdot a_{MeCl_3}} = \frac{\left[\overline{R_4N^+A^-\cdot MeCl_3}\right]}{\left[\overline{R_4N^+A^-}\right]\cdot[MeCl_3]} \cdot \frac{\gamma_{\overline{R_4N^+A^-\cdot MeCl_3}}}{\gamma_{\overline{R_4N^+A^-}} \cdot \gamma_{MeCl_3}} \quad \text{(Eq.32)}$$

$$K_{eHCl} = \frac{a_{\overline{R_4N^+Cl^-}} \cdot a_{\overline{HA}}}{a_{\overline{R_4N^+A^-}} \cdot a_{HCl}} = \frac{\left[\overline{R_4N^+Cl^-}\right]\cdot\left[\overline{HA}\right]}{\left[\overline{R_4N^+A^-}\right]\cdot[HCl]} \cdot \frac{\gamma_{\overline{R_4N^+Cl^-}} \cdot \gamma_{\overline{HA}}}{\gamma_{\overline{R_4N^+A^-}} \cdot \gamma_{HCl}} \quad \text{(Eq.33)}$$

The bar above the species denotes that they are in the organic phase.
In the equilibria equations, the activity coefficients (γ) of the organic and the aqueous neutral species are considered to be equal to 1.

3.2.2. Mass balances

The mass balances are based on the stoichiometry of the equilibria equations. Taking into account the equal volumes of the aqueous and the organic phases, the total concentration of the reagents involved in the reaction can be calculated as the sum of the species present in the system. Generalized mass balances for the equilibria of single extraction reactions (R.4 – R.13) can be written as follows:

REEs mass balance

$$[Me]_t = [Me^{3+}] + [MeCl^{2+}] + \left[MeCl_2^+\right] + [MeCl_3] + [\overline{Me}] \quad \text{(Eq.34)}$$

Chloride mass balance

$$[Cl^-]_t = [MeCl^{2+}] + 2\cdot\left[MeCl_2^+\right] + 3\cdot[MeCl_3] + 3\cdot[\overline{Me}] + \Delta[H^+] \quad \text{(Eq.35)}$$

AliOle mass balance

$$[\overline{E}]_t = [\overline{E_{free}}] + m\cdot[\overline{Me}] + \Delta[H^+] \quad \text{(Eq.36)}$$

Where the subscript *t* means the total concentration of the specie, which in turn is the initial concentration, the bar above the metallic species denotes that it belongs to the organic phase, $[\overline{E_{free}}]$ is the extractant concentration available after HCl and metal extraction, $\Delta[H^+]$ is equal to the concentration of HCl in the organic phase and m can be 1, 2 or 3 depending on the stoichiometry of the equilibria reaction considered.

3.2.3. Competitive extraction prediction

The models that better fitted the extraction performance of each REE individually as well as the optimized extraction and formation constants calculated in each case were used to forecast the behaviour of the multicomponent extraction process. In this regard, the mass balances of chloride (Eq.35) and AliOle IL (Eq.36) needed to be modified to embrace all the metallic species involved in the extraction system. The modified mass balances can be defined as follows:

Nd(III) mass balance

$$[\mathrm{Nd}]_t = [\mathrm{Nd}^{3+}] + [\mathrm{NdCl}^{2+}] + [\mathrm{NdCl_2}^{+}] + [\mathrm{NdCl_3}] + [\overline{\mathrm{Nd}}] \quad \text{(Eq.37)}$$

Tb(III) mass balance

$$[\mathrm{Tb}]_t = [\mathrm{Tb}^{3+}] + [\mathrm{TbCl}^{2+}] + [\mathrm{TbCl_2}^{+}] + [\mathrm{TbCl_3}] + [\overline{\mathrm{Tb}}] \quad \text{(Eq.38)}$$

Dy(III) mass balance

$$[\mathrm{Dy}]_t = [\mathrm{Dy}^{3+}] + [\mathrm{DyCl}^{2+}] + [\mathrm{DyCl_2}^{+}] + [\mathrm{DyCl_3}] + [\overline{\mathrm{Dy}}] \quad \text{(Eq.39)}$$

Chloride mass balance

$$\begin{aligned}[\mathrm{Cl}^-]_t = {} & [\mathrm{NdCl}^{2+}] + 2\cdot[\mathrm{NdCl_2}^{+}] + 3\cdot[\mathrm{NdCl_3}] + 3\cdot[\overline{\mathrm{Nd}}] \\ & + [\mathrm{TbCl}^{2+}] + 2\cdot[\mathrm{TbCl_2}^{+}] + 3\cdot[\mathrm{TbCl_3}] + 3\cdot[\overline{\mathrm{Tb}}] \\ & + [\mathrm{DyCl}^{2+}] + 2\cdot[\mathrm{DyCl_2}^{+}] + 3\cdot[\mathrm{DyCl_3}] + 3\cdot[\overline{\mathrm{Dy}}] + \Delta[\mathrm{H}^+]\end{aligned} \quad \text{(Eq.40)}$$

AliOle mass balance

$$[\overline{\mathrm{E}}]_t = [\overline{\mathrm{E_{free}}}] + \mathrm{m}\cdot[\overline{\mathrm{Nd}}] + \mathrm{n}\cdot[\overline{\mathrm{Tb}}] + \mathrm{p}\cdot[\overline{\mathrm{Dy}}] + \Delta[\mathrm{H}^+] \quad \text{(Eq.41)}$$

Where n and p can be 1, 2 or 3 depending on the stoichiometry of the equilibria reaction considered.

For the competitive extraction prediction Eq. 40 is used instead of Eq. 35 and Eq.41 instead of Eq. 36.

3.2.4. Model resolution

The calculations of the modelling of REEs extraction were performed using the mathematical software Matlab R2016a. The formation (Eq. 19 – 21) and extraction constants (Eq. 23 – 33) were used as the optimization parameters in order to find the values that make experimental and calculated data match with the minimum error. The resolution method applied has been described in chapter 3 (Figure 31).

Three different matrices were used to compile the experimental data of Nd(III), Tb(III) and Dy(III) separately (90 experimental points). The experimental matrices contained, in columns, the initial concentrations of the metals and the chloride anion in the aqueous phase, the initial concentration of AliOle, the concentration of protons in the aqueous phase before and after the extraction and the extraction percentages obtained experimentally. Next, the equilibria equations in the aqueous and the organic phase as well as the mass balances involved were introduced. Nine extraction models were tested, one for each of the equilibria equations described (Eq. 23 – 32). Initial concentration guesses of all the metal species in the system (X_0) were entered. The nonlinear system of equations was solved with the Matlab function *fsolve* and the extraction percentages were calculated (Eq.1). The optimization of the stability and equilibria constants was achieved by minimizing the function defined as the sum of the square of the differences between the calculated and the experimental percentages of extraction (Eq.4) using the Matlab function *fmincon.* Formation constants based on the literature and guessed equilibria constants were used to initialize the program (K_0). Table 19 depicts the stability constants of the chlorinated species in the aqueous phase found in the literature.

Table 19. Stability constants in the literature.

	Nd(III)			Tb(III)			Dy(III)		
	K_1	K_2	K_3	K_1	K_2	K_3	K_1	K_2	K_3
a	2.09	0.50	-	1.86	0.45	-	1.86	0.45	-
b	1.00	-	-	-	-	-	-	-	-
c	$8.32 \cdot 10^{-3}$	-	-	-	-	-	-	-	-
d	1.8	1.1	-	-	-	-	-	-	-

a. Medusa Software, KHT Royal Institute of Technology (Puigdomenech, 2013)
b. (Hogfeldt, 1982)
c. (Lee et al., 2005)
d. (Sastri, 2003)

The optimization led to the determination of the stability and equilibria constants, whose values allow the experimental extraction extension of the metals to be reproduced with the minimum error.

The simulation models created were applied to the extraction of Nd(III), Tb(III), and Dy(III) individually. The stability factors from the literature (table 19) were taken into account although there was not much information because of the recent surge in REEs interest. The reported formation constants were tested out for initialization of the models (K_0) but unfortunately, they were not able to reproduce the experimental extraction values of the metals for any of the proposed models. In this regard, it became necessary to find new constants beyond the literature, from scratch, in order to adjust the models to the experimental data of REEs solvent extraction.

The error, calculated as the sum of the absolute value of the differences between the calculated and the experimental extraction percentages of the metals for each point studied (Eq.4), as well as comparative plots between the experimental and the modelled results were used to discern which model, within the nine proposed, is the most appropriate for the reproduction of REEs experimental extraction data. Optimized stability and equilibria constants were determined in each case. Table 20 shows the optimized stability and extraction constants and the error value calculated for each model tested.

Table 20. Optimization parameters.

	Nd(III)				Tb(III)				Dy(III)				σ total
	K_{eq}	K_1	K_2	K_3	K_{eq}	K_1	K_2	K_3	K_{eq}	K_1	K_2	K_3	
Eq.6 (a)	7.88	0.09	0.94	0.13	7.62	$1.20 \cdot 10^{-3}$	0.24	0.69	6.79	0.16	0.33	0.06	8140.10
Eq.7 (b)	50223	0.75	1.17	0.72	63541	$5 \cdot 10^{-3}$	0.43	0.27	50965	1.94	1.92	1.90	5492
Eq.8 (c)	7837.70	0.44	$1.00 \cdot 10^{-5}$	0.07	13580	$3.00 \cdot 10^{-3}$	0.84	0.105	7737.9	4.363	0.732	0.13	4746.70
Eq.9 (d)	82.39	0.57	0.44	0.49	1850.90	0.67	1.84	1.05	2321.60	1.67	0.36	61.15	7345.80
Eq.10 (e)	3.54	3.25	124.12	0.32	1.34	0.05	0.03	0.81	3.21	20.48	2.44	2.68	2347
Eq.11 (f)	4223.02	37.14	0.15	$9.50 \cdot 10^{-4}$	5573.10	252.97	0.03	0.30	7259.50	98.39	0.02	1.00	599.25
Eq.12 (g)	5559.30	87.22	0.10	$7.65 \cdot 10^{-4}$	6515.50	84.04	0.08	$4.72 \cdot 10^{-6}$	5021.90	100.59	$3.30 \cdot 10^{-3}$	1.76	652.95
Eq.13 (h)	0.08	71.25	1.51	0.02	41.99	306.84	6.71	0.87	3.92	75.04	0.01	$1.10 \cdot 10^{-4}$	3239
Eq.14 (i)	53.67	39.66	149.98	0.12	56.58	253.39	25.73	0.16	84.11	99.17	18.89	0.42	1428
Eq.15 (j)	435.17	34.27	155.78	0.12	356.59	249.44	18.15	0.16	198.31	110.08	0.18	42.50	1427.60

The results show that the best-fitted model to the experimental data for Nd(III), Tb(III) and Dy(III) is the one corresponding to the reaction R.32a, which means that the metals are extracted by solvation and the stoichiometry metal – IL is 1:2:

$$2\ \overline{R_4N^+A^-} + MeCl^{2+} + 2\ Cl^- \overset{K_f}{\leftrightarrow} \overline{(R_4N^+Cl^-)_2 \cdot MeClA_2} \qquad \text{(R.32a)}$$

This finding is in agreement with the results obtained in the previous study dealing with the extraction of Nd(III) in chloride media using AliOle IL (E. Obón et al., 2017b). The comparative plots of Nd(III), Tb(III) and Dy(III) extraction from chloride media 2 and 4 mol·L^{-1} with AliOle IL show that it is possible to accurately recreate the experimental extraction of the metals.

Figure 55 shows a comparison between the results of the model obtained by using the optimized parameters calculated with Matlab software and the experimental extraction percentages.

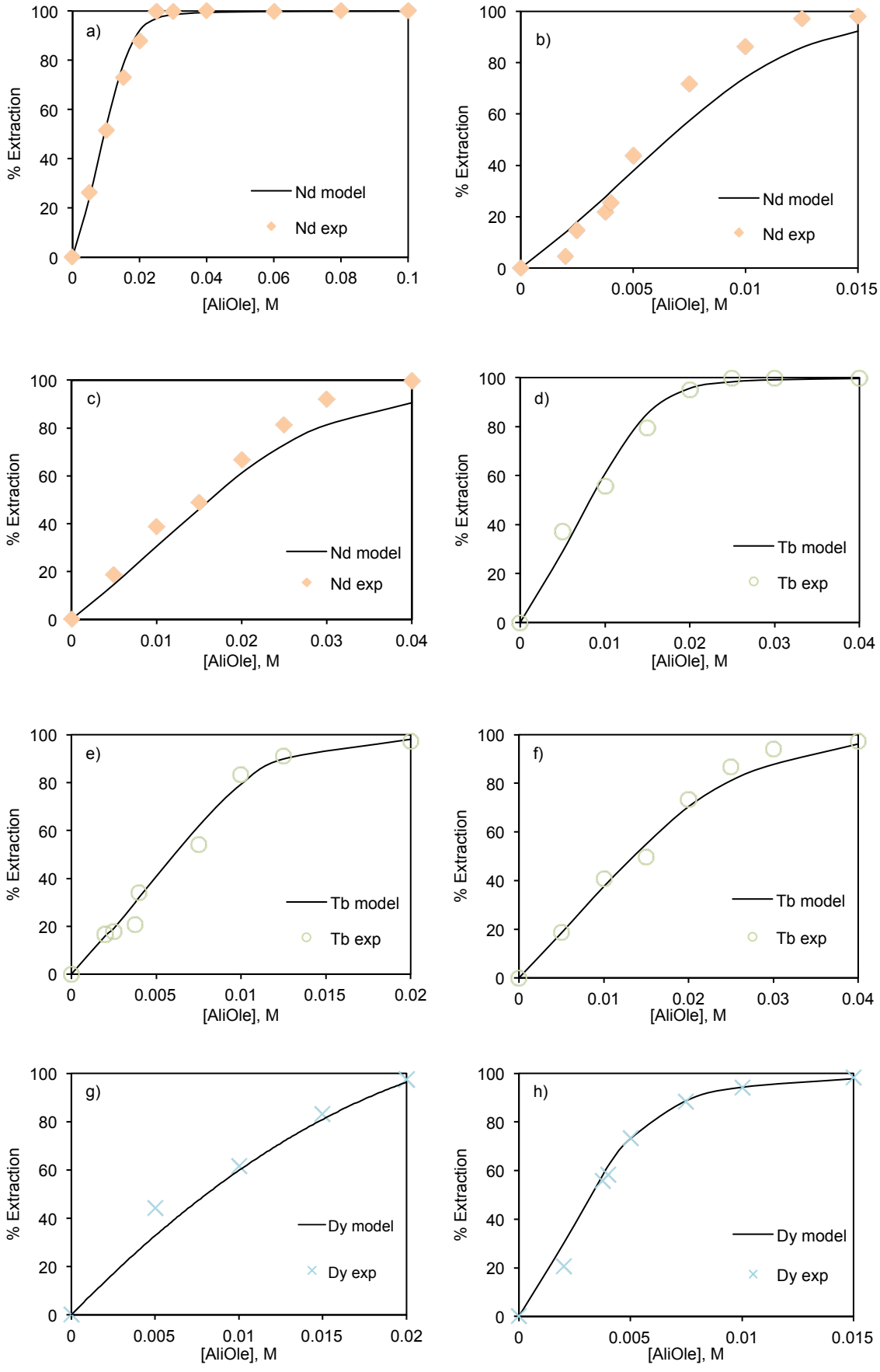
a)
% Extraction
[AliOle], M
Nd model
Nd exp
b)
% Extraction
[AliOle], M
Nd model
Nd exp
c)
% Extraction
[AliOle], M
Nd model
Nd exp
d)
% Extraction
[AliOle], M
Tb model
Tb exp
e)
% Extraction
[AliOle], M
Tb model
Tb exp
f)
% Extraction
[AliOle], M
Tb model
Tb exp
g)
% Extraction
[AliOle], M
Dy model
Dy exp
h)
% Extraction
[AliOle], M
Dy model
Dy exp

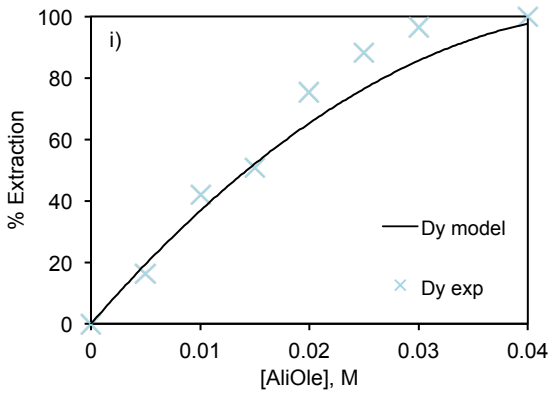

Figure 55. Comparative graphs between the simulated extraction results and the experimental extraction extension. a) aqueous phase: 0.007 mol·L^{-1} Nd(III), 4 mol·L^{-1} chloride; b) aqueous phase: 0.004 mol·L^{-1} Nd(III), 4 mol·L^{-1} chloride; c) aqueous phase: 0.007 mol·L^{-1} Nd(III), 2 mol·L^{-1} chloride; d) aqueous phase: 0.007 mol·L^{-1} ^{1} Tb(III), 4 mol·L^{-1} chloride; e) aqueous phase: 0.004 mol·L^{-1} Td(III), 4 mol·L^{-1} chloride; f) aqueous phase: 0.007 mol·L^{-1} Tb(III), 2 mol·L^{-1} chloride; g) aqueous phase: 0.006 mol·L^{-1} Dy(III), 4 mol·L^{-1} chloride; h) aqueous phase: 0.001 mol·L^{-1} Dy(III), 4 mol·L^{-1} chloride; i) aqueous phase: 0.006 mol·L^{-1} Dy(III), 2 mol·L^{-1} chloride.

As can be seen, the selected model is able to reproduce the experimental extraction yield of Nd(III), Tb(III) and Dy(III) using the optimized equilibrium parameters listed in table 19. The effect of the AliOle, the chloride anion and the REEs concentrations over the extraction process are taken as a reference and as can be observed, the model fits the experimental data with the minimum error.

The optimized stability and equilibrium constants calculated on this model were tested on an extraction system of the mixture of neodymium, terbium and dysprosium in the aqueous phase in order to determine if the model established for the single extraction of the metals was also useful to reproduce their competitive extraction. The effect of the AliOle and chloride concentrations in the aqueous phase on the simultaneous extraction of Nd(III), Tb(III) and Dy(III) was studied. Figure 56 shows the comparative graphs between the simulation results of the model and the extraction percentages obtained experimentally.

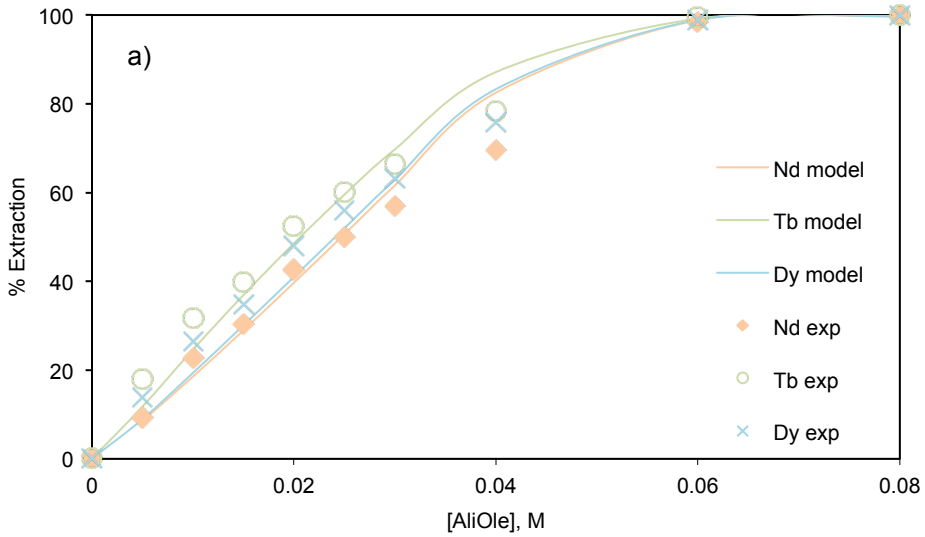

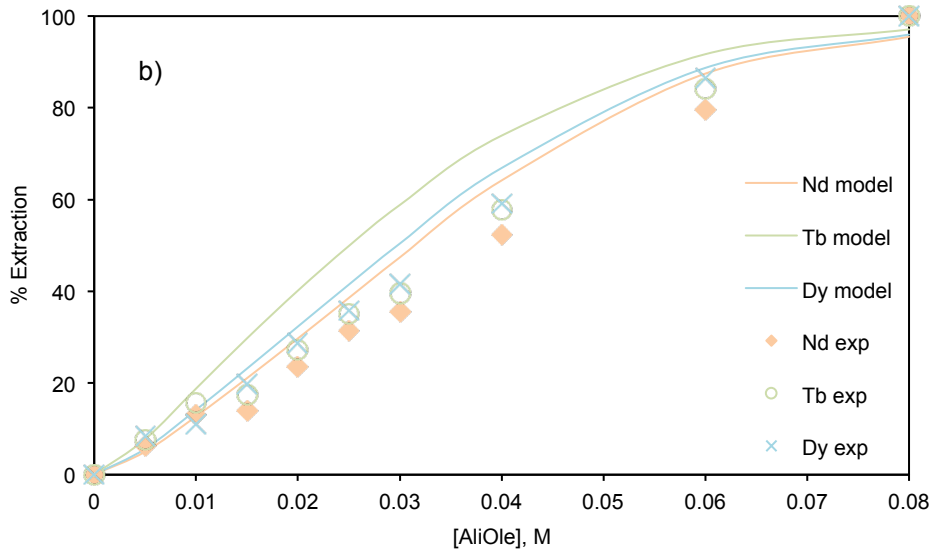

Figure 56. Comparative graphs between simulated extraction results and experimental extraction extension. a) aqueous phase: 1000 mg·L^{-1} of Nd(III), Tb(III) and Dy(III), 4 mol·L^{-1} chloride; b) aqueous phase: 1000 mg·L^{-1} of Nd(III), Tb(III) and Dy(III), 2 mol·L^{-1} chloride.

The proposed model, which involves solvating extraction of the metals by 1:2 stoichiometry, has proven to be a very handy tool to predict the extraction of REEs with AliOle in chloride media. This could also be very useful either to set the parameters for a new experimental study about any other REEs solvent extraction with AliOle, or to model their transport through SLM. It also could be successfully exploited for extraction prediction of REEs from end of life products (urban mining), requiring only minor adjustments of the equilibria equations and mass balances.

In conclusion, the model that better fitted the experimental data was found to be in agreement preliminary studies. The calculated formation constants of the aqueous Nd-Cl, Tb-Cl and Dy-Cl complexes formed in the aqueous phase were: $K_{1\ Nd}$ = 37.14; $K_{2\ Nd}$ = 0.15; $K_{3\ Nd}$ = $9.50 \cdot 10^{-4}$; $K_{1\ Tb}$ = 252.97; $K_{2\ Tb}$ =0.03; $K_{3\ Tb}$ = 0.30; $K_{1\ Dy}$ = 98.39; $K_{2\ Dy}$ = 0.02; $K_{3\ Dy}$ = 1.00. The equilibrium constants were calculated as: $K_{eq\ Nd}$ = 4223.02; $K_{eq\ Tb}$ = 5573.10; $K_{eq\ Dy}$ = 7259.50. The reliability of the method was proven by plotting the calculated extraction percentages versus the experimental extraction percentages.

3.3. Mathematical modelling of neodymium, terbium and dysprosium solvent extraction from chloride alkaline solution using methyltri(octyl/decyl)ammonium chloride

Based on the experimental study of the solvent extraction of neodymium, terbium and dysprosium from alkaline media using Aliquat 336 IL with the addition of citric acid, a mathematical modelling of Nd(III), Tb(III) and Dy(III) solvent extraction was developed. As in the model of neodymium, terbium and dysprosium extraction from chloride media using AliOle IL (E. Obón et al.,

2017a), the Matlab software was used. The proposed extraction model has proven to match the experimental extraction extension of the metals individually and to faithfully predict the simultaneous extraction of Nd(III), Tb(III) and Dy(III) from alkaline aqueous media. The validity of the approached equilibria constants was confirmed by comparing the plots of the experimental percentages versus the calculated data.

The mathematical model proposed was developed taking into account the equilibria equations involved in the REEs extraction process with Aliquat 336. Different equilibria (speciation and extraction) were considered regarding the speciation of the metals in chloride media in order to figure out the best-fitted extraction model.

3.3.1. Equilibria equations

The extraction mechanism of Nd(III), Tb(III) and Dy(III) has been superficially investigated in section 2.4 of this chapter. Neodymium, terbium and dysprosium citrates appear to be extracted in the form $MeCl_2Cit^{2-}$, nonetheless for modelling purposes, the speciation of the metals in the feed is taken into account. In this regard, the REEs distribution in the aqueous phase can be described as follows:

$$Me^{3+} + Cl^- \overset{K_1}{\leftrightarrow} MeCl^{2+} \quad \text{(R.38)}$$

$$MeCl^{2+} + Cl^- \overset{K_2}{\leftrightarrow} {MeCl_2}^+ \quad \text{(R.39)}$$

$${MeCl_2}^+ + Cl^- \overset{K_3}{\leftrightarrow} MeCl_3 \quad \text{(R.40)}$$

$$MeCl^{2+} + Cit^{3-} \overset{Kcit1}{\longleftrightarrow} MeClCit^- \quad \text{(R.19)}$$

$$MeCl_2^+ + Cit^{3-} \overset{Kcit2}{\longleftrightarrow} MeCl_2Cit^{2-} \quad \text{(R.20)}$$

$$Me^{3+} + Cit^{3-} \overset{Kcit3}{\longleftrightarrow} MeCit \quad \text{(R.21)}$$

In the reactions, Me can be Nd(III), Tb(III) or Dy(III) and K_1, K_2, K_3, K_{cit1}, K_{cit2}, K_{cit3} represent the stepwise stability constants.

The equilibria expressions of the formation constants are expressed as a function of the concentrations and activities of the species (a_i):

$$K_1 = \frac{a_{MeCl^{2+}}}{a_{Me^{3+}} \cdot a_{Cl^-}} = \frac{[MeCl^{2+}]}{[Me^{3+}]\cdot[Cl^-]} \cdot \frac{\gamma_{MeCl^{2+}}}{\gamma_{Me^{3+}}\cdot\gamma_{Cl^-}} \quad \text{(Eq.42)}$$

$$K_2 = \frac{a_{{MeCl_2}^+}}{a_{MeCl^{2+}} \cdot a_{Cl^-}} = \frac{[{MeCl_2}^+]}{[MeCl^{2+}]\cdot[Cl^-]} \cdot \frac{\gamma_{{MeCl_2}^+}}{\gamma_{MeCl^{2+}}\cdot\gamma_{Cl^-}} \quad \text{(Eq.43)}$$

$$K_3 = \frac{a_{MeCl_3}}{a_{{MeCl_2}^+} \cdot a_{Cl^-}} = \frac{[MeCl_3]}{[{MeCl_2}^+]\cdot[Cl^-]} \cdot \frac{\gamma_{MeCl_3}}{\gamma_{{MeCl_2}^+}\cdot\gamma_{Cl^-}} \quad \text{(Eq.44)}$$

$$K_{cit1} = \frac{a_{MeClCit^-}}{a_{MeCl^{2+}} \cdot a_{Cit^{3-}}} = \frac{[MeClCit^-]}{[MeCl^{2+}]\cdot[Cit^-]} \cdot \frac{\gamma_{MeClCit^-}}{\gamma_{MeCl^{2+}}\cdot\gamma_{Cit^-}} \quad \text{(Eq.45)}$$

$$K_{cit2} = \frac{a_{MeCl_2Cit^{2-}}}{a_{MeCl_2^+} \cdot a_{Cit^{3-}}} = \frac{[MeCl_2Cit^{2-}]}{[MeCl_2^+] \cdot [Cit^{3-}]} \cdot \frac{\gamma_{MeCl_2Cit^{2-}}}{\gamma_{MeCl_2^+} \cdot \gamma_{Cit^{3-}}} \quad \text{(Eq.46)}$$

$$K_{cit3} = \frac{a_{MeCit}}{a_{Me^{3+}} \cdot a_{Cit^{-}}} = \frac{[MeCit]}{[Me^{3+}] \cdot [Cit^{-}]} \cdot \frac{\gamma_{MeCit}}{\gamma_{Me^{3+}} \cdot \gamma_{Cit^{-}}} \quad \text{(Eq.47)}$$

Where γ_i are the activity coefficients of the *i* species. The stepwise stability constants can be converted to their accumulative form by taking their product: $\beta_1 = K_1$; $\beta_2 = K_1 \cdot K_2$; $\beta_3 = K_1 \cdot K_2 \cdot K_3$.

The Davies equation (Eq.22) was used to calculate the activity coefficients of the metal species provided that their ionic strength is > 0 (Eq.5).

According to the slopes obtained by plotting the logarithm of the distribution coefficient of the metals (D) versus the logarithm of Aliquat 336 IL concentration (Figure 51), the following extraction mechanism by anionic exchange was proposed:

$$MeCl_2Cit^{2-} + 2\,\overline{R_4N^+Cl^-} \overset{Kex}{\longleftrightarrow} \overline{(R_4N^+)_2MeCl_2Cit^{2-}} + 2\,Cl^- \quad \text{(R.24)}$$

In the proposed equilibria it is assumed that there is just one metal-organic species in the organic phase. The ionic exchange chloride/citrate is also taken into account:

$$Cit^{3-} + 3\,\overline{R_4N^+Cl^-} \overset{Kie}{\longleftrightarrow} \overline{(R_4N^+)_3Cit^{3-}} + 3\,Cl^- \quad \text{(R.18)}$$

The corresponding equilibria equations can be written as follows:

$$K_{ex} = \frac{a_{\overline{(R_4N^+)_2MeCl_2Cit^{2-}}} \cdot a_{Cl^-}^2}{a_{\overline{R_4N^+Cl^-}}^2 \cdot a_{MeCl_2Cit^{2-}}} = \frac{[\overline{(R_4N^+)_2MeCl_2Cit^{2-}}] \cdot [Cl^-]^2}{[\overline{R_4N^+Cl^-}]^2 \cdot [MeCl_2Cit^{2-}]} \cdot \frac{\gamma_{\overline{(R_4N^+)_2MeCl_2Cit^{2-}}} \cdot \gamma_{Cl^-}^2}{\gamma_{\overline{R_4N^+Cl^-}}^2 \cdot \gamma_{MeCl_2Cit^{2-}}} \quad \text{(Eq.48)}$$

$$K_{ie} = \frac{a_{\overline{(R_4N^+)_3Cit^{3-}}} \cdot a_{Cl^-}^3}{a_{\overline{R_4N^+Cl^-}}^3 \cdot a_{Cit^{3-}}} = \frac{[\overline{(R_4N^+)_3Cit^{3-}}] \cdot [Cl^-]^3}{[\overline{R_4N^+Cl^-}]^3 \cdot [Cit^{3-}]} \cdot \frac{\gamma_{\overline{(R_4N^+)_3Cit^{3-}}} \cdot \gamma_{Cl^-}^3}{\gamma_{\overline{R_4N^+Cl^-}}^3 \cdot \gamma_{Cit^{3-}}} \quad \text{(Eq.49)}$$

In the equilibria, the bar above the species means that they are in the organic phase. Their activity coefficients (γ) are considered to be equal to 1.

3.3.2. Mass balances

Mass balances of neodymium, terbium, dysprosium, citrate and Aliquat 336 are required to solve the model. In order to set it up, equal volumes of aqueous and organic phases are assumed. Therefore, the sum of each reagent in the equilibria is considered as follows:

Neodymium mass balance

$$[Nd]_t = [Nd^{3+}] + [NdCl^{2+}] + [NdCl_2^{+}] + [NdCl_3] + [NdClCit^{-}] + [NdCl_2Cit^{2-}] + \\ + [NdCit] + [\overline{(R_4N^+)_2NdCl_2Cit^{2-}}] \quad \text{(Eq.50)}$$

Terbium mass balance

$$[Tb]_t = [Tb^{3+}] + [TbCl^{2+}] + [TbCl_2^{+}] + [TbCl_3] + [TbClCit^{-}] + [TbCl_2Cit^{2-}] + \\ + [TbCit] + [\overline{(R_4N^+)_2TbCl_2Cit^{2-}}] \quad \text{(Eq.51)}$$

Dysprosium mass balance

$$[Dy]_t = [Dy^{3+}] + [DyCl^{2+}] + [DyCl_2^{+}] + [DyCl_3] + [DyClCit^{-}] + [DyCl_2Cit^{2-}] + \\ + [DyCit] + [\overline{(R_4N^+)_2DyCl_2Cit^{2-}}] \quad \text{(Eq.52)}$$

Chloride mass balance

$$[Cl^-]_t = [Cl^-]_{free} + [\overline{R_4N^+Cl^-}]_{free} + [NdCl^{2+}] + 2\cdot[NdCl_2^{+}] + 3\cdot[NdCl_3] + \\ + [NdClCit^-] + 2\cdot[NdCl_2Cit^{2-}] + 2\cdot[\overline{(R_4N^+)_2NdCl_2Cit^{2-}}] + [TbCl^{2+}] + \\ + 2\cdot[TbCl_2^{+}] + 3\cdot[TbCl_3] + [TbClCit^-] + 2\cdot[TbCl_2Cit^{2-}] + \\ + 2\cdot[\overline{(R_4N^+)_2TbCl_2Cit^{2-}}] + [DyCl^{2+}] + 2\cdot[DyCl_2^{+}] + 3\cdot[DyCl_3] + \\ + [DyClCit^-] + 2\cdot[DyCl_2Cit^{2-}] + 2\cdot[\overline{(R_4N^+)_2DyCl_2Cit^{2-}}] \quad \text{(Eq.53)}$$

Citrate mass balance

$$[Cit^{3-}]_t = [Cit^{3-}]_{free} + [NdClCit^-] + [NdCl_2Cit^{2-}] + [NdCit] + [TbClCit^-] + \\ + [TbCl_2Cit^{2-}] + [TbCit] + [DyClCit^-] + [DyCl_2Cit^{2-}] + [DyCit] + \\ + [\overline{(R_4N^+)_2NdCl_2Cit^{2-}}] + [\overline{(R_4N^+)_2TbCl_2Cit^{2-}}] + [\overline{(R_4N^+)_2DyCl_2Cit^{2-}}] + \\ + [\overline{(R_4N^+)_3Cit^{3-}}] \quad \text{(Eq. 54)}$$

Aliquat 336 mass balance

$$[\overline{E}]_t = [\overline{R_4N^+Cl^-}]_{free} + 2\cdot[\overline{(R_4N^+)_2NdCl_2Cit^{2-}}] + 2\cdot[\overline{(R_4N^+)_2TbCl_2Cit^{2-}}] + \\ + 2\cdot[\overline{(R_4N^+)_2DyCl_2Cit^{2-}}] + 3\cdot[\overline{(R_4N^+)_3Cit^{3-}}] \quad \text{(Eq.55)}$$

3.3.3. Model resolution

Matlab R2017b software was used to solve the mathematical model. The equilibria equations (Eq.42 – 47; Eq. 48 – 49) and the mass balances (Eq.50 – 55) were solved using the formation and equilibria constants (K) as optimization parameters so that the calculated values fit the experimental ones with the minimum error. The resolution method applied is described in Chapter 3 (Figure 31). The metal-chloride formation constants calculated in the mathematical modelling of neodymium, terbium and dysprosium extraction with AliOle in chloride media were used for initialization of the program (K_0):

Table 21. Stability constants of the metal-chloride species (E. Obón et al., 2017a).

	K_1	K_2	K_3
Nd(III)	37.14	0.15	$9.50 \cdot 10^{-4}$
Tb(III)	252.97	0.03	0.30
Dy(III)	98.39	0.02	1.00

The chloro-metal-citrate formation constants (K_{Cit}) and the extraction constants (K_{ex}) were used as optimization parameters. The optimization is meant to find the constant values that will make the model match the experimental extraction percentages with the minimum error.

3.3.4. Mathematical modelling results

The extraction model proposed was applied to the extraction of neodymium, terbium and dysprosium anionic species in the $MeCl_2Cit^{2-}$ form with Aliquat 336 IL. Optimized stability and equilibria constants (K) were determined by minimization of the error function F(x), defined as the sum of the squared differences between the calculated and the experimental extraction data (Eq.4). Minimizing F(x) using the Matlab *fmincon* function, a set of the most optimized stability and equilibria constants (K) was determined. Table 22 shows the constants found and the error value associated.

Table 22. Stability and equilibria optimized constants

	K_{cit1}	K_{cit2}	K_{cit2}	K_{ex}	K_{ie}	σ total*
Nd(III)	15.91	2614.45	1.55	94.18	-	952
Tb(III)	9.38	578.60	0.39	261.01	-	
Dy(III)	0.56	1011.00	7.92	253.50	-	
Cit^{3-}	-	-	-	-	1.87	

The stability and equilibria constants in the table proved to fit the proposed model with the minimum error. Calculated and experimental data were plotted in order to get a better picture of the accuracy of the fitting. Figure 57 shows the comparative graphs between the simulated results of the model and the extraction percentages obtained experimentally.

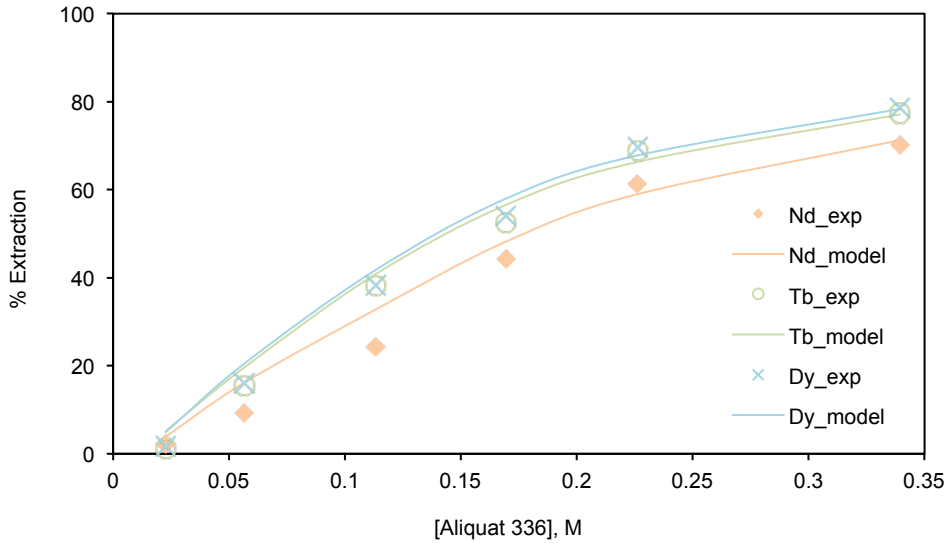

Figure 57. Comparative graph between simulated and experimental extraction values as a function of the Aliquat 336 IL molar concentration on the extraction of Nd(III), Tb(III) and Dy(III). $[Metal]_i$ = 7 mmol·L^{-1} each; [Citric acid] = 42 mmol·L^{-1}; $[Cl^-]$ = 0.1 mol·L^{-1}.

As shown, the proposed model is able to reproduce the experimental extraction extension when it comes to the effect of the Aliquat 336 IL concentration.

The optimized stability and equilibria constants calculated were also tested to forecast the single extraction of neodymium, terbium and dysprosium. The effect of the Aliquat 336 IL concentration was also studied in this case. Figure 58 shows comparative plots between the simulated results of the model and the extraction percentages obtained experimentally.

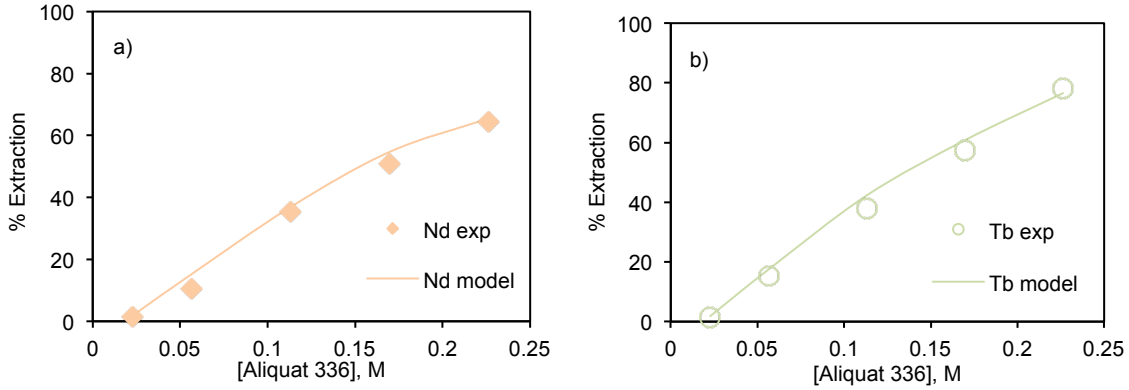

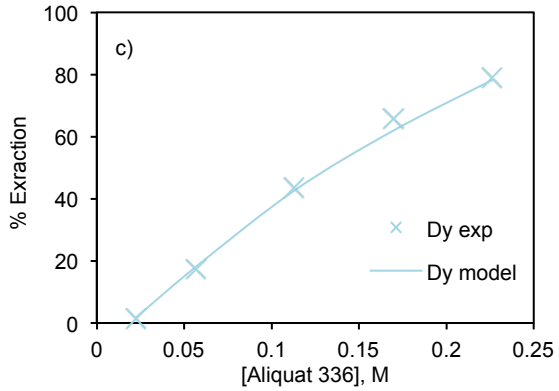

Figure 58. Comparative graph between simulated and experimental extraction values as a function of the Aliquat 336 molar concentration on the extraction of single Nd(III), Tb(III) and Dy(III). $[Metal]_i$ = 7 mmol·L^{-1} each; [Citric acid] = 14 mmol·L^{-1}; [Cl^-] = 0.1 mol·L^{-1}.

As can be seen, the calculated equilibrium constants allow to faithfully recreate the extraction of Nd(III), Tb(III) and Dy(III) individually.

The proposed mathematical modelling developed with Matlab software, which involves extraction of the $MeCl_2Cit^{2-}$ species by 1:2 stoichiometry, has proven to be a handy tool to predict and reproduce both single and combined metal extraction with Aliquat 336 IL in chloride media taking into account the stability constants of the metal chlorinated species defined in previous studies. The calculated stability constants of the chloro-metal-citrate species formed in the aqueous phase were: $K_{cit1\text{-}Nd}$ = 15.91; $K_{cit2\text{-}Nd}$ = 2614.45; $K_{cit3\text{-}Nd}$ = 1.55; $K_{cit1\text{-}Tb}$ = 9.38; $K_{cit2\text{-}Tb}$ = 578.60; $K_{cit3\text{-}Tb}$ = 0.39; $K_{cit1\text{-}Dy}$ = 0.56; $K_{cit2\text{-}Dy}$ = 1011.00 and $K_{cit3\text{-}Dy}$ = 7.92; and the extraction constants: $K_{ex\text{-}Nd}$ = 94.18; $K_{ex\text{-}Tb}$ = 261.01; $K_{ex\text{-}Dy}$ = 253.50; K_{ie} = 1.87. It might be a convenient instrument to be used for extraction and separation prediction of other rare earth elements from end of life products, requiring minor adjustments of the equilibria equations and mass balances.

4. Studies on implementation of supported liquid membranes for extraction of Nd(III), Tb(III) and Dy(III) from alkaline media using Aliquat 336 IL as a carrier

The most convenient experimental conditions for the liquid-liquid extraction of neodymium, terbium and dysprosium chloro-citrate species from alkaline media with Aliquat 336 IL were used for implementation of supported liquid membranes experiments. The transport of the metallic species through the membrane is not necessarily comparable to the extraction extension achieved via solvent extraction. In the SLM procedure, the physical factors involved such as the size of the metallic molecules or the viscosity of the extractant typically have an impact on the REEs extraction.

The transport of the anionic species of neodymium, terbium and dysprosium in alkaline media using Aliquat 336 IL as a carrier was studied as a function of the stripping phase. As in the liquid-liquid stripping procedure, two stripping agents

were used to perform the SLM trials. The permeability of the membranes was calculated for each stripping solution maintaining the same operation conditions:

- Feed: 100 $mg \cdot L^{-1}$ of Nd(III), Tb(III) and Dy(III); 0.1 $mol \cdot L^{-1}$ Cl^-; 42 $mmol \cdot L^{-1}$ citrate; pH = 10.5.
- Organic phase: 10% Aliquat 336 IL diluted in decanol/kerosene 10% v/v (0.23 $mol \cdot L^{-1}$).

The experimental assembly used has been widely depicted in Chapter 3. The permeability of the membranes was calculated taking the mass balances involved in each experiment. Figure 59 shows the metal transportation achieved in the SLM trials using H_2SO_4 and HCl 0.5 $mol \cdot L^{-1}$ as stripping solutions.

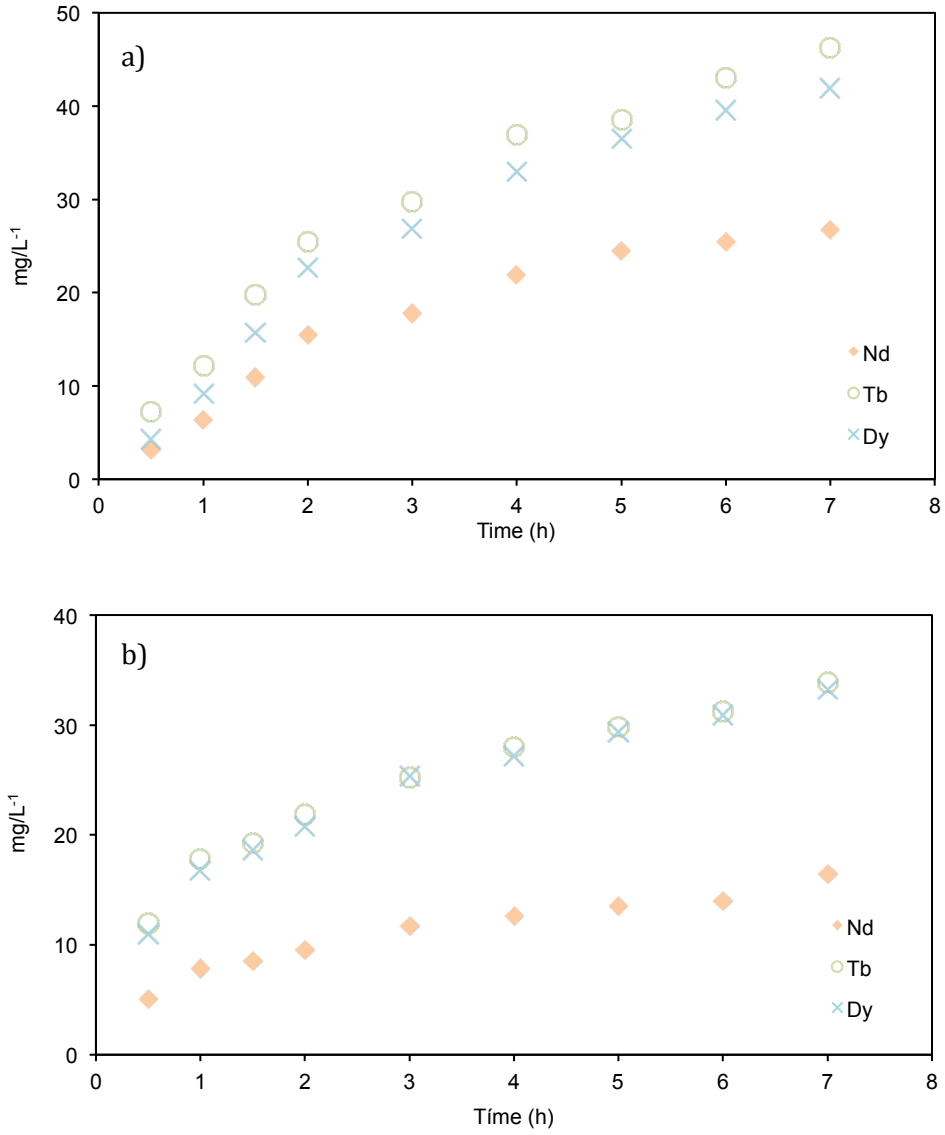

Figure 59. Nd(III), Tb(III) and Dy(III) concentration transferred to the stripping cells. $[Metal]_i$ = 0.7 $mmol \cdot L^{-1}$ each; [Citric acid] = 42 $mmol \cdot L^{-1}$; $[Cl^-]$ = 0.1 $mol \cdot L^{-1}$; pH = 10.5; [Aliquat 336] = 0.23 $mol \cdot L^{-1}$. Stripping solutions: a) 0.5 $mol \cdot L^{-1}$ H_2SO_4; b) 0.5 $mol \cdot L^{-1}$ HCl.

As can be observed, the concentration of metals in the stripping cells increases over time. As in the liquid-liquid stripping (figure 52), the sulphuric acid solution achieves higher REEs stripping yields than the hydrochloric acid solution. However, the extraction of the metals through SLM is slow compared to that of the L-L extraction. After 7 hours, 26.8% of Nd, 43.6% of Tb and 42.0% of Dy had been transferred to the H_2SO_4 stripping cell; and 16.4% of Nd, 34.0% of Tb and 33.3% of Dy to the HCl stripping cell; whereas with L-L extraction, in one contact, and using the same concentration of Aliquat 336, 61.3% of neodymium, 69.6% of terbium and 70% of dysprosium were extracted. This is caused primarily by the differences in the exchange surface, which is much smaller in SLM than in the emulsion formed in solvent extraction after shaking the aqueous and organic phases. Nonetheless, the implementation of the supported liquid membranes seems to be promising for the separation of neodymium from terbium and dysprosium, which may be incurred by the differences in the size of the molecules, which in turn is determined by the lanthanide contraction.

To quantify the transport of the metallic species and calculate the permeability of the SLMs, the mass balances of the $MeCl_2Cit^{2-}$ species in the cells were taken. The permeability is a key factor that enables to determine the most favourable experimental conditions to work with. The permeability coefficient was calculated according to the following demonstration:

Metal balance in the feed cell:

~~Input +~~ ~~Generation~~ = Output + Accumulation (Eq.56)

In this particular case the input and generation terms are 0 because it is a closed cell without external inputs or generation of metals.

Output = - Accumulation (Eq. 57)

Accumulation is defined as:

$$A = \frac{dn}{dt} \quad \text{(Eq.58)}$$

Where: n represents the metals concentration and t means time.
Applying the accumulation equation to the balance:

$$\frac{dn}{dt} = -\frac{S}{A} = -N \quad \text{(Eq.59)}$$

The output flow (N) is then related to the Fick equation and replaced in the previous equation:

$$\frac{\mathrm{dn}}{\mathrm{dt}} = -\mathrm{D} \cdot \mathrm{A} \cdot \left(\mathrm{C}_{\mathrm{feed}} - \mathrm{C}_{\mathrm{stripping}}\right)/\mathrm{e} \qquad \text{(Eq.60)}$$

Where C_{feed} and $C_{stripping}$ are the metals concentration in the feed cell and the stripping cell, respectively; e is the membrane width; A is the exchange surface and D is the diffusivity constant. In this case, $C_{stripping}$ is equal to 0 since the $MeCl_2Cit^{2-}$ species are not present in acidic media.

The variation in the metals concentration (dn) can be expressed as:

$$\mathrm{dn}_{\mathrm{feed}} = \mathrm{C}_{\mathrm{feed}} \cdot \mathrm{V}_{\mathrm{cell}} \qquad \text{(Eq. 61)}$$

Thus, replacing this expression in Eq. 60:

$$\frac{V \cdot dC_{feed}}{dt} = \frac{-D \cdot A}{e} \cdot C_{feed} \qquad \text{(Eq. 62)}$$

Grouping the factors and integrating the equation the following expression is obtained:

$$-\frac{V}{A} \cdot Ln \frac{C_{0\,feed} - C_{stripping}}{C_{0\,feed}} = P \cdot t \qquad \text{(Eq.63)}$$

Where V is the cell volume; A is the exchange surface; $C_{0\ feed}$ is the initial concentration of Nd, Tb and Dy in the feed cell; $C_{stripping}$ is the concentration of the metals in the stripping cells; P is the permeability of the membrane (P = D/e) and t is the time elapsed.

The representation of the expression $-\frac{V}{A} \cdot Ln \frac{C_{0\,feed} - C_{stripping}}{C_{0\,feed}}$ versus time will generate a linear regression in which the slope is the permeability coefficient. Figure 60 shows the representation of the linear regression corresponding to the mass balance involved taking into account the transport values obtained experimentally:

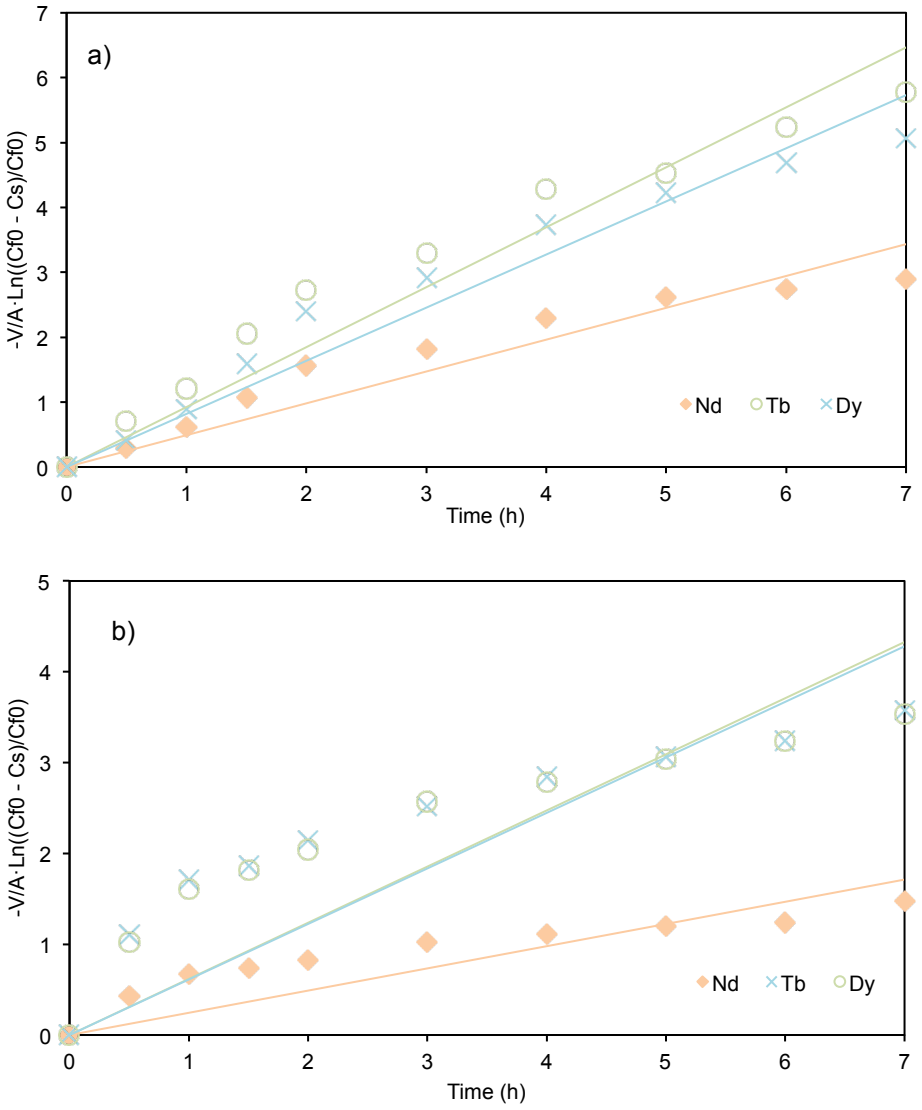

Figure 60. Representation of the SLM mass balances. a) Stripping solution: 0.5 mol·L^{-1} H_2sO_4. Calculated permeabilities: Nd(III) = 0.5 m/h; Tb(III) = 0.9 m/h; Dy(III) = 0.8 m/h; b) Stripping solution: 0.5 mol·L^{-1} HCl. Calculated permeabilities: Nd(III) = 0.2 m/h; Tb(III) = 0.6 m/h; Dy(III) = 0.6 m/h.

As can be seen, applying the Eq. 63 to the stripping points obtained and adjusting a regression line, it is possible to estimate the permeability values of each metal based on the experimental conditions.

The permeability values obtained with the H_2SO_4 stripping solution were higher than those obtained with HCl. The differences in the permeability values are determined by the speed in which the metals are transferred from the feed to the stripping cell. Furthermore, higher permeabilities were obtained for terbium and dysprosium compared to neodymium regardless of the stripping solution, which makes the SLM systems proposed stand as handy tools for the separation of LREE from HREE anionic species using Aliquat 336 IL as a carrier.

5. A multi-step leaching process for the recovery of rare earth elements from fluorescent lamp waste fractions

During the stay in the Chemical Engineering Department at the Chalmers University of Technology (Gothenburg, Sweden) in 2016, the multi-step leaching process proposed by Tunsu et al. (Tunsu et al., 2014c) was tested for the recovery of rare earth elements from end-of-life fluorescent lamps. The material used was obtained from the mechanical fractioning of fluorescent lamps previously treated to eliminate the largest part of the glass and the plastic, and baked in the oven at 600ºC during 12 hours to transform the phosphates in oxides to facilitate the leachate of the metals. The resulting sample containing primarily small pieces of glass and fibers generated during the crushing of the lamps, rare earth metals in different forms (oxides, phosphates, etc.), calcium and other impurities, was then treated with a water-based wet process and thermally processed to remove mercury. The dry fine powder obtained afterwards was used to carry on the leaching of the metals. Table 23 displays the composition of the sample after separation of large impurities and dissolution with aqua regia at 90ºC during 2 hours (solid:liquid ratio of 10% w/v).

The chemical diversity in the sample presents a challenge when it comes to the recovery of the rare earth elements. The chemical forms in which the REEs are found require acidic agents for an efficient leaching. The chemical process for the leaching of REEs from their corresponding phosphors using acidic solutions has been described in the R.3 – R.5 of this manuscript. The acid concentration plays an important role in the leaching of rare earth metals since consumption of protons takes place in the reactions.

The multi-step leaching process followed involved different stages: first of all, the leaching of a certain amount of the solid sample with a volume ten times higher of acidic solution 1 $mol \cdot L^{-1}$ was carried out during 10 min to get rid of the non-ferreous impurities, especially calcium with minimum losses of REEs. Then, the resulting amount of dry residue obtained after the first stage was treated again with a volume ten times higher of the same acidic solution 2 $mol \cdot L^{-1}$ during 22 hours. The resulting leachate was rich in Y/Eu, and contained small quantities of Ca, other REEs (Ce, La, Tb, Gd) and some impurities. The solid residue obtained after the second leaching stage can be treated with NaOH (1:1) and baked in the oven at 800ºC during 2-4 hours to oxidate the metals and facilitate the acidic dissolution for further separation by solvent extraction.

Table 23. Characterisation of the sample investigated. Adapted from (Tunsu et al., 2014c).

Metals	Average metal content (ppm)
Al	7700
B	1531
Ba	4500
Ca	87800
Cd	40
Ce	678
Cr	36
Cu	220
Eu	10800
Fe	7200
Gd	978
Hg	Not detected
K	619
La	609
Mg	1100
Mn	3300
Mo	61
Na	2300
Ni	133
Pb	310
Sb	1200
Si	268
Sn	43
Sr	3100
Ti	468
Tb	416
W	435
Y	162300
Zn	193
Zr	20

The leaching process described in Tunsu's work was applied to the sample kindly supplied by the university. As a first approach, the leaching process was carried out with hydrochloric acid following the stages depicted above. Hydrochloric acid was selected for the leaching experiments, since the majority of the investigations carried out in the course of this thesis were performed in chloride media, to facilitate the implementation of the solvent extraction and transport techniques previously proposed for the recovery and separation of REEs. Figure 61 shows a comparison between the leachates compositions

obtained by (Tunsu et al., 2016) using nitric acid and the experimental results obtained using hydrochloric acid in this investigation.

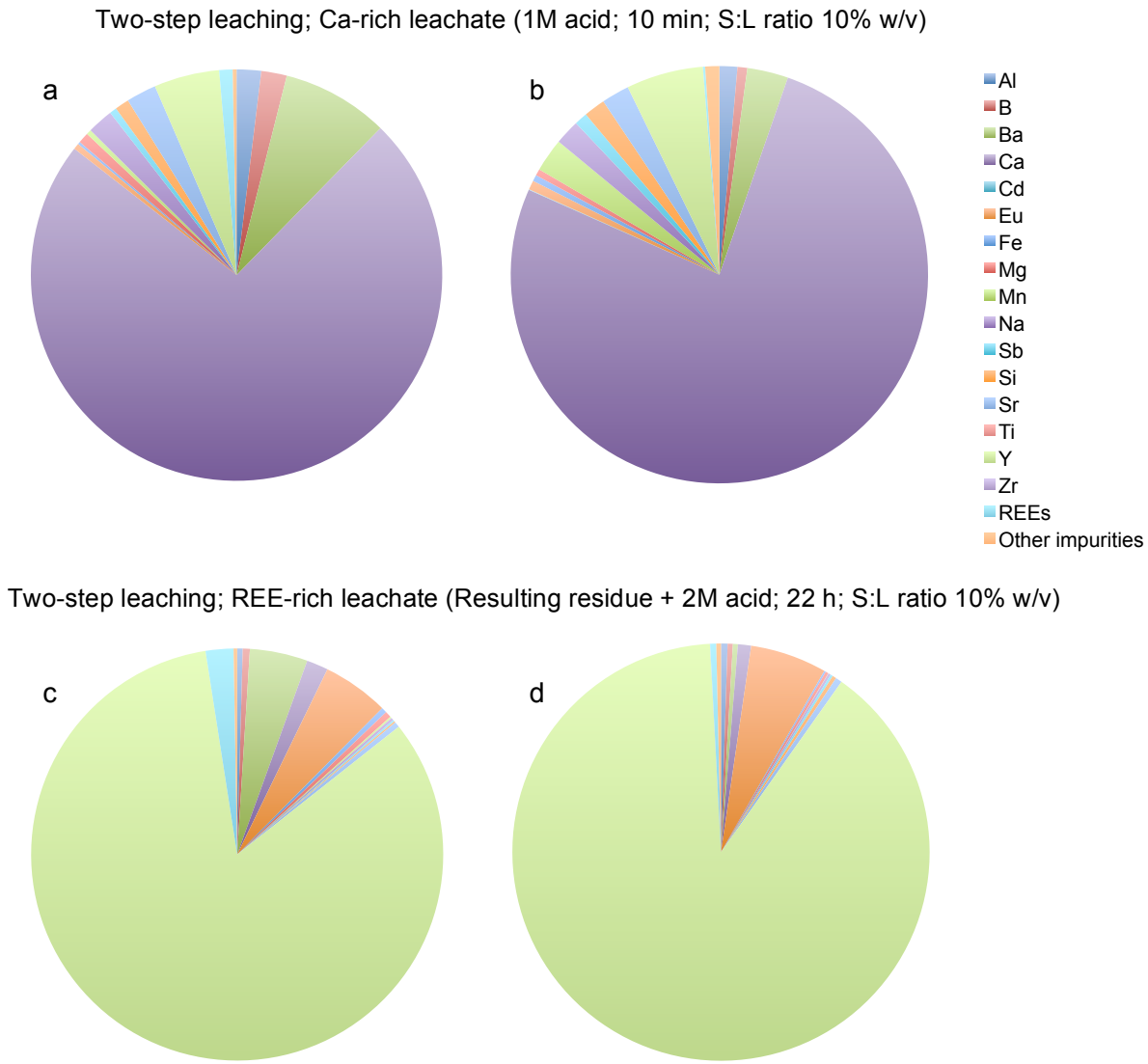

Figure 61. Representation of the leachates compositions as a function of the acidic solution used in the leaching process. Diagrams a) and c) collect the results obtained with HCl acidic solutions and b) and d) the results obtained by (Tunsu et al., 2016) with HNO_3 acidic solution. The REEs section compiles: Ce, Gd, La and Tb. The other impurities section compiles: Cr, Cu, K, Mo, Ni, Pb, Sn, W and Zn.

As can be observed, the overall composition of the leachates was very similar regardless of the acidic solution used. The Ca-rich leachates obtained after the first step of the leaching process contained 73.2% of Ca (HCl leaching solution) and 76.3% of Ca (HNO_3 leaching solution). The REEs losses in this step were 1% in HCl leachates and 0.2% in HNO_3 leachates. The main difference between the leachates compositions was spotted in the Ba concentration since 8% of the Ba was extracted from the sample in the first stage with HCl whereas only 3% was removed with HNO_3.

The metal composition of the REE-rich leachates was also very similar, 83.2% of Y and 5.2% Eu were dissolved in the HCl solution after 22 hours, whilst 89.4% of Y and 5.9% of Y were dissolved in the HNO_3 solution. The REE losses in this step were higher for the HCl solution (2.2%) compared to the HNO_3 solution (0.5%). To all readers interested in a more complete summary, the concentrations of the metals in the solutions obtained after leaching of the samples using the two steps leaching process described with nitric and hydrochloric acid can be found in the Appendix 1 of this thesis.

Based on the results obtained, different solvent extraction methods could be applied to recover/separate Y and Eu from the REE-rich leachates. The metals can be recovered from their leachates by using selective extractants. Tunsu et.al proposed the use of Cyanex 923 and Cyanex 527 for the recovery and separation of REMs from nitric media. However, future research is needed to carry on recovery of the rare earth metals contained in the HCl leachates. In this regard, we highly suggest implementation of the hydrometallurgical routes depicted in this thesis and especially, the transport through SLM since it has shown to be promising for the separation of rare earth elements as a function of their ionic radius.

Chapter 5. Conclusions, Contributions and Future Work

1. Conclusions

This chapter summarizes the main conclusions obtained in the course of this thesis and highlights the areas identified as being in need of further investigation. The work in this thesis involved the application of established hydrometallurgical routes for the recovery of rare earth elements from aqueous solutions and mathematical modelling of the proposed extraction systems. The contributions of this work may be stated as the development of a consolidated framework of REE separation techniques, which future researchers will be able to build on to achieve recycling rates high enough to be economically viable for application in the urban mining industry.

This research program has focused on the dual goals of: developing the state of art surrounding the rare earth elements to bring into focus their importance for the development of modern industry and green technologies; and to investigate hydrometallurgical routes to recover these essential metals for eventual implementation in urban mining operations. Within the field of REM-related research this thesis presents an attempt at identifying the hydrometallurgical processes described in the literature and then begins the work of developing new routes through experimental investigations. Matemathical modelling of the reported extraction systems has been undertaken to generate a computational tool for prediction of other collecting processes requiring minor adjustments. The conclusions of this work are as follows:

- New hydrometallurgical routes involving the use of ionic liquids as carriers for the recovery and separation of neodymium, terbium and dysprosium from aqueous solutions have been developed.

- The efficiency of the ionic liquids synthetized in the laboratory for the solvent extraction of REMs has been demonstrated.
    - The ionic liquids AliCy, AliDec, AliD2EHPA and AliOle were prepared in the laboratory by reacting the quaternary amine salt Aliquat 336 with equimolar amounts of Oleic Acid, Cyanex 272, Decanoic Acid and D2EHPA, respectively.
    - The homemade ionic liquids showed greater extraction potentials than the commercial acidic and solvating extractants tested under the experimental conditions employed.

- The liquid-liquid solvent extraction of neodymium, terbium and dysprosium from acidic aqueous solutions using AliOle IL has been reported.
    - The optimum experimental conditions for the extraction and stripping of neodymium, terbium and dysprosium from acidic aqueous solutions using AliOle IL as a carrier were investigated.
    - The AliOle IL was found to be not selective enough for separation of the lanthanides under the experimental conditions set but, because of its extraction ability, it might be used for the recovery of rare earths from mixed solutions containing other metals.

- The liquid-liquid extraction of neodymium, terbium and dysprosium from alkaline solutions using Aliquat 336 IL with the addition of a complexing agent has been investigated.
    - The optimum experimental conditions for the extraction and stripping of neodymium, terbium and dysprosium from alkaline solutions using Aliquat 336 as a carrier with the addition of citric acid were investigated.
    - The linear regression analysis of the metals distribution (log D) as a function of the Aliquat 336 concentration was conducted to assess the extraction mechanism involved in the solvent extraction system under the experimental conditions employed.

- Mathematical models have been created to reproduce the experimental data and predict the extraction extension of the metals involved. The mathematical models provided were created for application in different extraction systems requiring minor adjustments of the equilibria equations and mass balances.
    - Preliminary modelling studies of neodymium solvent extraction with AliOle IL from chloride media were carried out. The proposed models, which have proven to be able to feasibily reproduce the experimental extraction extension, assume extraction of Nd^{3+} species at low chloride concentrations (0.05 $mol \cdot L^{-1}$) and $NdCl^{2+}$ species at high chloride concentrations (> 2 $mol \cdot L^{-1}$).
    - Mathematical modelling of neodymium, terbium and dysprosium solvent extraction from chloride media using AliOle IL as extractant was conducted. The preliminary modelling studies of neodymium solvent extraction were taken as a basis for development of the model. The Matlab software was used to solve the equilibria equations and mass balances involved in the extraction systems in order to determine the equilibria constants. The validity of the models was confirmed by comparison of the experimental data plotted versus the calculated data. The

proposed model can be tailored to predict the extraction extension in separation systems entailing other REEs and different organic extractants.

- Mathematical modelling of neodymium, terbium and dysprosium solvent extraction from chloride alkaline solution using Aliquat 336 IL as a carrier was performed. The experimental analysis of the metals distribution (Log D) as a function of the Aliquat 336 concentration was taken as a base to build the model. The Matlab software was used to solve the equilibria equations and mass balances involved in the extraction system and to determine the equilibria constants. The proposed extraction model has proven to match the experimental extraction extension of the metals individually and to faithfully predict the simultaneous extraction of Nd(III), Tb(III) and Dy(III) from alkaline aqueous media. The validity of the approached equilibria constants was confirmed by comparing the plots of the experimental percentages versus the calculated data.

- The use of supported liquid membranes has been evaluated for extraction and selective separation of neodymium, terbium and dysprosium from alkaline media using Aliquat 336 IL as a carrier.
  - The optimum experimental conditions for the solvent extraction of neodymium, terbium and dysprosium chloro-citrate species from alkaline solutions with Aliquat 336 were used for implementation of SLM experiments. The mass balances of the anionic species in the cells were used to quantify the transport and calculate the permeability of the membrane. Higher permeabilities were obtained for terbium and dysprosium compared to neodymium, which opens an important path for further investigation on potential separation of LREE from HREE anionic species using Aliquat 336 IL as a carrier.

- A multi-step leaching process has been applied for the recovery of rare earth elements from end-of-life fluorescent lamps to assess the recycling potential of the resulting REE-rich leachates.
  - The two-steps leaching process proposed by Tunsu et al. was tested for the recovery of rare earth elements from end-of-life fluorescent lamps using hydrochloric acid as the leaching solution. Two different leachates were obtained, the first one was rich in calcium and the second one was rich in REE, specially yttrium and europium. The overall composition of the HCl leachates was found to be very similar to the HNO_3 leachates depicted in the literature. The hydrometallurgical routes proposed in this thesis appear to be

promising for the separation of rare earth elements from the REE-rich leachate achieved in the second step of the leaching process.

2. Future work

The recovery of REEs from end-of-life products will require a great deal of future research work. As discussed in the previous section, this thesis provides a framework on which to build up the processing knowledge surrounding the recycling of the rare earth elements. Certain specific areas in need of further investigation have been identified:

- To carry on solvent extraction studies such as the ones that have been performed in the course of this thesis but using AliCy, AliDec and AliD2EHPA instead of AliOle or Aliquat 336, to assess the extraction / separation capabilities of these homemade ILs.
- The hydrometallurgical routes described involving the use of ionic liquids as carriers should be applied for evaluation of the recovery and separation of rare earth elements other than neodymium, terbium and dysprosium.
- Testing of the mathematical models proposed for prediction of the performance of different extraction systems involving rare earths individually and mixtures with other metallic species.
- Implementation of the SLM technology using Aliquat 336 IL as a carrier should be tested for separation of REEs anionic species from prepared mixtures of different elements simulating alkaline leachates.
- To carry on solvent extraction studies for separation of Y and Eu from the REE-rich leachate obtained with the leaching of end-of-life fluorescent powders with HCl proposed.
- Application of the two-steps leaching procedure described using hydrochloric acid for the recovery of rare earth elements from different samples of end-of-life products, such as permanent magnets powders and NiMH batteries.

References

Aba, Y.B., Ubota, F.K., Amiya, N.K., Oto, M.G., 2011. Recent Advances in Extraction and Separation of Rare-Earth Metals Using Ionic Liquids. J. Chem. Eng. Japan 44, 679–685. doi:https://doi.org/10.1252/jcej.10we279

Abedini, A., Butcher, C., Nemcko, M.J., Kurukuri, S., Worswick, M.J., 2017. Constitutive characterization of a rare-earth magnesium alloy sheet (ZEK100-O) in shear loading: Studies of anisotropy and rate sensitivity. Int. J. Mech. Sci. 128–129, 54–69. doi:10.1016/j.ijmecsci.2017.04.013

Adunka, R., Virginia Orna, M., 2018. Discoveries Among the Rare Earths 3.1 Ytterby and Beyond. SpringerBriefs Hist. Chem. doi:10.1007/978-3-319-77905-8_3

Agilent Technologies, 2016. Microwave Plasma Atomic Emission Spectroscopy (MP-AES), Application eHandbook.

Akah, A., 2017. Application of rare earths in fluid catalytic cracking: A review. J. Rare Earths 35, 941–956. doi:10.1016/S1002-0721(17)60998-0

Alonso, E., Sherman, A.M., Wallington, T.J., Everson, M.P., Field, F.R., Roth, R., Kirchain, R.E., 2012. Evaluating rare earth element availability: a case with revolutionary demand from clean technologies. Environ. Sci. Technol. 46, 3406–14. doi:10.1021/es203518d

Assumpçao, D., Moura, A., Alberto, J., Tenório, S., 2009. Spent NiMH batteries-The role of selective precipitation in the recovery of valuable metals. J. Power Sources 193, 914–923. doi:10.1016/j.jpowsour.2009.05.014

Assumpçao, D., Moura, A., Alberto, J., Tenório, S., 2006. Spent NiMH batteries: Characterization and metal recovery through mechanical processing. J. Power Sources 160, 1465–1470. doi:10.1016/j.jpowsour.2006.02.091

Banda, R., Jeon, H., Lee, M., 2012a. Solvent extraction separation of Pr and Nd from chloride solution containing La using Cyanex 272 and its mixture with other extractants. Sep. Purif. Technol. 98, 481–487. doi:10.1016/j.seppur.2012.08.015

Banda, R., Jeon, H.S., Lee, M.S., 2012b. Solvent extraction separation of La from chloride solution containing Pr and Nd with Cyanex 272. Hydrometallurgy 121–124, 74–80. doi:10.1016/j.hydromet.2012.04.003

Baolu, Z., Zhongxue, L., Congcong, C., 2017. Global Potential of Rare Earth Resources and Rare Earth Demand from Clean Technologies. Minerals 7. doi:10.3390/min7110203

Batchu, N.K., Hoogerstraete, T. Vander, Banerjee, D., Binnemans, K., 2017. Non-aqueous solvent extraction of rare-earth nitrates from ethylene glycol to n-dodecane by Cyanex 923. Sep. Purif. Technol. 174, 544–553. doi:10.1016/j.seppur.2016.10.039

Berthod, A., Ruiz-Ángel, M.J., Carda-Broch, S., 2018. Recent advances on ionic liquid uses in separation techniques. J. Chromatogr. A 1559, 2–16. doi:10.1016/j.chroma.2017.09.044

Binnemans, K., Jones, P.T., Blanpain, B., Van Gerven, T., Yang, Y., Walton, A., Buchert, M., 2013. Recycling of rare earths: a critical review. J. Clean. Prod. 51, 1–22. doi:10.1016/j.jclepro.2012.12.037

Blankson Abaka-Wood, G., Quast, K., Zanin, M., Addai-Mensah, J., Skinner, W., 2019. A study of the feasibility of upgrading rare earth elements minerals from iron-oxide-silicate rich tailings using Knelson concentrator and Wilfley shaking table. Powder Technol. 334, 897–913.

doi:10.1016/j.powtec.2018.12.005
Böhm, M., Tietze, A.A., Heimer, P., Chen, M., Imhof, D., 2014. Ionic liquids as reaction media for oxidative folding and native chemical ligation of cysteine-containing peptides. J. Mol. Liq. 192, 67–70. doi:10.1016/j.molliq.2013.08.020
Charbonniere, L.J., 2011. Luminescent Lanthanide Labels. Curr. Inorg. Chem. 1, 2–16. doi:10.2174/1877945X11101010002
Chen, Z., 2011. Global rare earth resources and scenarios of future rare earth industry. J. Rare Earths. doi:10.1016/S1002-0721(10)60401-2
Cossu, R., Bonifazi, G., 2013. The Urban Mining concept. Waste Manag. 33, 497–498. doi:10.1016/j.wasman.2013.01.010
Cotton, S., 2006. Lanthanide and Actinide Chemistry and Spectroscopy, American Chemical Society. doi:10.1002/0470010088
Cousland, G.P., Cui, X.Y., Smith, A.E., Stampfl, A.P.J., Stampfl, C.M., 2018. Mechanical properties of zirconia, doped and undoped yttria-stabilized cubic zirconia from first-principles. J. Phys. Chem. Solids 122, 51–71. doi:10.1016/j.jpcs.2018.06.003
Cui, J., Kramer, M., Zhou, L., Liu, F., Gabay, A., Hadjipanayis, G., Balasubramanian, B., Sellmyer, D., 2018. Current progress and future challenges in rare-earth-free permanent magnets. Acta Mater. 158, 118–137. doi:10.1016/j.actamat.2018.07.049
Desouky, O.A., Daher, A.M., Abdel-Monem, Y.K., Galhoum, A.A., 2008. Liquid-liquid extraction of yttrium using primene-JMT from acidic sulfate solutions. Hydrometallurgy 96, 313–317. doi:10.1016/j.hydromet.2008.11.009
Dickman, 2008. Diodelaser Pumped Nd : YAG Laser.
Dupont, D., Binnemans, K., 2015. Recycling of rare earths from NdFeB magnets using a combined leaching/extraction system based on the acidity and thermomorphism of the ionic liquid [Hbet][Tf 2 N]. Green Chem. 17, 2150–2163. doi:10.1039/C5GC00155B
Ella Y. Lin, Astrid Rahmawati, Jo-Hsin Ko, Jhy-Chern Liu, 2018. Extraction of yttrium and europium from waste cathode-ray tube (CRT) phosphor by subcritical water. Sep. Purif. Technol. 1921, 166–175. doi:http://dx.doi.org/10.1016/j.seppur.2017.10.004
EURare, 2017. Research and development for the Rare Earth Element supply chain in Europe.
EURare, 2013. EURARE sustainable exploitation [WWW Document].
European Comission, 2014a. Report on Critical raw materials for the EU.
European Comission, 2014b. ERECON: Strengthening the European Rare Earths Supply-Chain, Challenges and policy options.
European Commission, 2017. Study on the review of the list of critical raw materials, Study on the review of the list of critical raw materials. Criticality Assessments. doi:10.2873/876644
Fatahi, M.R., Farzanegan, A., 2018. An analysis of multiphase flow and solids separation inside Knelson Concentrator based on four-way coupling of CFD and DEM simulation methods. Miner. Eng. 126, 130–144. doi:10.1016/j.mineng.2018.07.004
Fernandes, A., Afonso, J.C., Junqueira, A., Dutra, B., 2013. Separation of nickel(II), cobalt(II) and lanthanides from spent Ni-MH batteries by hydrochloric acid leaching, solvent extraction and precipitation. Hydrometallurgy 133, 37–43. doi:10.1016/j.hydromet.2012.11.017

Grabda, M., Panigrahi, M., Oleszek, S., Kozak, D., Eckert, F., Shibata, E., Nakamura, T., 2014. COSMO-RS screening for efficient ionic liquid extraction solvents for NdCl3 and DyCl3. Fluid Phase Equilib. 383, 134–143.
Gupta, D.C.C.K., Krishnamurthy, N., 2005. Extractive Metallurgy of Rare Earths.
Habashi, F., 2013. Extractive metallurgy of rare earths Historical introduction. Can. Metall. Q. 52, 224–233. doi:10.1179/1879139513Y.0000000081
Habib, K., Wenzel, H., 2014. Exploring rare earths supply constraints for the emerging clean energy technologies and the role of recycling. J. Clean. Prod. 84, 348–359. doi:10.1016/j.jclepro.2014.04.035
Hidayah, N.N., Abidin, Z., 2018. The evolution of mineral processing in extraction of rare earth elements using liquid-liquid extraction: A review. Miner. Eng. 121, 146–157. doi:10.1016/j.mineng.2018.03.018
Hiskey, J.B., Copp, R.G., 2018. Solvent extraction of yttrium and rare earth elements from copper pregnant leach solutions using Primene JM-T. Miner. Eng. 125, 265–270. doi:10.1016/j.mineng.2018.06.014
Hitachi, 2010. Hitachi Develops Recycling Technologies for Rare Earth Metals.
Hogfeldt, E., 1982. Stability Constants of Metal-Ion Complexes, Part A: Inorganic Ligands (IUPAC Chemical Data Series), 2nd ed. Pergamon Press.
Hoogerstraete, T. Vander, Blanpain, B., Van Gerven, T., Binnemans, K., 2014. From NdFeB magnets towards the rare-earth oxides: a recycling process consuming only oxalic acid. RSC Adv. 4, 64099–64111. doi:10.1039/c4ra13787f
Innocenzi, V., De Michelis, I., Ferella, F., Vegliò, F., 2017a. Leaching of yttrium from cathode ray tube fluorescent powder: Kinetic study and empirical models. Int. J. Miner. Process. 168, 76–86. doi:10.1016/j.minpro.2017.09.015
Innocenzi, V., Maria Ippolito, N., De Michelis, I., Prisciandaro, M., Medici, F., Vegli, F., 2017b. A review of the processes and lab-scale techniques for the treatment of spent rechargeable NiMH batteries. J. Power Sources 362, 202–218. doi:10.1016/j.jpowsour.2017.07.034
Innocenzi, V., Maria Ippolito, N., Pietrelli, L., Centofanti, M., Piga, L., Vegli, F., 2018. Application of solvent extraction operation to recover rare earths from fluorescent lamps. J. Clean. Prod. 172, 2840–2852. doi:10.1016/j.jclepro.2017.11.129
Innocenzi, V., Vegliò, F., 2012. Recovery of rare earths and base metals from spent nickel-metal hydride batteries by sequential sulphuric acid leaching and selective precipitations. J. Power Sources 211, 184–191. doi:10.1016/j.jpowsour.2012.03.064
IPT, 2017. A future for rare earths in Brazil A future for rare earths in Brazil.
Jordens, A., 2016. The beneficiation of rare earth element-bearing minerals. McGill University.
Jordens, A., Cheng, Y.P., Waters, K.E., 2013. A review of the beneficiation of rare earth element bearing minerals. Miner. Eng. 41, 97–114. doi:10.1016/j.mineng.2012.10.017
Jowitt, S.M., Werner, T.T., Weng, Z., Mudd, G.M., Thakur, V.K., Kumar Gupta, R., Matharu, A.S., 2018. Current Opinion in Green and Sustainable Chemistry. Curr. Opin. Green Sustain. Chem. 13, 1–7. doi:10.1016/j.cogsc.2018.02.008

Kubota, F., Shimobori, Y., Baba, Y., 2011. Application of ionic liquids to extraction separation of rare earth metals with an effective diglycol amic acid extractant. J. Chem. Eng. Japan 44, 307–312.
Kumar Jha, M., Kumari, A., Panda, R., Kumar, J.R., Yoo, K., Lee, J.Y., 2016. Review on hydrometallurgical recovery of rare earth metals. doi:10.1016/j.hydromet.2016.01.035
Kumari, A., Panda, R., Jha, M.K., Pathak, D.D., 2018. Extraction of rare earth metals by organometallic complexation using PC88A. Comptes Rendus Chim. 21, 1029–1034. doi:10.1016/j.crci.2018.09.005
Kumari, A., Panda, R., Kumar Jha, M., Rajesh Kumar, J., Lee, J.Y., 2015. Process development to recover rare earth metals from monazite mineral: A review. Miner. Eng. 79, 102–115. doi:10.1016/j.mineng.2015.05.003
Kumari, A., Sinha, M.K., Pramanik, S., Kumar Sahu, S., 2018. Recovery of rare earths from spent NdFeB magnets of wind turbine: Leaching and kinetic aspects. Waste Manag. 75, 486–498. doi:10.1016/j.wasman.2018.01.033
Larsson, K., Binnemans, K., 2015. Metal Recovery from Nickel Metal Hydride Batteries Using Cyanex 923 in Tricaprylylmethylammonium Nitrate from Chloride Aqueous Media. J. Sustain. Metall. 1, 161–167. doi:10.1007/s40831-015-0017-5
Larsson, K., Binnemans, K., 2014. Selective extraction of metals using ionic liquids for nickel metal hydride battery recycling. Green Chem. 16, 4595. doi:10.1039/c3gc41930d
Larsson, K., Ekberg, C., Ødegaard-Jensen, A., 2013a. Dissolution and characterization of HEV NiMH batteries. Waste Manag. 33, 689–698. doi:10.1016/j.wasman.2012.06.001
Larsson, K., Ekberg, C., Ødegaard-Jensen, A., 2013b. Using Cyanex 923 for selective extraction in a high concentration chloride medium on nickel metal hydride battery waste Part II: mixer-settler experiments. Hydrometallurgy 133, 168–175. doi:10.1016/j.hydromet.2013.01.012
Larsson, K., Ekberg, C., Ødegaard-Jensen, A., 2012. Using Cyanex 923 for selective extraction in a high concentration chloride medium on nickel metal hydride battery waste. Hydrometallurg 120–130, 35–42. doi:10.1016/j.hydromet.2012.08.011
Lee, C.-H., Chen, Y.-J., Liao, C.-H., Popuri, S.R., Tsai, S.-L., Hung, C.-E., 2013. Selective Leaching Process for Neodymium Recovery from Scrap Nd-Fe-B Magnet. Metall. Mater. Trans. A 44A, 5825–5833. doi:10.1007/s11661-013-1924-3
Lee, G.S., Uchikoshi, M., Mimura, K., Isshiki, M., 2009. Distribution coefficients of La, Ce, Pr, Nd, and Sm on Cyanex 923-, D2EHPA-, and PC88A-impregnated resins. Sep. Purif. Technol. 67, 79–85. doi:10.1016/j.seppur.2009.03.033
Lee, M.-S., Lee, J.-Y., Kim, J.-S., Lee, G.-S., 2005. Solvent extraction of neodymium ions from hydrochloric acid solution using PC88A and saponified PC88A. Sep. Purif. Technol. 46, 72–78. doi:10.1016/j.seppur.2005.04.014
Leif, R.C., Vallarino, L.M., Becker, M.C., Yang, S., 2006. Increasing the Luminescence of Lanthanide Complexes. Int. Soc. Anal. Cytol. 69A, 767–778. doi:10.1002/cyto.a.20321
Long, K.; Van Gosen, B.; Foley, N.; Cordier, D., 2010. The Principal Rare Earth Elements Deposits of the United States-A Summary of Domestic Deposits

and a Global Perspective.
Loy, S. Van, Binnemans, K., Van Gerven, T., 2017. Recycling of rare earths from lamp phosphor waste: Enhanced dissolution of LaPO 4 :Ce 3þ ,Tb 3þ by mechanical activation. J. Clean. Prod. 156, 226–234. doi:10.1016/j.jclepro.2017.03.160
Lyman, W.J., Palmer, R.G., 1992. Scrap Treatment Method For Rare Earth Transition Metal Alloys. US patent 5129945 A.
Ma, L., Zhao, Z., Dong, Y., Sun, X., 2017. A synergistic extraction strategy by [N 1888][SOPAA] and Cyphos IL 104 for heavy rare earth elements separation. Sep. Purif. Technol. 174, 474–481. doi:10.1016/j.seppur.2016.10.046
Mathworks, 1984. Matlab Software.
Miceli, H., Rossi, M.G., Neumann, R., Marcelo Tavares, L., 2017. Contaminant removal from manufactured fine aggregates by dry rare-earth magnetic separation. Miner. Eng. 113, 15–22. doi:10.1016/j.mineng.2017.07.017
Michaud, S., Miguirditchian, M., Deblonde, G., Dinh, B., Hérès, X., Andreoletti, G., 2012. Modelling of Thorium Extraction by TBP. Procedia Chem. 7, 251–257. doi:10.1016/j.proche.2012.10.041
Miskufova, A., Kochmanova, A., Havlik, T., Horvathova, H., Kuruc, P., 2018. Leaching of yttrium, europium and accompanying elements from phosphor coatings. Hydrometallurgy 176, 216–228. doi:10.1016/j.hydromet.2018.01.010
Mohammadi, M., Forsberg, K., Kloo, L., Martinez De La Cruz, J., Rasmuson, Å., 2015. Separation of ND(III), DY(III) and Y(III) by solvent extraction using D2EHPA and EHEHPA. Hydrometallurgy 156, 215–224. doi:10.1016/j.hydromet.2015.05.004
Molycorp, I., 1994. A LANTHANIDE LANTHOLOGY Part II, M-Z A LANTHANIDE LANTHOLOGY Part II, M-Z CONTENTS.
Moustafa, M.I., Abdelfattah, N.A., 2010. Physical and chemical beneficiation of the egyptian beach monazite. Resour. Geol. 60, 288–299. doi:10.1111/j.1751-3928.2010.00131.x
Nan, J., Han, D., Yang, M., Cui, M., Hou, X., 2006. Recovery of metal values from a mixture of spent lithium-ion batteries and nickel-metal hydride batteries. Hydrometallurgy 84, 75–80. doi:10.1016/j.hydromet.2006.03.059
Ni'am, A.C., Wang, Y.-F., Chen, S.-W., You, S.-J., 2019. Recovery of rare earth elements from waste permanent magnet (WPMs) via selective leaching using the Taguchi method. J. Taiwan Inst. Chem. Eng. 18, 30. doi:10.1016/j.jtice.2019.01.006
Obón, E., Fortuny, A., Coll, M.T., Sastre, A.M., 2017a. Mathematical modelling of neodymium, terbium and dysprosium solvent extraction from chloride media using methyl-tri(octyl/decyl)ammonium oleate ionic liquid as extractant. Hydrometallurgy 173, 84–90. doi:10.1016/j.hydromet.2017.08.011
Obón, E., Fortuny, A., Coll, M.T., Sastre, A.M., 2017b. Experimental and modeling studies of neodymium solvent extraction from chloride media with methyl-tri(octyl/decyl)ammonium oleate ionic liquid diluted in kerosene. Hydrometallurgy 174, 216–226. doi:10.1016/j.hydromet.2017.10.021
Obón, E., Fortuny, A., Coll, M.T., Sastre, A.M., 2017. Experimental and modelling studies of neodymium solvent extraction from chloride media with methyl-tri(octyl/decyl)ammonium oleate ionic liquid diluted in kerosene.

Hydrometallurgy 174, 261–226. doi:10.1016/j.hydromet.2017.10.021
Önal Recai, M.A., Jönsson, C., Zhou, W., Van Gerven, T., Guo, M., Walton, A., Blanpain, B., 2017. Comparative oxidation behavior of Nd-Fe-B magnets for potential recycling methods: Effect of hydrogenation pre-treatment and magnet composition. J. Alloys Compd. 728, 727–738. doi:10.1016/j.jallcom.2017.09.046
Onoda, H., Nakamura, R., 2014. Recovery of neodymium from an iron-neodymium solution using phosphoric acid. J. Environ. Chem. Eng. 2, 1186–1190. doi:10.1016/j.jece.2014.04.019
Padhan, E., Nayak, A.K., Sarangi, K., 2017. Recovery of neodymium and dysprosium from NdFeB magnet swarf. Hydrometallurgy 174, 210–215. doi:10.1016/j.hydromet.2017.10.015
Padhan, E., Sarangi, K., 2017. Recovery of Nd and Pr from NdFeB magnet leachates with bi-functional ionic liquids based on Aliquat 336 and Cyanex 272. Hydrometallurgy 167, 134–140. doi:10.1016/j.hydromet.2016.11.008
Padwal, N., Prakash, S.S., Thakkar, S., Deshpande, T., 2018. Supported Liquid Membrane Technology: Advances and Review of its Applications. Indian J. Adv. Chem. Sci. 6, 2018. doi:10.22607/IJACS.2018.601003
Pana Rabatho, J., Tongamp, W., Takasaki, Y., Haga, K., Shibayama, A., 2013. Recovery of Nd and Dy from rare earth magnetic waste sludge by hydrometallurgical process. J Mater Cycles Waste Manag. 15, 171–178. doi:10.1007/s10163-012-0105-6
Panda, N., Devi, N., Mishra, S., 2012a. Solvent extraction of neodymium(III) from acidic nitrate medium using Cyanex 921 in kerosene. J. Rare Earths 30, 794–797. doi:10.1016/S1002-0721(12)60132-X
Panda, N., Devi, N., Mishra, S., 2012b. Solvent extraction of neodymium(III) from acidic nitrate medium using Cyanex 921 in kerosene. J. Rare Earths 30, 794–797. doi:10.1016/S1002-0721(12)60132-X
Parmentier, D., Valia, Y.A., Metz, S.J., Burheim, O.S., Kroon, M.C., 2015a. Regeneration of the ionic liquid tetraoctylammonium oleate after metal extraction. Hydrometallurgy 158, 56–60. doi:10.1016/j.hydromet.2015.10.006
Parmentier, D., Vander Hoogerstraete, T., Metz, S.J., Binnemans, K., Kroon, M.C., 2015b. Selective Extraction of Metals from Chloride Solutions with the Tetraoctylphosphonium Oleate Ionic Liquid. Ind. Eng. Chem. Res. 54, 5149–5158. doi:10.1021/acs.iecr.5b00534
Pavón, S., Fortuny, A., Coll, M.T., Sastre, A.M., 2018a. Rare earths separation from fluorescent lamp wastes using ionic liquids as extractant agents. Waste Manag. 82, 241–248. doi:10.1016/j.wasman.2018.10.027
Pavón, S., Fortuny, A., Coll, M.T., Sastre, A.M., 2018b. Neodymium recovery from NdFeB magnet wastes using Primene 81R·Cyanex 572 IL by solvent extraction. J. Environ. Manage. 222, 359–367. doi:10.1016/j.jenvman.2018.05.054
Peelman, S., Sun, Z.H.I., Sietsma, J., Yang, Y., 2016. Rare Earths Industry. Elsevier. doi:10.1016/B978-0-12-802328-0.00021-8
Peng, C.-Y., Tsai, T.-H., 2014. Solvent extraction of palladium(II) from acidic chloride solutions using tri-octyl/decyl ammonium chloride (Aliquat 336). Desalin. Water Treat. 52, 1101–1121. doi:10.1080/19443994.2013.826616
Petranikova, M., Herdzik-Koniecko, I., Steenari, B.-M., Ekberg, C., 2017. Hydrometallurgical processes for recovery of valuable and critical metals

from spent car NiMH batteries optimized in a pilot plant scale. Hydrometallurgy 171, 128–141. doi:10.1016/j.hydromet.2017.05.006
Pietrelli, L., Bellomo, B., Fontana, D., Montereali, M.R., 2002. Rare earths recovery from NiMH spent batteries. Hydrometallurgy 66, 135–139.
Porvali, A., Wilson, B.P., Lundström, M., 2018. Lanthanide-alkali double sulfate precipitation from strong sulfuric acid NiMH battery waste leachate. Waste Manag. 71, 381–389. doi:10.1016/j.wasman.2017.10.031
Provazi, K., Campos, B.A., Crocce, D., Espinosa, R., Alberto, J., Tenório, S., 2011. Metal separation from mixed types of batteries using selective precipitation and liquid-liquid extraction techniques. Waste Manag. 31, 59–64. doi:10.1016/j.wasman.2010.08.021
Puigdomenech, I., 2013. Medusa Software.
Quinn, J.E., Soldenhoff, K.H., Stevens, G.W., 2017. Solvent extraction of rare earth elements using a bifunctional ionic liquid. Part 2_ Separation of rare earth elements. doi:10.1016/j.hydromet.2017.04.003
Rabie, K.A., 2006. A group separation and purification of Sm, Eu and Gd from Egyptian beach monazite mineral using solvent extraction. Hydrometallurgy 81–86. doi:10.1016/j.hydromet.2005.12.012
Rayner-Canham, G., 2000. Química Inorgánica Descriptiva, 2a edición. ed.
Regel-Rosocka, M., Materna, K., 2014. Ionic Liquids in Separation Technology, Ionic Liquids in Separation Technology. Elsevier. doi:10.1016/B978-0-444-63257-9.00004-3
Richard, A.R., Fan, M., 2018. Rare earth elements: Properties and applications to methanol synthesis catalysis via hydrogenation of carbon oxides. J. Rare Earths 36, 1127–1135. doi:10.1016/j.jre.2018.02.012
Rout, A., Binnemans, K., 2014a. Influence of the ionic liquid cation on the solvent extraction of trivalent rare-earth ions by mixtures of Cyanex 923 and ionic liquids. Dalt. Trans. 44, 1379. doi:10.1039/c4dt02766c
Rout, A., Binnemans, K., 2014b. Liquid-liquid extraction of europium(III) and other trivalent rare-earth ions using a non-fluorinated functionalized ionic liquid. Dalton Trans. 43, 1862–72. doi:10.1039/c3dt52285g
Rout, A., Binnemans, K., 2014c. Solvent Extraction of Neodymium(III) by Functionalized Ionic Liquid Trioctylmethylammonium Dioctyl Diglycolamate in Fluorine-free Ionic Liquid Diluent. Ind. Eng. Chem. Res. 53, 6500–6508. doi:10.1021/ie404340p
Rout, A., Binnemans, K., 2014. Separation of rare earths from transition metals by liquid-liquid extraction from a molten salt hydrate to an ionic liquid phase. Dalton Trans. 43, 3186–3195. doi:10.1039/c3dt52541d
Rout, A., Kotlarska, J., Dehaen, W., Binnemans, K., 2013. Liquid-liquid extraction of neodymium(iii) by dialkylphosphate ionic liquids from acidic medium: The importance of the ionic liquid cation. Phys. Chem. Chem. Phys. 15, 16533–16541. doi:10.1039/c3cp52218k
Sastri, V.S., 2003. Modern aspects of rare earths and their complexes. Elsevier.
Skokov, K.P., Gutfleisch, O., 2018. Heavy rare earth free, free rare earth and rare earth free magnets - Vision and reality. Scr. Mater. 154, 289–294. doi:10.1016/j.scriptamat.2018.01.032
Smith Stegen, K., 2015. Heavy rare earths, permanent magnets, and renewable energies: An imminent crisis. Energy Policy 79, 1–8. doi:10.1016/j.enpol.2014.12.015
Srivastava, A.M.., Sommerer, T.J., 1998. Fluorescent Lamp Phosphors.

Electrochem. Soc. Interface.
Sturza, C.M., Boscencu, R., Nacea, V., 2008. The lanthanides: Physico-chemical properties relevant for their biomedical applications. Farmacia 56, 326–338.
Sun, P., Huang, K., Wang, X., Song, W., Zheng, H., Liu, H., 2017. Separation of V from alkaline solution containing Cr using acidified primary amine N1923 with the addition of trisodium citrate. Sep. Purif. Technol. 179, 504–512. doi:10.1016/j.seppur.2017.02.035
Sunil Kumar Tripathy, Y. Ramamurthy, C. Raghu Kumar, 2010. Modeling of high-tension roll separator for separation of titanium bearing minerals. Powder Technol. 201, 181–186. doi:doi:10.1016/j.powtec.2010.04.005
Swain, B., Otu, E.O., 2011. Competitive extraction of lanthanides by solvent extraction using Cyanex 272: Analysis, classification and mechanism. Sep. Purif. Technol. 83, 82–90. doi:10.1016/j.seppur.2011.09.015
Swain, N., Mishra, S., 2019. A review on the recovery and separation of rare earths and transition metals from secondary resources. J. Clean. Prod. 220, 884–898. doi:10.1016/j.jclepro.2019.02.094
SX Kinetics, 2002. Sorbent extraction technology. J. Pharm. Biomed. Anal. 5, 755. doi:10.1016/0731-7085(87)80091-2
Tanabe, E.H., Schlemmer, D.F., Aguiar, L., Dotto, G.L., Bertuol, D.A., 2016. Recovery of valuable materials from spent NIMH batteries using spouted bed elutriation. J. Environ. Manage. 171, 177–183. doi:10.1016/j.jenvman.2016.02.011
Tanvar, H., Dhawan, N., 2019. Extraction of rare earth oxides from discarded compact fluorescent lamps. Miner. Eng. 135, 95–104. doi:10.1016/j.mineng.2019.02.041
Tian, Y., Liu, Z., Zhang Guoqing, 2019. Recovering REEs from NdFeB wastes with high purity and efficiency by leaching and selective precipitation process with modified agents. J. Rare Earths 37, 205–210.
Tunsu, C., Ekberg, C., Foreman, M., Retegan, T., 2014a. Studies on the Solvent Extraction of Rare Earth Metals from Fluorescent Lamp Waste Using Cyanex 923. Solvent Extr. Ion Exch. 32, 650–668. doi:10.1080/07366299.2014.925297
Tunsu, C., Ekberg, C., Gregoric, M., Retegan, T., 2014b. Recovery of La, Ce, Eu, Gd, Tb and Y from fluorescent lamp waste using solvent extraction: solvent choice studies., in: Proceedings of the 20th International Solvent Extraction Conference. Wurtzburg, Germany, pp. 07–11.
Tunsu, C., Ekberg, C., Retegan, T., 2014c. Characterization and leaching of real fluorescent lamp waste for the recovery of rare earth metals and mercury. Hydrometallurgy 144–145, 91–98. doi:10.1016/j.hydromet.2014.01.019
Tunsu, C., Petranikova, M., Ekberg, C., Retegan, T., 2016. A hydrometallurgical process for the recovery of rare earth elements from fluorescent lamp waste fractions. Sep. Purif. Technol. 161, 172–186. doi:10.1016/j.seppur.2016.01.048
Tunsu, C., Petranikova, M., Gergorić, M., Ekberg, C., Retegan, T., 2015a. Reclaiming rare earth elements from end-of-life products: A review of the perspectives for urban mining using hydrometallurgical unit operations. Hydrometallurgy 156, 239–258. doi:10.1016/j.hydromet.2015.06.007
Tunsu, C., Petranikova, M., Gergorić, M., Ekberg, C., Retegan, T., 2015b.

Reclaiming rare earth elements from end-of-life products: A review of the perspectives for urban mining using hydrometallurgical unit operations. Hydrometallurgy 156, 239–258. doi:10.1016/j.hydromet.2015.06.007
Tunsu, C., Retegan, T., 2016. Chapter 6 - Hydrometallurgical Processes for the Recovery of Metals from WEEE. doi:10.1016/B978-0-12-803363-0.00006-7
U.S. Geological Survey, 2018. Mineral Commodity Summaries 2018. doi:10.3133/70194932
U.S Department of Energy, 2011. Critical Materials Strategy.
Usapein, P., Lothongkum, A.W., Ramakul, P., Pancharoen, U., 2009. Efficient transport and selective extraction of Cr(VI) from waste pickling solution of the stainless steel-cold rolled plate process using Aliquat 336 via HFSLM. Korean J. Chem. Eng. 26, 791–798. doi:10.1007/s11814-009-0132-8
Van Gosen, B.S., Verplanck, P.L., Seal, R.R., II, Long, K.R., Gambogi, J., 2017. Critical mineral resources of the United States— Economic and environmental geology and prospects for future supply. U.S. Geol. Surv. . doi:10.3133/pp1802O
Voncken, J.H.., 2016a. 1. The Rare Earth Elements - A Special Group of Metals, in: The Rare Earth Elements. Springer US, pp. 21–41. doi:10.1007/978-3-319-26809-5
Voncken, J.H.., 2016b. 3. Physical and Chemical Properties of the Rare Earths, in: The Rare Earth Elements. Springer US, pp. 98–125. doi:10.1007/978-3-319-26809-5
Wang, Q., He, Z., Li, G., Li, B., Zhu, C., Chen, P., 2017. Numerical investigation of desulfurization behavior in electroslag remelting process. Int. J. Heat Mass Transf. 104, 943–951. doi:10.1016/j.ijheatmasstransfer.2016.09.022
Welton, T., 2018. Ionic liquids: a brief history. Biophys. Rev. 10, 691–706. doi:10.1007/s12551-018-0419-2
Wu, F., Xu, S., Li, L., Chen, S., Xu, G., Xu, J., 2009. Recovery of valuable metals from anode material of hydrogen-nickel battery. Trans. Nonferrous Met. Soc. China 19, 468–473. doi:10.1016/S1003-6326(08)60297-6
Wu, Y., Yin, X., Zhang, Q., Wang, W., Mu, X., 2014. The recycling of rare earths from waste tricolor phosphors in fluorescent lamps: A review of processes and technologies. "Resources, Conserv. Recycl. 88, 21–31. doi:10.1016/j.resconrec.2014.04.007
Wübbeke, J., 2013. Rare earth elements in China: Policies and narratives of reinventing an industry. Resour. Policy 38, 384–394. doi:10.1016/j.resourpol.2013.05.005
Xie, F., Zhang, T.A., Dreisinger, D., Doyle, F., 2014. A critical review on solvent extraction of rare earths from aqueous solutions. Miner. Eng. 56, 10–28. doi:10.1016/j.mineng.2013.10.021
Yang, F., Kubota, F., Baba, Y., Kamiya, N., Goto, M., 2013. Selective extraction and recovery of rare earth metals from phosphor powders in waste fluorescent lamps using an ionic liquid system. J. Hazard. Mater. 254–255, 79–88. doi:10.1016/j.jhazmat.2013.03.026
Yang, X., Zhang, J., Fang, X., 2014. Rare earth element recycling from waste nickel-metal hydride batteries. J. Hazard. Mater. 279, 384–388. doi:10.1016/j.jhazmat.2014.07.027
Yin, X., Tian, X., Wu, Y., Zhang, Q., Wang, W., Li, B., Gong, Y., Zuo, T., 2018. Recycling rare earth elements from waste cathode ray tube phosphors: Experimental study and mechanism analysis. J. Clean. Prod. 205, 58–66.

doi:10.1016/j.jclepro.2018.09.055
Yoon, H.-S., Kim, C.-J., Chung, K.-W., Kim, S.-D., Lee, J.-Y., Kumar, J.R., 2016. Solvent extraction, separation and recovery of dysprosium (Dy) and neodymium (Nd) from aqueous solutions: Waste recycling strategies for permanent magnet processing. Hydrometallurgy. doi:10.1016/j.hydromet.2016.01.028
Yun, X., Liansheng, X., Jiying, T., Zhaoyang, L., Li, Z., 2015. Recovery of rare earths from acid leach solutions of spent nickel-metal hydride batteries using solvent extraction. J. RARE EARTHS 33, 1348. doi:10.1016/S1002-0721(14)60568-8
Zhan, W., Guo, Y., Gong, X., Guo, Y., Wang, Y., Lu, G., 2014. Current status and perspectives of rare earth catalytic materials and catalysis. Chinese J. Catal. 35, 1238–1250. doi:10.1016/S1872-2067(14)60189-3
Zhang, P., Yokoyama, T., Itabashi, O., Wakui, Y., Suzuki, T.M., Inoue, K., 1998. Hydrometallurgical process for recovery of metal values from spent nickel-metal hydride secondary batteries, Hydrometallurgy.

Appendix 1

Concentration of the metals in the aqueous solutions after leaching of fluorescent lamp powders using the two-step leaching approach with hydrochloric and nitric acid

	Leachate type and concentration of the metals in solution (%)			
Elements	1M HNO3; 10 min; S:L ratio 10% w/v	1M HCl; 10 min; S:L ratio 10% w/v	Resulting residue + 2M HNO3; 22 h; S:L ratio 10% w/v	Resulting residue + 2M HCl; 22 h; S:L ratio 10% w/v
Al	1.93	1.39	0.43	0.51
B	2.01	0.76	0.56	0.40
Ba	8.40	3.18	4.54	0.39
Ca	73.20	76.33	1.69	1.02
Cd	-	0.05	-	0.00
Eu	0.47	0.71	5.22	5.93
Fe	0.19	0.49	0.43	0.13
Mg	0.84	0.50	0.49	0.23
Mn	0.39	2.59	0.13	0.02
Na	2.04	1.93	0.21	0.18
Sb	0.56	1.01	0.13	0.19
Si	1.11	1.66	0.12	0.30
Sr	2.36	2.16	0.42	0.50
Ti	-	0.01	-	0.01
Y	5.14	5.96	83.20	89.35
Zr	-	0.01	-	0.02
REEs	1.05	0.17	2.18	0.47
Other impurities	0.3	1.09	0.28	0.36

Appendix 2

2017a Hydrometallurgy Journal Paper

ATTENTION¡¡

Pages 163 to 173 of the thesis, containing the article

Experimental and modelling studies of neodymium solvent extraction from chloride media with methyl-tri(octyl/decyl)ammonium oleate ionic liquid diluted in kerosene

are available at the editor's web

https://www.sciencedirect.com/science/article/pii/S0304386X17302773

Appendix 3

2017b Hydrometallurgy Journal Paper

ATTENTION¡¡

Pages 175 to 181 of the thesis, containing the article

Mathematical modelling of neodymium, terbium and dysprosium solvent extraction from chloride media using methyl-tri(octyl/decyl)ammonium oleate ionic liquid as extractant

are available at the editor's web

https://www.sciencedirect.com/science/article/abs/pii/S0304386X17304176

Appendix 4

2019 Paper submitted to Solvent Extraction & Ion Exchange Journal (In review)

EXTRACTION STUDY AND MATHEMATICAL MODELLING OF NEODYMIUM, TERBIUM AND DYSPROSIUM FROM CHLORIDE ALKALINE SOLUTION USING METHYLTRI(OCTYL/DECYL)AMMONIUM CHLORIDE

E. Obón[a], A. Fortuny[a], M.T. Coll[a], A.M. Sastre[b]

[a] *Chemical Engineering Department, Universitat Politècnica de Catalunya, EPSEVG, Av. Víctor Balaguer 1, 08800 Vilanova i la Geltrú, Spain.*
[b] *Chemical Engineering Department, Universitat Politècnica de Catalunya, ESTEIB, Av. Diagonal 647, 08028 Barcelona, Spain.*

Abstract

In the present paper, a study on the extraction of neodymium, terbium and dysprosium anionic species from chloride alkaline solutions with methyltri(octyl/decyl)ammonium chloride (Aliquat 336) was carried out. The addition of citrate to the aqueous phase was needed to create anionic extractable species of the metals. The pH of the feed did not affect the extraction extension working in the range 8–11. Increasing the concentration of chloride in the aqueous phase was detrimental since it was found to shift the equilibrium slowing down the extraction of the metallic species. The effect of Aliquat 336 concentration on the extraction extension was studied and used as a base for the mathematical modelling with Matlab Software. Sulphuric and hydrochloric acids were tested as stripping solutions.
A mathematical model was calculated based on the obtained experimental results. The proposed model includes competitive extraction of citrate ions from the media. The model proved to be reliable since it was able to accurately reproduce the experimental extraction yield of the individual metallic species as well as from their mixture.

Highlights

- Solvent extraction of REEs anionic species from aqueous solution.
- Addition of citrate ion is required to form extractable anionic species.
- The proposed mathematical model is able to reproduce the experimental data accurately.

Keywords
Rare Earth Elements; chloride media; citrate; Aliquat 336; extraction model

1. Introduction

The use of the Rare Earth Elements is continuously growing since they are essential ingredients for the development of the modern industry and high technology products used in our daily lives (Kumar Jha et al., 2016). Because of their unique properties, they are being used in a large variety of applications such as the manufacturing of permanent magnets for wind turbines, speakers and phones; fluorescent lamps and nickel metal hydride (NiMH) batteries for hybrid vehicles (Tunsu et al., 2015a). Despite the large demand of these elements, they are regarded as being among the most critical chemical elements. Their critical status is related to their heterogeneous geological location, meaning that they cannot be found all over the earth but just in specific areas, their low concentration in the ores, which make them hard to be mined, and the environmental issues that are often associated with their production (European Comission, 2014b).

Solvent extraction has become one of the most important methods used in hydrometallurgy for the recovery of Rare Earth Elements (REEs) from end of life products (Batchu et al., 2017). The extraction efficiency of many ionic liquids (ILs) has been tested for the development of several REEs extraction systems. They are considered the best substitutes for the conventional volatile organic diluents since they are tailored extractants that can be modified by the combination of cationic and anionic partners to solve the specific needs of the extraction systems (Tunsu et al., 2015b). Moreover, their unique physicochemical properties such as their melting point under 100ºC, their negligible vapour pressure, low flammability, high thermal stability and large electrochemical window among others (Grabda et al., 2014), have promoted them as clean alternatives for safer and more environmentally friendly extraction processes (Böhm et al., 2014).

Anionic extractants such as primary or tertiary amines have proven to be useful to separate anionic species of REEs from impurities in mixed alkaline solutions. Nonetheless, the use of anionic extractants to recover lanthanides from aqueous solutions has been sparsely studied. Aliquat 336 and Primene JMT have been tested since they are strong-base anion exchangers (Kumar Jha et al., 2016). However, solvent extraction of REEs from acidic solutions is still predominant in the metal recovery field. D2EHPA is the most widely studied extractant for rare earth separation (Kumar Jha et al., 2016). Conventional extractants such as Cyanex 921 (Panda et al., 2012b), TBP (Michaud et al., 2012), Cyanex 923 (Larsson et al., 2012) and Cyanex 272 (Banda et al., 2012b) seem to have fallen behind the use of synergic mixtures of solvents such as the synthesised ionic liquids formed from Aliquat 336 (methyltri(octyl/decyl)ammonium chloride) and EHEHPA (2-ethylhexyl phosphonic acid 2-ethylhexyl ester, also known as P507 or PC88A) (Quinn et

al., 2017) or oleic acid (Obón et al., 2017), the nonfluorinated ionic liquid system consisting of the ionic liquid methyltri(octyl/decyl)ammonium dioctyl diglycolamate ([A336][DGA]) in the ionic liquid diluent methyl-tri(octyl/decyl)ammonium nitrate ([A336][NO_3]) (A. Rout and Binnemans, 2014) or the mixture of the methyltrioctylammonium sec-octylphenoxy acetate ([N_{1888}][SOPAA]) and Cyphos 104 (Ma et al., 2017).

The present manuscript describes a study on the solvent extraction of neodymium, terbium and dysprosium from alkaline media using Aliquat 336. Adding citric acid to acidic solutions containing Nd(III), Tb(III) and Dy(III) and adjusting the pH beyond 8 form anionic species that are easily extracted by methyltri(octyl/decyl)ammonium chloride (Aliquat 336). Mathematical modelling of single Nd(III), Tb(III) and Dy(III) solvent extraction has been developed. As in the model of neodymium, terbium and dysprosium extraction from chloride media using AliOle IL done in a previous study (Obón et al., 2017), Matlab R2017b software has been used. The experimental trials were used to find out a suitable model. The proposed extraction model has proven to adjust perfectly to the experimental single extraction and to predict accurately the extraction of Nd(III), Tb(III) and Dy(III) simultaneously.

2. Experimental procedure

2.1. Reagents

Neodymium(III), terbium(III) and dysprosium(III) feed solutions were prepared dissolving 99.9% purity Nd_2O_3, Tb_2O_3 and Dy_2O_3 (Sigma Aldrich; Ref. 228656, 590509 and 289264, respectively) by an acid attack with the minimal amount of HCl. NaCl was added, when needed, up to the required chloride concentration in the aqueous phase. Citric acid (Sigma Aldrich; Ref. 251275) was added to the solution and the initial pH was adjusted with NaOH in order to form anionic citrates. HCl and H_2SO_4 solutions were used as stripping agents.

As extractant, the ionic liquid Aliquat 336 (Methyltri(octyl/decyl)ammonium chloride, 90.6%) provided by Alfa Aesar (Ref. A17247) was used dissolved in a kerosene/ decanol 90/10% v/v solution.

2.2. Procedure

The extraction experiments were carried out by shaking equal volumes of the aqueous and organic phases (10 mL) in separatory funnels with an MVH-40 SBS horizontal mechanical shaker (150 rpm) at room temperature for 15 minutes. After phase separation, the aqueous phase was collected and its pH was measured with a calibrated Crison micropH 2002 pH meter.

Then, Nd(III), Tb(III) and Dy(III) concentrations were measured by Microwave Plasma Atomic Emission Spectroscopy using an MP-AES 4100 spectrophotometer (Agilent Technologies).
The organic phase was reserved for stripping experiments. Hydrochloric and sulphuric acid solutions were used to close the mass balance and strip the REEs from the organic phase. The stripping experiments were performed in the same conditions as the extraction experiments.

In this study, the effect of the citric acid concentration, the pH, the chloride concentration and the Aliquat 336 concentration on the extraction efficiency were studied.

The mathematical model was based on the experimental results obtained. The Matlab R2017b software was used to solve the equilibria equations and mass balances involved in the solvent extraction system.

3. Results

3.1. Liquid-liquid extraction

A series of batch trials was carried out to evaluate the feasibility of removing simultaneously Nd(III), Tb(III) and Dy(III) from the feed solution. Citric acid capability to form anionic species with REEs was tested. The effect of the chloride concentration in the aqueous media, the pH of the aqueous phase and the extractant concentration on the extraction yield was investigated.

First of all, the effectiveness of the extraction system was tested by comparing the extraction of Nd(III), Tb(III) and Dy(III) anionic species from chloride media by adding citric acid to the aqueous phase and adjusting the pH with NaOH. Figure 1 shows the effect of the citric acid addition on the extraction extension.

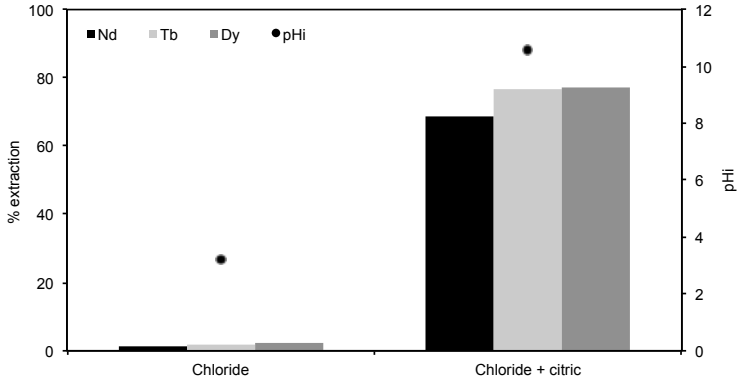

Fig.1.(1-COLUMN FITTING IMAGE) The effect of the citric acid addition in the feed on the Nd(III), Tb(III) and Dy(III) extraction. [Metal ions]$_i$ = 7 mmol·L^{-1} each; [Cl$^-$] = 0.1 mol·L^{-1}, [Aliquat336] = 10%, [Citric acid] = 42 mmol·L^{-1}

As expected, the addition of citric acid into the feed along with an increase in the pH using sodium hydroxide, leads to the formation of metal anionic complexes that can be extracted by the IL Aliquat 336.

The effect of the citric acid concentration in the aqueous phase was also addressed. The total concentration of the metals (21 mmol·L^{-1} in total, 7 mmol·L^{-1} each) was taken as a benchmark and the citric acid concentration was increased from there. A series of experiments were done at 21, 42 and 60 mmol·L^{-1} citric acid to achieve 1:1, 1:2 and 1:3 metal-citrate stoichiometries, respectively. Figure 2 displays the effect of the metal-citrate stoichiometry on the extraction performance.

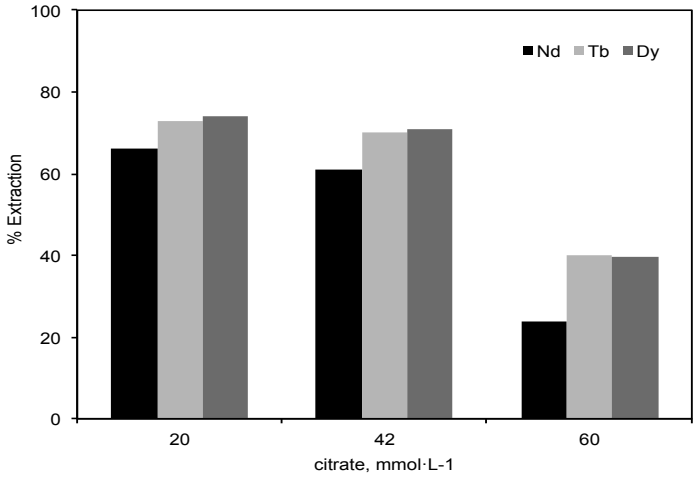

Fig.2.(1-COLUMN FITTING IMAGE) The effect of the citrate concentration in the feed on the Nd(III), Tb(III) and Dy(III) extraction. [Metal ions]$_i$ = 7 mmol·L^{-1} each; [Cl$^-$] = 0.1 mol·L^{-1}, [Aliquat336] = 10% (0.23 mol·L^{-1}).

As can be seen, increasing the citrate concentration in the aqueous phase from 21 to 60 mmol·L^{-1} causes a decrease in the extraction yield of the metals, around 50% in the case of terbium and dysprosium and approximately 40% in the case of neodymium, indicating that there might be competitive extraction of citrate by anionic exchange with Aliquat 336:

$$\mathrm{Cit^{3-}} + 3\,\overline{\mathrm{R_4N^+Cl^-}} \overset{\mathrm{Kie}}{\leftrightarrow} \overline{(\mathrm{R_4N^+})_3\mathrm{Cit^{3-}}} + 3\,\mathrm{Cl^-} \qquad \text{(R.1)}$$

Moreover, metal precipitation was observed in the aqueous phase for the 21 mmol·L^{-1} citrate concentration experiment, which seems to confirm this assumption. Having a metal-citric acid molar ratio of 1:1, the extraction of citrate might leave free metal ions in the solution that would precipitate in the $Me(OH)_3$ form when increasing the pH in the feed. In this regard, the extraction percentages obtained after analysis of the 1:1 raffinate would be distorted because of the precipitation issues.

Thus, to avoid precipitation and minimize the competitive extraction of citrate at the same time, the citric acid concentration in the feed was set to 42 mmol·L^{-1}, which is twice the total concentration of metals in the aqueous phase. The potential extraction of citrate by anionic exchange will be taken into account further on in the mathematical modelling section of the paper.

3.2. Effect of the pH

First of all, the distribution of citrate ions in the aqueous phase was studied. The Medusa Software (Puigdomenech, 2013) was used to figure out the citrate speciation in the feed. Figure 3 shows the effect of the pH on the citrate speciation in the media.

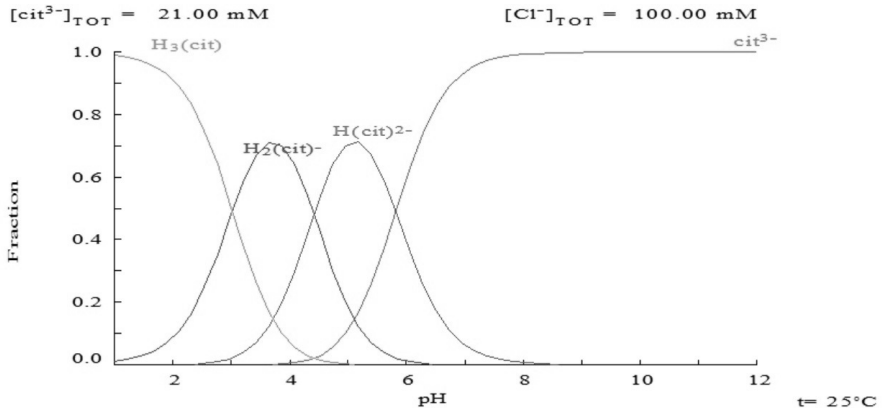

Fig.3.(1-COLUMN FITTING IMAGE) Effect of the pH in the aqueous media on the citrate ion distribution. [Citric acid] = 21 mmol·L^{-1}; [Cl^-] = 0.1 mol·L^{-1}; pH within 1–12.

As can be seen, the pH determines the formation of citrate species in the aqueous phase. As the pH increases, the proton concentration declines, which promotes the formation of cit^{3-} ions. Since the effect of the pH was tested in the pH range 8–11, it can be assumed that the citrate species available to form anionic complexes with the metals is cit^{3-}

The effect of the feed pH on the extraction performance was investigated as well. Figure 4 shows the extraction extension of the metals as a function of the pH in the feed.

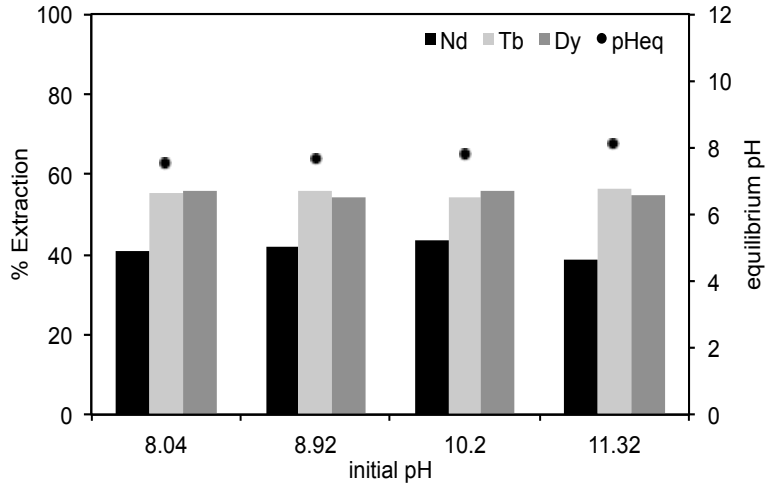

Fig.4.(1-COLUMN FITTING IMAGE) The effect of the pH in the aqueous media on the metals extraction yield. $[Metal]_i$ = 7 mmol·L^{-1} each; [Citric acid] = 42 mmol·L^{-1}; [Cl^-] = 0.1 mol·L^{-1}; [Aliquat 336] = 0.23 mol·L^{-1}

Based on the experimental results obtained, it can be assumed that the pH in the aqueous phase does not have a significant effect on the metal extraction efficiency in the working pH range. As can be observed, the extraction extension remains constant and the equilibrium pH is maintained all the way.
The pH of the solution does not affect the extraction because hydroxide ions are not involved in the formation of chloro-metal-citrate species (R.2 to R.4). Since the main citrate species in the feed, in the working pH range, is cit^{3-} (Fig.3) the formation of chloro-metal-citrate species relies only on the stability constants:

$$MeCl^{2+} + Cit^{3-} \overset{Kcit1}{\longleftrightarrow} MeClCit^{-} \quad \text{(R.2)}$$

$$MeCl_2^{+} + Cit^{3-} \overset{Kcit2}{\longleftrightarrow} MeCl_2Cit^{2-} \quad \text{(R.3)}$$

$$Me^{3+} + Cit^{3-} \overset{Kcit3}{\longleftrightarrow} MeCit \quad \text{(R.4)}$$

And the list could go on because of the excess of citric acid in the media, which may lead to formation of more metal chlorinated anionic species. In the reactions, Me can be Nd(III), Tb(III) or Dy(III) and $Kcit_1$, $Kcit_2$ and $Kcit_3$ represent the stepwise stability constants of the potential anionic complexes formed.

Nonetheless, since the equilibrium pH did not change regardless of the initial pH in the feed, the competitive extraction of hydroxide ions from the aqueous phase must be taken into account:

$$\overline{R_4N^+Cl^-} + OH^- \overset{Kex\ OH}{\longleftrightarrow} \overline{R_4N^+OH^-} + Cl^- \quad \text{(R.5)}$$

As can be seen, the competitive extraction of hydroxide ions does not affect the metal extraction efficiency in the experimental conditions established, because of the excess of Aliquat 336 (0.23 mol·L^{-1}) compared to the OH^- concentration in the aqueous phase.

3.3. Effect of chloride concentration in aqueous phase

The metal extraction performance was studied as a function of the chloride concentration in the feed to determine the effect of the salting out reagent on the extraction extension of the metals. Figure 5 depicts the influence of the Cl^- concentration in the feed on the metal extraction percentages.

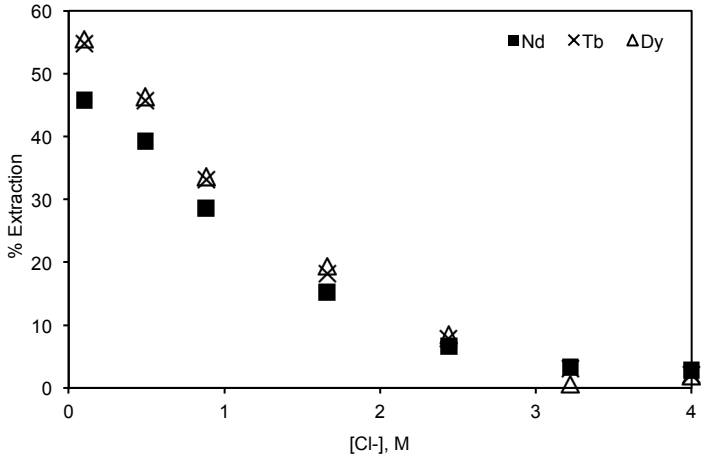

Fig.5(1-COLUMN FITTING IMAGE) The effect chloride concentration in the aqueous phase on the extraction performance. $[Metal]_i$ = 7 mmol·L^{-1} each; [Citric acid] = 42 mmol·L^{-1}; [Aliquat336] = 0.17 mol·L^{-1}; pH = 10.3

As can be observed, low concentrations of chloride ions in the aqueous phase lead to higher extraction values. High chloride concentrations in the feed have a detrimental effect on the extraction performance. Increasing the chloride concentration in the aqueous phase may harm the extraction performance of the metals by shifting the extraction equilibrium towards the release of the REE anionic species to the aqueous phase:

$$\overline{R_4N^+Cl^-} + X^- \overset{Kex}{\longleftrightarrow} \overline{R_4N^+X^-} + Cl^- \qquad \text{(R.6)}$$

Where X^- represents whatever metallic anionic species extracted

In fact, NaCl has been tested as a stripping agent in the literature when working with Aliquat 336 to recover the metals from the organic phase and close the mass balance (Peng and Tsai, 2014; Usapein et al., 2009).

3.4. Effect of Aliquat 336 concentration in the organic phase

The effect of the Aliquat 336 concentration on the extraction performance was studied as well. Several trials were carried out using Aliquat 336 dissolved in kerosene / decanol (90/10 %v/v) to cover a concentration range of 0.023 – 0.34 mol·L^{-1}. Figure 6 shows the neodymium, terbium and dysprosium extraction extension as a function of the ionic liquid concentration in the organic solution.

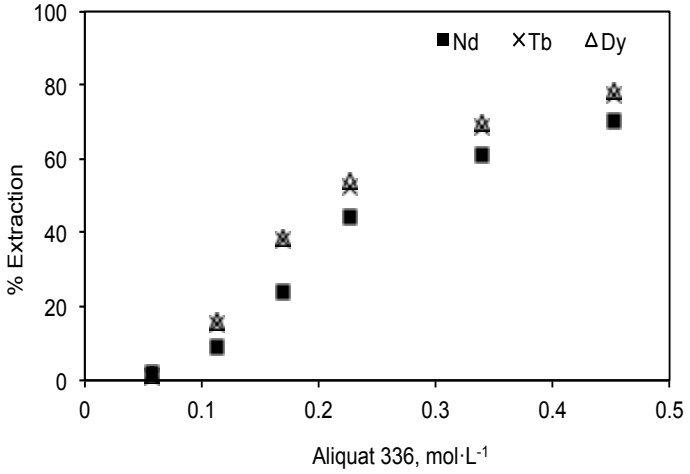

Fig.6.(1-COLUMN FITTING IMAGE) Effect of the Aliquat 336 molar concentration on the extraction of Nd(III), Tb(III) and Dy(III). $[Metal]_i$ = 7 mmol·L^{-1} each; [Citric acid] = 42 mmol·L^{-1}; pH = 10.3.

As expected, an increase of Aliquat 336 concentration leads to an increase in the extraction yield because of the higher extraction capability of the organic phase. At this point, in order to get closer to the extraction mechanism involved in the extraction system, the logarithm of the distribution coefficient (D) of the metals, which is described as: $[Metal\ ion]_{aq}$ / $[Metal\ ion]_{org}$ was plotted vs. the logarithm of Aliquat 336 concentration. Figure 7 shows the effect of Aliquat 336 concentration on the neodymium, terbium and dysprosium distribution coefficients:

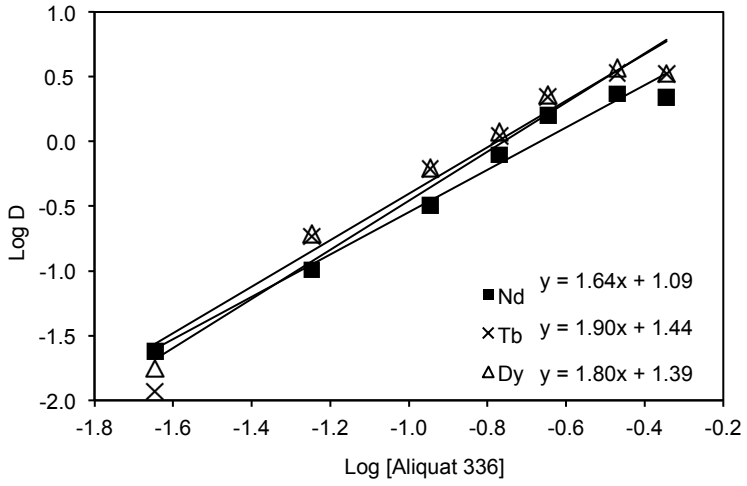

Fig.7.(1-COLUMN FITTING IMAGE) Effect of the [Aliquat 336] on the extraction of Nd(III), Tb(III) and Dy(III). [Citric acid] = 42 mmol·L^{-1}; pH = 10.3.

The linear regression analysis of Log D versus Log [Aliquat 336] of the extraction data gave straight lines with slope values of 1.76 for neodymium, 2.05 for terbium and 1.96 for dysprosium. This suggests that 2 molecules of Aliquat 336 are involved in the extraction of the metals. Therefore, taking into account the speciation of citrate in the aqueous media, the extraction of Nd(III), Tb(III) and Dy(III) is most likely to occur via a $MeCl_2Cit^{2-}$ complex in combination with two IL molecules:

$$\mathrm{MeCl_2Cit^{2-}} + 2\,\overline{\mathrm{R_4N^+Cl^-}} \overset{\mathrm{Kex}}{\leftrightarrow} \overline{\mathrm{(R_4N^+)_2MeCl_2Cit^{2-}}} + 2\,\mathrm{Cl^-} \qquad \text{(R.7)}$$

This was used as a starting point to develop the Matlab modelling of the solvent extraction of Nd(III), Tb(III) and Dy(III) which can be found further on in section 4 of this paper.

3.5. Stripping studies

Stripping studies using acidic solutions were performed for the recovery of the metals from the loaded Aliquat 336. Since Nd(III), Tb(III) and Dy(III) chloro-citrate complexes are anionic species, they may be easily stripped by ion exchange.

Hydrochloric and sulphuric acids were used as stripping agents. The stripping of neodymium, terbium and dysprosium occurs according to the general reactions written below:

$$\overline{\mathrm{(R_4N^+)_2MeCl_2Cit^{2-}}} + 3\,\mathrm{HCl} \leftrightarrow 2\,\overline{\mathrm{R_4N^+Cl^-}} + \mathrm{Me^{3+}} + \mathrm{H_3Cit} + 3\,\mathrm{Cl^-} \qquad \text{(R.8)}$$

$$2\,\overline{(R_4N^+)_2MeCl_2Cit^{2-}} + 3\,H_2SO_4 \;\leftrightarrow\; 2\,\overline{(R_4N^+)_2SO_4} + 2\,Me^{3+} + 2\,H_3Cit + 4\,Cl^- + SO_4^{2-} \qquad \text{(R.9)}$$

The stripping performance was assessed as a function of the hydrochloric and sulphuric acid concentrations in the stripping solutions. Figure 8 shows the effect of HCl and H_2SO_4 concentrations on the stripping of the metals after the first contact.

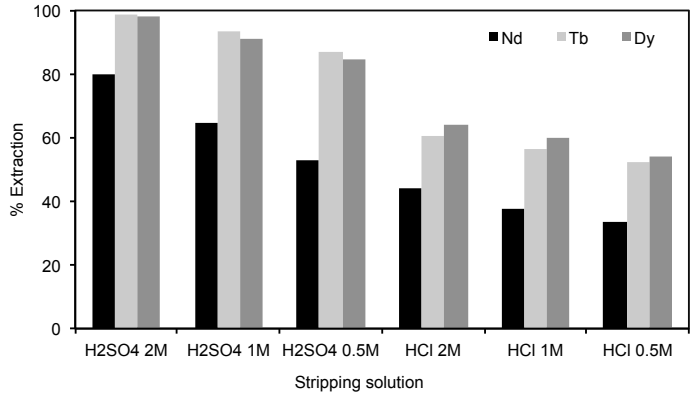

Fig.8.(1-COLUMN FITTING IMAGE) Effect of the Stripping agent on the stripping performance of Nd(III), Tb(III) and Dy(III). $[Metal]_I$ = 7 mmol·L^{-1} each; [Aliquat336] = 0.17 mol·L^{-1}, [Citric acid] = 42 mmol·L^{-1}, [Cl^-] = 0.1 mol·L^{-1}.

The stripping performance was found to rely significantly on the acidic solution. Higher stripping performances were achieved with the sulphuric acid solutions. The ionic strength of the stripping solutions tested may explain this trend:

$$I_m = 0.5 \sum z_i^2 c_i \qquad \text{(Eq.1)}$$

Where c_i represents the molar concentration of the ions in the solution and z_i is the charge of each ion.

According to Eq.1 the ionic strength of H_2SO_4 1 mol·L^{-1} is 3, whereas the ionic strength of HCl 2 mol·L^{-1} is 2. The higher amount of ions available for the ionic exchange of the metals in the sulphuric solutions may be the reason why the sulphuric acid 1 mol·L^{-1} leads to higher stripping values than the HCl 2 mol·L^{-1}. Two stripping contacts were required to remove the metals completely from the loaded organic phase with H_2SO_4 2 mol·L^{-1}.

Regarding the effect of concentration of the acidic solutions, it was noted that increasing HCl and H_2SO_4 concentration improves the stripping performance. Moreover, it can be seen that the stripping of neodymium is lower than the stripping of terbium and dysprosium. This could provide a basis to investigate the REEs separation in the future.

4. Mathematical modelling

The mathematical model proposed was developed taking into account the obtained experimental results. Metal speciation in chloride media and extraction equilibria were considered in order to figure out the best-fitted extraction model.

4.1. Equilibria equations

The extraction mechanism of Nd(III), Tb(III) and Dy(III) has been superficially investigated in section 3.4 of this paper. Neodymium, terbium and dysprosium citrates appear to be extracted in the form $MeCl_2Cit^{2-}$, nonetheless as discussed before, several metallic species can be formed in the aqueous media and they have to be taken into account as well. Therefore, the REEs distribution in the aqueous phase can be described as follows:

$$Me^{3+} + Cl^- \overset{K_1}{\leftrightarrow} MeCl^{2+} \quad \text{(R.10)}$$

$$MeCl^{2+} + Cl^- \overset{K_2}{\leftrightarrow} MeCl_2{}^{+} \quad \text{(R.11)}$$

$$MeCl_2{}^{+} + Cl^- \overset{K_3}{\leftrightarrow} MeCl_3 \quad \text{(R.12)}$$

$$MeCl^{2+} + Cit^{3-} \overset{Kcit1}{\longleftrightarrow} MeClCit^- \quad \text{(R.2)}$$

$$MeCl_2^{+} + Cit^{3-} \overset{Kcit2}{\longleftrightarrow} MeCl_2Cit^{2-} \quad \text{(R.3)}$$

$$Me^{3+} + Cit^{3-} \overset{Kcit3}{\longleftrightarrow} MeCit \quad \text{(R.4)}$$

In the reactions, Me can be Nd(III), Tb(III) or Dy(III) and K_1, K_2, K_3, K_{cit1}, K_{cit2}, K_{cit3} represent the stepwise stability constants.

The equilibria expressions of the formation constants are expressed as a function of the concentrations and activities of the species (a_i):

$$K_1 = \frac{a_{MeCl^{2+}}}{a_{Me^{3+}} \cdot a_{Cl^-}} = \frac{[MeCl^{2+}]}{[Me^{3+}]\cdot[Cl^-]} \cdot \frac{\gamma_{MeCl^{2+}}}{\gamma_{Me^{3+}}\cdot\gamma_{Cl^-}} \quad \text{(Eq.2)}$$

$$K_2 = \frac{a_{MeCl_2{}^{+}}}{a_{MeCl^{2+}} \cdot a_{Cl^-}} = \frac{[MeCl_2{}^{+}]}{[MeCl^{2+}]\cdot[Cl^-]} \cdot \frac{\gamma_{MeCl_2{}^{+}}}{\gamma_{MeCl^{2+}}\cdot\gamma_{Cl^-}} \quad \text{(Eq.3)}$$

$$K_3 = \frac{a_{MeCl_3}}{a_{MeCl_2{}^{+}} \cdot a_{Cl^-}} = \frac{[MeCl_3]}{[MeCl_2{}^{+}]\cdot[Cl^-]} \cdot \frac{\gamma_{MeCl_3}}{\gamma_{MeCl_2{}^{+}}\cdot\gamma_{Cl^-}} \quad \text{(Eq.4)}$$

$$K_{cit1} = \frac{a_{MeClCit^-}}{a_{MeCl^{2+}} \cdot a_{Cit^{3-}}} = \frac{[MeClCit^-]}{[MeCl^{2+}]\cdot[Cit^-]} \cdot \frac{\gamma_{MeClCit^-}}{\gamma_{MeCl^{2+}}\cdot\gamma_{Cit^-}} \quad \text{(Eq.5)}$$

$$K_{cit2} = \frac{a_{MeCl_2Cit^{2-}}}{a_{MeCl_2{}^{+}} \cdot a_{Cit^{3-}}} = \frac{[MeCl_2Cit^{2-}]}{[MeCl_2{}^{+}]\cdot[Cit^{3-}]} \cdot \frac{\gamma_{MeCl_2Cit^{2-}}}{\gamma_{MeCl_2{}^{+}}\cdot\gamma_{Cit^{3-}}} \quad \text{(Eq.6)}$$

$$K_{cit3} = \frac{a_{MeCit}}{a_{Me^{3+}} \cdot a_{Cit^-}} = \frac{[MeCit]}{[Me^{3+}]\cdot[Cit^-]} \cdot \frac{\gamma_{MeCit}}{\gamma_{Me^{3+}}\cdot\gamma_{Cit^-}} \quad \text{(Eq.7)}$$

Where γ_i are the activity coefficients of the *i* species. The stepwise stability constants can be converted to their accumulative form by taking their product: $\beta_1 = K_1$; $\beta_2 = K_1 \cdot K_2$; $\beta_3 = K_1 \cdot K_2 \cdot K_3$.

The Davies equation was used to calculate the activity coefficients of the metal species provided that their ionic strength is > 0:

$$\log_{10} \gamma_i = -0.5102 \cdot z_i \cdot \left(\frac{\sqrt{I_m}}{(1+\sqrt{I_m})} - 0.3 \cdot I_m \right) \quad \text{(Eq.8)}$$

$$I_m = 0.5 \sum z_i^2 c_i \quad \text{(Eq.1)}$$

Where z_i is the charge of the species *i*, I_m is the ionic strength and c_i the concentration of the metals.

According to the slopes obtained by plotting the logarithm of the distribution coefficient (D) of the metals vs. the logarithm of Aliquat 336 concentration (Fig. 7), the following extraction mechanism by anionic exchange is proposed:

$$MeCl_2Cit^{2-} + 2\,\overline{R_4N^+Cl^-} \overset{Kex}{\leftrightarrow} \overline{(R_4N^+)_2MeCl_2Cit^{2-}} + 2\,Cl^- \quad \text{(R.13)}$$

In the proposed equilibria it is assumed that there is just one metal-organic species in the organic phase. The ionic exchange chloride/citrate is also taken into account:

$$Cit^{3-} + 3\,\overline{R_4N^+Cl^-} \overset{Kie}{\leftrightarrow} \overline{(R_4N^+)_3Cit^{3-}} + 3\,Cl^- \quad \text{(R.1)}$$

The corresponding equilibria equations can be written as follows:

$$K_{ex} = \frac{a_{\overline{(R_4N^+)_2MeCl_2Cit^{2-}}} \cdot a_{Cl^-}^2}{a_{\overline{R_4N^+Cl^-}}^2 \cdot a_{MeCl_2Cit^{2-}}} = \frac{[\overline{(R_4N^+)_2MeCl_2Cit^{2-}}] \cdot [Cl^-]^2}{[\overline{R_4N^+Cl^-}]^2 \cdot [MeCl_2Cit^{2-}]} \cdot \frac{\gamma_{\overline{(R_4N^+)_2MeCl_2Cit^{2-}}} \cdot \gamma_{Cl^-}^2}{\gamma_{\overline{R_4N^+Cl^-}}^2 \cdot \gamma_{MeCl_2Cit^{2-}}} \quad \text{(Eq.9)}$$

$$K_{ie} = \frac{a_{\overline{(R_4N^+)_3Cit^{3-}}} \cdot a_{Cl^-}^3}{a_{\overline{R_4N^+Cl^-}}^3 \cdot a_{Cit^{3-}}} = \frac{[\overline{(R_4N^+)_3Cit^{3-}}] \cdot [Cl^-]^3}{[\overline{R_4N^+Cl^-}]^3 \cdot [Cit^{3-}]} \cdot \frac{\gamma_{\overline{(R_4N^+)_3Cit^{3-}}} \cdot \gamma_{Cl^-}^3}{\gamma_{\overline{R_4N^+Cl^-}}^3 \cdot \gamma_{Cit^{3-}}} \quad \text{(Eq.10)}$$

In the equilibria, the bar above the species means that they are in the organic phase. Their activity coefficients (γ) are considered to be equal to 1.

4.2. Mass balances

Mass balances of neodymium, terbium, dysprosium, citrate and Aliquat 336 are required to solve the model. In order to set it up, equal volumes of aqueous and organic phases are assumed. Therefore, the sum of each reagent in the equilibria is considered as follows:

Neodymium mass balance

$$[Nd]_t = [Nd^{3+}] + [NdCl^{2+}] + [NdCl_2^{+}] + [NdCl_3] + [NdClCit^{-}] + [NdCl_2Cit^{2-}] + \\ + [NdCit] + [\overline{(R_4N^+)_2NdCl_2Cit^{2-}}] \quad \text{(Eq.11)}$$

Terbium mass balance

$$[Tb]_t = [Tb^{3+}] + [TbCl^{2+}] + [TbCl_2^{+}] + [TbCl_3] + [TbClCit^{-}] + [TbCl_2Cit^{2-}] + \\ + [TbCit] + [\overline{(R_4N^+)_2TbCl_2Cit^{2-}}] \quad \text{(Eq.12)}$$

Dysprosium mass balance

$$[Dy]_t = [Dy^{3+}] + [DyCl^{2+}] + [DyCl_2^{+}] + [DyCl_3] + [DyClCit^{-}] + [DyCl_2Cit^{2-}] + \\ + [DyCit] + [\overline{(R_4N^+)_2DyCl_2Cit^{2-}}] \quad \text{(Eq.13)}$$

Chloride mass balance

$$[Cl^-]_t = [Cl^-]_{free} + [\overline{R_4N^+Cl^-}]_{free} + [NdCl^{2+}] + 2\cdot[NdCl_2^{+}] + 3\cdot[NdCl_3] + \\ + [NdClCit^-] + 2\cdot[NdCl_2Cit^{2-}] + 2\cdot[\overline{(R_4N^+)_2NdCl_2Cit^{2-}}] + [TbCl^{2+}] + \\ + 2\cdot[TbCl_2^{+}] + 3\cdot[TbCl_3] + [TbClCit^-] + 2\cdot[TbCl_2Cit^{2-}] + \\ + 2\cdot[\overline{(R_4N^+)_2TbCl_2Cit^{2-}}] + [DyCl^{2+}] + 2\cdot[DyCl_2^{+}] + 3\cdot[DyCl_3] + \\ + [DyClCit^-] + 2\cdot[DyCl_2Cit^{2-}] + 2\cdot[\overline{(R_4N^+)_2DyCl_2Cit^{2-}}] \quad \text{(Eq.14)}$$

Citrate mass balance

$$[Cit^{3-}]_t = [Cit^{3-}]_{free} + [NdClCit^-] + [NdCl_2Cit^{2-}] + [NdCit] + [TbClCit^-] + \\ + [TbCl_2Cit^{2-}] + [TbCit] + [DyClCit^-] + [DyCl_2Cit^{2-}] + [DyCit] + \\ + [\overline{(R_4N^+)_2NdCl_2Cit^{2-}}] + [\overline{(R_4N^+)_2TbCl_2Cit^{2-}}] + [\overline{(R_4N^+)_2DyCl_2Cit^{2-}}] + \\ + [\overline{(R_4N^+)_3Cit^{3-}}] \quad \text{(Eq. 15)}$$

Aliquat 336 mass balance

$$[\overline{E}]_t = [\overline{R_4N^+Cl^-}]_{free} + 2\cdot[\overline{(R_4N^+)_2NdCl_2Cit^{2-}}] + 2\cdot[\overline{(R_4N^+)_2TbCl_2Cit^{2-}}] + \\ + 2\cdot[\overline{(R_4N^+)_2DyCl_2Cit^{2-}}] + 3\cdot[\overline{(R_4N^+)_3Cit^{3-}}] \quad \text{(Eq.16)}$$

4.3. Model resolution

To solve the model the Matlab R2017b software was used. The equilibria equations (Eq.2–7; Eq. 9 – 10) and the mass balances (Eq. 11–16) were solved using the formation and equilibria constants (K) as optimization parameters so that the calculated values fit the experimental ones with the minimum error. The

resolution method applied is described in a previous work regarding the mathematical modelling of neodymium, terbium and dysprosium extraction with methyltri(octyl/decyl)ammonium oleate ionic liquid (AliOle) (Obón et al., 2017). The metal-chloride formation constants calculated in that paper were used for initialization of the program (K_0):

Table 1
Stability constants in the literature (Obón et al., 2017).

	K_1	K_2	K_3
Nd(III)	37.14	0.15	$9.5 \cdot 10^{-4}$
Tb(III)	252.97	0.03	0.3
Dy(III)	98.39	0.02	1.0

The chloro-metal-citrate formation constants (K_{Cit}) and the extraction constants (K_{ex}) were used as optimization parameters. The optimization is meant to find the constant values that will make the model match the experimental extraction extension with the minimum error.

4.4. Mathematical modelling results

The extraction model proposed was applied to the extraction of neodymium, terbium and dysprosium anionic species in the $MeCl_2Cit^{2-}$ form with Aliquat 336 IL. Optimized stability and equilibrium constants (K) were determined by minimization of the error function F(x), defined as the square root of the sum of the squared differences between the calculated and experimental extraction data:

$$F(x) = \sum \left| \left(\%E_{icalc} - \%E_{iexp} \right)^2 \right| \qquad \text{(Eq.17)}$$

Where E_{icalc} and E_{iexp} are the calculated and experimental extraction values.

Minimizing F(x) using the Matlab *fmincon* function, a set of the most optimized stability and equilibria constants (K) was determined. Table 2 shows the constants found and the error value associated.

Table 2
Stability and equilibria optimized constants

	K_{cit1}	K_{cit2}	K_{cit2}	K_{ex}	K_{ie}	σ total*
Nd(III)	15.91	2614.45	1.55	94.18	-	952
Tb(III)	9.38	578.60	0.39	261.01	-	
Dy(III)	0.56	1011.00	7.92	253.50	-	
Cit^{3-}	-	-	-	-	1.87	

The stability and equilibria constants in the table proved to fit the proposed model with the minimum error. Calculated and experimental data were plotted in order to get a better picture of the accuracy of the fitting. Figure 9 shows a comparative graph between the calculated extraction extension using the optimized constants with the Matlab software versus the experimental extraction percentages of Nd(III), Tb(III) and Dy(III).

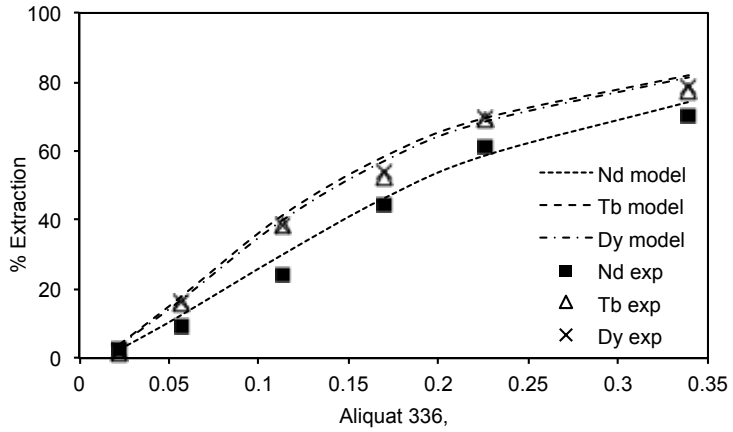

Fig.9. (1-COLUMN FITTING IMAGE) Comparative graph between simulated and experimental extraction values regarding the effect of the Aliquat 336 molar concentration on the extraction of Nd(III), Tb(III) and Dy(III). $[Metal]_i$ = 7 mmol·L^{-1} each; [Citric acid] = 42 mmol·L^{-1}; [Cl^-] = 0.1 mol·L^{-1}.

As shown, the proposed model is able to reproduce the experimental extraction extension when it comes to the effect of the extractant concentration.

The optimized stability and equilibria constants calculated were also tested to forecast the single extraction of neodymium, terbium and dysprosium. The effect of Aliquat 336 was also studied in this case. Figure 10 shows comparative plots between the simulation results of the model and the extraction percentages obtained experimentally.

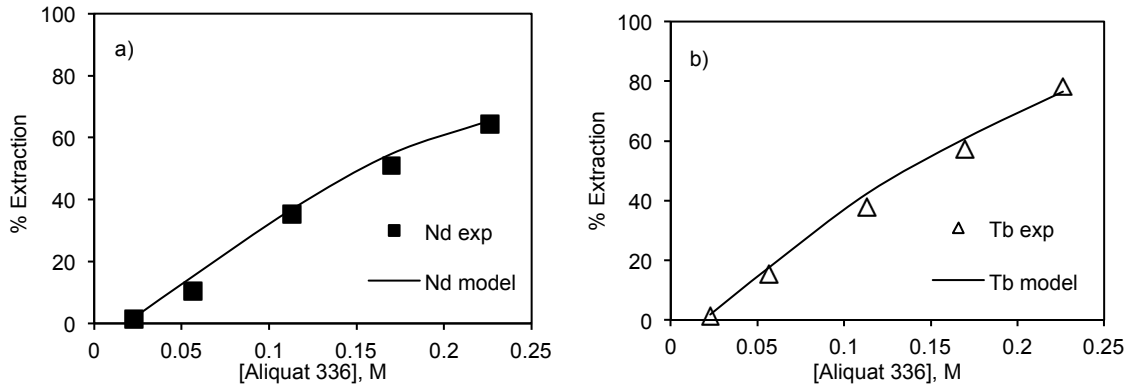

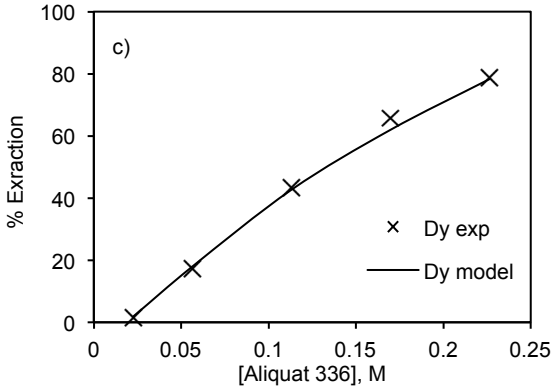

Fig.10. (2-COLUMN FITTING IMAGES) Comparative graph between simulated and experimental extraction values regarding the effect of the Aliquat 336 molar concentration on the extraction of single Nd(III), Tb(III) and Dy(III). $[Metal]_i$ = 7 mmol·L^{-1} each; [Citric acid] = 14 mmol·L^{-1}.

As can be seen, the calculated equilibrium constants allow to faithfully recreate the extraction of Nd(III), Tb(III) and Dy(III) individually.

The proposed mathematical model, which involves extraction of the $MeCl_2Cit^{2-}$ species by 1:2 stoichiometry, has proven to be a handy tool to predict and reproduce both single and combined metal extraction with Aliquat 336 in chloride media. It might be a convenient instrument to be used for extraction and separation prediction of other rare earth elements from end of life products, involving minor adjustments of the equilibria equations and mass balances.

5. Conclusions

This study reports on the extraction of Nd(III), Tb(III) and Dy(III) anionic species from chloride media with Aliquat 336. First of, the effectiveness of the citrate addition to create extractable anionic species of the metals was confirmed. The pH was found to be non-critical when working in the range 8–11, since the main citrate species in the feed is the cit^{3-} ion and therefore, the formation of chloro-metal-citrate species relies only on the stability constants. The effect of chloride in the aqueous phase was studied and it was seen that high concentrations are detrimental since chloride ions seem to shift the equilibrium decreasing the extraction of the metallic species. The effect of Aliquat 336 concentration on the extraction extension was investigated. The results were used as a base for the mathematical modelling with Matlab Software. The stripping performance was found to rely significantly on the ionic strength of the acidic solution; the stripping yield achieved with sulphuric acid was higher than with hydrochloric acid.

A mathematical model is proposed. The model was developed with Matlab software taking into account the experimental results obtained. The calculated stability constants of the chloro-metal-citrate species formed in the aqueous

phase were: $K_{cit1\text{-}Nd}$ = 15.91; $K_{cit2\text{-}Nd}$ = 2614.45; $K_{cit3\text{-}Nd}$ = 1.55; $K_{cit1\text{-}Tb}$ = 9.38; $K_{cit2\text{-}Tb}$ = 578.60; $K_{cit3\text{-}Tb}$ = 0.39; $K_{cit1\text{-}Dy}$ = 0.56; $K_{cit2\text{-}Dy}$ = 1011.00 and $K_{cit3\text{-}Dy}$ = 7.92; and the extraction constants: $K_{ex\text{-}Nd}$ = 94.18; $K_{ex\text{-}Tb}$ = 261.01; $K_{ex\text{-}Dy}$ = 253.50; K_{ie} = 1.87. The reliability of the model was proved since it was able to reproduce and feasibly predict the experimental extraction extension with a standard deviation of 952.

This work provides a base for the recovery of REEs as anionic species using Aliquat 336 as extractant and appears to be very promising to be used in urban mining recycling systems. The proposed model could also be useful to set the background for rare earths transport and separation in a SLM system.

Acknowledgements

This work was funded by the Ministry of Science and Innovation of Spain (Project No. CTM 2017-83581R). E.O. acknowledges The Ministry of Science and Innovation the fellowship received (BES-2012-057589).

References

Aba, Y.B., Ubota, F.K., Amiya, N.K., Oto, M.G., 2011. Recent Advances in Extraction and Separation of Rare-Earth Metals Using Ionic Liquids. J. Chem. Eng. Japan 44, 679–685. doi:https://doi.org/10.1252/jcej.10we279

Abedini, A., Butcher, C., Nemcko, M.J., Kurukuri, S., Worswick, M.J., 2017. Constitutive characterization of a rare-earth magnesium alloy sheet (ZEK100-O) in shear loading: Studies of anisotropy and rate sensitivity. Int. J. Mech. Sci. 128–129, 54–69. doi:10.1016/j.ijmecsci.2017.04.013

Adunka, R., Virginia Orna, M., 2018. Discoveries Among the Rare Earths 3.1 Ytterby and Beyond. SpringerBriefs Hist. Chem. doi:10.1007/978-3-319-77905-8_3

Agilent Technologies, 2016. Microwave Plasma Atomic Emission Spectroscopy (MP-AES), Application eHandbook.

Akah, A., 2017. Application of rare earths in fluid catalytic cracking: A review. J. Rare Earths 35, 941–956. doi:10.1016/S1002-0721(17)60998-0

Alonso, E., Sherman, A.M., Wallington, T.J., Everson, M.P., Field, F.R., Roth, R., Kirchain, R.E., 2012. Evaluating rare earth element availability: a case with revolutionary demand from clean technologies. Environ. Sci. Technol. 46, 3406–14. doi:10.1021/es203518d

Assumpçao, D., Moura, A., Alberto, J., Tenório, S., 2009. Spent NiMH batteries-The role of selective precipitation in the recovery of valuable metals. J. Power Sources 193, 914–923. doi:10.1016/j.jpowsour.2009.05.014

Assumpçao, D., Moura, A., Alberto, J., Tenório, S., 2006. Spent NiMH batteries:

Characterization and metal recovery through mechanical processing. J. Power Sources 160, 1465–1470. doi:10.1016/j.jpowsour.2006.02.091

Banda, R., Jeon, H., Lee, M., 2012a. Solvent extraction separation of Pr and Nd from chloride solution containing La using Cyanex 272 and its mixture with other extractants. Sep. Purif. Technol. 98, 481–487. doi:10.1016/j.seppur.2012.08.015

Banda, R., Jeon, H.S., Lee, M.S., 2012b. Solvent extraction separation of La from chloride solution containing Pr and Nd with Cyanex 272. Hydrometallurgy 121–124, 74–80. doi:10.1016/j.hydromet.2012.04.003

Baolu, Z., Zhongxue, L., Congcong, C., 2017. Global Potential of Rare Earth Resources and Rare Earth Demand from Clean Technologies. Minerals 7. doi:10.3390/min7110203

Batchu, N.K., Hoogerstraete, T. Vander, Banerjee, D., Binnemans, K., 2017. Non-aqueous solvent extraction of rare-earth nitrates from ethylene glycol to n-dodecane by Cyanex 923. Sep. Purif. Technol. 174, 544–553. doi:10.1016/j.seppur.2016.10.039

Berthod, A., Ruiz-Ángel, M.J., Carda-Broch, S., 2018. Recent advances on ionic liquid uses in separation techniques. J. Chromatogr. A 1559, 2–16. doi:10.1016/j.chroma.2017.09.044

Binnemans, K., Jones, P.T., Blanpain, B., Van Gerven, T., Yang, Y., Walton, A., Buchert, M., 2013. Recycling of rare earths: a critical review. J. Clean. Prod. 51, 1–22. doi:10.1016/j.jclepro.2012.12.037

Blankson Abaka-Wood, G., Quast, K., Zanin, M., Addai-Mensah, J., Skinner, W., 2019. A study of the feasibility of upgrading rare earth elements minerals from iron-oxide-silicate rich tailings using Knelson concentrator and Wilfley shaking table. Powder Technol. 334, 897–913. doi:10.1016/j.powtec.2018.12.005

Böhm, M., Tietze, A.A., Heimer, P., Chen, M., Imhof, D., 2014. Ionic liquids as reaction media for oxidative folding and native chemical ligation of cysteine-containing peptides. J. Mol. Liq. 192, 67–70. doi:10.1016/j.molliq.2013.08.020

Charbonniere, L.J., 2011. Luminescent Lanthanide Labels. Curr. Inorg. Chem. 1, 2–16. doi:10.2174/1877945X11101010002

Chen, Z., 2011. Global rare earth resources and scenarios of future rare earth industry. J. Rare Earths. doi:10.1016/S1002-0721(10)60401-2

Cossu, R., Bonifazi, G., 2013. The Urban Mining concept. Waste Manag. 33, 497–498. doi:10.1016/j.wasman.2013.01.010

Cotton, S., 2006. Lanthanide and Actinide Chemistry and Spectroscopy, American Chemical Society. doi:10.1002/0470010088

Cousland, G.P., Cui, X.Y., Smith, A.E., Stampfl, A.P.J., Stampfl, C.M., 2018. Mechanical properties of zirconia, doped and undoped yttria-stabilized cubic zirconia from first-principles. J. Phys. Chem. Solids 122, 51–71. doi:10.1016/j.jpcs.2018.06.003

Cui, J., Kramer, M., Zhou, L., Liu, F., Gabay, A., Hadjipanayis, G., Balasubramanian, B., Sellmyer, D., 2018. Current progress and future challenges in rare-earth-free permanent magnets. Acta Mater. 158, 118–137. doi:10.1016/j.actamat.2018.07.049

Desouky, O.A., Daher, A.M., Abdel-Monem, Y.K., Galhoum, A.A., 2008. Liquid-liquid extraction of yttrium using primene-JMT from acidic sulfate solutions. Hydrometallurgy 96, 313–317. doi:10.1016/j.hydromet.2008.11.009

Dickman, 2008. Diodelaser Pumped Nd : YAG Laser.

Dupont, D., Binnemans, K., 2015. Recycling of rare earths from NdFeB magnets using a combined leaching/extraction system based on the acidity and thermomorphism of the ionic liquid [Hbet][Tf 2 N]. Green Chem. 17, 2150–2163. doi:10.1039/C5GC00155B

Ella Y. Lin, Astrid Rahmawati, Jo-Hsin Ko, Jhy-Chern Liu, 2018. Extraction of yttrium and europium from waste cathode-ray tube (CRT) phosphor by subcritical water. Sep. Purif. Technol. 1921, 166–175. doi:http://dx.doi.org/10.1016/j.seppur.2017.10.004

EURare, 2017. Research and development for the Rare Earth Element supply chain in Europe.

EURare, 2013. EURARE sustainable exploitation [WWW Document].

European Comission, 2014a. Report on Critical raw materials for the EU.

European Comission, 2014b. ERECON: Strengthening the European Rare Earths Supply-Chain, Challenges and policy options.

European Commission, 2017. Study on the review of the list of critical raw materials, Study on the review of the list of critical raw materials. Criticality Assessments. doi:10.2873/876644

Fatahi, M.R., Farzanegan, A., 2018. An analysis of multiphase flow and solids separation inside Knelson Concentrator based on four-way coupling of CFD and DEM simulation methods. Miner. Eng. 126, 130–144. doi:10.1016/j.mineng.2018.07.004

Fernandes, A., Afonso, J.C., Junqueira, A., Dutra, B., 2013. Separation of nickel(II), cobalt(II) and lanthanides from spent Ni-MH batteries by hydrochloric acid leaching, solvent extraction and precipitation. Hydrometallurgy 133, 37–43. doi:10.1016/j.hydromet.2012.11.017

Grabda, M., Panigrahi, M., Oleszek, S., Kozak, D., Eckert, F., Shibata, E., Nakamura, T., 2014. COSMO-RS screening for efficient ionic liquid

extraction solvents for NdCl3 and DyCl3. Fluid Phase Equilib. 383, 134–143.

Gupta, D.C.C.K., Krishnamurthy, N., 2005. Extractive Metallurgy of Rare Earths.

Habashi, F., 2013. Extractive metallurgy of rare earths Historical introduction. Can. Metall. Q. 52, 224–233. doi:10.1179/1879139513Y.0000000081

Habib, K., Wenzel, H., 2014. Exploring rare earths supply constraints for the emerging clean energy technologies and the role of recycling. J. Clean. Prod. 84, 348–359. doi:10.1016/j.jclepro.2014.04.035

Hidayah, N.N., Abidin, Z., 2018. The evolution of mineral processing in extraction of rare earth elements using liquid-liquid extraction: A review. Miner. Eng. 121, 146–157. doi:10.1016/j.mineng.2018.03.018

Hiskey, J.B., Copp, R.G., 2018. Solvent extraction of yttrium and rare earth elements from copper pregnant leach solutions using Primene JM-T. Miner. Eng. 125, 265–270. doi:10.1016/j.mineng.2018.06.014

Hitachi, 2010. Hitachi Develops Recycling Technologies for Rare Earth Metals.

Hogfeldt, E., 1982. Stability Constants of Metal-Ion Complexes, Part A: Inorganic Ligands (IUPAC Chemical Data Series), 2nd ed. Pergamon Press.

Hoogerstraete, T. Vander, Blanpain, B., Van Gerven, T., Binnemans, K., 2014. From NdFeB magnets towards the rare-earth oxides: a recycling process consuming only oxalic acid. RSC Adv. 4, 64099–64111. doi:10.1039/c4ra13787f

Innocenzi, V., De Michelis, I., Ferella, F., Vegliò, F., 2017a. Leaching of yttrium from cathode ray tube fluorescent powder: Kinetic study and empirical models. Int. J. Miner. Process. 168, 76–86. doi:10.1016/j.minpro.2017.09.015

Innocenzi, V., Maria Ippolito, N., De Michelis, I., Prisciandaro, M., Medici, F., Vegli, F., 2017b. A review of the processes and lab-scale techniques for the treatment of spent rechargeable NiMH batteries. J. Power Sources 362, 202–218. doi:10.1016/j.jpowsour.2017.07.034

Innocenzi, V., Maria Ippolito, N., Pietrelli, L., Centofanti, M., Piga, L., Vegli, F., 2018. Application of solvent extraction operation to recover rare earths from fluorescent lamps. J. Clean. Prod. 172, 2840–2852. doi:10.1016/j.jclepro.2017.11.129

Innocenzi, V., Vegliò, F., 2012. Recovery of rare earths and base metals from spent nickel-metal hydride batteries by sequential sulphuric acid leaching and selective precipitations. J. Power Sources 211, 184–191. doi:10.1016/j.jpowsour.2012.03.064

IPT, 2017. A future for rare earths in Brazil A future for rare earths in Brazil.

Jordens, A., 2016. The beneficiation of rare earth element-bearing minerals. McGill University.

Jordens, A., Cheng, Y.P., Waters, K.E., 2013. A review of the beneficiation of rare earth element bearing minerals. Miner. Eng. 41, 97–114. doi:10.1016/j.mineng.2012.10.017

Jowitt, S.M., Werner, T.T., Weng, Z., Mudd, G.M., Thakur, V.K., Kumar Gupta, R., Matharu, A.S., 2018. Current Opinion in Green and Sustainable Chemistry. Curr. Opin. Green Sustain. Chem. 13, 1–7. doi:10.1016/j.cogsc.2018.02.008

Kubota, F., Shimobori, Y., Baba, Y., 2011. Application of ionic liquids to extraction separation of rare earth metals with an effective diglycol amic acid extractant. J. Chem. Eng. Japan 44, 307–312.

Kumar Jha, M., Kumari, A., Panda, R., Kumar, J.R., Yoo, K., Lee, J.Y., 2016. Review on hydrometallurgical recovery of rare earth metals. doi:10.1016/j.hydromet.2016.01.035

Kumari, A., Panda, R., Jha, M.K., Pathak, D.D., 2018. Extraction of rare earth metals by organometallic complexation using PC88A. Comptes Rendus Chim. 21, 1029–1034. doi:10.1016/j.crci.2018.09.005

Kumari, A., Panda, R., Kumar Jha, M., Rajesh Kumar, J., Lee, J.Y., 2015. Process development to recover rare earth metals from monazite mineral: A review. Miner. Eng. 79, 102–115. doi:10.1016/j.mineng.2015.05.003

Kumari, A., Sinha, M.K., Pramanik, S., Kumar Sahu, S., 2018. Recovery of rare earths from spent NdFeB magnets of wind turbine: Leaching and kinetic aspects. Waste Manag. 75, 486–498. doi:10.1016/j.wasman.2018.01.033

Larsson, K., Binnemans, K., 2015. Metal Recovery from Nickel Metal Hydride Batteries Using Cyanex 923 in Tricaprylylmethylammonium Nitrate from Chloride Aqueous Media. J. Sustain. Metall. 1, 161–167. doi:10.1007/s40831-015-0017-5

Larsson, K., Binnemans, K., 2014. Selective extraction of metals using ionic liquids for nickel metal hydride battery recycling. Green Chem. 16, 4595. doi:10.1039/c3gc41930d

Larsson, K., Ekberg, C., Ødegaard-Jensen, A., 2013a. Dissolution and characterization of HEV NiMH batteries. Waste Manag. 33, 689–698. doi:10.1016/j.wasman.2012.06.001

Larsson, K., Ekberg, C., Ødegaard-Jensen, A., 2013b. Using Cyanex 923 for selective extraction in a high concentration chloride medium on nickel metal hydride battery waste Part II: mixer-settler experiments. Hydrometallurgy 133, 168–175. doi:10.1016/j.hydromet.2013.01.012

Larsson, K., Ekberg, C., Ødegaard-Jensen, A., 2012. Using Cyanex 923 for selective extraction in a high concentration chloride medium on nickel

metal hydride battery waste. Hydrometallurg 120–130, 35–42. doi:10.1016/j.hydromet.2012.08.011

Lee, C.-H., Chen, Y.-J., Liao, C.-H., Popuri, S.R., Tsai, S.-L., Hung, C.-E., 2013. Selective Leaching Process for Neodymium Recovery from Scrap Nd-Fe-B Magnet. Metall. Mater. Trans. A 44A, 5825–5833. doi:10.1007/s11661-013-1924-3

Lee, G.S., Uchikoshi, M., Mimura, K., Isshiki, M., 2009. Distribution coefficients of La, Ce, Pr, Nd, and Sm on Cyanex 923-, D2EHPA-, and PC88A-impregnated resins. Sep. Purif. Technol. 67, 79–85. doi:10.1016/j.seppur.2009.03.033

Lee, M.-S., Lee, J.-Y., Kim, J.-S., Lee, G.-S., 2005. Solvent extraction of neodymium ions from hydrochloric acid solution using PC88A and saponified PC88A. Sep. Purif. Technol. 46, 72–78. doi:10.1016/j.seppur.2005.04.014

Leif, R.C., Vallarino, L.M., Becker, M.C., Yang, S., 2006. Increasing the Luminescence of Lanthanide Complexes. Int. Soc. Anal. Cytol. 69A, 767–778. doi:10.1002/cyto.a.20321

Long, K.; Van Gosen, B.; Foley, N.; Cordier, D., 2010. The Principal Rare Earth Elements Deposits of the United States-A Summary of Domestic Deposits and a Global Perspective.

Loy, S. Van, Binnemans, K., Van Gerven, T., 2017. Recycling of rare earths from lamp phosphor waste: Enhanced dissolution of LaPO 4 :Ce 3þ ,Tb 3þ by mechanical activation. J. Clean. Prod. 156, 226–234. doi:10.1016/j.jclepro.2017.03.160

Lyman, W.J., Palmer, R.G., 1992. Scrap Treatment Method For Rare Earth Transition Metal Alloys. US patent 5129945 A.

Ma, L., Zhao, Z., Dong, Y., Sun, X., 2017. A synergistic extraction strategy by [N 1888][SOPAA] and Cyphos IL 104 for heavy rare earth elements separation. Sep. Purif. Technol. 174, 474–481. doi:10.1016/j.seppur.2016.10.046

Mathworks, 1984. Matlab Software.

Miceli, H., Rossi, M.G., Neumann, R., Marcelo Tavares, L., 2017. Contaminant removal from manufactured fine aggregates by dry rare-earth magnetic separation. Miner. Eng. 113, 15–22. doi:10.1016/j.mineng.2017.07.017

Michaud, S., Miguirditchian, M., Deblonde, G., Dinh, B., Hérès, X., Andreoletti, G., 2012. Modelling of Thorium Extraction by TBP. Procedia Chem. 7, 251–257. doi:10.1016/j.proche.2012.10.041

Miskufova, A., Kochmanova, A., Havlik, T., Horvathova, H., Kuruc, P., 2018. Leaching of yttrium, europium and accompanying elements from phosphor coatings. Hydrometallurgy 176, 216–228.

doi:10.1016/j.hydromet.2018.01.010

Mohammadi, M., Forsberg, K., Kloo, L., Martinez De La Cruz, J., Rasmuson, Å., 2015. Separation of ND(III), DY(III) and Y(III) by solvent extraction using D2EHPA and EHEHPA. Hydrometallurgy 156, 215–224. doi:10.1016/j.hydromet.2015.05.004

Molycorp, I., 1994. A LANTHANIDE LANTHOLOGY Part II, M-Z A LANTHANIDE LANTHOLOGY Part II, M-Z CONTENTS.

Moustafa, M.I., Abdelfattah, N.A., 2010. Physical and chemical beneficiation of the egyptian beach monazite. Resour. Geol. 60, 288–299. doi:10.1111/j.1751-3928.2010.00131.x

Nan, J., Han, D., Yang, M., Cui, M., Hou, X., 2006. Recovery of metal values from a mixture of spent lithium-ion batteries and nickel-metal hydride batteries. Hydrometallurgy 84, 75–80. doi:10.1016/j.hydromet.2006.03.059

Ni'am, A.C., Wang, Y.-F., Chen, S.-W., You, S.-J., 2019. Recovery of rare earth elements from waste permanent magnet (WPMs) via selective leaching using the Taguchi method. J. Taiwan Inst. Chem. Eng. 18, 30. doi:10.1016/j.jtice.2019.01.006

Obón, E., Fortuny, A., Coll, M.T., Sastre, A.M., 2017a. Mathematical modelling of neodymium, terbium and dysprosium solvent extraction from chloride media using methyl-tri(octyl/decyl)ammonium oleate ionic liquid as extractant. Hydrometallurgy 173, 84–90. doi:10.1016/j.hydromet.2017.08.011

Obón, E., Fortuny, A., Coll, M.T., Sastre, A.M., 2017b. Experimental and modeling studies of neodymium solvent extraction from chloride media with methyl-tri(octyl/decyl)ammonium oleate ionic liquid diluted in kerosene. Hydrometallurgy 174, 216–226. doi:10.1016/j.hydromet.2017.10.021

Obón, E., Fortuny, A., Coll, M.T., Sastre, A.M., 2017. Experimental and modelling studies of neodymium solvent extraction from chloride media with methyl-tri(octyl/decyl)ammonium oleate ionic liquid diluted in kerosene. Hydrometallurgy 174, 261–226. doi:10.1016/j.hydromet.2017.10.021

Önal Recai, M.A., Jönsson, C., Zhou, W., Van Gerven, T., Guo, M., Walton, A., Blanpain, B., 2017. Comparative oxidation behavior of Nd-Fe-B magnets for potential recycling methods: Effect of hydrogenation pre-treatment and magnet composition. J. Alloys Compd. 728, 727–738. doi:10.1016/j.jallcom.2017.09.046

Onoda, H., Nakamura, R., 2014. Recovery of neodymium from an iron-neodymium solution using phosphoric acid. J. Environ. Chem. Eng. 2, 1186–1190. doi:10.1016/j.jece.2014.04.019

Padhan, E., Nayak, A.K., Sarangi, K., 2017. Recovery of neodymium and dysprosium from NdFeB magnet swarf. Hydrometallurgy 174, 210–215. doi:10.1016/j.hydromet.2017.10.015

Padhan, E., Sarangi, K., 2017. Recovery of Nd and Pr from NdFeB magnet leachates with bi-functional ionic liquids based on Aliquat 336 and Cyanex 272. Hydrometallurgy 167, 134–140. doi:10.1016/j.hydromet.2016.11.008

Padwal, N., Prakash, S.S., Thakkar, S., Deshpande, T., 2018. Supported Liquid Membrane Technology: Advances and Review of its Applications. Indian J. Adv. Chem. Sci. 6, 2018. doi:10.22607/IJACS.2018.601003

Pana Rabatho, J., Tongamp, W., Takasaki, Y., Haga, K., Shibayama, A., 2013. Recovery of Nd and Dy from rare earth magnetic waste sludge by hydrometallurgical process. J Mater Cycles Waste Manag. 15, 171–178. doi:10.1007/s10163-012-0105-6

Panda, N., Devi, N., Mishra, S., 2012a. Solvent extraction of neodymium(III) from acidic nitrate medium using Cyanex 921 in kerosene. J. Rare Earths 30, 794–797. doi:10.1016/S1002-0721(12)60132-X

Panda, N., Devi, N., Mishra, S., 2012b. Solvent extraction of neodymium(III) from acidic nitrate medium using Cyanex 921 in kerosene. J. Rare Earths 30, 794–797. doi:10.1016/S1002-0721(12)60132-X

Parmentier, D., Valia, Y.A., Metz, S.J., Burheim, O.S., Kroon, M.C., 2015a. Regeneration of the ionic liquid tetraoctylammonium oleate after metal extraction. Hydrometallurgy 158, 56–60. doi:10.1016/j.hydromet.2015.10.006

Parmentier, D., Vander Hoogerstraete, T., Metz, S.J., Binnemans, K., Kroon, M.C., 2015b. Selective Extraction of Metals from Chloride Solutions with the Tetraoctylphosphonium Oleate Ionic Liquid. Ind. Eng. Chem. Res. 54, 5149–5158. doi:10.1021/acs.iecr.5b00534

Pavón, S., Fortuny, A., Coll, M.T., Sastre, A.M., 2018a. Rare earths separation from fluorescent lamp wastes using ionic liquids as extractant agents. Waste Manag. 82, 241–248. doi:10.1016/j.wasman.2018.10.027

Pavón, S., Fortuny, A., Coll, M.T., Sastre, A.M., 2018b. Neodymium recovery from NdFeB magnet wastes using Primene 81R·Cyanex 572 IL by solvent extraction. J. Environ. Manage. 222, 359–367. doi:10.1016/j.jenvman.2018.05.054

Peelman, S., Sun, Z.H.I., Sietsma, J., Yang, Y., 2016. Rare Earths Industry. Elsevier. doi:10.1016/B978-0-12-802328-0.00021-8

Peng, C.-Y., Tsai, T.-H., 2014. Solvent extraction of palladium(II) from acidic chloride solutions using tri-octyl/decyl ammonium chloride (Aliquat 336). Desalin. Water Treat. 52, 1101–1121. doi:10.1080/19443994.2013.826616

Petranikova, M., Herdzik-Koniecko, I., Steenari, B.-M., Ekberg, C., 2017. Hydrometallurgical processes for recovery of valuable and critical metals from spent car NiMH batteries optimized in a pilot plant scale. Hydrometallurgy 171, 128–141. doi:10.1016/j.hydromet.2017.05.006

Pietrelli, L., Bellomo, B., Fontana, D., Montereali, M.R., 2002. Rare earths recovery from NiMH spent batteries. Hydrometallurgy 66, 135–139.

Porvali, A., Wilson, B.P., Lundström, M., 2018. Lanthanide-alkali double sulfate precipitation from strong sulfuric acid NiMH battery waste leachate. Waste Manag. 71, 381–389. doi:10.1016/j.wasman.2017.10.031

Provazi, K., Campos, B.A., Crocce, D., Espinosa, R., Alberto, J., Tenório, S., 2011. Metal separation from mixed types of batteries using selective precipitation and liquid-liquid extraction techniques. Waste Manag. 31, 59–64. doi:10.1016/j.wasman.2010.08.021

Puigdomenech, I., 2013. Medusa Software.

Quinn, J.E., Soldenhoff, K.H., Stevens, G.W., 2017. Solvent extraction of rare earth elements using a bifunctional ionic liquid. Part 2_ Separation of rare earth elements. doi:10.1016/j.hydromet.2017.04.003

Rabie, K.A., 2006. A group separation and purification of Sm, Eu and Gd from Egyptian beach monazite mineral using solvent extraction. Hydrometallurgy 81–86. doi:10.1016/j.hydromet.2005.12.012

Rayner-Canham, G., 2000. Química Inorgánica Descriptiva, 2a edición. ed.

Regel-Rosocka, M., Materna, K., 2014. Ionic Liquids in Separation Technology, Ionic Liquids in Separation Technology. Elsevier. doi:10.1016/B978-0-444-63257-9.00004-3

Richard, A.R., Fan, M., 2018. Rare earth elements: Properties and applications to methanol synthesis catalysis via hydrogenation of carbon oxides. J. Rare Earths 36, 1127–1135. doi:10.1016/j.jre.2018.02.012

Rout, A., Binnemans, K., 2014a. Influence of the ionic liquid cation on the solvent extraction of trivalent rare-earth ions by mixtures of Cyanex 923 and ionic liquids. Dalt. Trans. 44, 1379. doi:10.1039/c4dt02766c

Rout, A., Binnemans, K., 2014b. Liquid-liquid extraction of europium(III) and other trivalent rare-earth ions using a non-fluorinated functionalized ionic liquid. Dalton Trans. 43, 1862–72. doi:10.1039/c3dt52285g

Rout, A., Binnemans, K., 2014c. Solvent Extraction of Neodymium(III) by Functionalized Ionic Liquid Trioctylmethylammonium Dioctyl Diglycolamate in Fluorine-free Ionic Liquid Diluent. Ind. Eng. Chem. Res. 53, 6500–6508. doi:10.1021/ie404340p

Rout, A., Binnemans, K., 2014. Separation of rare earths from transition metals by liquid-liquid extraction from a molten salt hydrate to an ionic liquid phase. Dalton Trans. 43, 3186–3195. doi:10.1039/c3dt52541d

Rout, A., Kotlarska, J., Dehaen, W., Binnemans, K., 2013. Liquid-liquid extraction of neodymium(iii) by dialkylphosphate ionic liquids from acidic medium: The importance of the ionic liquid cation. Phys. Chem. Chem.

Phys. 15, 16533–16541. doi:10.1039/c3cp52218k

Sastri, V.S., 2003. Modern aspects of rare earths and their complexes. Elsevier.

Skokov, K.P., Gutfleisch, O., 2018. Heavy rare earth free, free rare earth and rare earth free magnets - Vision and reality. Scr. Mater. 154, 289–294. doi:10.1016/j.scriptamat.2018.01.032

Smith Stegen, K., 2015. Heavy rare earths, permanent magnets, and renewable energies: An imminent crisis. Energy Policy 79, 1–8. doi:10.1016/j.enpol.2014.12.015

Srivastava, A.M.., Sommerer, T.J., 1998. Fluorescent Lamp Phosphors. Electrochem. Soc. Interface.

Sturza, C.M., Boscencu, R., Nacea, V., 2008. The lanthanides: Physico-chemical properties relevant for their biomedical applications. Farmacia 56, 326–338.

Sun, P., Huang, K., Wang, X., Song, W., Zheng, H., Liu, H., 2017. Separation of V from alkaline solution containing Cr using acidified primary amine N1923 with the addition of trisodium citrate. Sep. Purif. Technol. 179, 504–512. doi:10.1016/j.seppur.2017.02.035

Sunil Kumar Tripathy, Y. Ramamurthy, C. Raghu Kumar, 2010. Modeling of high-tension roll separator for separation of titanium bearing minerals. Powder Technol. 201, 181–186. doi:doi:10.1016/j.powtec.2010.04.005

Swain, B., Otu, E.O., 2011. Competitive extraction of lanthanides by solvent extraction using Cyanex 272: Analysis, classification and mechanism. Sep. Purif. Technol. 83, 82–90. doi:10.1016/j.seppur.2011.09.015

Swain, N., Mishra, S., 2019. A review on the recovery and separation of rare earths and transition metals from secondary resources. J. Clean. Prod. 220, 884–898. doi:10.1016/j.jclepro.2019.02.094

SX Kinetics, 2002. Sorbent extraction technology. J. Pharm. Biomed. Anal. 5, 755. doi:10.1016/0731-7085(87)80091-2

Tanabe, E.H., Schlemmer, D.F., Aguiar, L., Dotto, G.L., Bertuol, D.A., 2016. Recovery of valuable materials from spent NIMH batteries using spouted bed elutriation. J. Environ. Manage. 171, 177–183. doi:10.1016/j.jenvman.2016.02.011

Tanvar, H., Dhawan, N., 2019. Extraction of rare earth oxides from discarded compact fluorescent lamps. Miner. Eng. 135, 95–104. doi:10.1016/j.mineng.2019.02.041

Tian, Y., Liu, Z., Zhang Guoqing, 2019. Recovering REEs from NdFeB wastes with high purity and efficiency by leaching and selective precipitation process with modified agents. J. Rare Earths 37, 205–210.

Tunsu, C., Ekberg, C., Foreman, M., Retegan, T., 2014a. Studies on the Solvent Extraction of Rare Earth Metals from Fluorescent Lamp Waste Using Cyanex 923. Solvent Extr. Ion Exch. 32, 650–668. doi:10.1080/07366299.2014.925297

Tunsu, C., Ekberg, C., Gregoric, M., Retegan, T., 2014b. Recovery of La, Ce, Eu, Gd, Tb and Y from fluorescent lamp waste using solvent extraction: solvent choice studies., in: Proceedings of the 20th International Solvent Extraction Conference. Wurtzburg, Germany, pp. 07–11.

Tunsu, C., Ekberg, C., Retegan, T., 2014c. Characterization and leaching of real fluorescent lamp waste for the recovery of rare earth metals and mercury. Hydrometallurgy 144–145, 91–98. doi:10.1016/j.hydromet.2014.01.019

Tunsu, C., Petranikova, M., Ekberg, C., Retegan, T., 2016. A hydrometallurgical process for the recovery of rare earth elements from fluorescent lamp waste fractions. Sep. Purif. Technol. 161, 172–186. doi:10.1016/j.seppur.2016.01.048

Tunsu, C., Petranikova, M., Gergorić, M., Ekberg, C., Retegan, T., 2015a. Reclaiming rare earth elements from end-of-life products: A review of the perspectives for urban mining using hydrometallurgical unit operations. Hydrometallurgy 156, 239–258. doi:10.1016/j.hydromet.2015.06.007

Tunsu, C., Petranikova, M., Gergorić, M., Ekberg, C., Retegan, T., 2015b. Reclaiming rare earth elements from end-of-life products: A review of the perspectives for urban mining using hydrometallurgical unit operations. Hydrometallurgy 156, 239–258. doi:10.1016/j.hydromet.2015.06.007

Tunsu, C., Retegan, T., 2016. Chapter 6 - Hydrometallurgical Processes for the Recovery of Metals from WEEE. doi:10.1016/B978-0-12-803363-0.00006-7

U.S. Geological Survey, 2018. Mineral Commodity Summaries 2018. doi:10.3133/70194932

U.S Department of Energy, 2011. Critical Materials Strategy.

Usapein, P., Lothongkum, A.W., Ramakul, P., Pancharoen, U., 2009. Efficient transport and selective extraction of Cr(VI) from waste pickling solution of the stainless steel-cold rolled plate process using Aliquat 336 via HFSLM. Korean J. Chem. Eng. 26, 791–798. doi:10.1007/s11814-009-0132-8

Van Gosen, B.S., Verplanck, P.L., Seal, R.R., II, Long, K.R., Gambogi, J., 2017. Critical mineral resources of the United States— Economic and environmental geology and prospects for future supply. U.S. Geol. Surv. . doi:10.3133/pp1802O

Voncken, J.H.., 2016a. 1. The Rare Earth Elements - A Special Group of Metals, in: The Rare Earth Elements. Springer US, pp. 21–41. doi:10.1007/978-3-319-26809-5

Voncken, J.H.., 2016b. 3. Physical and Chemical Properties of the Rare Earths, in: The Rare Earth Elements. Springer US, pp. 98–125. doi:10.1007/978-3-319-26809-5

Wang, Q., He, Z., Li, G., Li, B., Zhu, C., Chen, P., 2017. Numerical investigation of desulfurization behavior in electroslag remelting process. Int. J. Heat Mass Transf. 104, 943–951. doi:10.1016/j.ijheatmasstransfer.2016.09.022

Welton, T., 2018. Ionic liquids: a brief history. Biophys. Rev. 10, 691–706. doi:10.1007/s12551-018-0419-2

Wu, F., Xu, S., Li, L., Chen, S., Xu, G., Xu, J., 2009. Recovery of valuable metals from anode material of hydrogen-nickel battery. Trans. Nonferrous Met. Soc. China 19, 468–473. doi:10.1016/S1003-6326(08)60297-6

Wu, Y., Yin, X., Zhang, Q., Wang, W., Mu, X., 2014. The recycling of rare earths from waste tricolor phosphors in fluorescent lamps: A review of processes and technologies. "Resources, Conserv. Recycl. 88, 21–31. doi:10.1016/j.resconrec.2014.04.007

Wübbeke, J., 2013. Rare earth elements in China: Policies and narratives of reinventing an industry. Resour. Policy 38, 384–394. doi:10.1016/j.resourpol.2013.05.005

Xie, F., Zhang, T.A., Dreisinger, D., Doyle, F., 2014. A critical review on solvent extraction of rare earths from aqueous solutions. Miner. Eng. 56, 10–28. doi:10.1016/j.mineng.2013.10.021

Yang, F., Kubota, F., Baba, Y., Kamiya, N., Goto, M., 2013. Selective extraction and recovery of rare earth metals from phosphor powders in waste fluorescent lamps using an ionic liquid system. J. Hazard. Mater. 254–255, 79–88. doi:10.1016/j.jhazmat.2013.03.026

Yang, X., Zhang, J., Fang, X., 2014. Rare earth element recycling from waste nickel-metal hydride batteries. J. Hazard. Mater. 279, 384–388. doi:10.1016/j.jhazmat.2014.07.027

Yin, X., Tian, X., Wu, Y., Zhang, Q., Wang, W., Li, B., Gong, Y., Zuo, T., 2018. Recycling rare earth elements from waste cathode ray tube phosphors: Experimental study and mechanism analysis. J. Clean. Prod. 205, 58–66. doi:10.1016/j.jclepro.2018.09.055

Yoon, H.-S., Kim, C.-J., Chung, K.-W., Kim, S.-D., Lee, J.-Y., Kumar, J.R., 2016. Solvent extraction, separation and recovery of dysprosium (Dy) and neodymium (Nd) from aqueous solutions: Waste recycling strategies for permanent magnet processing. Hydrometallurgy. doi:10.1016/j.hydromet.2016.01.028

Yun, X., Liansheng, X., Jiying, T., Zhaoyang, L., Li, Z., 2015. Recovery of rare earths from acid leach solutions of spent nickel-metal hydride batteries using solvent extraction. J. RARE EARTHS 33, 1348. doi:10.1016/S1002-0721(14)60568-8

Zhan, W., Guo, Y., Gong, X., Guo, Y., Wang, Y., Lu, G., 2014. Current status and perspectives of rare earth catalytic materials and catalysis. Chinese J. Catal. 35, 1238–1250. doi:10.1016/S1872-2067(14)60189-3

Zhang, P., Yokoyama, T., Itabashi, O., Wakui, Y., Suzuki, T.M., Inoue, K., 1998. Hydrometallurgical process for recovery of metal values from spent nickel-metal hydride secondary batteries, Hydrometallurgy.